LABORATORY AND THEORETICAL INVESTIGATION OF THE NEAR CRITICAL PHASE BEHAVIOUR OF HYDROCARBON - INJECTION GAS SYSTEMS

by

NIKOS VAROTSIS, Dip.Eng,MEng.

Doctor of Philosophy

Heriot-Watt University,

Department of Petroleum Engineering

November, 1983

T A B L E O F C O N T E N T S

PART I (CONTD)

D E T A I L E D S E C T I O N T I T L E S

GENERAL INTRODUCTION TO GAS MISCIBLE FLOODING PROCESS

PART I

DEVELOPMENT OF A THEORETICAL MODEL TO PREDICT PHASE BEHAVIOUR OF MULTICOMPONENT GAS/OIL MIXTURES

LIST OF TABLES

TABLE

TABLE

LIST OF FIGURES

LIST OF PLATES

ACKNOWLEDGEMENTS

I would like to thank all the people both within and outside the Department who have been immensely helpful during this study.

In particular I wish to thank:

Professor George Stewart for his advice and encouragement throughout this project and for his valuable suggestions concerning the theoretical part of the work.

Dr A C Todd for his advice and helpful discussions as to the design and running of the experimental appratus.

Mr Charlie McLeod for the original design and construction of the experimental system.

Mr G Pratt for his continuous and enthusiastic cooperation at all times in the design and commissioning of the laboratory apparatus.

Mr A Reid for his valuable help in the development of the composition analysis techniques and his enthusiastic and helpful cooperation at all times.

In addition, I would like to thank Professor Jim Brown under whose interest and inspiration this project has started.

Sincere thanks are extended to the workshop team under Mr Alan Brown for their superb workmanship and unfailing support.

I wish also to express my thanks to the UK Department of Energy for generously sponsoring this investigation.

Finally, I am indebted to Carol Paton for her dedication and often long worked hours in typing this manuscript.

Above all, I wish to express my gratitude to Leanne, whose continuous support and encouragement at a difficult time, made the completion of this study possible.

ABSTRACT

The evaluation of an oil recovery scheme based on gas injection requires knowledge of the mass transfer effects which will take place in the reservoir as a result of the solution of the injected gas in the oil phase and vapourisation of hydrocarbons into the gas phase.

This study describes the design and use of an experimental system, as well as the development of a theoretical model to study the phase behaviour and PVT properties of injection gas-reservoir fluid mixtures at reservoir conditions of pressure and temperature.

The Peng-Robinson, or the Modified Soave-Redlich-Kwong, or the Modified Redlich-Kwong equation of state is solved implicitly with the material balance and thermodynamic equilibria equations model to predict the phase behaviour and physical properties of injection gas and hydrocarbon mixtures in equilibrium. The iteration method used requires a minimum number of variables for which simultaneous iteration is required and a solution technique based on the Broyden's modification of the full Newton step gives consistent phase properties and rapid convergence even near the very sensitive critical point region for a miscible displacement.

A series of experiments including saturation pressure determination, density and composition measurements of the phases resulting from single and multiple contacts, were performed on CO_2-hydrocarbon mixtures. The ability of CO_2 to extract hydrocarbons from the reservoir fluid and, at the same time, to condense into the oil changing the physical properties of the liquid phase, is demonstrated. Techniques to tune the phase

behaviour simulator are discussed and the point is argued that the interchange of information between the experimental work and a robust computer model is necessary for a comprehensive study of the phase behaviour of reservoir fluids encountered in a gas miscible flooding process.

NOMENCLATURE

The following list of nomenclature only includes the generalised symbols used in the text. Symbols which have been used to represent different quantities have been defined as they arose within the text.

SYMBOL	DESCRIPTION
A,a	Parameters in equation of state
API	API gravity
B,b	Parameters in equation of state
d	Density
F	Moles of feed, mathematical function
f	Fugacity
G	Energy
K	Equilibium ratio
k	Binary interaction coefficient
L	Moles of liquid phase
M	Mass
m	Parameter in equation of state
MW	Molecular weight
N	Number of components
n	Number of moles or number of mathematical variables
P	Pressure
R	Universal gas constant
S	Entropy
T	Temperature
V	Moles of vapour

NOMENCLATURE (CONTD)

v	Molar volume
x,y	Mole fractions
Z	Compressibility factor
z	Overall mole fractions

SUBSCRIPTS

B	Boiling
C	Critical
i,j	Component identifiers
L	Liquid
o	Standard reference state
r	Reduced
S	Saturation
V	Vapour

SUPERSCRIPTS

A	Phase identifier
B	Phase identifier

GREEK LETTERS

μ	Chemical potential
Φ	Fugacity coefficient
Φ	Equation residual
ω	Acentric factor
Θ	Angle or scalar

INTRODUCTION

The efficiency of a displacement of a reservoir fluid by an injection gas depends on a variety of factors. The phase behaviour of the gas reservoir fluid mixtures generated during the displacement, the densities and viscosities of the phases present, the relative permeabilities to individual phases together with complications during the displacement such as dispersion, fingering, reservoir heterogenities, determine decisively the efficiency of the enhanced oil recovery process.

Interpretation of the effects of phase behaviour on displacement efficiency becomes difficult due to the complexity of the interaction between injection gas-reservoir fluid mixtures. The co-existence of multiple phases in equilibrium, such as the liquid-liquid-vapour equilibrium for some CO_2 and crude oil systems at temperatures not too far above the critical temperature of CO_2 (31^oC), or as in the vapour-liquid-solid equilibrium exhibited by crude oil mixtures rich in asphaltenes, is one of the difficulties in the phase behaviour study.

The variety of mechanisms responsible for the mass transfer between the injection gas and reservoir fluid phase, which leads through a continuous change in compositions to one homogeneous phase miscible fluid, constitutes another difficulty. In miscible processes knowledge of the phase behaviour in the vicinity of the critical point is very significant. However in this region the interfaces between the different phases become very difficult to detect and the calculation of the physical properties often becomes problematic. These factors contribute as well to the difficulties of a gas miscible enhanced oil recovery study. The prediction of the multiple phase behaviour is complicated because

generally the high pressure makes the heavy hydrocarbons very soluble in the gas phase, and it also makes the supercritical light components very soluble in the liquid phase, resulting in near critical and sometimes retrograde behaviour.

There are two approaches for the investigation of the phase behaviour of injection gas-reservoir fluid mixtures. These two approaches should complement each other. The first approach is to obtain experimental results in the laboratory at the conditions required, covering most of the interesting areas of the phase envelope. Because of the complex nature of petroleum reservoir fluids and the often complicated phase behaviour observed at elevated temperature and pressure conditions, the fluid properties and phase behaviour historically have been measured experimentally. The second approach is the mathematical modelling of the processes. The development of reliable equations of state, applicable to both phases under a very wide range of pressure and temperature conditions, and the use of fast computer systems allow us now to predict with sufficient accuracy and reliability, the phase equilibria of multicomponent mixtures. This approach makes use of theoretical models based on thermodynamic principles and the whole phase envelope and the physical properties of any mixture can be predicted in minimal time.

Both approaches exhibit serious disadvantages if considered seperately. The time and manpower required to run the experiments as well as the great number of runs needed to obtain an overall conception of the phase behaviour, reduce significantly the attractiveness of the first approach when used solely. On the other hand, theoretical predictions based on empirical functions

without any tuning to the real system under study, given the complexity of the chemical nature of the hydrocarbon mixtures, often appear meaningless.

The approach taken in this study is to build up an experimental system which will allow independent measurements of phase behaviour and fluid properties to be made. These results are subsequently going to be used to tune the numerical simulation model shortly to be described. By doing only a few experiments and tuning the model to match these experimental data, the simulator can then be used to predict, reliably and accurately, the phase behaviour of the mixture under study for different regions of the phase envelope. A valid and reliable theoretical model can decrease dramatically the cost of a miscible flooding study as only a few experimental results, which are very expensive and time consuming, have to be obtained. The use of the simulator before any experimental work has been done allows the investigator to focus his attention on the interesting areas of the phase envelope, so that the number of the experiments required to validate the computer predictions can be optimised. The interchange of information between the experimental work and computer model, cuts drastically the time required for an enhanced oil recovery study, provides a double check on the derived data, helps to clarify areas of uncertainty and assists with the explanation and physical interpretation of the obtained results. The use of both approaches is necessary in order to establish a complete and comprehensive view of the phase behaviour of the mixtures of reservoir fluids and injection gases encountered in a gas miscible enhanced oil recovery process.

Based on the arguments above, this study can be divided into three main sections. The first one describes in detail the development of the theoretical model to be used and discusses other methods. The second section describes the experimental equipment which has been set up for the laboratory study of the phase behaviour, and describes the experimental procedures and methods. Finally, the last section compares the laboratory data obtained against the computer predictions and discusses the advantages and disadvantages of the methods as well as their limitations.

C H A P T E R 1

T H E R E C O V E R Y O F O I L
F R O M P E T R O L E U M R E S E R V O I R S

1.1 INTRODUCTION - PRIMARY AND SECONDARY RECOVERY

1.2 ENHANCED OIL RECOVERY

1.2.1 Entrapment of Oil into the Reservoir During Primary and Secondary Recovery

1.2.2 Applicable Enhanced Oil Recovery Methods

1.1 INTRODUCTION - PRIMARY AND SECONDARY RECOVERY

Oil is found filling the porous rocks of the reservoirs at depths even greater than 10,000 feet, at temperatures of the order of 350°K and pressures of up to 800 bar. As far as the origin is concerned the reservoir rocks were normally laid down in marine sedimentary environments so that saline water occupied the pores. The saline water was displaced at some later stages by the migrating oil. Thin films of water remained, coating the surfaces of the rocks, or water droplets remained in small pores of the rock matrix. The water which could not be displaced by the oil and which co-exists with the hydrocarbons in the reservoir, is called connate water and can claim between 10 - 15% of the pore space.[1]

The reservoir rock consists of a mixture of various minerals whose grains are usually irregular and which comprise a complex interconnected capillary system shared by oil, gas and water. As oil is produced from the reservoir, the pressure declines unless another fluid enters the reservoir, to replace the produced oil. Reservoir pressure decline, adversely affects the rate of oil production by diminishing the pressure differential force that drives oil into the well bore. A second and very important consequence of the pressure drop is that the oil becomes very quickly saturated, gas is released in the reservoir and the gas phase, more mobile than the oil phase, flows in increasing ratio towards the well at the expense of oil production.

Only a few oil reservoirs are fortunate enough to have a contiguous aquifer which is able to supply water as fast as the oil is normally produced[1]. In undersaturated reservoirs the decline in

pressure is either eliminated, or at least reduced by the injection of water through selected injection wells. Naturally in offshore fields the injected fluid is seawater which can cause problems due to its salinity and high solids content. Without either fluid injection or an active natural water drive, oil recovery is usually restricted to a small percentage of the oil originally in place and by that time further production is limited. Historically, the pressure maintenance in the reservoirs by water injection has been called "secondary recovery" because the fluid injection results in a "second crop" of oil from the reservoir[2]. Waterflooding's popularity is accounted for by the general availability of water, particularly in offshore fields and its efficiency in displacing oil[2].

Waterflooding was first used over 100 years ago, but it was not until the 1950's that it gained popularity when field applications increased at a rapidly escalating rate[17]. Waterflooding has been the universal secondary recovery agent.

1.2 ENHANCED OIL RECOVERY

The presence of the remaining 65 - 70% of oil in place after the secondary recovery has been applied, has prompted interest and experimentation in "tertiary" or "enhanced" recovery methods to recover a "third crop of oil". These methods make use of substances added before or during fluid injection to increase the recovery efficiency of the injected water or gas. These more efficient methods may be applied immediately without utilising the older "secondary recovery" methods, hence the name "tertiary recovery" may not be truly applicable.

The field need not be completely watered out before the inception of enhanced recovery, indeed economic considerations militate against this, but certainly large portions of the reservoir will be at the waterflood residual oil saturation. Hence any proposed EOR process should definitely be effective in displacing oil in the presence of a high water saturation.

1.2.1 Entrapment of Oil into the Reservoir During Primary and Secondary Recovery

Before embarking on a technical description of the various enhanced recovery methods, it is important to investigate the physical mechanisms whereby primary production methods result in such large amounts of oil being retained in place.

The disposition of the immiscible phases within the pore structure during and after waterflooding depends on the wettability characteristics of the oil-water-rock system. Most reservoir rocks are preferentially water-wet, but a variety of states is possible, ranging from completely water-wet to preferentially oil-wet. Some of the oil that has been left behind, is present in those macroscopic regions within the reservoir which were not contacted by the water drive. This is conceptually related to the sweep efficiency of the flooding and Figure 1-1 illustrates this factor. This is exemplified by the 5-spot pattern at depletion, where water has swept most but not all of the pattern area[17]. Large unswept areas remain after a flood has been abandoned. Different mobilities of the injected water with respect to the displaced hydrocarbons are responsible for the existence of unswept pockets at the end of waterflooding. Obviously, being less viscous, the

water tends to move through the reservoir fluid rather than to push against it.

In reservoirs with high variations in permeability, water moves faster through the more permeable parts of the reservoir, and it appears in the production well having left significant quantities of oil behind.

Any additional water injected is going to flow through the already established channel to the production well, as the capillary forces and interfacial tensions are absent, thus making it the more attractive way. This fingering is due to the high permeability variations and not to the mobility ratios difference. In the non-swept zones the oil saturation is presumably high enough for the oil phase to remain continuous. Even in the zones of the reservoir that have been swept macroscopically by water, some factor of the swept volume has not been reached by the injected fluid. Shown on the cross-section (Figure 1-b) is the water swept reservoir and the oil bank; however, not all of the swept region has been contacted by water. By-passed regions or islands have been left behind. Reservoir heterogeneities, lensing, faulting, shale barriers or permeability variations can be blamed for the non-contacted areas, Docher and Wise speculated that this effect could be especially noticeable in carbonates and that recovery of oil from these pores would depend on diffusion rather than direct frontal displacement[3].

Another fraction of the oil remaining in place is trapped into the reservoir by capillary forces applied by the surrounding aqueous phase. Oil droplets are left in individual pores as well as in

dead-end pores or minute crevices which contain both water and oil as a result of the original accumulation process. A simple model of trapped oil in a capillary is illustrated in Figure 1-2. Water flowing through adjacent and communicating capillaries establishes a pressure gradient across the trapped drop. The drop moves in the direction closest to the gradient direction, subject to pore wall constraints, until a pore constriction is met that is too small to permit further advance.

For simplicity, assume that the oil-water-rock system is completely water-wet, the advancing and receding contact angles are θ_2 and θ_1 respectively and also that the capillary is sufficiently small so that these interfaces are spherical. The angles θ_1 and θ_2 are controlled by the intermolecular forces and are a measure of the wettability of the system[4].

Laplace's equation can be used to calculate the capillary pressure Pc across the curved interface[5]. Thus

$$P_{c_1} = P_o - P_{w_1} = \frac{2\gamma\cos\theta_1}{r_1} \quad \text{. . . . . Eq 1-1}$$

$$P_{c_2} = P_o - P_{w_2} = \frac{2\gamma\cos\theta_2}{r_2} \quad \text{. . . . . Eq 1-2}$$

It follows that a water phase pressure difference over the trapped ganglion in excess of

$$\Delta p = P_{w_2} - P_{w_1} = 2\gamma\left[\frac{\cos\theta_1}{r_1} - \frac{\cos\theta_2}{r_2}\right] \quad \text{. . . . . Eq 1-3}$$

will be required to exceed the capillary force retaining the drop and cause it to flow.

To describe the entrapment of oil within pores, some qualitative description of the porous system of the natural rock is necessary. Figure 1-3 shows how oil can become trapped and can indicate how the amount of trapped oil may be expected to vary as conditions of displacement are changed. The water front in the two differently sized capillaries, with common inlet and outlet, will generally move with different velocities as the fluids respond to the combined effects of viscous and capillary forces[4].

In Figure 1-3a the oil-water interface enters through the common inlet to both pores. The pressure drop across each pore is the sum of the pressure drops caused by the viscous forces along the capillary and the capillary pressure exerted on the fluid in the pore.

$$\Delta p = \Delta p_{visc} + P_{cap} \quad \text{. . . . . Eq 1-4}$$

The pressure drop due to viscous forces is given by the Poiseuille equation

$$\Delta p = 8Qn\ell/\pi r_1^4 \text{ for pore 1}$$

$$\Delta p = 8Qn\ell/\pi r_2^4 \text{ for pore 2} \quad \text{. . . . . Eq 1-5}$$

where Q is the flow rate in the pore, n is the viscosity of the fluid, ℓ and r are the length and radius of the capillary.

When the pressure of the displacement is high and the flow rate is high, Equation 1-5 predominates and the pore with the smaller radius r_2 causes the larger pressure drop. In that case, the oil-water interface in arm "1" reaches the common outlet first, thus trapping oil in the small capillary (Fig 1-3b). If the pressure is small, the capillary forces then become significant and

control the movement of the oil-water interfaces, and hence the entrapment of oil. In that case the entrapment will now occur in the larger capillary (Figure 1-3c). For mixed wettability rock, as the oil-water interface passes through the pore, oil can become stuck on the oil-wet portions which can then break off from the main body of the oil and become trapped as a droplet. Typically the residual oil is 60% to 90% of all remaining oil after waterflood. The porous structure of the natural rock is, of course, much more complicated than a system of simple capillaries. The dimensions of the interconnected pores change from place to place and thereby the capillary pressures do not remain constant. Despite that, the simplified model used above, provides a very useful qualitative interpretation of what is happening as the oil and water move into the reservoir.

From the oil that exists originally in place in a reservoir, some 60% of it on average, remains in situ after waterflooding is abandoned, due to one of the reasons mentioned previously. It is the recovery of this oil that enhanced oil recovery is aimed.

1.2.2 Applicable Enhanced Oil Recovery Methods

The term "enhanced oil recovery" refers to a collection of techniques that seek to enhance or overcome the natural forces that impede recovery of oil. While the broad umbrella of EOR covers many methods, the techniques can be grouped under four main headings[1a]:-

(i) Thermal methods
- Steam drive
- In situ combustion
- Hot waterflooding

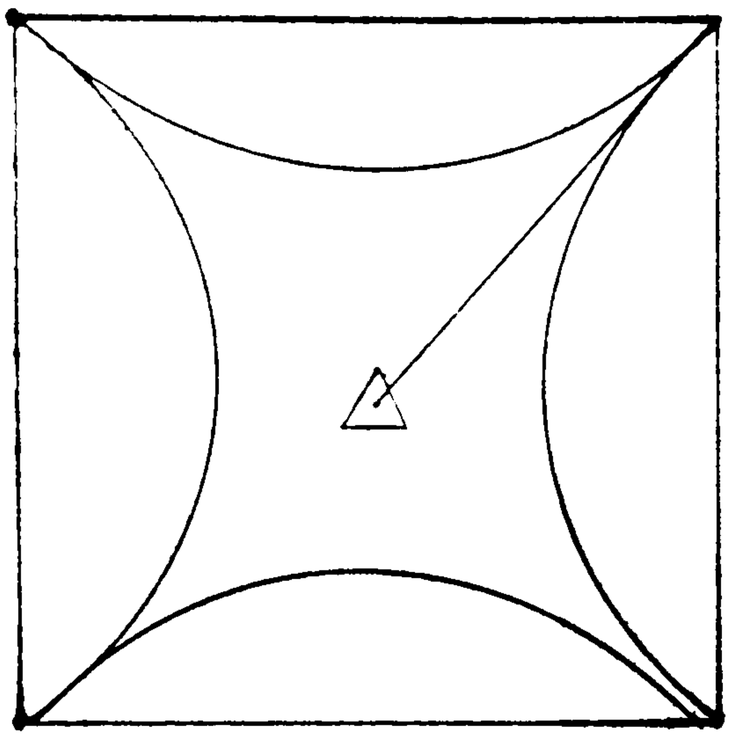

FIGURE 1-1a

5-SPOT PATTERN AT DEPLETION

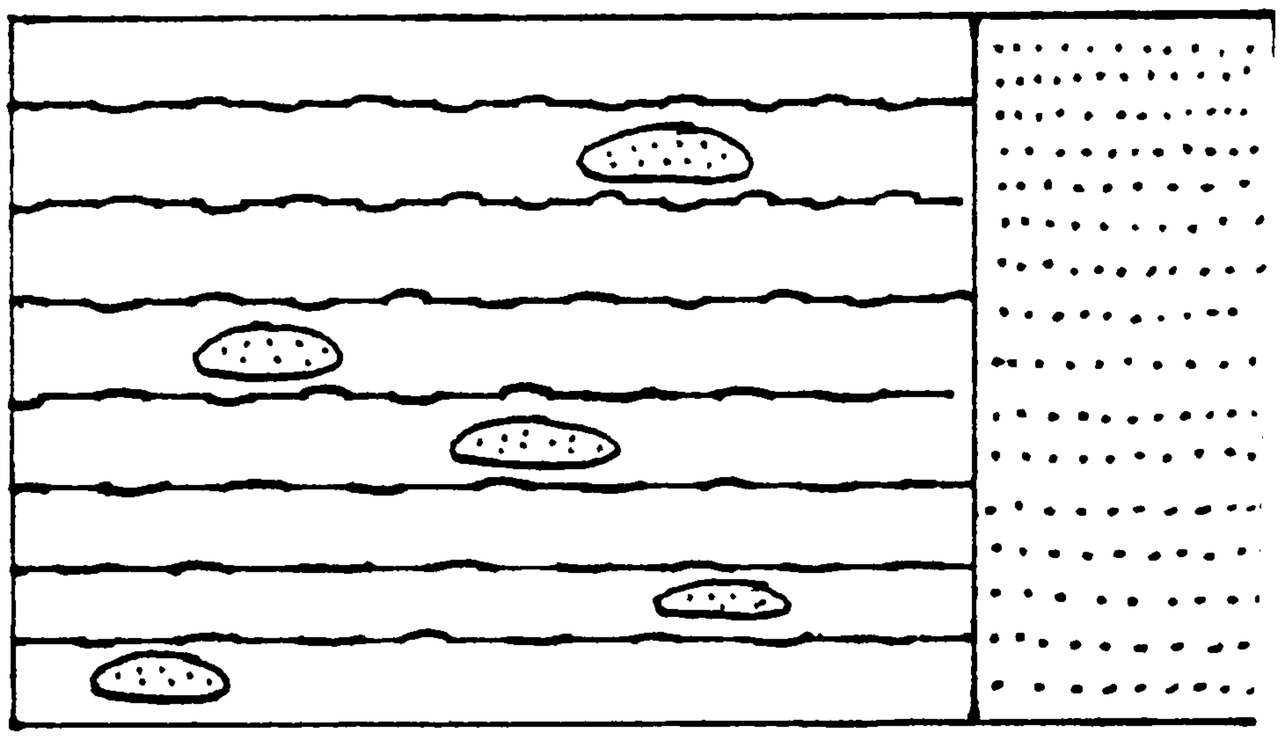

FIGURE 1-1b

CROSS SECTION OF WATER SWEPT RESERVOIR[17]

5-SPOT PATTERN AT DEPLETION

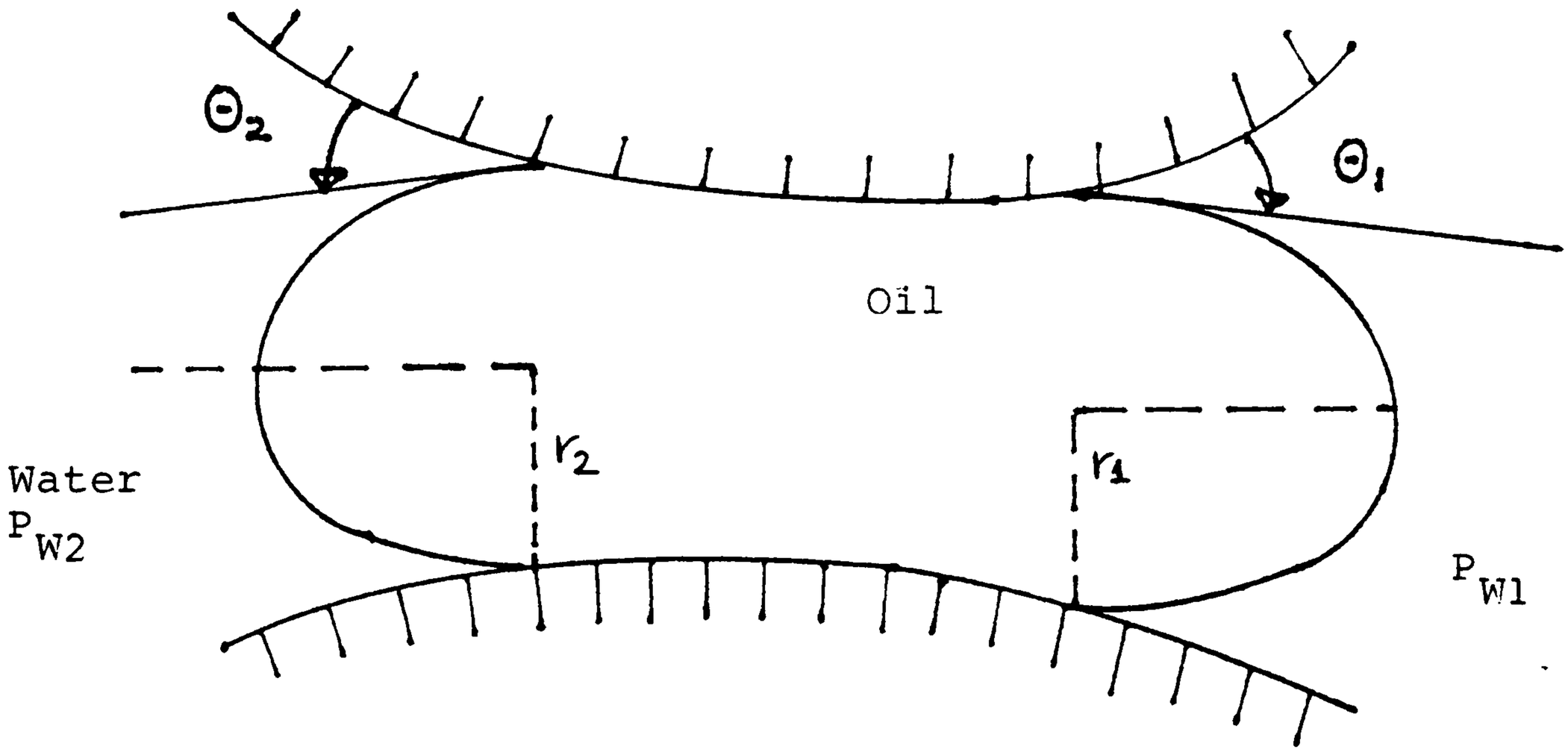

FIGURE 1-2

OIL DROPLET TRAPPED IN A CAPILLARY[17]

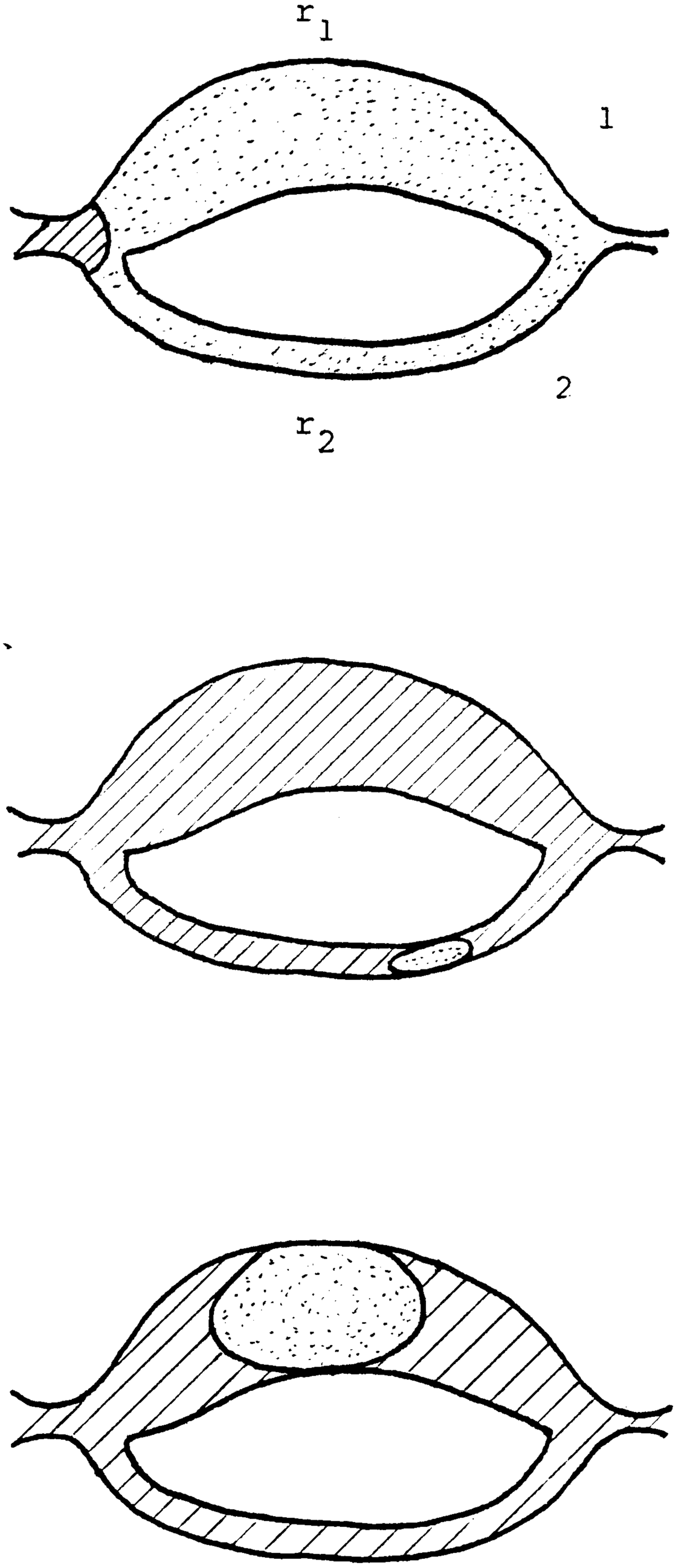

FIGURE 1-3

OIL ENTRAPMENT WITHIN PORES

(ii)	Gas Flooding	- Carbon dioxide flooding
		- Inert gas flooding
		- Natural gas flooding
(iii)	Chemical Flooding	- Surfactant flooding
		- Polymer augmented waterflooding
		- Alkaline flooding
(iv)	Novel Technologies	- Electrical methods
		- Microbiology
		- Oil mining

Enhanced oil recovery techniques, either chemical, miscible or thermal, aim at improving the recovery efficiency of a reservoir over and above that achievable with conventional methods, by altering different parameters of the system and to eliminating one of the previously mentioned causes that keep oil trapped in place. The first group of methods improves the mobility of the hydrocarbon phase by reducing its viscosity. The second one, which includes the miscible processes, eliminates the capillary pressures that are holding the oil droplets in the rock pores. The third group of methods reduces the interfacial tension, alters the rock wettability (surfactant, alkaline flooding) or increases the viscosity of water (polymer injection) to achieve more favourable mobility ratios.

Although each EOR method has its own range of application, these methods are to a large extent complementary and thus together cover a wide range of reservoir conditions. It is most likely that future recovery methods will be a combination of these techniques, each designed to correct or overcome problems that have led to the entrapment of oil in a specific reservoir. In spite of the considerable effort spent on research and field testing during the last 30 years, enhanced oil recovery techniques are, on the whole, still very much in an early stage of development. Most successful so far have been thermal recovery methods, particularly those employing steam[6]. For many years steam drive has been applied on a large scale. Chemical flooding processes are still in the testing stage, although considerable progress has been made towards the understanding of their mechanisms. The novel technologies are at the moment at their initial stage of development and they can be possibly applied in the future only in reservoirs which have certain characteristics[18]. The prospects for gas injection miscible recovery floodings (including for example non-miscible nitrogen injection) are promising. Large scale miscible gas injection projects are underway in various parts of the world[7,8,9,10,11,12,13,14,15,16].

LIST OF REFERENCES

1. Levorsen: "Geology of Petroleum", W.H. Freeman & Co, 2nd Edition.

2. Craig, F.F. Jr:
"The Reservoir Engineering Aspects of Waterflooding"
SPE Monograph Vol. 3.

3. Docher, T.M. and Wise, F.A.:
SPE paper No. 5800 March 1976.

4. Dawe, R.A. and Egbogah, E.O.:
Contemp. Physic. 1978 Vol. 19 p. 355.

5. Mahers, E.G. and Dawe, R.A.:
Paper presented at 2nd European EOR Conference, Paris 1982.

6. Haan, H.J. and Van Breen, H.M.L.:
Report presented at 2nd European EOR Conference, Paris 1982.

7. Stalkup, F.I.:
Journal of Petroleum Technology, April 1983, p. 815.

8. Porter, R.E. and Cover, A.E.:
Proc.,ERDA Enhanced Oil and Gas Recovery and Improved Drilling Methods Tulsa (1977) 1, C5.

9. Kane, A.V.:
Journal of Petroleum Technology, Feb. 1979 p. 217.

10. Bleakley, W.B.:
Oil and Gas Journal, March 25, 1974, pp. 69–78.

11. Intl. Petroleum Encyclopedia:
Petroleum Publishing Co., Tulsa 1977 pp.282–294.

12. Matheny, S.L.:
Oil and Gas Journal, March 31, 1980, 79.

13. Pontius, S.B. and Tham, M.J.:
Journal of Petroleum Technology, Dec. 1978, p. 1706.

14. Hansen, P.W.:
SPE paper No. 6747 presented at the 1977 SPE Annual Technical Conference and Exhibition, Denver, Oct. 9, 1977.

15. Thrash, J.C.:
SPE paper No. 8382 presented at the 1979 SPE Annual Technical Conference and Exhibition, Las Vegas, Sept. 23–26, 1979.

16. Goodrich, J.H.:
SPE paper No. 8832 presented at the 1980 SPE/DOE EOR Symposium, Tuba, April 20–23, 1980.

17. Herbeck, E.R., Heintz, R.C. and Hastings, J.R.:
Petroleum Engineer, Jan. 1976 p. 33.

18. Kuuskraa, V.A.:
Report presented at 2nd European EOR Conference, Paris 1982.

CHAPTER 2

INTRODUCTION TO GAS MISCIBLE DISPLACEMENT

The purpose of gas miscible displacement methods is to inject a substance miscible with the oil inside the reservoir. Miscibility overcomes the capillary forces which lock residual oil droplets in the pores and permits dynamic movement of the injected fluid to dislodge the oil and move it to the producing well. Any liquid hydrocarbon such as naptha, kerosene or gasoline is miscible with reservoir oil. Also miscible are liquified petroleum gas products such as ethane, propane or butane[1,2]. These liquid hydrocarbons have first contact miscibility with oil which means that they are miscible with oil immediately on contact. This feature distinguishes this method from the high pressure lean gas process or the CO_2 or nitrogen injection schemes, in which the injection gases are not miscible with oil on initial contact, but become so after multiple contacts[3,4,5,6]. Any enhancement process fluid should be able to contact by-passed areas or release and reduce the trapped oil; preferably it should do both. Careful engineering of the injection processes can have zones which have been previously by-passed by water, invaded by the injected gas. The waterflooding profiles shown in Figure 2-1, show the effect of gravity segregation in a reservoir at two differect times after waterflooding has started. Water segregates in the lower regions of the reservoir and leaves regions of the upper part unswept. The use of a gaseous substance for enhanced oil recovery ensures, because of the density difference, that the injected gas will sweep the areas not invaded by water in the reservoir. On the other hand, a disadvantage of the gas flooding compared with waterflooding, results from the low viscosity of the injection gas relative with that of oil. The mobility ratio of the reservoir oils with displacing agents will be much more unfavourable than the

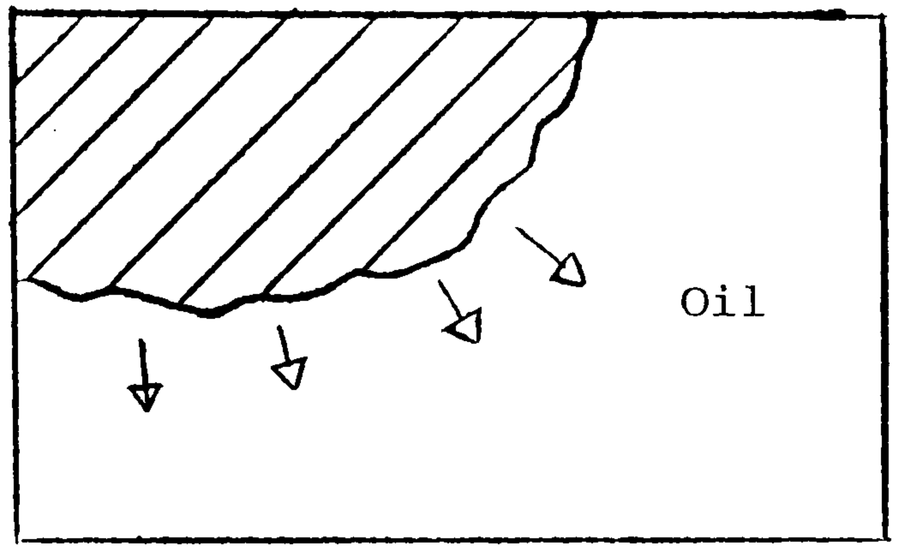

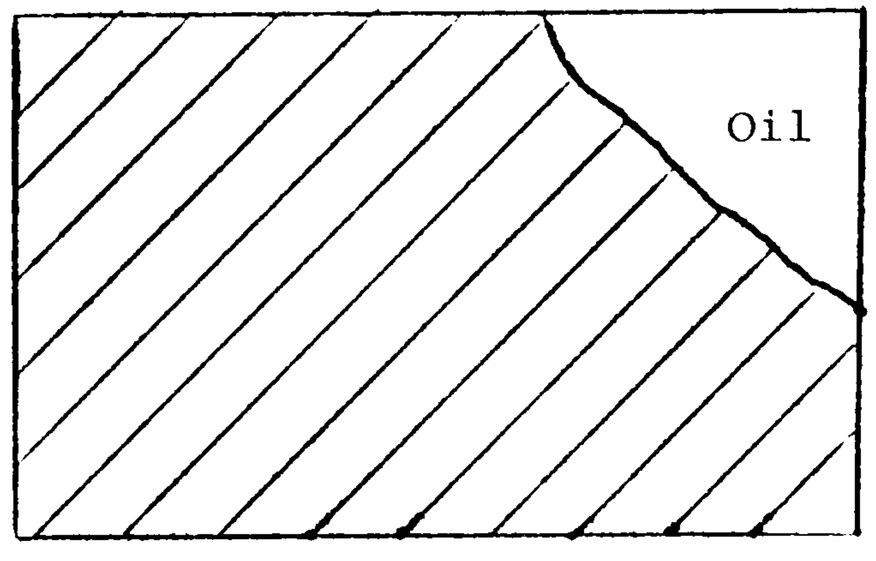

Water Swept Regions

FIGURE 2-1

GRAVITY SEGREGATION IN A WATERFLOODED RESERVOIR

mobility ratio with water. For these reasons, reservoirs containing oil of relatively high viscosity are not prospective candidates for gas injection[7,8].

Several techniques to reduce the unfavourable mobility ratios of gas flooding projects have been investigated, such as:

(i) installation of well packers and perforating techniques to isolate certain layers;

(ii) shutting in production wells to eliminate low pressure sinks[9];

(iii) addition of surfactant to water, alternatively injected with gas to cause a foam or emulsion to be formed[10,11,12];

(iv) the alternative injection of water and gas slugs (WAG PROCESS) which has been the most widely used mobility control method so far[13,14,15,16]. Although injected water invades the zones previously invaded by gas, subsequently injected gas is not diverted completely to other zones. As a result, gas channeling is reduced temporarily.

The residual oil saturation can be reduced through a mass transfer process between the injection gas phase and the reservoir oil phase. The mass transfer that takes place during gas injection operations can be taken advantage of, to create miscible conditions and theoretically recover all of the reservoir oil. This is possible because miscibility eliminates the capillary and interfacial forces which retain substantial quantities of oil even after successful flooding under immiscible conditions[16].

An engineering evaluation of the recovery efficiency of a gas injection, requires a knowledge of three factors[7]:

(i) the efficiency with which the gas displaces the oil on a pore scale;

(ii) the horizontal sweep efficiency which refers to the area contacted on a horizontal plane;

(iii) the vertical sweep efficiency of the injected fluid as it advances through layers of different physical and fluid properties.

A gas-oil displacement can be either immiscible or miscible. If we neglect all phase behaviour effects between the injected gas and the residual oil and gas phases, in other words consider the displacement to be only immiscible, all methods for determining the horizontal and vertical efficiencies of the displacement hinge on two basic theories. These theories consider either simultaneous flow of the displacing and resident fluids behind the injection front[17], or separate flow of each phase; the oil ahead of the front and the gas behind[18].

There are a number of field projects of gas injection where complete miscibility is not practical but where near miscible conditions are feasible, ie nitrogen flooding projects, due to the very intensive conditions needed to achieve miscibility.

Predicting reservoir performance under this type of gas injection programme, where the fluids are only partially miscible, requires the same factors which influence immiscible displacement to be considered plus the effect of interphase mass transfer between the

injected gas and the reservoir oil which results in a redistribution of composition and liquid and gas saturations.

Miscibility is the ability of two or more substances to mix and form a single homogeneous phase. If two miscible fluids are mixed, they will blend into each other without any interface. Without the interface there will be no capillary forces and the oil droplet shown in Figure 1-2 could be dislodged by the dynamic or viscous forces. All gases are completely miscible with each other, but the solubility of gases in liquids depends on the chemical similarity of the fluids, the pressure and the temperature of the system. Chemical similarity implies that hydrocarbon gases would dissolve more readily in hydrocarbon liquids and other organic solvents, than they would in connate water. Pressure affects solubility in the way that gases dissolve in liquids more readily as the pressure of the system increases. In contrast, increasing temperatures diminish the solubility of gases in liquids.

In applying the process, a slug of injection gas equal to a small fraction of the reservoir's pore volume is injected. The displacing fluid is usually followed either by water and/or natural gas which pushes the slug through the reservoir. The slug can be envisioned as a ring expanding in radius around the injection well as the gas pushes it outward[19]. As the slug moves through the reservoir it displaces both oil and flowable water. The resulting mass transfer alters the physical properties of both the residual oil phase and the gas phase[23]. For an oil bank to form, the nature of these changes must be to mobilise some of the residual oil which is then pushed ahead of the injection gas front to form the oil bank. Successful modelling of the mass transfer occurring in the

transition zone, should determine the amount of oil pushed ahead of the injection gas front to form the oil bank. The water moves ahead of the oil and is produced. The injected gas, after having either partly condensed in the reservoir fluid and/or extracted various hydrocarbon fractions out of it (intermediates and components even heavier than C_{20})[20,21], moves onward through the reservoir. Following it, however, is new "fresh" gas which again contacts reservoir oil so that mass transfer takes place continuously. When full miscibility is achieved, the "two" phases of the injected gas and the oil in place have identical compositions and intensive properties, so that they become one identical miscible, phase, and a sharp interface no longer exists between them. As the oil is pushed away from the injection well, breaks occur in the miscible front exposing new reservoir oil to injected gas. Whenever this occurs, the exchange of components from gas to oil is repeated until miscibility is regained[22].

In moving outward from the injection well, the gas may travel only a few feet before the miscible front forms. The distance varies depending on pressure, oil composition and oil saturation. The oil contacted while the miscible front is forming and from which intermediates have been stripped, is left behind. Injected gas moving over this oil continues to vapourise it until only an asphaltine residue is left. That asphaltine residue cannot be produced and occupies up to about 5% of the pore volume.

The minimum pressure required to bring about the required component exchange between the gas and the oil phase and develop miscibility between the two, depends on the composition of the gas and of the oil and on the reservoir temperature, and is called <u>Minimum</u>

Miscibility Pressure (MMP)[24,25,26,27]. In miscible gas drives, either the injected gas is first contact miscible with the reservoir oil or the miscible drive is being formed in situ. Liquified petroleum gas products, such as ethane, propane, butane, naptha, kerosene or other hydrocarbons normally in the liquid state, are used in the first case.

The cost of such expensive solvents for enhanced oil recovery makes their use economically non-practical. Lean gas or non-hydrocarbon gases, like carbon dioxide or nitrogen, are used in the second case where the miscible front is developed in the reservoir by multiple contacts between the displacing and the displaced phase. One possibility involves the "enriched gas drive", in which the injected gas contains enough light condensible hydrocarbons (eg propane and butane) to form the miscible zone as a result of the reservoir pressure and contacts with the reservoir oil. This is called condensing gas drive. Another possibility is the vapourising gas drive, in which volatile components of the reservoir oil enter the gas phase so that by repeated contacts a miscible zone is formed. A schematic representation of the gas miscible process between the injection and the production well in a reservoir is given in Figure 2-2.

FIGURE 2-2

SCHEMATIC REPRESENTATION OF A GAS MISCIBLE PROCESS IN A RESERVOIR

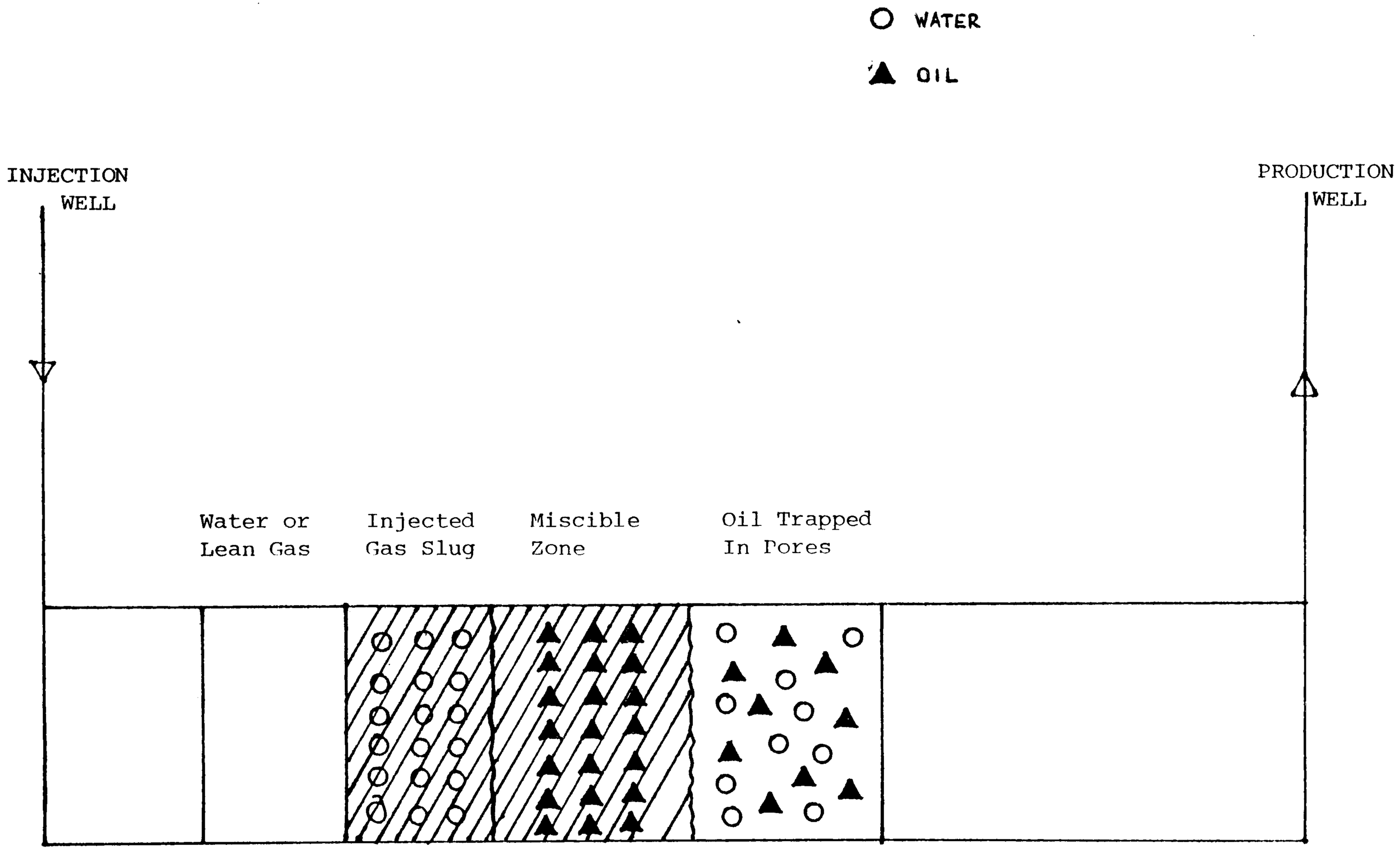

LIST OF REFERENCES

1. Koch, H.A., Jr and Slobod, R.L
.:
Trans. Am. Inst. Mech. Engrs, p. 40, (1957).

2. Hall, H.N. and Geffen, T.M.:
Trans. Am. Inst. Mech. Engrs. p. 48, (1957).

3. Slobod, R.L. and Koch, H.A., Jr:
Amer. Petrol. Inst. Drilling and Production Practice, p. 82, (1953).

4. Whorton, L.P. and Kiesehnick:
Oil and gas journal p. 78, (1950).

5. Whorton, L.P. and Brownscombe, E.R.:
U.S. patent No. 2724437 (November 26, 1955).

6. Kehn, D.M., Pyndus, G.T. and Gaskell, M.H.:
Am. Inst. Mech. Engrs., Fall Meeting, Dallas, Texas, (1957).

7. Herbeck, E.F., Heintz, R.C. and Hastings, J.R.:
Petroleum Engineer, January 1976 p. 35.

8. Holm, L.W. and Josendal, V.A.:
Am. Inst. Mining, Metal and Petrol. Engrs., SPE paper No. 4736, 1974.

9. Kane, A.V.:
Journal of Petroleum Technology (Feb. 1979) p. 217-231.

10. Bernard, G.G., Holm, L.W. and Harvey, C.P.:
Society of Petroleum Engrs. Paper No.8370, 1979.

11. Bernard, G.G., and Holm, L.W.:
Society of Petroleum Engrs.Journal Dec. 1965 pp. 295-300.

12. Bernard, G.G., Holm, L.W. and Jacobs, W.L.:
Society of Petroleum Engrs. Journal (Dec. 1965).

13. Tiffin, D.L. and Yellig, W.F.:
SPE paper No. 10687 presented at the 1982 SPE/DOE EOR Symposium Tulsa, April 1982.

14. Caudle, B.H. and Dyes, A.B.:
Trans. AIME (1958), 213 p. 281.

15. Blackwell, R.J., Terry, W.M., Rayne, W.M., Lindley, D.C. and Henderson, J.R.:
Trans. AIME (1960), 219, 293-300.

16. Hutchinson, C.A. and Braun, P.H.:
Amer. Instit. Chem. Engineering, March 1961, p. 64.

17. Buckley, S.E. and Leverett, M.C.:
Trans. AIME, 1941 pp. 146, 107.

18. Dietz, D.N.:
Konikl Ned. Akad. Wetenschap (1953) Proc. B56, 83.

19. Herbeck, E.F., Heintz, R.C. and Hastings, J.R.:
Petroleum Engineer, Feb. 1976 p.62.

20. Rathmell, J.J., Stalkup, F.I. and Hassinger, R.C.:
SPE paper No. 3483 presented at SPE-AIME 46th Annual Fall Meeting, New Orleans, Oct 3-6, 1971.

21. Kumar, N and Von Gonten, W.D.:
SPE paper No. 4581 presented at SPE-AIME 48th Annual Fall Meeting, Las Vegas, Sept. 30 - Oct. 3, 1973.

22. Herbeck, E.F., Heintz, R.C. and Hastings, J.R.:
Petroleum Engineer, April 1976 p 66.

23. Shearn, R:
Report presented at DOE, EOR Seminar Imperial College London,April 1982.

24. Yellig, W.F. and Metcalfe, R.S.:
Journal of Petroleum Technology Jan. 1980, p. 160-168.

25. National Petroleum Council:
Enhanced Oil Recovery - An Analysis of the Potential for EOR from Known Fields in the United States - 1976 to 2000, (Dec. 1976), Washington, D.C..

26. Sigmund, P.M., Aziz, K., Lee, J.I., Nghiem, L.X. and Mehra, R.:
World Petroleum Congress, Bucharest, Romania, Sept. 1979, PD10 (5).

27. Holm, L.W. and Josendal, V.A.:
Journal of Petroleum Technology, May 1980 p. 870.

CHAPTER 3

SPECIAL CHARACTERISTICS OF CO_2 FLOODING

One of todays more promising enhanced oil recovery techniques is miscible CO_2 flooding. Use of carbon dioxide to increase oil recovery is not a new idea. Carbon dioxide has been investigated for miscible displacement, for immiscible displacement of reservoir oil and for producing well stimulation. Current industry interest in CO_2 miscible flooding is high, as evidenced by the level of activity in field testing and CO_2 source development[1,2,3,4,5].

Apart from the miscible displacement of oil by the CO_2, the other minor mechanisms of achieving enhanced oil recovery by injection of CO_2 are:

1. Oil swelling: The high solubility of CO_2 in hydrocarbons, causes swelling of the reservoir oil because the CO_2-oil mixture has a higher specific volume than the original oil and therefore some fluid must migrate due to expansion. More CO_2 could be dissolved in oil at higher pressures; the higher the GOR the higher will be the swelling factor. The solubility of CO_2 in oil decreases at higher temperatures and the swelling factor shows a corresponding drop which is characteristic of the solubility of gases in liquids. Oil swelling results in an increase in production and a decrease in residual oil saturation due to an increase in the relative permeability. Figure 3-1 shows the relative oil volume versus pressure for a 40^{o} API crude oil and CO_2 or natural gas at $190^{o}F$[18].

2. Reduction of oil viscosity: The internal friction between the molecules of the flowing fluid is the essential feature of viscosity and the dissolution of CO_2 into the oil phase reduces

that friction. Consequently a large reduction in the viscosity of crude oils occurs as they become saturated with CO_2 at increasing pressures which makes it easier for the contacted oil to flow into the porous media. A larger reduction occurs in the viscosity of the more viscous crudes (Figure 3-2)[6,7,8].

3. Increase in oil density: The CO_2-oil mixture has a higher density than the reservoir oil. The density of liquid carbon dioxide at 2000 psi and 70°F is about 0.9 g/cc which, when mixed with oil of lower density than itself, causes an increase in the density of the system.

4. High solubility in water: CO_2 also has an effect on the water or brine that is present in the reservoir when displacement processes are in operation. There is some expansion of water when CO_2 goes into solution and the water density decreases. Consequently when CO_2 is injected, the densities of the oil and water become closer to each other which lessens the chances for gravity segregation of these fluids and the resultant overriding of the CO_2-water mixture.

5. Acidic effect on rock: The acidic effect of CO_2 on the rock has been shown to increase the injectivity of water by direct action on carbonate portions of the rock and by stabilising action on clays in the rock[9,10,11].

6. Lower interfacial tension of crude oils: Simon et al[12] have studied the change in interfacial tension versus pressure and CO_2 concentration for a reservoir oil. Figure 3-3 gives the calculated and experimentally measured interfacial tensions where

it becomes evident that they approach zero as composition and pressure approach critical conditions.

7. Forms a non-wetting phase like the natural gas in the reservoir rock.

So far, carbon dioxide has been used to recover additional oil in many situations. It was used in sandstone, limestone, dolomite and chert reservoirs, to depths greater than 10,000 ft, in formations with very low permeabilities, at bottom hole temperatures up to 250°F with crudes varying in gravities from 15-50° API. More than 36 field trials of CO_2 injection processes have been undertaken to date[13].

Four large field applications of CO_2 flooding are currently in progress. The largest project is a secondary recovery flood in the SACROC Unit in Texas[14]. More than 30,000 acres of the 2-bbl oil field are being flooded with CO_2. Oil recovery from this miscible CO_2 flooding project is approaching 90 million bbl, about 7% OOIP. Incremental oil recovery for CO_2 miscible projects has ranged from a low of about 3.5% OOIP to a high of about 18% OOIP. Figure 3-4 shows that the enhanced recovery began after injection of about 0.1 to 0.2 HCPV (hydrocarbon pore volume)[13]. After a period of almost linear increase in incremental recovery with cumulative injection, the recovery curves bend over and gradually approach the ultimate recovery value.

Lower than anticipated CO_2 injectivity has been observed in a number of field trials[15,2]. Operating problems have been reported to be more severe than in waterflooding with corrosion, leaks and

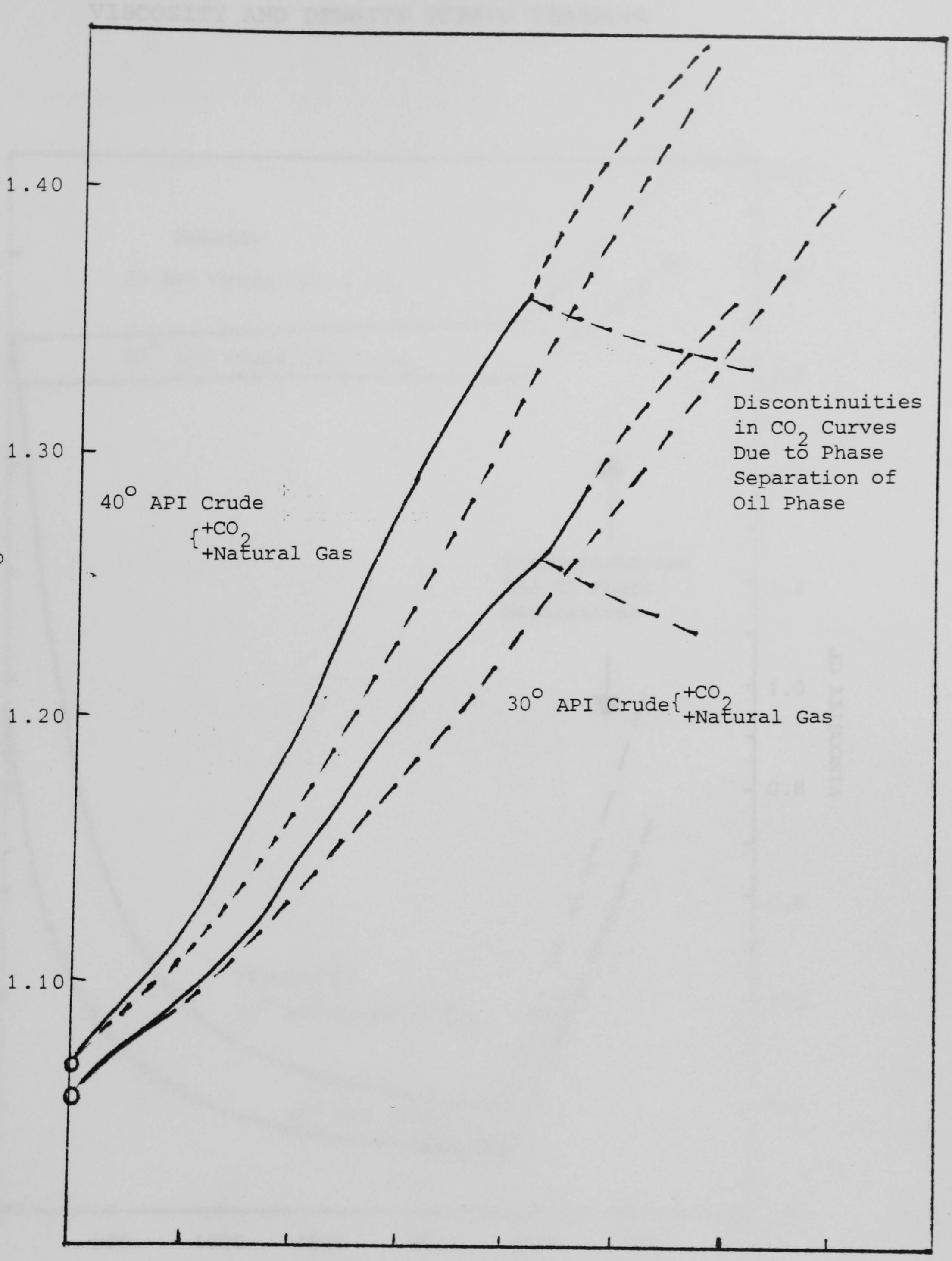

FIGURE 3-1

RELATIVE OIL VOLUME VERSUS PRESSURE[18]

FIGURE 3-2

VISCOSITY AND DENSITY VERSUS PRESSURE[7]

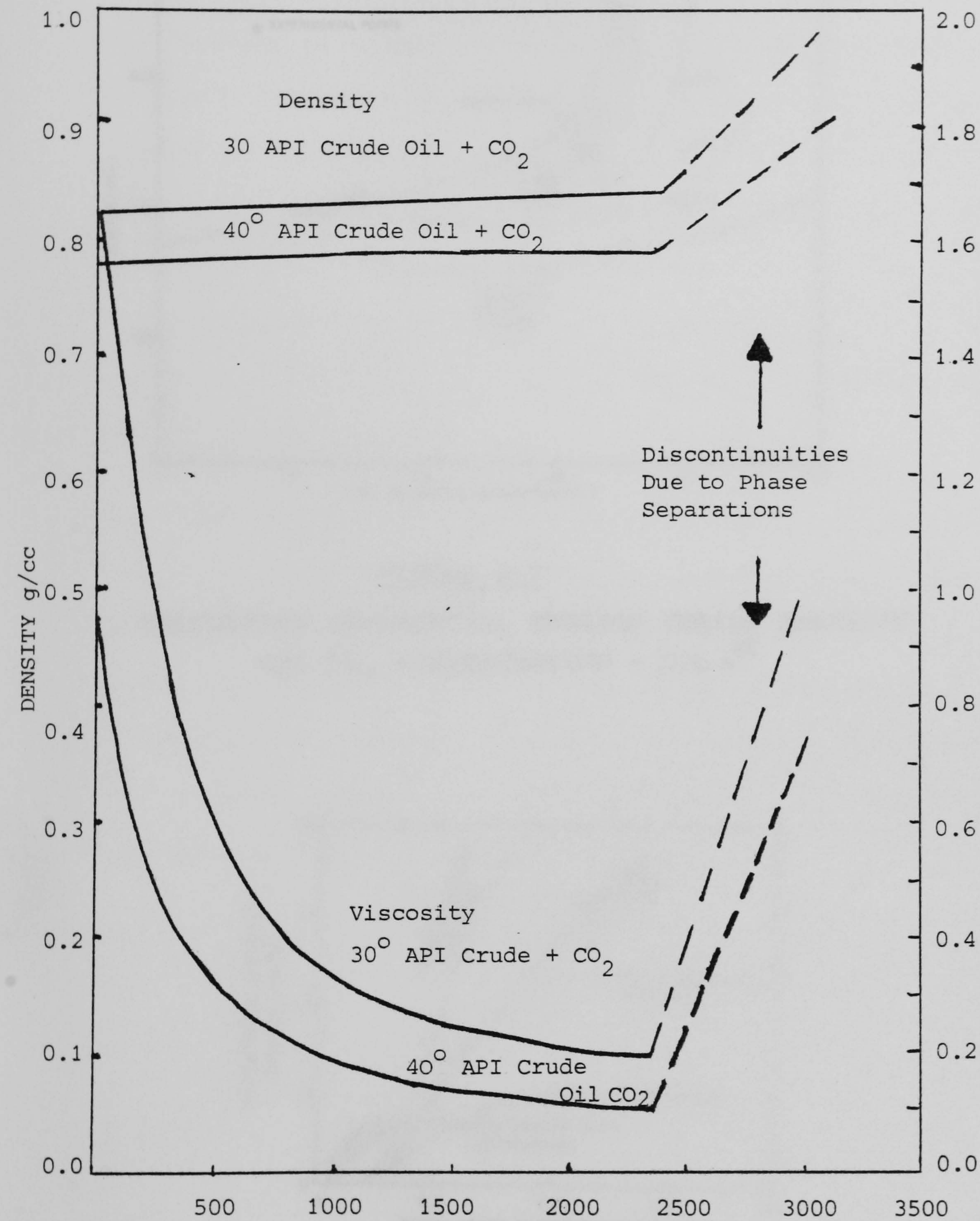

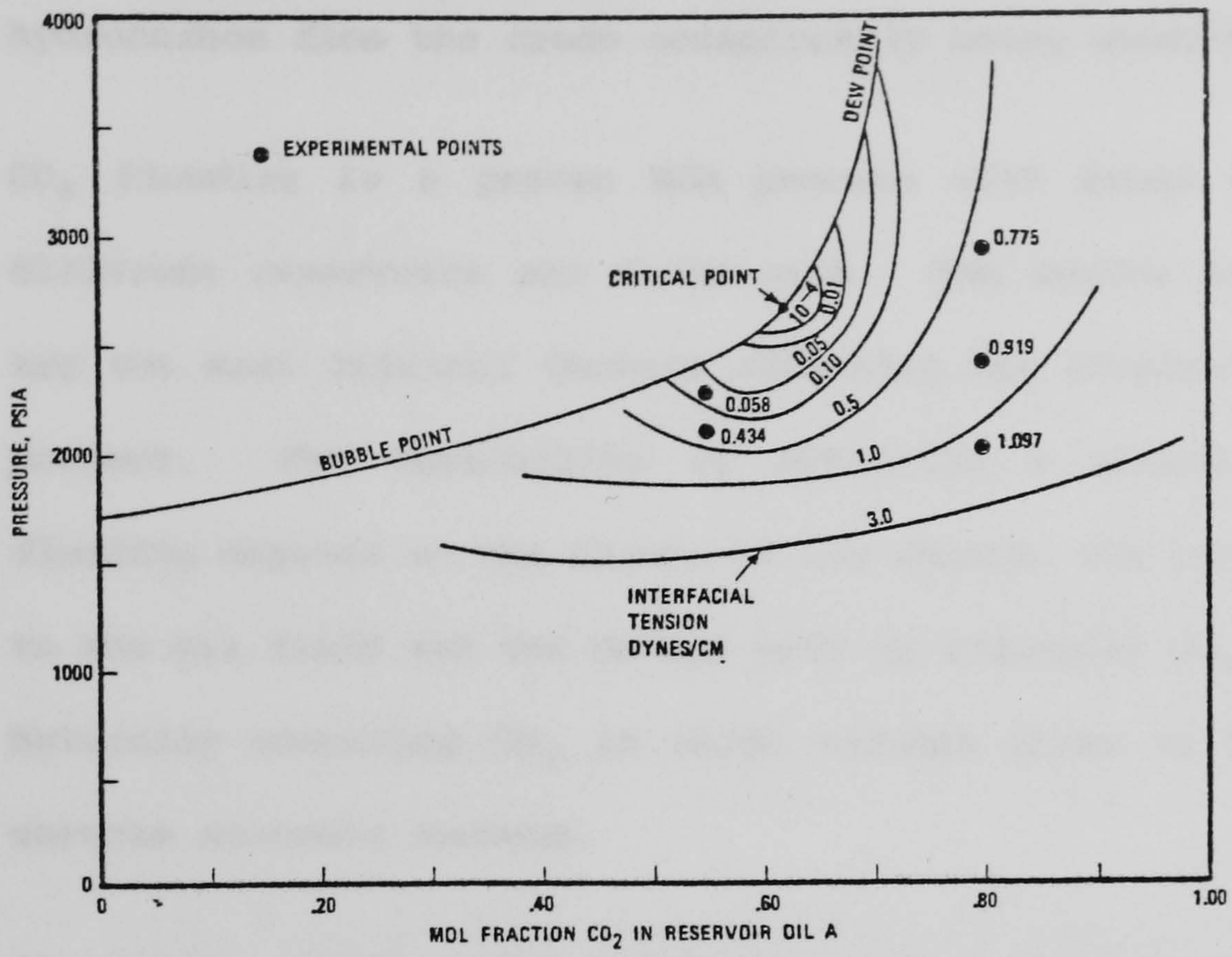

FIGURE 3-3

CALCULATED INTERFACIAL TENSION VERSUS PRESSURE AND CO_2 CONCENTRATION - OIL A[12]

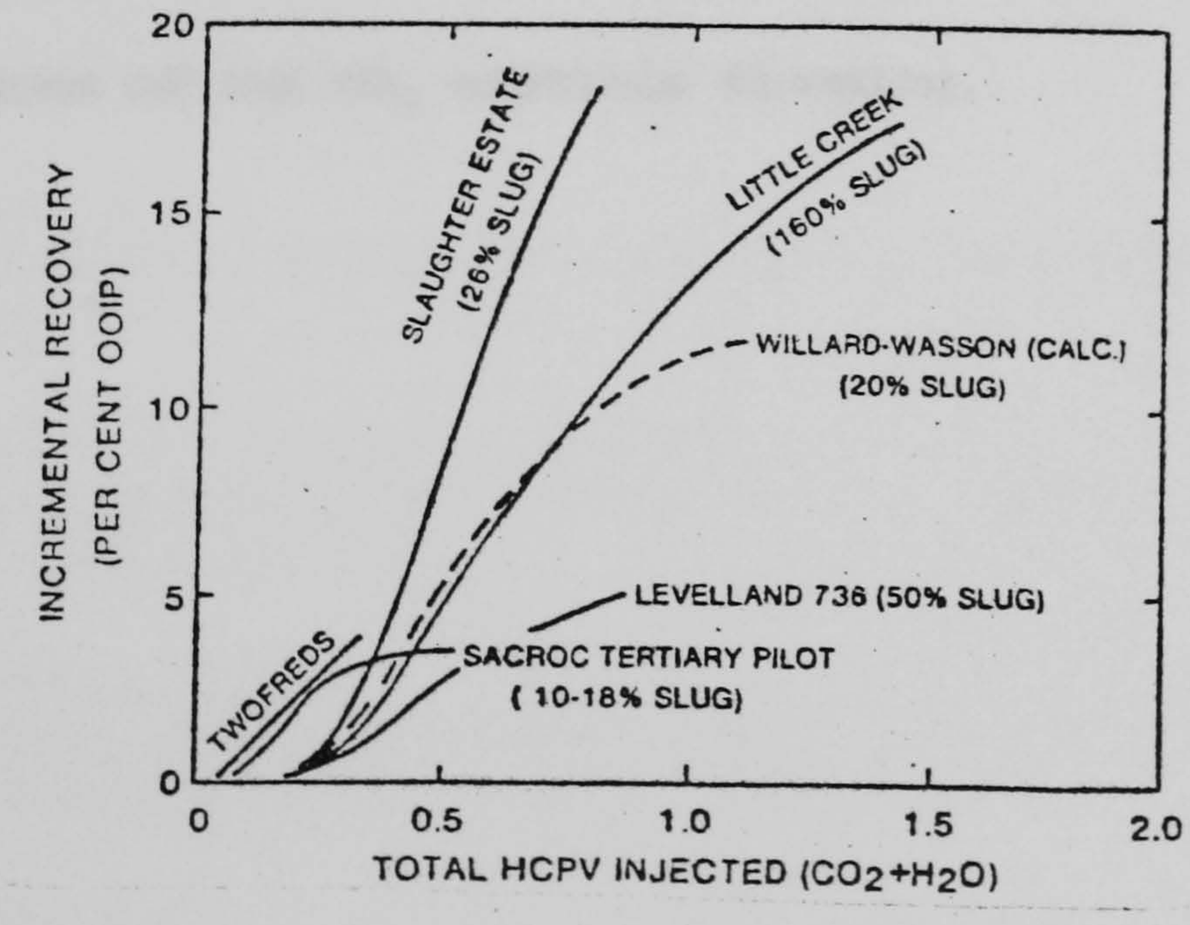

FIGURE 3-4

RELATIVE OIL VOLUME OF A WEST TEXAS RESERVOIR FLUID VERSUS PRESSURE AT 144°F

scaling being mentioned in addition to precipitation of a heavy hydrocarbon from the crude occasionally being observed[14,2,16].

CO_2 flooding is a proven EOR process with broad application to different reservoirs and crude oils. The source and cost of CO_2 are the most critical factors affecting the economic success of a project. The feasibility of obtaining a source for oilfield flooding depends on the nature of the source, its location relative to the oil field and the method used to transport CO_2 to the field. Naturally occurring CO_2 in large volumes close to the oil fields ensures economic success.

At todays prices, the production of a barrel of oil by CO_2 injection, costs $26 - $39. Transportation of CO_2 to the oil fields can be economical even when the CO_2 sources are up to 500 miles from the oil field[17]. The future of CO_2 enhanced oil recovery projects depends largely on the price of the barrel of oil. Higher prices for crudes would boost the research and applications of the CO_2 miscible flooding.

LIST OF REFERENCES

1. Dicharry, R.M. et al:
Evaluation and Design of CO_2 Miscible Flood Project, SACROC Unit-Kelly-Snyder Field, Journal of Petroleum Technology, Nov. 1973 p. 1309.

2. Pontious, S.B. and Tham, M.J.:
Journal of Petroleum Technology, Dec. 1978 p. 1706.

3. Thrash, J.C.:
SPE paper No. 8382 presented at the 54th Annual Technical Conference and Exhibition, Las Vegas, Sept. 1979.

4. Hansen, P.W.:
SPE paper No. 6747 presented at the SPE 52nd Annual Technical Conference and Exhibition, Denver, Oct. 1977.

5. Reid, T.B. and Robinson, H.J.:
Journal of Petroleum Technology Sept. 1981 p. 1723.

6. Holm, L.W.:
CO_2 Slug and Carbonated Water Oil Recovery Process, Prod. Monthly Sept. 1963, 6.

7. Simon, R. and Graue, D.J.:
Journal of Petroleum Technology Jan. 1965 pp. 102-106.

8. Beeson, S.M. and Ortloff, G.D.:
Trans. AIME (1959) 216, pp. 388-391.

9. Crawford, H.R. et al:
Journal of Petroleum Technology, March 1963,237.

10. CO_2 - A New Shot in the Arm for Acid Frac. Jobs,
Oil and Gas Journal, Oct. 1962 pp. 92-97.

11. Ross, G.H.:
Phd Thesis, Heriot-Watt University Petroleum Engineering, 1982.

12. Simon, R., Rosman, A and Zana, E.:
Phase Behaviour Properties of CO_2 - Rservoir Oil Systems, SPE paper No. 6387.

13. Stalkup, F.I.:
Status of Miscible Displacement, Journal of Petroleum Technology, April 1983 p. 815.

14. Kane, A.V.:
Journal of Petroleum Technology, Feb. 1979 pp. 217-231.

15. Rowe, H.G., York, S.D. and Ader, J.C.:
Journal of Petroleum Technology March 1982, pp. 613-620.

16. Crockett, D.H.:
Proc., 22nd Annual Southwestern Petroleum Short Course,
Texas Tech. U., Lubbock (1975) 159–164.

17. Kuuskraa, V.A.:
Report presented at 2nd European Conference on EOR,
Paris 1982.

18. Holm, L.W. and Josendal, V.A.:
SPE paper No. 4736 presented at the Improved Oil Recovery
Symposium of AIME, Tulsa April 1974.

CHAPTER 4

MECHANISMS AND REPRESENTATION OF THE GAS MISCIBLE FLOODING PROCESS

4.1 INTRODUCTION

4.2 TERNARY REPRESENTATION OF PHASE EQUILIBRIUM

4.3 QUATERNARY REPRESENTATION FOR HYDROCARBON

- INJECTION GAS MIXTURES

4.1 INTRODUCTION

To study the mechanisms under which miscibility can be achieved when a gas is injected into a reservoir, one has to investigate the mass transfer of the different components between the various phases present in the reservoir during the process. The phase equilibria problem is not a simple one, because quite often more than two phases co-exist and the components present can migrate from one phase to another. For mixtures of reservoir oils and carbon dioxide, four phases have been observed[2,3,4,5,6] such as hydrocarbon-rich liquid, CO_2-rich liquid, vapour and asphaltenes. Experimental results suggest that liquid-liquid and liquid-liquid-vapour equilibria occur for CO_2-crude oil mixtures at temperatures below about 50°C (120°F) and that development of miscibility occurs by extraction of hydrocarbons from the oil into a CO_2 rich liquid phase in such systems. Figure 4-1 demonstrates the complexity of the phase behaviour of a crude oil and CO_2 mixture at different pressures and temperatures[1].

On the other hand, asphalt or asphaltenes precipitation induced by compositional changes in a miscible drive or by pressure variation, may have a pronounced effect on the flow of reservoir fluids, and therefore they have to be taken into consideration. The study of the solid phase precipitation is beyond the scope of this work. North Sea reservoirs, as they are deep reservoirs, have a temperature much higher than the 50°C limit for the appearance of the second liquid phase for CO_2 injection (North Sea reservoir average temperature 200°F) and given that the objective of this project is to study the application of the EOR methods to the North

Sea oil fields, only the two phase (vapour-liquid) equilibria will be investigated.

The experimental results on the multiple contact miscible flooding of injection gases and reservoir oils indicate that there are two main mechanisms which can be identified as being responsible for the achievement of miscibility. These are the vapourisation of light and intermediate components to the gas phase, and the condensation of the injected gas to the oil phase[4,7]. Hydrocarbons which are mainly intermediates are extracted from the oil phase by the advancing gas. High pressures and temperatures are favourable conditions for this mechanism. Through successive contacts, the vapour phase becomes richer and richer in hydrocarbons until the critical composition has been achieved, no interfacial tension exists between the two phases and a one phase miscible fluid results.

4.2 TERNARY REPRESENTATION OF PHASE EQUILIBRIUM

The development of miscibility by gas A and a reservoir oil, in a displacement controlled by a vapourisation mechanism, can be visualised conceptually using a ternary diagram representation where the gas A and two pseudo-components' mole fractions, which characterise the oil, are the three apexes of the triangle at a given pressure and temperature (Figure 4-2). The L and H usually are a light and a heavy fraction. Point B represents the reservoir fluid composition and the line AB which connects point B with the injected gas composition, is called the dilution line[12] and is the locus where the overall compositions of all the mixtures of injection gas and oil lie. For the BC part of the dilution line,

the gas A concentration in the mixture is not enough to saturate the reservoir oil. When the percentage of gas A exceeds a certain value the dilution line intersects the phase envelope at C, which determines the saturation (bubble point) composition for the given pressure and temperature. At C, the first gas bubble is formed and as the mixture is being enriched with gas A, the vapour phase becomes dominant as the mixture moves towards the 100% gas A composition.

For any overall composition D, there is a single line which intersects the phase envelope at G and E, where G, the intersection with the dew point curve (100% vapour), gives the vapour composition in equilibrium with a liquid composition E, the intersection with the bubble point curve (100% liquid). These equilibrium lines are called tie-lines. The curve AGKCF is the phase envelope for the mixture and it encloses in it the region where the liquid and vapour co-exist. The AGK curve represents the saturated vapour while the KCEF, the saturated liquid. The critical point K is the transition from 100% liquid to 100% vapour and determines the composition of a critical fluid which can be classified as neither liquid nor vapour.

The fact that a ternary representation provides only two degrees of freedom (two independent compositions) and the third component's mole fraction can be determined by the restrictive equation on the mole fractions $z_i + z_j + z_m = 1$, makes the representation of the phase equilibria inadequate. Different phase envelopes can be obtained for a multicomponent system for different selections of j and m and, therefore, the use of ternary diagrams should be made with caution.

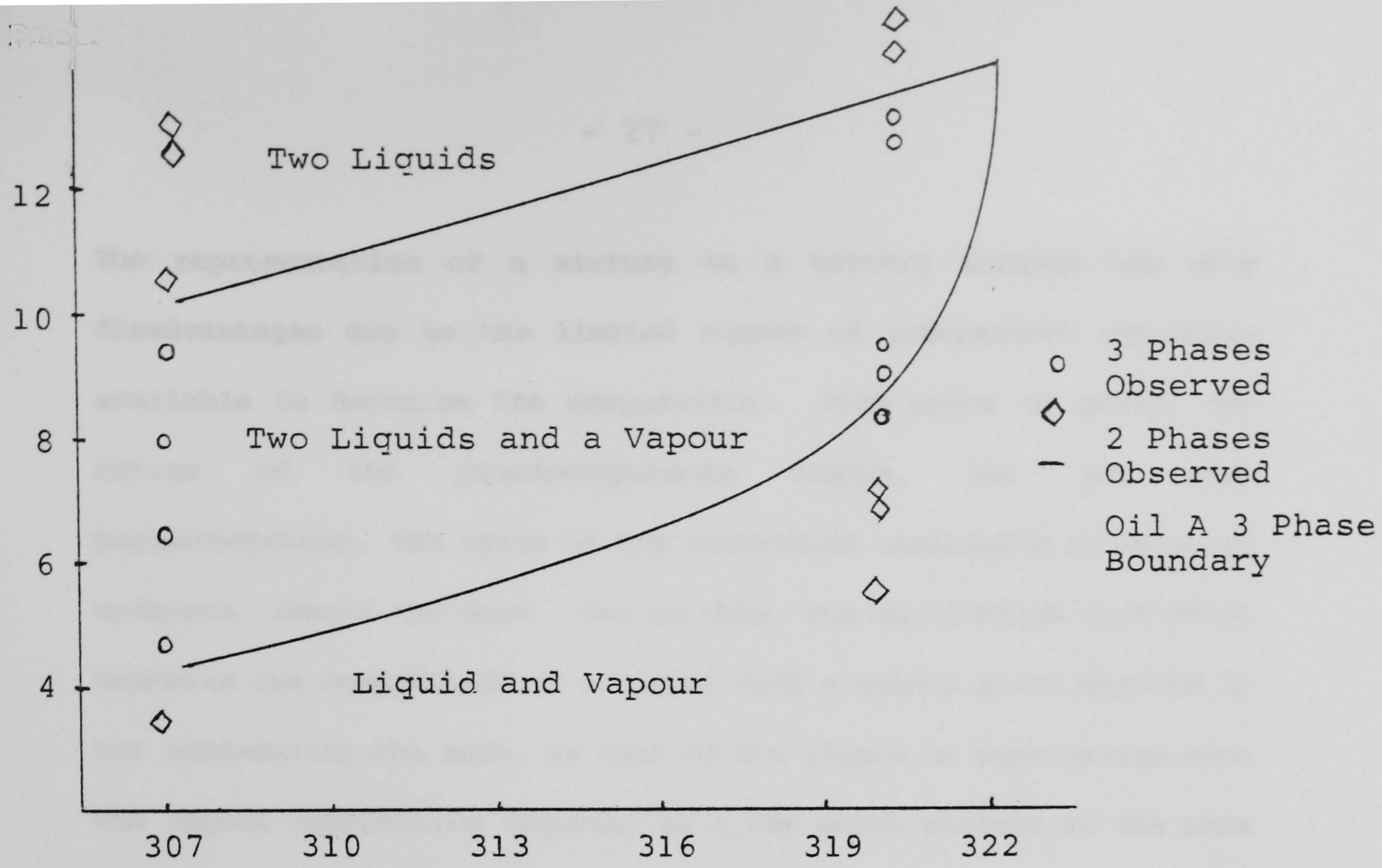

FIGURE 4-1

MULTIPLE PHASE REGION FOR CO_2 - OIL COIL MICROCORE DISPLACEMENTS[1]

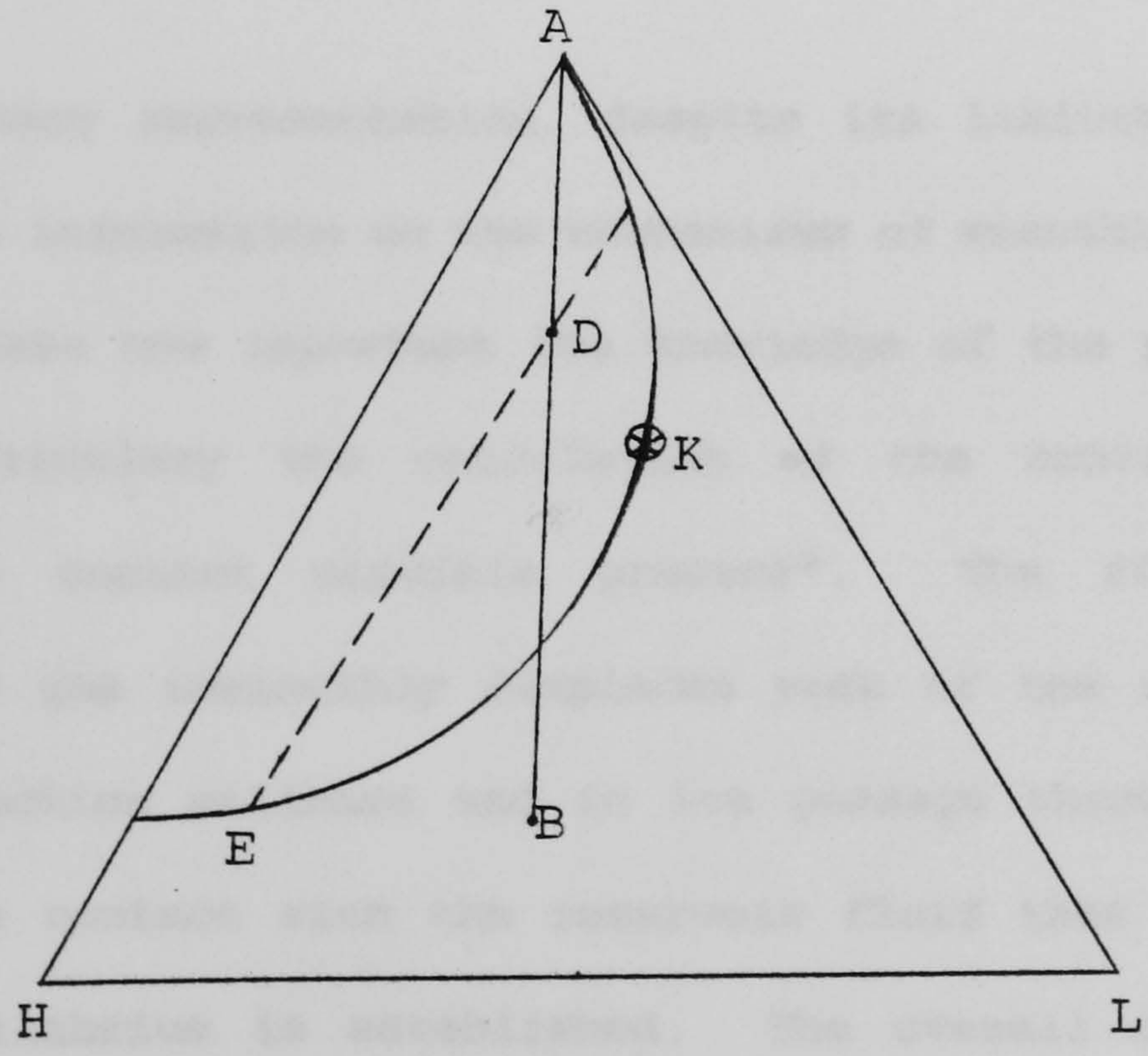

FIGURE 4-2

TERNARY REPRESENTATION OF PHASE BEHAVIOUR

The representation of a mixture on a ternary diagram has many disadvantages due to the limited number of independent variables available to describe the composition. From point to point, the ratios of the pseudocomponents change, but for each pseudocomponent, the ratio of the individual components of which it consists, remain the same. Due to this, the equilibrium line which connects the composition of a vapour with a bubble point mixture is not necessarily the same, as that of the liquid in equilibrium with the vapour composition regarded as a dew point mixture at the same pressure and temperature. In other words, if the KCEF curve has been determined as the locus of liquid compositions in equilibrium with the dew point mixtures of the AGK curve, then the locus of the vapour compositions in equilibrium with the bubble point mixtures of the KCEF curve, does not necessarily coincide with the AGK curve.

The ternary representation, despite its limitations, can provide valuable information on the mechanisms of miscible displacement and demonstrate how important the knowledge of the phase behaviour is and particulary the calculation of the critical point for a multiple contact miscible process[6]. The first increment of injected gas immiscibly displaces some of the reservoir oil near the injection wellbore and in its passage through the reservoir, comes in contact with the reservoir fluid that was not displaced and equilibrium is established. The overall composition of the mixture and the compositions of the vapour and liquid phases lie on the line AR (Figure 4-30)[7]. With the conditions of pressure and temperature of the reservoir, the resulting mixture M_1 consists of an equilibrium gas G_1 and an equilibrium liquid L_1, defined by the

intersections of the tie-line which passes through M_1, and the dew and bubble point-curves.

Following the advancing front of the injected gas , we find that the gas G_1 has been displaced further into the reservoir by the second increment of injected CO_2, where it contacts fresh reservoir fluid yielding the new overall composition M_2. The new overall composition consists of gas G_2 and liquid L_2 in equilibrium. The gas G_2 flows ahead and contacts more reservoir fluid. The same process is repeated over again in the reservoir rock until the advancing gas, by a continuous enrichment process, obtains the critical composition. The distinct phases exist no more and there is only one phase present there; the critical phase. The tie-line at the critical point becomes in fact the tangent of the phase envelope at that point, as it has only one point of intersection with it.

Obviously, if a tie-line or its extension passes through the reservoir oil composition R (Figure 4-3), then further enrichment of the gas G is not possible, because the tie-line imposes the conditions of equilibrium for any mixtures lying on it. Consequently, for miscibility to be achieved, the reservoir oil composition should lie either on the right of the tangent to the phase boundary at the critical point (critical tie-line), or above it. Figure 4-4 shows the areas where miscibility is or is not achievable. When the dilution line for a reservoir fluid composition does not intersect the phase envelope, then the injection gas is first contact miscible with the oil.

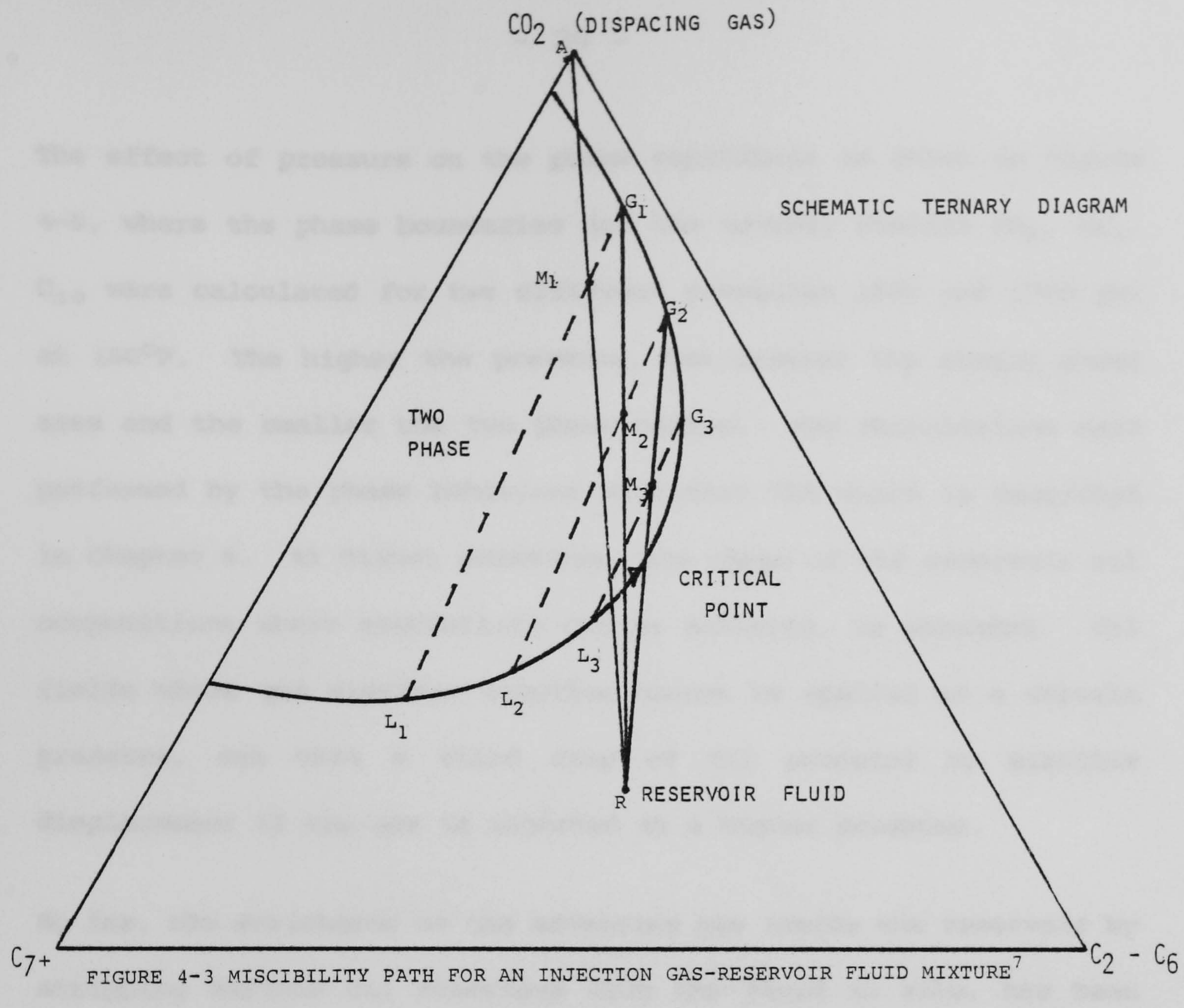

FIGURE 4-3 MISCIBILITY PATH FOR AN INJECTION GAS-RESERVOIR FLUID MIXTURE[7]

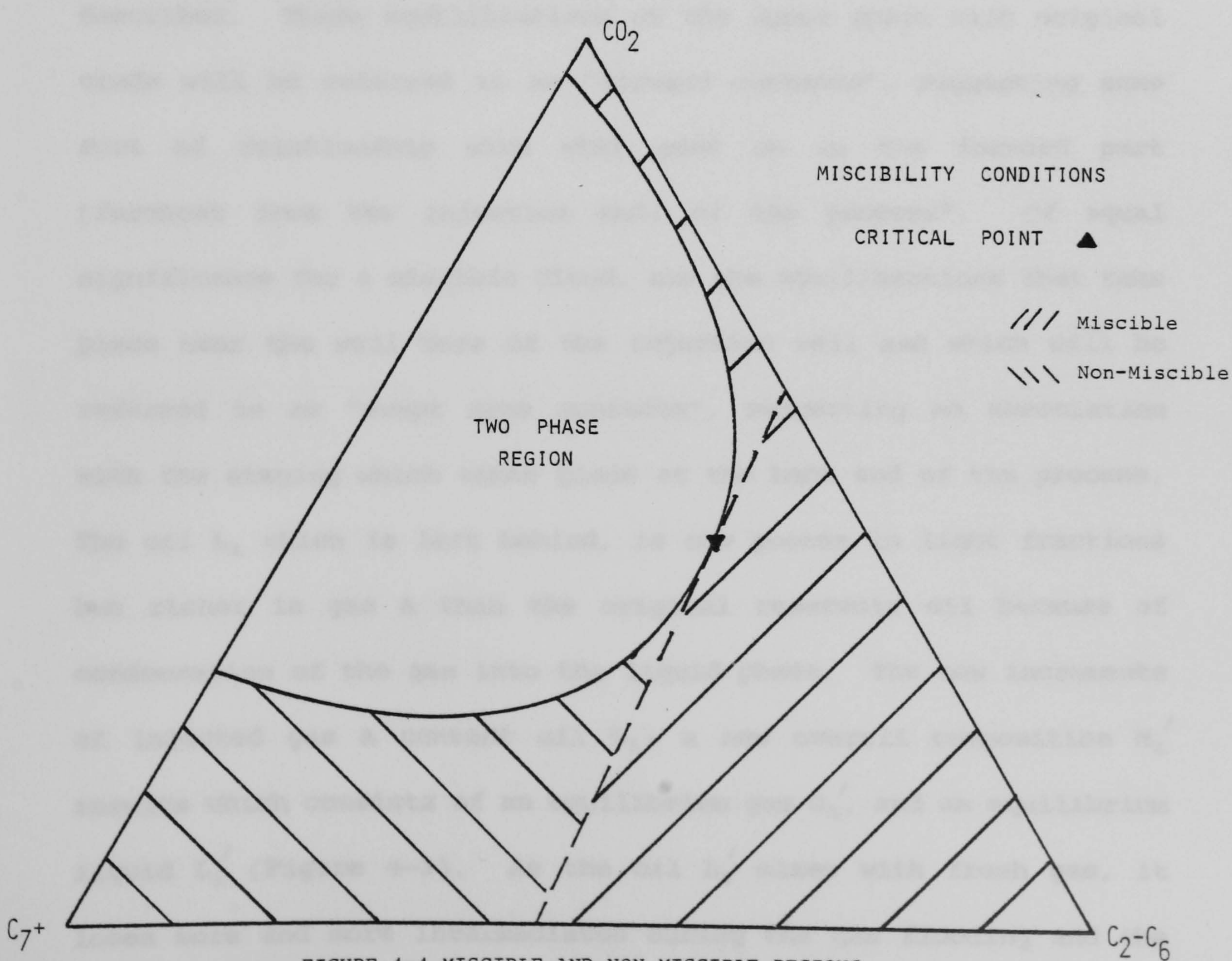

FIGURE 4-4 MISCIBLE AND NON MISCIBLE REGIONS

The effect of pressure on the phase equilibria is shown in Figure 4-5, where the phase boundaries for the ternary mixture CO_2, nC_5, C_{10} were calculated for two different pressures 1500 and 1700 psi at 160°F. The higher the pressure, the greater the single phase area and the smaller the two phase region. The calculations were performed by the phase behaviour simulator VLE which is described in Chapter 6. At higher pressures, the range of the reservoir oil compositions where miscibility can be achieved, is extended. Oil fields where gas miscible flooding cannot be applied at a certain pressure, can have a third crop of oil produced by miscible displacement if the gas is injected at a higher pressure.

So far, the enrichment of the advancing gas inside the reservoir by stripping various oil fractions from the fluid in situ, has been described. These equilibrations of the upper phase with original crude will be referred to as "forward contacts", suggesting some sort of relationship with what goes on in the forward part (farthest from the injection end) of the process[9]. Of equal significance for a miscible flood, are the equilibrations that take place near the well bore of the injection well and which will be referred to as "swept zone contacts", suggesting an association with the staging which takes place at the back end of the process. The oil L_1 which is left behind, is now poorer in light fractions but richer in gas A than the original reservoir oil because of condensation of the gas into the liquid phase. The new increments of injected gas A contact oil L_1; a new overall composition M_1' results which consists of an equilibrium gas G_1', and an equilibrium liquid L_1' (Figure 4-3). As the oil L_1' mixes with fresh gas, it loses more and more intermediates during the gas flooding and the

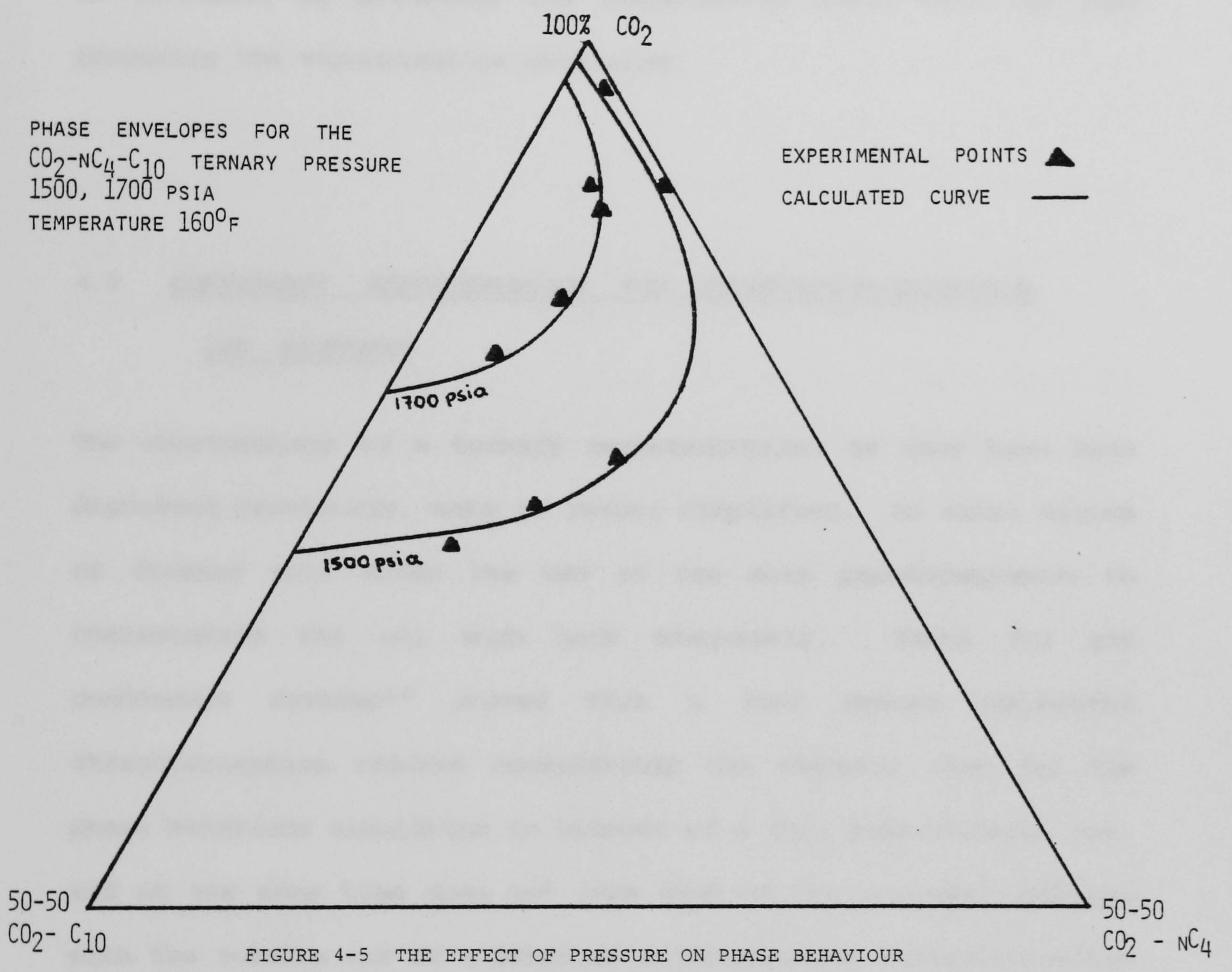

FIGURE 4-5 THE EFFECT OF PRESSURE ON PHASE BEHAVIOUR

result is that residuum is deposited all along the displacement path with heavier precipitates near the injection well. The amount of residuum deposited will depend on oil composition as well as flood pressure. High asphaltene content should result in large residuum deposition. The condensation of gas into the liquid phase is favoured, by pressures and temperatures lower than the ones favouring the vapourisation mechanism.

4.3 QUATERNARY REPRESENTATION FOR HYDROCARBON-INJECTION GAS MIXTURES

The shortcomings of a ternary representation, as they have been discussed previously, make it rather simplified. An extra degree of freedom will allow the use of one more pseudocomponent to characterise the oil much more adequately. Tests for gas condensate systems[10] proved that a four pseudo components characterisation reduces considerably the computer time for the phase behaviour simulation in respect of a full compositional one, and at the same time does not lose much of the accuracy compared with the results out of a detailed multicomponent characterisation run.

A quaternary phase diagram can be defined by a pyramid where the basal triangle has all its sides equal to each other and equal to the height of the pyramid; (CD) = (CB) = (DB) = (OA) = 1.0 (Figure 4-6). The apexes A,B,C,D represent the mole fractions of four pure components or groups of components. The C component mole fraction is determined on the BC line (0 - 1.0), the D component on the CD

line and the B component on the DB line. The A component mole fraction takes values on the OA line with 0.0 on O and 1.0 on A. For 0.0 mole fraction A the phase behaviour is represented by the ternary CDB, with lengths (DC) = (DB) = (BC) = 1.0 and mole fractions from 0.0 to 1.0.

It has to be proved that any point in the pyramid can represent a four-component mixture adequately, which means that the sum of the mole fractions of the four components equals to unity everywhere in the quaternary diagram. Consider a mixture having (OT) gas A mole fraction (Figure 4-7). The cross section KHG of the pyramid by a plane vertical to OA at T, gives the locus of all saturated mixtures of the three components B,C,D with (OT) mole fraction gas A. The lengths (KG) = (GH) = (KH) of the ternary should be equal to 1.0 - (OT), in other words the components B,C,D mole fractions can take values from 0 to 1 - (OT). Basic geometrical relations give

$$\frac{(CM)}{(CL)} = \frac{(CK)}{(CA)} \qquad \text{Eq 4-1}$$

$$\frac{(CK)}{(CA)} = \frac{(OT)}{(OA)} = (OT) \qquad \text{Eq 4-2}$$

$$(CL) = \cos 30^{o} * (OC) = \sqrt{3}/2 \cdot 2/3 \cdot \sqrt{3}/2 = 1/2 \qquad \text{Eq 4-3}$$

From Eq 4-1, 4-2, 4-3:

$$(CM) = (OT)/2,\ (NB) = (OT)/2,\ (KG) = (GH) = (KH) = 1 - (OT)$$

The two phase region in this case is represented by the solid AOPK (Figure 4-8), the phase boundaries by the surface surrounding it and the critical locus is a line in the 3-dimensional space lying

on the saturation surface. In Figure 4-8, the bubble and dew saturation surfaces are shown as well as the vapour and liquid single phase regions. The intersection of the phase envelope with the base of the pyramid gives the ternary phase envelope of mixtures of reservoir oil at that pressure and temperature. Also, the intersection, if any, of the two phase solid with the other three faces of the pyramid give the ternaries for the corresponding three components' mixtures. Obviously, when the ternary phase envelope on one face intersects an edge of the pyramid, the ternary diagram on the adjacent face should intersect the common edge at the same points. The tie-lines lie on the 3-D space and connect equilibrium points on the phase surface. Criteria for miscibility similar to the ones for the ternary representation are difficult to define because the selection of a critical tie-line on a quaternary plot is arbitrary since an infinite number is possible[11].

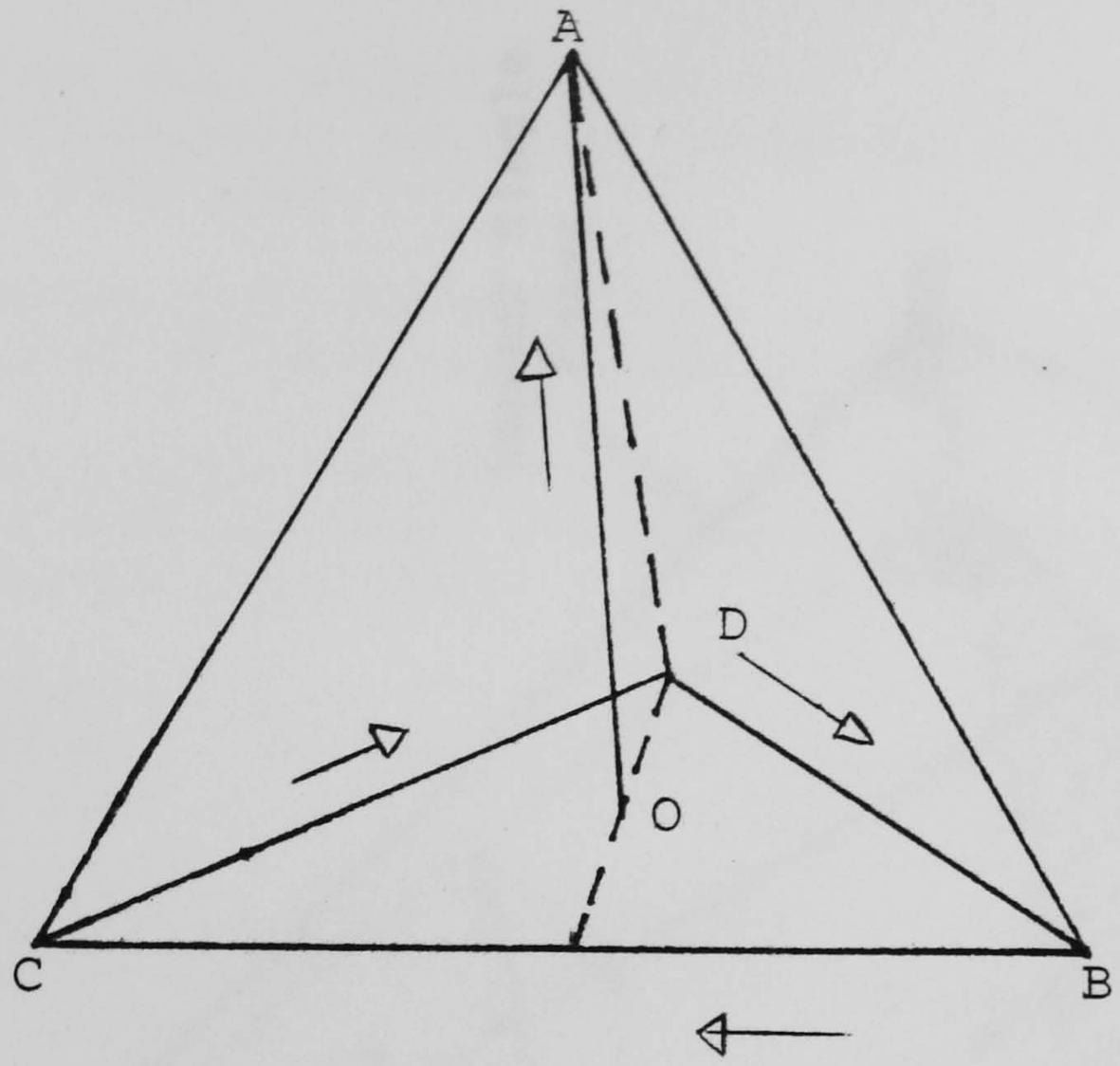

FIGURE 4-6

QUATERNARY REPRESENTATION

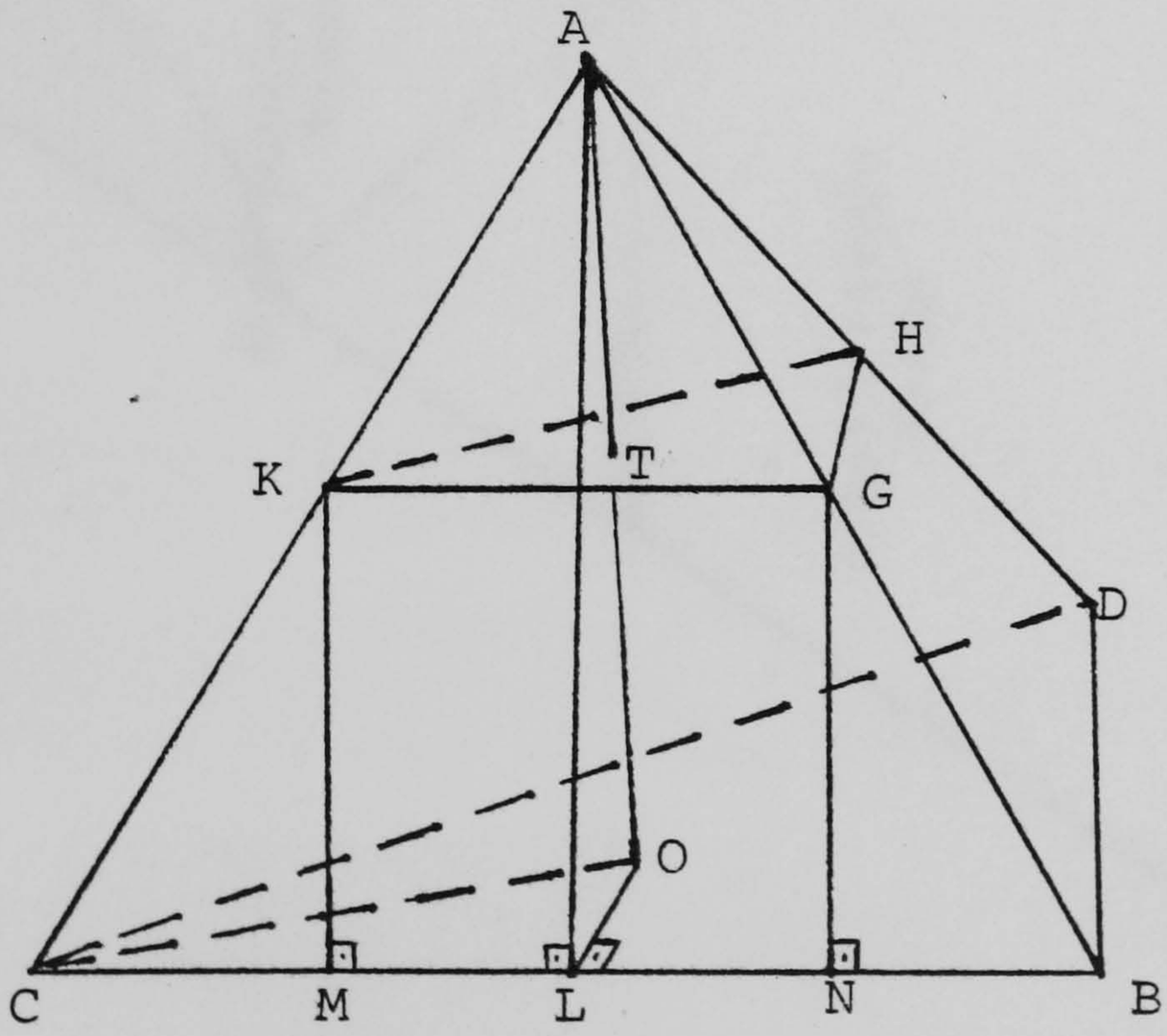

FIGURE 4-7

QUATERNARY PHASE DIAGRAM

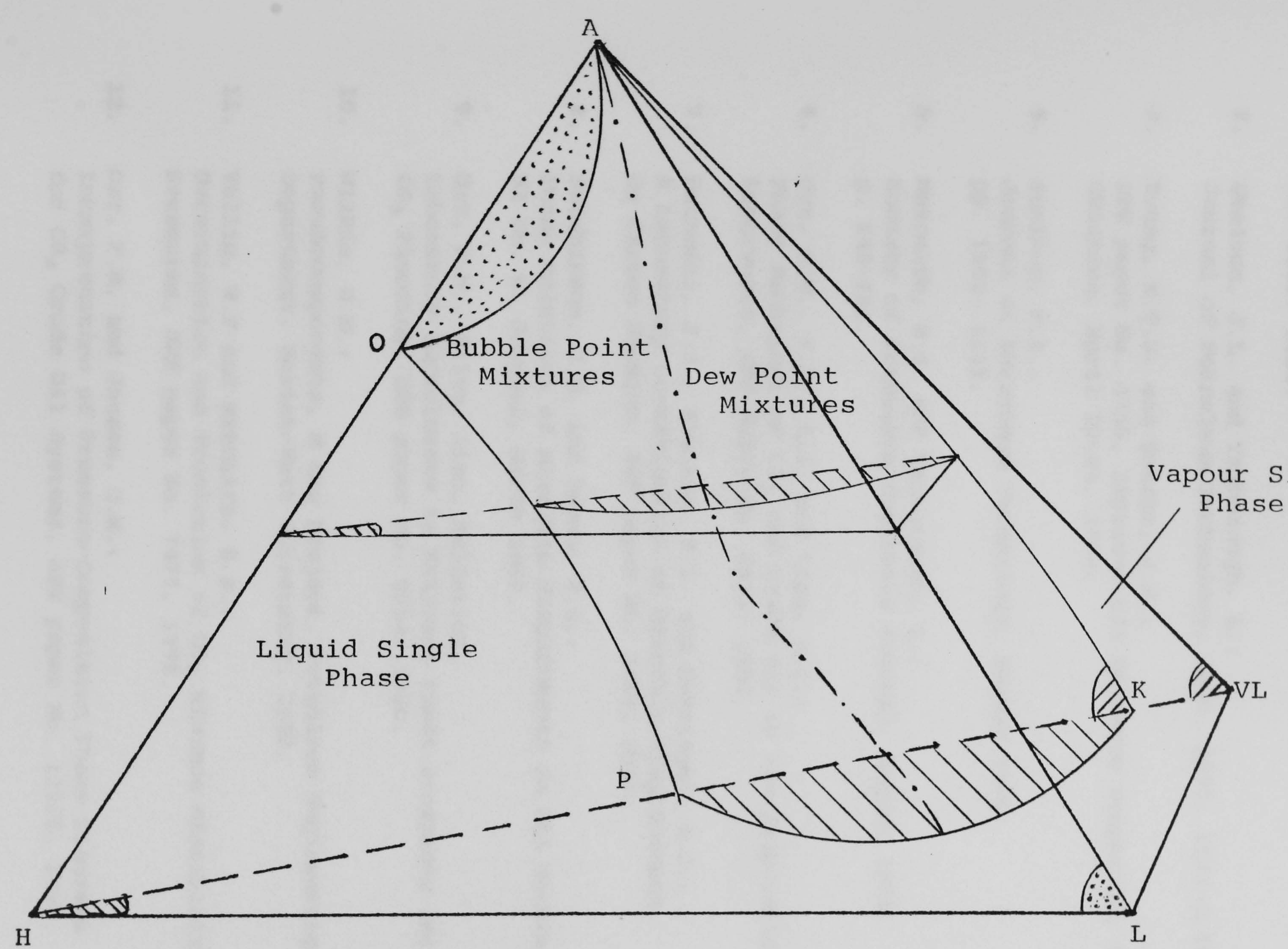

FIGURE 4-8

QUATERNARY REPRESENTATION OF THE PHASE BEHAVIOUR OF A MIXTURE

LIST OF REFERENCES

1. Henry, R.L. and Metcalfe, R.S.:
Multiple phase Generation During CO_2 Flooding, SPE paper No. 8812, 1980.

2. Shelton, J.L. and Yarborough, L.:
Journal of Petroleum Technology, Sept. 1977, 1171-1178.

3. Huang, E.T.S. and Tracht, J.H.:
SPE paper No. 4735, Improved Oil Recovery Symposium, Tulsa, Oklahoma, April 22-24, 1974.

4. Stalkup, F.I.:
Journal of Petroleum Technology, August 1978, pp. 1102- 1112.

5. Metcalfe, R.S. and Yarborough, L.:
Society of Petroleum Engineers Journal, August 1979, p. 242-252.

6. Orr, F.M., Y.U., A.D. and Lien, C.L.:
Phase Behaviour of CO_2 and Crude Oil in Low Temperature Reservoirs, SPE paper No. 8813, 1980.

7. Rathmell, J.J., Stalkup, F.I. and Hessinger, R.C.:
A Laboratory Investigation of Miscible Displacement by Carbon Dioxide, SPE paper No. 3483, 1971.

8. Hutchinson, J.R. and Braun, P.H.:
Phase Relations of Miscible Displacement in Oil Recovery, AI ch. E. Journal, March 1961.

9. Orr, F.M., Silva, Lien, Pelletier:
Laboratory Experiments to Evaluate Field Prospects for CO_2 Flooding, SPE paper No. 9534, 1980.

10. Wilkie, D.H.:
Pseudocomponents, M Eng Project, Petroleum Engineering Department, Heriot-Watt University, 1982.

11. Yellig, W.F and Metcalfe, R.S.:
Determination and Prediction of CO_2 Minimum Miscibility Pressures, SPE paper No. 7477, 1978.

12. Orr, F.M. and Jensen, C.M.:
Interpretation of Pressure-Composition Phase Diagrams for CO_2 Crude Oil Systems, SPE paper No. 11125, 1982.

P A R T I

DEVELOPMENT OF A THEORETICAL MODEL TO PREDICT PHASE BEHAVIOUR OF MULTICOMPONENT GAS/OIL MIXTURES

CHAPTER 5

PREDICTION OF PHYSICAL PROPERTIES OF MULTICOMPONENT SYSTEMS

5.1 METHODS FOR CALCULATING THE PHYSICAL PROPERTIES BASED ON THERMODYNAMIC PRINCIPLES

For petroleum engineering application, the method used should:

(a) be applicable to multicomponent mixtures

(b) be accurate in predicting thermodynamic equilibrium and volumetric properties over a wide range of conditions of temperature and pressure, and specifically be accurate around the critical point

(c) preferably require only pure component data or binary data which is either readily available from literature or derivable from available data.

In the case of the experimental determination, expensive and time consuming experiments have to be run for each particular reservoir fluid at any set of conditions and, therefore, calculation is highly desirable.

The methods associated with phase equilibrium prediction are classified as:

(i) Methods which involve empirical curve fitting to experimental data

(ii) Methods which are based on thermodynamic principles

The first group of methods assume that the equilibrium ratios are only functions of pressure and temperature and independent of composition. That approach lacks consistency in the phase properties near the critical point and they do not provide the possibility of varying the parameters of the equation of state to match experimental or field data.

The methods based on thermodynamic principles are based on approaches radically different from each other and therefore need further subdivision:

(i) Methods based on the principle of corresponding states

(ii) Methods based on molecular thermodynamics

(iii) Methods based on semi-empirical equations of state.

5.2 METHODS BASED ON THE PRINCIPLE OF CORRESPONDING STATES

The principle of corresponding states is based on the assumption that all gases, when compared at the same reduced temperature and reduced pressure, have the same compressibility factor and all deviate from ideal gas behaviour to about the same degree. This can be applied to generating graphs or through a reduced equation of state, to evaluate the compressibility factor of a pure component or mixture by using reduced pressure and temperature evaluations. The problem that comes in applying the principle to mixtures of complex molecules, which deviate from the behaviour of the simple reference fluid, was faced by several workers with the introduction of parameters which consider the molecular deviation. Pitzer's acentric factor ω which is defined in terms of a vapour pressure datum is based on a reduced temperature of 0.7, such that ω is zero for argon. Other investigators have tried different methods based on the principle of corresponding states[1,2,3,4,5]. These methods have the disadvantage of requiring numerous lengthy iterative calculations and they have been reported to fail in the retrograde region.

5.3 METHODS BASED ON MOLECULAR THERMODYNAMICS

Molecular thermodynamics is a combination of classical thermodynamic techniques applied to macroscopic systems and statistical mechanics which involve analytical expressions, which are often complex, to describe the size and shape of molecules and the distances and forces between them. With an accurate knowledge of how to describe the distance and energy between two interacting molecules, the properties of a mixture of real fluid would be calculated from pure component data. These methods are collectively termed perturbation or variational approaches to the equation of state. Theoretical aspects of the method and types of perturbation methods are described in a review by Gubbins[6]. At this stage, the use of such techniques can involve very complex theory and require lengthy and complex mathematical solution techniques. Thus, although molecular thermodynamics may eventually provide the ability to predict the properties of multicomponent non-ideal systems, its application at present is limited.

5.4 METHODS BASED ON EMPIRICAL EQUATIONS OF STATE

5.4.1 Thermodynamic Concepts of the EOS

The equations of state relate quantitatively the thermodynamic properties which describe the state of equilibrium of different homogeneous phases, which are free to interchange energy and matter. A phase at equilibrium is defined as homogeneous when at any region in the space it occupies, the intensive properties which are the properties independent of the mass, the shape or the

size of the phase (like density, pressure, temperature, composition), are everywhere the same.

Consider a two phase, N components system in equilibrium at pressure P and temperature T. To describe the state of two phases which are free to interact and which have reached equilibrium, some of their equilibrium properties have to be specified so that the remaining ones can be determined. The number of intensive properties which must be specified so that the state of equilibrium is determined, is given by the Gibbs phase rule

$$\begin{array}{l}\text{Number of independent}\\ \text{intensive properties}\end{array} = \begin{array}{l}\text{Number of components}\\ \text{- Number of phases + 2}\end{array}$$

The number of primary variables involved in this case is 2N (N - 1 compositions of phase A, N -1 compositions of phase B, pressure and temperature). The remaining N dependent variables can be calculated from the N independent variables using thermodynamic relationships. For the two phase, N components system, the phase rule shows that N, any N, intensive properties have to be specified to determine the equilibrium condition of the system.

Thermodynamics show the way to the answer by providing the mathematical language in which abstract solution of the phase equilibrium problem is readily available. The approach to the answer consists of three steps. The first step is to project the physical problem into abstract terms, in other words to find the suitable mathematical functions to describe it. The second step involves the choice of the appropriate solution technique to solve the equations and in the third step, the results of the equations have to be translated back into terms of physical significance.

The third step is usually outside the realm of classic thermodynamics. This is because the latter gives us important but also severely limited information on the relation between abstract thermodynamic quantities, on the one hand chemical potential, and fugacity, and on the other real experimentally accessible data like pressure, temperature or composition.

The quantitative criterion for equilibrium is that the change of Gibbs free energy in the system should be zero. The energy of the system can be expressed as a function of the pressure and temperature and the mole fraction of each component:

$$G = G(T,P,n_1,n_2 \ldots\ldots n_N) \quad \ldots\ldots\ldots \quad \text{Eq 5-1}$$

The differential of the energy is then

$$dG = \left.\frac{\partial G}{\partial T}\right]_{P,n_1\ldots\ldots n_N} dT + \left.\frac{\partial G}{\partial P}\right]_{T,n_1\ldots\ldots n_N} dP +$$

$$\left.\frac{\partial G}{\partial n_1}\right]_{T,P,n_2,\ldots\ldots n_N} dn_1 + \ldots\ldots +$$

$$\left.\frac{\partial G}{\partial n_N}\right]_{T,P,n_1,\ldots\ldots n_{N-1}} dn_N \quad \ldots\ldots\ldots \quad \text{Eq 5-2}$$

or

$$dG = \left.\frac{\partial G}{\partial T}\right]_{P,n} dT + \left.\frac{\partial G}{\partial P}\right]_{T,n} dP + \sum_i^N \left.\frac{\partial G}{\partial n_i}\right]_{P,T,n} dn_i \quad \text{Eq 5-3}$$

or

$$dG = -SdT + VdP + \sum_i^N \mu_i dn_i \quad \ldots\ldots\ldots\ldots \quad \text{Eq 5-4}$$

where

$$\mu_i = \left.\frac{\partial G}{\partial n_i}\right]_{P,T,n}$$ is the chemical potential

The chemical potential states that with no chemical reaction involved, if a free energy change takes place at constant temperature and pressure then mass must be transferred from one phase to another. Absolute values for μ cannot be calculated, only its changes can be measured. The Gibbs free energy function is preferred because it relates directly the temperature, pressure and compositions; intensive properties readily measured in the laboratory.

At constant temperature and pressure

$$dG = \sum_{i}^{N} \mu_i dn_i \quad . . . . . \quad \text{Eq 5-5}$$

For N components two phase system Eq 5-5 becomes

$$\mu^A_1 dn^A_1 + \mu^A_2 dn^A_2 + ... \mu^A_N dn^A_N +$$

$$\mu^B_1 dn_1 + \mu^B_2 dn^B_2 + ... \mu^B_N dn^B_N = dG \quad \text{Eq 5-6}$$

At constant T and P, and at equilibrium conditions and since the total mass of each component is constant for a mechanically closed system

$$dn^A_1 + dn^A_2 + ... + dn^A_N = 0$$

$$dn^B_1 + dn^B_2 + ... + dn^B_N = 0 \quad . . . . . \quad \text{Eq 5-7}$$

Consequently

$$\mu_1^A = \mu_1^B$$
$$\mu_2^A = \mu_2^B$$
$$\vdots$$
$$\mu_N^A = \mu_N^B \quad \ldots\ldots\ldots\ldots\ldots\ldots \quad \text{Eq 5-8}$$

The equilibrium state has been expressed as the equalities of the chemical potentials of the different components in the two phases. To relate the abstract concept of the chemical potential to variables experimentally measured, like T,P,x_i, auxiliary functions much closer to our physical senses have to be introduced.

From Equation 5-4, $\left.\frac{\partial \mu}{\partial P}\right]_T = v$ and substituting the ideal-gas equation and integrating

$$\mu_i - \mu_{oi} = RT\ln\frac{P}{P_o} \quad \ldots\ldots\ldots\ldots \quad \text{Eq 5-9}$$

where μ_{oi} and P_o are the chemical potential and pressure at a reference state.

Lewis generalised Equation 5-9 to apply to any component in any system by introducing the fugacity ie

$$\mu_i - \mu_{oi} = RT\ln\frac{f_i}{f_o} \quad \ldots\ldots\ldots\ldots \quad \text{Eq 5-10}$$

where f_o is the fugacity at the reference state. The fugacity is given by $f_i = \phi y_i P$ where ϕ_i is the fugacity coefficient which has a value of 1 as pressure approaches zero and fugacity becomes equal to the partial pressure of the component.

The relation between fugacity and chemical potential is of conceptual aid in performing the translation from thermodynamic to physical variables and helps to make the transition from pure thermodynamics to the theory of intermolecular forces. The fugacity seen as corrected pressure for non-ideal components copes with the non-idealities which can be interpreted further by molecular thermodynamics.

Substituting Equation 5-10 to Equation 5-8 gives:

$$\begin{aligned} \mu_{o1}^{A} + RT\ln\frac{f_1^{A}}{f_{o1}^{A}} &= \mu_{o1}^{B} + RT\ln\frac{f_1^{B}}{f_{o1}^{B}} \\ \vdots \quad & \quad \vdots \quad \vdots \quad \vdots \qquad \ldots \qquad \text{Eq 5-11} \\ \mu_{oN}^{A} + RT\ln\frac{f_N^{A}}{f_{oN}^{A}} &= \mu_{oN}^{B} + RT\ln\frac{f_N^{B}}{f_{oN}^{B}} \end{aligned}$$

Assuming the same standard state for all components in both phases

$$\begin{aligned} f_1^{A} &= f_1^{B} \\ &\vdots \\ f_N^{A} &= f_N^{B} \qquad \ldots \ldots \ldots \ldots \ldots \qquad \text{Eq 5-12} \end{aligned}$$

The quantitative criterion for equilibrium has been expressed as the equalities of the fugacities of each component in both phases. To express the equilibrium in terms of the laboratory measured properties, fugacity has to be related mathematically with volume, pressure and composition. From the thermodynamic theory, the fugacities at constant temperature and composition are given by

$$RT\ln\frac{f_i}{y_i P} = \int_v^{\infty}\left[\left(\frac{\partial P}{\partial n_i}\right)_{T,v,n_j} - \frac{RT}{v}\right]dv - RT\ln Z \qquad \ldots \qquad \text{Eq 5-13}$$

To solve Equation 5-13 for fugacity, a mathematical expression relating the fundamental thermodynamic properties, volume, pressure, temperature and composition is needed.

$$P = F(T,V,n_1, \ldots n_N) \quad \ldots\ldots\ldots\ldots \quad \text{Eq 5-14}$$

These mathematical relations are called equation of state (EOS) and are usually of pressure explicit type.

5.4.2 The Van der Waals Type of EOS

The equations of state have some theoretical basis, but are built on simplified assumptions which make possible the pure components PVT data to be fitted by analytical expressions. To extend the application of the equations to mixtures, their parameters must take into account the composition of the mixture. The accuracy of the predictions of the EOS increases as the number of the parameters used in the equation is increased, but the complexity and the computer cost for the calculations increase as well.

The Van der Waals equation of state was proposed in 1873[7]

$$(P + a/v^2)(v-b) = RT$$

where parameters a and b are functions of P_C and T_C. Despite its simplicity, recent developments in molecular thermodynamics have proved its relative accuracy. Many authors have proposed modifications to the Van der Waals equation in attempts to produce an accurate equation of state relating pressure, temperature and molar volume of a fluid. Such equations generally express the pressure as a sum of two terms, a repulsion pressure P_R and an attraction pressure P_A

$$P = P_A + P_R$$

The modern equations of state have their origin in that of Van der

Waals and the more recent and more commonly used modifications of the original, are two parameter cubic equations in terms of volume.

In the two phase region the cubic equations of state give either one or three real roots. When applied for the vapour phase, in the case of the three real roots, the largest one is selected as the vapour compressibility factor, while for the liquid phase the smallest corresponds to the liquid compressibility factor. Clausius (1880), Berthelot (1899), Wohl (1914), proposed improved versions of the Van der Waals equation. Benedict, Webb and Rubin (1940)[8] proposed an eight adjustable constant equation. This equation being power six in volume and using such a great number of parameters, requires enormous quantities of data to be handled and does not have an analytical solution. The equation of state whose modifications are now widely preferred for their accuracy and simplicity, is that of Redlich Kwong, proposed in 1949[9]. Its three main modifications are the equations used in this study and are presented extensively together with the original Redlich Kwong equation later.

5.4.3 EOS Used in this Study

The EOS used in this study are the following:

1. Peng - Robinson
2. Modified Soave Redlich - Kwong
3. Modified Redlich - Kwong

5.4.4 Peng - Robinson Equation of State[10]

In pressure explicit terms, the relation of the fundamental thermodynamic properties is given by

$$P = \frac{RT}{v - b} - \frac{a(T)}{v(v + b) + b(v - b)} \quad \ldots\ldots \quad \text{Eq 5-16}$$

or in terms of the compressibility factor

$$Z^3 - (1 - B)Z^2 + (A - 3B^2 - 2B)Z - (AB - B^2 - B^3) = 0 \quad \ldots\ldots \quad \text{Eq 5-17}$$

where

$$A = \frac{aP}{R^2T^2}, \quad B = \frac{bp}{RT}$$

and for pure components the coefficients a and b are given by

$$a(T) = a(T_C) * (1 + m(1 - T_r^{0.5}))^2$$

$$m = 0.37464 + 1.5422\omega - 0.26992\omega^2$$

$$a(T_C) = 0.45724 \frac{R^2T_C^2}{P_C}$$

$$b = 0.0778 \frac{RT_C}{P_C} \quad \ldots\ldots \quad \text{Eq 5-18}$$

The a and b parameters for each pure component are calculated at the critical point where

$$\left.\frac{\partial p}{\partial v}\right]_T = 0 \qquad \text{and} \qquad \left.\frac{\partial^2 p}{\partial v^2}\right]_T = 0$$

The thermodynamic fundamentals give finally the following expression for the fugacity coefficient of any component which is either in the liquid or in the vapour phase and is used for deriving fugacities using the equation of state

$$\ln\phi_i = \int_v^\infty \left[\frac{1}{RT}\frac{\partial P}{\partial n_i} - \frac{1}{v}\right]dv - \ln Z$$

The fugacity coefficient for a pure component can be calculated from the equation

$$\ln\phi_i = Z - 1 - \ln(Z - B) - \frac{A}{2\sqrt{2}B}\ln\left[\frac{Z + 2.414B}{Z - 0.414B}\right]$$

. . . . . Eq 5-19

5.4.5 Modified Soave Redlich - Kwong

In 1972 Soave presented a modified Redlich - Kwong equation of state to improve the prediction of thermodynamic properties of pure components and multicomponent mixtures[11]. In terms of pressure this may be represented as follows:

$$P = \frac{RT}{v - b} - \frac{a(T)}{v(v + b)} \quad . . . . . \quad \text{Eq 5-20}$$

or in terms of the compressibility factor

$$Z^3 - Z^2 + (A - B - B^2)Z - AB = 0 \quad . . . . . \quad \text{Eq 5-21}$$

where the temperature and the acentric factor dependence of a(T) is given by

$$a(T) = 0.42727\frac{R^2Tc^2}{Pc}(1 + m(1 - Tr^{1/2}))^2$$

$$m = 0.48 + 1.544\omega - 0.15613\omega^2$$

$$b = 0.08664\ R\ Tc/Pc \quad . . . . . \quad \text{Eq 5-22}$$

For this study's applications, a slightly modified equation for m due to Graboski was used[12]:

$$m = 0.48508 + 1.5571\omega - 0.15613\omega^2 \quad . . . . . \quad \text{Eq 5-23}$$

The fugacity coefficient for a pure component can be calculated from the equation

$$\ln\Phi_i = Z - 1 - \ln(Z - B) - \frac{A}{B}\ln\left[\frac{Z + B}{Z}\right]$$

. . . . . Eq 5-24

5.4.6 Modified Redlich - Kwong EOS

The original Redlich - Kwong EOS (1949) received in the last years great attention and has been widely used in chemical engineering calculations. The Redlich Kwong Equation of state has the form

$$p = \frac{RT}{v - b} - \frac{aT^{-1/2}}{v(v + b)}$$

Several attempts have been made in order to improve the original equation [13,14,15,16,17,18,19]. The most interesting development has been to introduce a modified temperature dependence of the a_i and b_i parameters. In that way, the a_i and b_i constant for each component,

$$a_i = 0.4278R^2Tc_i^{2.5}/Pc_i$$

$$b_i = 0.0867RTc_i/Pc_i \quad . . . . . \quad \text{Eq 5-25}$$

can be written

$$a_i = \Omega_{ai}R^2Tc_i^{2.5}/Pc_i$$

$$b_i = \Omega_{bi}RTc_i/Pc_i$$

where Ω_{ai}, Ω_{bi} are temperature dependent coefficients.

The fugacity coefficient for a single compound is given by

$$\ln\phi_i = Z - 1 - \ln(Z - BP) - \frac{A^2}{B} \ln\left[1 + \frac{BP}{Z}\right] \quad \text{Eq 5-26}$$

Each substance has its own characteristic pair of omega functions matched to experimental data. At the critical point the three real roots for Z coincide with the value $Z_c = 1/3$. Since all components we deal with, have Z_c values between 0.27 and 0.29, the calculated Z_c can be more than 20% in error. Furthermore, to generate three coinciding Z values at critical conditions, the Ω_{ai} and Ω_{bi} must have the Van der Waals values (Equation 5-25) at T_c. These values, because of the critical anomaly never lie on the omega curves derived from empirical data[20].

This error finally is only of minor influence on equilibrium prediction near the critical point, because the critical fugacity coefficient is only 5 - 6% in error and one is mainly interested in the equality of the two fugacities rather than in their individual numerical value. Zudkevitch and Joffe calculate Ω_{ai} and Ω_{bi} for each component i at a given temperature, using the component's saturation pressure, saturated liquid density and Lyckman's fugacity coefficient[21]. Coats[22] calculates Ω_{ai} and Ω_{bi} as the two unknowns, from two equations:

$$f_{iL} = f_{iV}$$

and

$$Z_L = Z_i^*$$

where Z_i^* is the saturated liquid Z factor of the component at the saturation pressure at the given temperature. The two equations are solved by a Newton - Raphson iteration method. For this study, generalised correlations established by Hamam et al[23] for Ω_{ai} and Ω_{bi} were used with the modified Redlich - Kwong EOS. The Ω_{ai} and

Ω_{bi} were correlated in terms of T_r and acentric factor ω. The expressions are simple and adequately tested for components having acentric factors as high as 0.5 in the subcritical region. For components in the supercritical state, values of Ω_{ai} and Ω_{bi} obtained at the critical temperature (T_r = 1.0) were used, and the predicted results compared with experimental data.

A deviation less than 1.5% was observed in the calculation of the saturation pressure. In Table 5-1 values of the parameters Ω_{ai} and Ω_{bi} calculated from the correlations are compared against those obtained by Coats[22] and Fussell[24] for a ternary mixture of C_1 - nC_4 - C_{10} at 160°F (344.3K). For the same mixture and for composition (mole fraction)

CH_4 : 0.253

nC_4 : 0.661

nC_{10} : 0.086

the equilibrium (K) values and the saturation pressure estimated using the phase behaviour simulator which is described in Chapter 6 and the Modified Redlich Kwong equation of state compared to the values predicted by Coats and to the experimental ones are given in Table 5-2.

5.5 APPLICATION OF THE EOS TO MIXTURES

To apply the equations of state for mixtures, a relation has to be found which states how the constants a and b for the mixture depend on the composition. If we interpret 'a' as a term which reflects the strength of attractions between two molecules, then for a mixture we usually express 'a' by averaging over all molecular pairs

$$a = \sum_{i=1}^{N} \sum_{j=1}^{N} y_i y_j a_{ij} \quad \text{. . . . . Eq 5-27}$$

where a_{ij} is a measure of the strength of attraction between a molecule i and a molecule j. The values for a_{ij} for hydrocarbon mixtures are recommended to be calculated by the equation (Soave - Graboski - Daubert)

$$a_{ij} = (a_i a_j)^{1/2} \quad \text{. . . . . Eq 5-28}$$

A more generalised equation for a_{ij} is given as[11]

$$a_{ij} = (a_i a_j)^{1/2}(1 - k_{ij}) \quad \text{. . . . . Eq 5-29}$$

especially when polar molecules are present in the system. The binary coefficient k_{ij} is an empirical factor which must be determined from binary mixture data and can take zero for nonpolar hydrocarbon pairs (Soave - Graboski - Daubert). A good approximation of the empirical k_{ij} can be obtained from the so called characteristic constant[17]. The binary constant represents the deviation from the geometric mean for T_{cij}. Chueh et al claim that the values for k_{ij} to a good approximation should be independent of the temperature, density and composition of the system[18]. On the contrary, Kato et al report that these parameters have an obvious temperature dependence[25]. Experience has shown that the interaction parameters are necessary for CO_2-hydrocarbon mixtures and also between methane and heavy fractions. Whitson[26] claims that the coefficients for C_1 - C_{7+} pairs have a relatively strong temperature dependence for many reservoir fluids. Turek et al extended it to CO_2 mixtures[27]. Katz et al and Lee et al[29] attempted to correlate the interaction

parameters. The trend observed is that coefficients increase with increasing molecular size. Varotsis et al at 1983[30] proved the interaction parameters for CO_2, N_2, C_1 to be functions of the reduced pressure and temperature and they have expressed them as generalised functions of the acentric factor, reduced pressure and temperature.

Conrand et al go further to consider the interaction coefficients as pure mathematical parameters without any physical sense, that can take any values in order that the EOS predictions match the experimental data. Shearn[33] suggested the use of ternary interaction parameters for mixtures involving CO_2 and methane.

If the constant b is interpreted as a term proportional to the size of the molecules, the molecular volumes can be averaged by applying the mixing rule

$$b = \sum_{i}^{N} \sum_{j}^{N} y_i y_j b_{ij} \quad \text{. . . . . Eq 5-30}$$

Wilson and Chueh and Prausnitz have proposed that Equation 5-30 be replaced with the simpler relationship[34,35]:

$$b = \sum_{i=1}^{N} y_i b_i, \quad y_i = \text{mole fraction} \quad \text{. . . . . Eq 5-31}$$

Equation 5-31 is equivalent to assuming the combining rule

$$b_{ij} = \frac{1}{2}(b_i + b_j) \quad \text{. . . . . Eq 5-32}$$

This mixing rule is based on an assumption that is rather arbitrary and other rules could be proposed. For mixtures whose

molecules are not too dissimilar in size, the particular mixing rule used for b does not significantly affect the results. Turek suggested the use of another binary interaction parameter D_{ij} for the first mixing rule for CO_2 mixtures.[27] Equation 5-30 becomes

$$bm = \frac{1}{z} \sum_{i}^{N} \sum_{j}^{N} z_i z_j (1 + D_{ij})(b_i + b_j) \quad \ldots\ldots\ldots \quad \text{Eq 5-33}$$

For the purposes of the present study Equations 5-31 and 5-27 were used as mixing rules. ω is the acentric factor by Pitzer which theoretically comes from the second virial coefficient and is a macroscopic measure for each component, of the extent to which the force field around a molecule deviates from spherical symmetry. The acentric factor is essentially zero for spherical, non-polar molecules such as the noble gases and for small, highly symmetric molecules such as methane. The operational definition of ω is

$$\omega = -\log_{10}\left[\frac{Ps}{Pc}\right]_{T/T_C=0.7} - 1.0 \quad \ldots\ldots\ldots \quad \text{Eq 5-34}$$

where Ps is the vapour pressure at $T_r = 0.7$

The success of an equation of state in predicting vapour, liquid equilibria (VLE) behaviour depends on its ability to account for nonidealities in both the vapour phase and the liquid phase. Seldom does a given equation of state perform equally well in the subcritical, critical and supercritical regions[32]. Thus the choice of the EOS depends on what region of the PVT space is considered. Further, the type of compounds and the type of mixture can also influence which is the most appropriate equation of state. Most modifications to the Van der Waals EOS have

emphasised improvement in predicting equilibrium ratios by improving the prediction for liquid phase nonideality. There are, however, cases where a "two-equation" approach is more viable. Such calculations represent the liquid phase nonideality through an activity coefficient model and the vapour phase through an equation of state. However, the equations of state, despite their limitations, possess a simple mathematical form and a small number of adjustable parameters, while achieving a sufficient degree of accuracy to be of practical interest. The fact that they can be applied in both phases makes them a very versatile tool for the prediction of physical properties of hydrocarbon mixtures.

TABLE 5-1

CALCULATION OF THE Ω_A, Ω_B PARAMETERS FOR THE REDLICH-KWONG EOS

CH_4-N-BUTANE-N-DECANE MIXTURE

160°F

	Ω_A	Ω_B	Ω_A coats	Ω_B coats	Ω_A fuss	Ω_B fuss
C_1	0.4265	0.0862	0.042617	0.8617	0.4251	0.0859
nC_4	0.4198	0.0794	0.4194	0.0794	0.4154	0.0759
nC_{10}	0.4638	0.734	0.4519	0.07045	0.4651	0.0726

TABLE 5-2

K VALUES SATURATION PRESSURE MODIFIED REDLICH-KWONG EOS

	K-Values Coats	K-Vol Our Model	K-Values Exper
C_1	3.173	3.174	3.174
nC_4	0.297	0.297	0.297
C_{10}	0.008	0.0081	0.013
Saturation Pressure (psia)	927.7	975.1	1000

LIST OF REFERENCES

1. Knapp, H.: Chem. Ing. Tech., 1977, 49, 12 955-965.

2. Plocker, V. and Knapp, H.: Ind. Eng. Chem. P.D.D., 1978, 17, 3, 324-332.

3. Gunn, R.D.: A. I. Ch. E. J., 1972, 18, 1, 183-188.

4. Rowlinson, J.S.: "Prediction of Thermodynamic Properties" Amer. Chem. Soc. Symp. Series 60, ed. Storvick and Sandler, A.C.S., 1977, 316-330.

5. Elliot, P.G.: "Thermophysical Properties; Their Effect on Cryogenic Gas Processing", Ibid, 289-309.

6. Gubbins, K.E.: A.I.Ch.E.J., 1973, 19, 4, 684-697.

7. Van der Waals, J.D. Doctoral Dissertation, Leiden, Holland 1873.

8. Benedict, M, Webb, G.B. and Rubin, L.C.: J. Chem. Phys., 1940, 8, 334.

9. Redlich, O. and Kwong, J.N.S.: Chem. Rev., 1941, 44, 233-243.

10. Peng, D.Y., Robinson, D.B. and Ng, H.J.: Procc. 56th Annual Conf. Gas Processors Ass., Dallas, (21-23 March 1977), 11-17.

11. Soave, G.: Chem. Eng. Sci. 27 pp 1197-1203 (1972).

12. Gravoski, M. and Daubert, T.E.: Ind. Eng. Chem. P.D.D., 1978, 17, 4, 443-454.

13. Wilson, G.M.: Adv. Cryog. Eng. 1964, 9, 168.

14. Zudkevitch, D., Joffe, J. A.I.Ch.E.J. 1970, 16 (1), 112.

15. Joffe, J., Schneder, G.M., Zudkevitch, D.: A.I.Ch.E.J., 1970, 16 (3), 496.

16. Chang, S.D., Lu, B.C.Y.: Can. J. Chem. Eng. 1976, 54, 595.

17. Chueh, P.L., Prausnitz, J.M.: Ind. Eng. Chem. Fundam., 1967, 6, 492.

18. Chueh, P.L., Prausnitz, J.M.: A.I.Ch.E.J., 1967, 13, 1099.

19. Peng, D.Y., Robinson, D.B.: Ind. Eng. Chem. Fundam., 1976, 15, 59.

20. Harmens, A.: Cryogenics, 15, 217 (1975).

21. Lyckman, E.W., Eckert, C.A. and Prausnitz, J.M.: Chem. Engng. Sci., 1965, 20, 685.

22. Coats, K.H.: SPEJ, October 1980 p 363.

23. Hamam, S., Chung, W.: Ind. Eng. Chem. Process. Des. Dev., Vol 16, No 1 1977.

24. Fussell, D.D., Yanosik, J.L: SPEJ, June 1978.

25. Kato, Nagahama, Hirata: Fluid Phase Equilibria, 1981, 7, pp 219–231.

26. Whitson, c.: "Effect of Physical Properties Estimation on Equation of State Predictions", SPE paper No 11200, 1982.

27. Turek, E., Metcalfe, R., Yarborough, L., Robinson, R.: "Phase Equilibria in CO_2-Multicomponent Hydrocarbon Systems Experimental Data and an Improved Prediction Technique", SPE paper No 9231.

28. Katz, D.L., Firoozabadi, A.: J. Petr. Tech., November 1978, pp 1649–1655, Trans. AIME, 228.

29. Lee, S.T., Jacoby, R.H., Chen, W.H., Culham: W.E. paper SPE 8398, September 23–26, 1979.

30. Varotsis, N., Stewart, G., Clancy, M.: "An Experimental and Theoretical Study of the Phase Behaviour of North Sea Reservoir Fluids with Special Reference to Miscibility with the Injection Gases CO_2, N_2 and CH_4", submitted for the 1984 SPE EOR Symposium to be held April 15–18, 1984 in Tulsa.

31. Conrard, P., Gravier, J.F.: Oil and Gas Journal, 21 April, 1980.

32. Tavakad, R., Spencer, C., Adler, S.: Pulman Kellogg Houston Texas, 1978.

33. Shearn, R.B.: "Mass Transfer in Miscible Displacements" Report written for the DOE Seminar, April 1983.

34. Wilson, G.M.: International Advances in Cryogenic Engineering, 1964, 9, 108.

35. Chueh and Prausnitz: A.I.Ch.E.Jl., 1967, 13, 1099.

CHAPTER 6

SIMULATION OF THE VAPOUR - LIQUID EQUILIBRIA OF RESERVOIR FLUID SYSTEMS

6.1 INTRODUCTION

The physical behaviour of the processes under investigation can be described by a system of mathematical equations. The calculation of the physical properties of the vapour and the liquid phases are all based on the assumption of thermodynamic equilibrium at the given temperature and pressure. A fluid mixture of known overall composition is equilibrated at the temperature and pressure of interest. The components in the mixture will be distributed in a vapour and a liquid phase. The composition of each phase, the volume ratios, the molar ratios and the densities of the phases will be determined mathematically.

Figure 6-1 demonstrates on a Pressure-Temperature (P-T) diagram the different possibilities of the phase behaviour of a hydrocarbon mixture. Mixtures lying on the bubble point locus (1) are single liquid phases in equilibrium with the first bubble of released gas. On the other hand, mixtures lying on the dew point curve (2) are vapour phases in equilibrium with the first drop of condensed liquid. Mixtures inside the phase envelope consist of two phases in equilibrium. For mixtures outside the phase envelope, those which lie on the left of the critical point (*) are undersaturated liquids and those on the right of the critical point undersaturated vapours. At this stage it is useful to define the equilibrium ratio or K-value for component i as:

$$K_i = y_i/x_i$$

where y_i, x_i are the vapour and liquid mole fractions.

6.2 MATHEMATICAL FORMULATION OF PHASE EQUILIBRIUM PROBLEMS

6.2.1 Isothermal Flash Calculation

Consider the following simple separation scheme (Figure 6-2). A mixture of F moles consisting of N components with overall composition z_i, i=1, N (mole fractions), is held at pressure P and temperature T. Its phase behaviour in equilibrium at the conditions of interest has to be determined. The F moles of the feed at the conditions of the test are separated into V moles of vapour at composition y_i (mole fractions) and L moles of liquid at composition x_i (mole fractions).

The overall material balance for the number of moles is expressed by the equation

$$F = L + V \quad \ldots\ldots\ldots\ldots\ldots\ldots \quad \text{Eq 6-1}$$

Given that there is no gain or loss of mass in the system, the number of moles of each component present remains constant during the process. The overall component material balance is given by the equation

$$Lx_i + Vy_i = Fz_i \qquad i = 1,N \quad \ldots\ldots\ldots \quad \text{Eq 6-2}$$

The resulting compositions of the two phases expressed as mole fractions should satisfy the equation

$$\sum_{i=1}^{N} x_i = 1 \text{ or } \sum_{i=1}^{N} y_i = 1 \quad \ldots\ldots\ldots\ldots \quad \text{Eq 6-3}$$

Only one of the two equations (6-3) should be used with the system of equations which describe the state of equilibrium, because

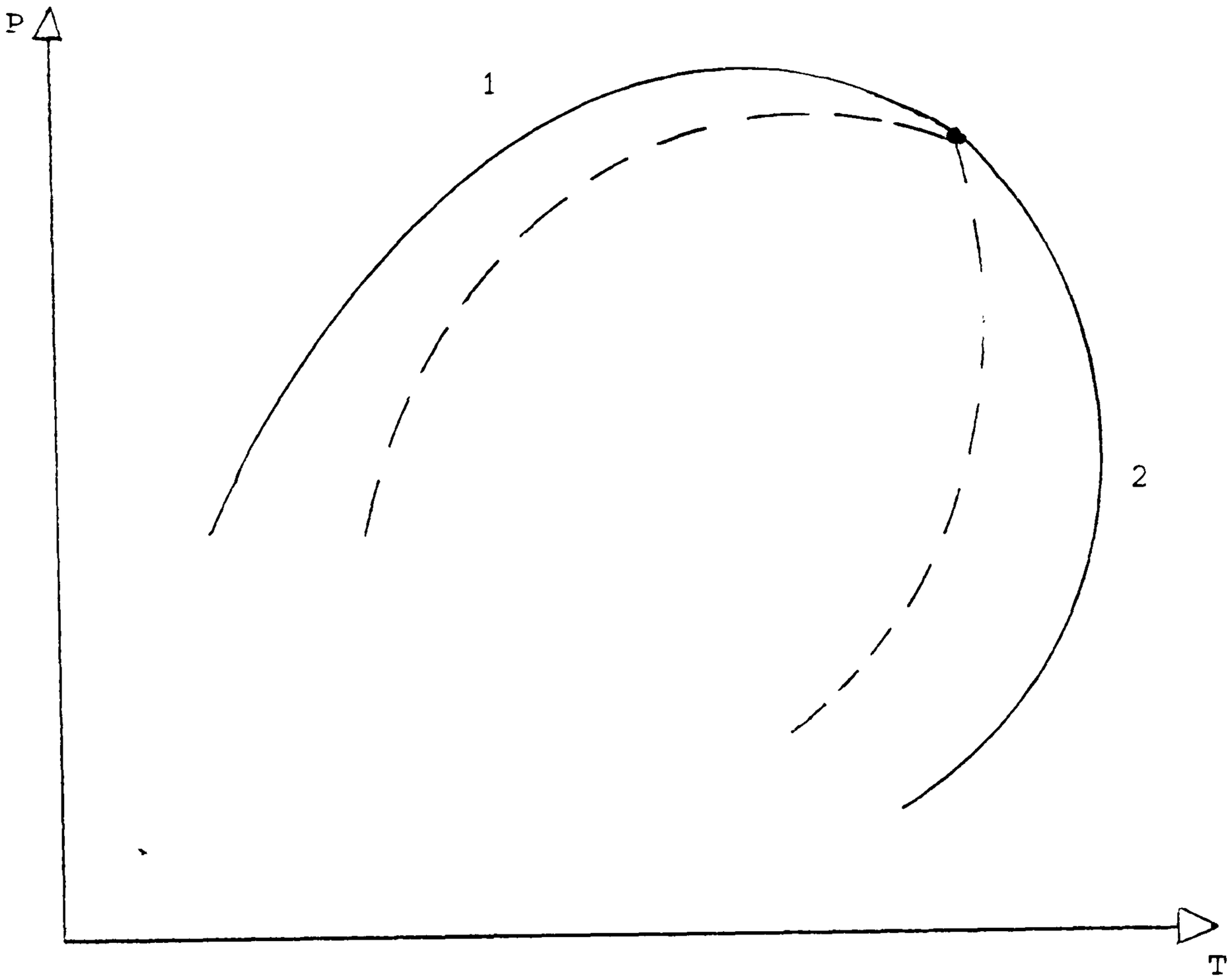

FIGURE 6-1

PRESSURE-TEMPERATURE PHASE ENVELOPE

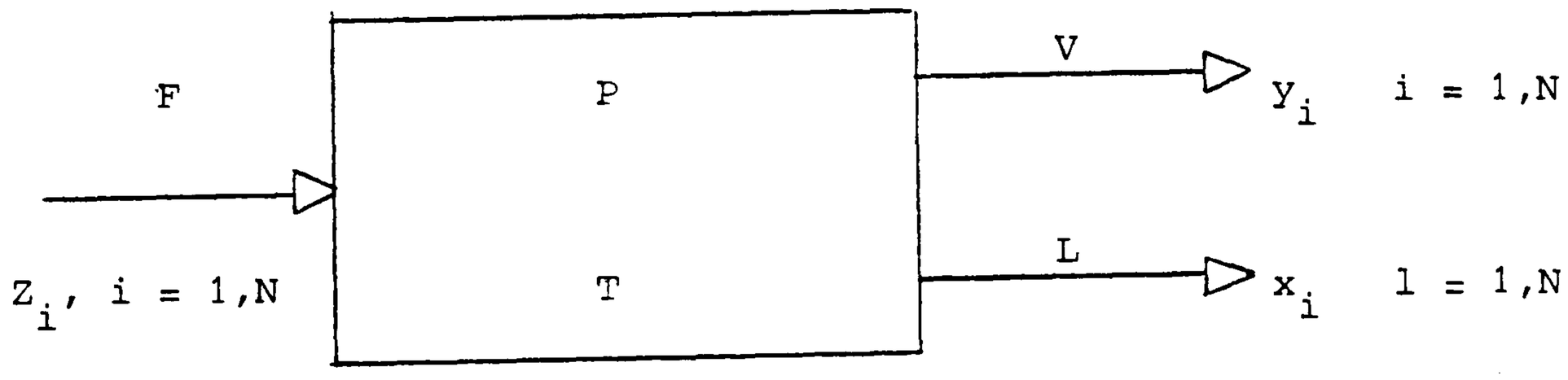

FIGURE 6-2

SEPARATION SCHEME

given one, the second may be derived by combining the given equation with Equation 6-1 and 6-2.

To express the thermodynamic equilibria, as it was presented in Chapter 5, the component fugacity is used to develop a criterion for thermodynamic equilibria. In physical terms the fugacity of a component in one phase with respect to the fugacity of that component in the second phase is a measure of the potential for transfer of the component to the phase where its fugacity is lower[1]. Therefore, the thermodynamic equilibria is expressed by

$$f_{iL} = f_{iV} \qquad i = 1,N \quad . \; . \; . \; . \; . \; . \; . \; . \; . \; . \; . \qquad \text{Eq 6-4}$$

where

$$f_{iL} = f_{iL}(x_j,P,T), \qquad f_{iV} = f_{iV}(Y_j,P,T) \qquad j = 1,N$$

The system of the Equations 6-1, 6-2, 6-3, 6-4, has to be solved to describe the equilibrium of the mixture. The equations are highly non-linear and therefore have to be solved simultaneously by an iteration method.

6.2.2 Bubble Point Calculation

The phase behaviour of mixtures lying on the saturated liquid part of the phase envelope (Figure 6-1), can be described mathematically using the thermodynamic equilibria equations that were used for the description of the isothermal flash problem. The problem in this case is either to find the bubble point pressure for a given feed temperature and composition, or to find the bubble point temperature for a given feed composition and pressure. The vapour phase properties are also to be determined.

Equations

A saturated liquid phase of composition ($x_i = z_i$, i = 1,N) co-exists in equilibrium with a first bubble of gas which has composition y_i, i = 1,N at

a specified temperature T. In this case the vapour phase is of negligible amount and the overall material balance can be written

$$F = L$$

The restrictive equation on the unknown (vapour) phase composition is written

$$\sum_{1}^{N} y_i = 1$$

and the thermodynamic equilibria is expressed by

$$f_{iL} = f_{iV}, \quad i = 1,N$$

where

$$f_{iL} = f_{iL}(z_j,P,T) \qquad f_{iV} = f_{iV}(y_j,P,T) \qquad j = 1,N$$

6.2.3 Dew Point Calculation

The problem in this case is either to find the pressure at which the first drop of liquid is formed out of undersaturated vapour at a given temperature, or to find the dew point temperature for a given feed composition and a specified pressure. The liquid phase properties are also to be determined. The overall material balance equation can be written

$$F = V$$

The restrictive equation on the unknown (liquid) phase composition is written

$$\sum_{1}^{N} x_i = 1$$

and the thermodynamic equilibria is expressed by

$$f_{iL} = f_{iV}, \quad i = 1,N$$

where

$$f_{iL} = f_{iL}(x_j,P,T) \qquad f_{iV} = f_{iV}(z_j,P,T) \qquad j = 1,N$$

6.3 ITERATIVE SOLUTION METHODS

6.3.1 Iteration Methods used for the Solution of Phase Equilibrium Problems

The next step is to develop an iteration method to solve the system of the algebraic equations presented in section 6.1. Consider the system of simultaneous, nonlinear algebraic equations of the form:

$$\begin{aligned} F_1(\underline{x}_1, \underline{x}_2, \ldots\ldots, \underline{x}_n) &= 0 \\ F_2(\underline{x}_1, \underline{x}_2, \ldots\ldots, \underline{x}_n) &= 0 \\ &\vdots \\ F_N(\underline{x}_1, \underline{x}_2, \ldots\ldots, \underline{x}_n) &= 0 \end{aligned} \qquad \text{Eq 6-5}$$

which can be written compactly in vector notation as

$$\bar{F}(\bar{\underline{x}}) = 0 \qquad \text{Eq 6-6}$$

where

$$\bar{\underline{x}} = (\underline{x}_1, \underline{x}_2, \ldots\ldots, \underline{x}_n)^T$$

$$\bar{F} = (F_1, F_2, \ldots\ldots, F_n)^T$$

$$F_i = F_i(\underline{x}_1, \underline{x}_2, \ldots\ldots, \underline{x}_n) \qquad i = 1,n$$

There are two different approaches to tackle the problem

(i) A direct iteration method can be used. The functions F_i are expressed in the following form

$$F_i = \underline{x}_i - g_i(\underline{\bar{x}}) \quad \ldots\ldots\ldots \quad \text{Eq 6-7}$$

where

$$g_i(\underline{\bar{x}}) = g_i(\underline{x}_1, \underline{x}_2, \ldots\ldots, \underline{x}_n)$$

The system of equations can now be written

$$\bar{F}(\underline{\bar{x}}) = \underline{\bar{x}} - \bar{g}(\underline{\bar{x}}) = 0 \quad \ldots\ldots\ldots \quad \text{Eq 6-8}$$

A direct iteration of the form

$$\underline{\bar{x}}^{k+1} = \bar{g}(\underline{\bar{x}}^{k}) \quad \ldots\ldots\ldots \quad \text{Eq 6-9}$$

is constructed where k is the number of the iteration. The method is regarded converged when the difference

$$| \underline{\bar{x}}^{k} - \bar{g}(\underline{\bar{x}}^{k}) | \quad \text{or} \quad | \bar{g}(\underline{\bar{x}}^{k-1}) - \bar{g}(\underline{\bar{x}}^{k}) |$$

is smaller than a specified tolerance.

The success of direct iteration depends on the selection of the functions $\bar{g}(\underline{\bar{x}})$. The absolute slope of these functions should be less than unity for convergence to be achieved. When the slope is greater than unity the method diverges. Figure 6-3a demonstrates a case of convergence and Figure 6-3b a case of divergence using one-variable functions[2].

The direct iteration method applicable to phase equilibrium problems is the successive substitution method (SSM). For the isothermal flash calculation

FIGURE 6-3a

DIRECT ITERATION METHOD - CONVERGENCE ACHIEVED

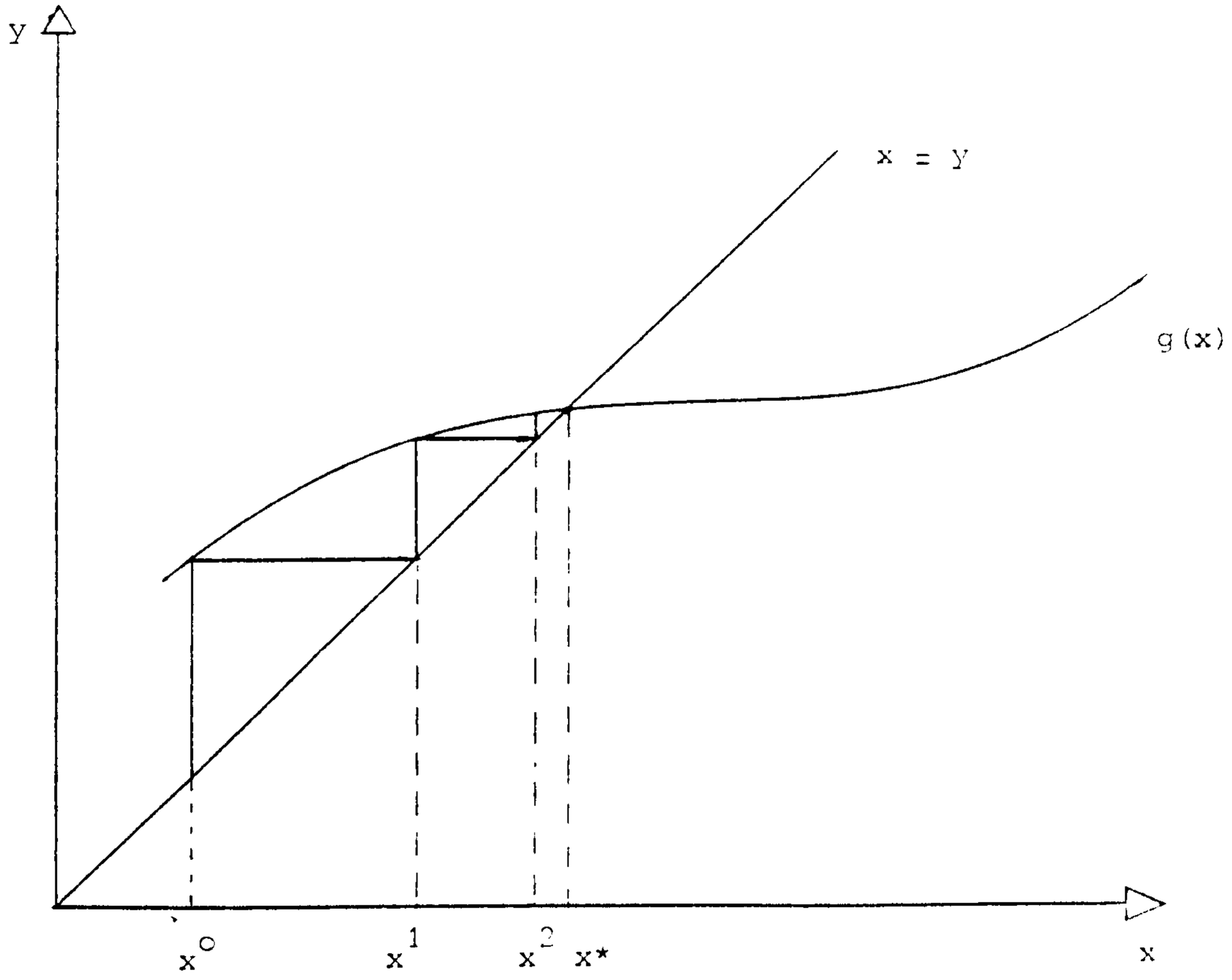

FIGURE 6-3b

DIRECT ITERATION METHOD - CONVERGENCE NOT ACHIEVED

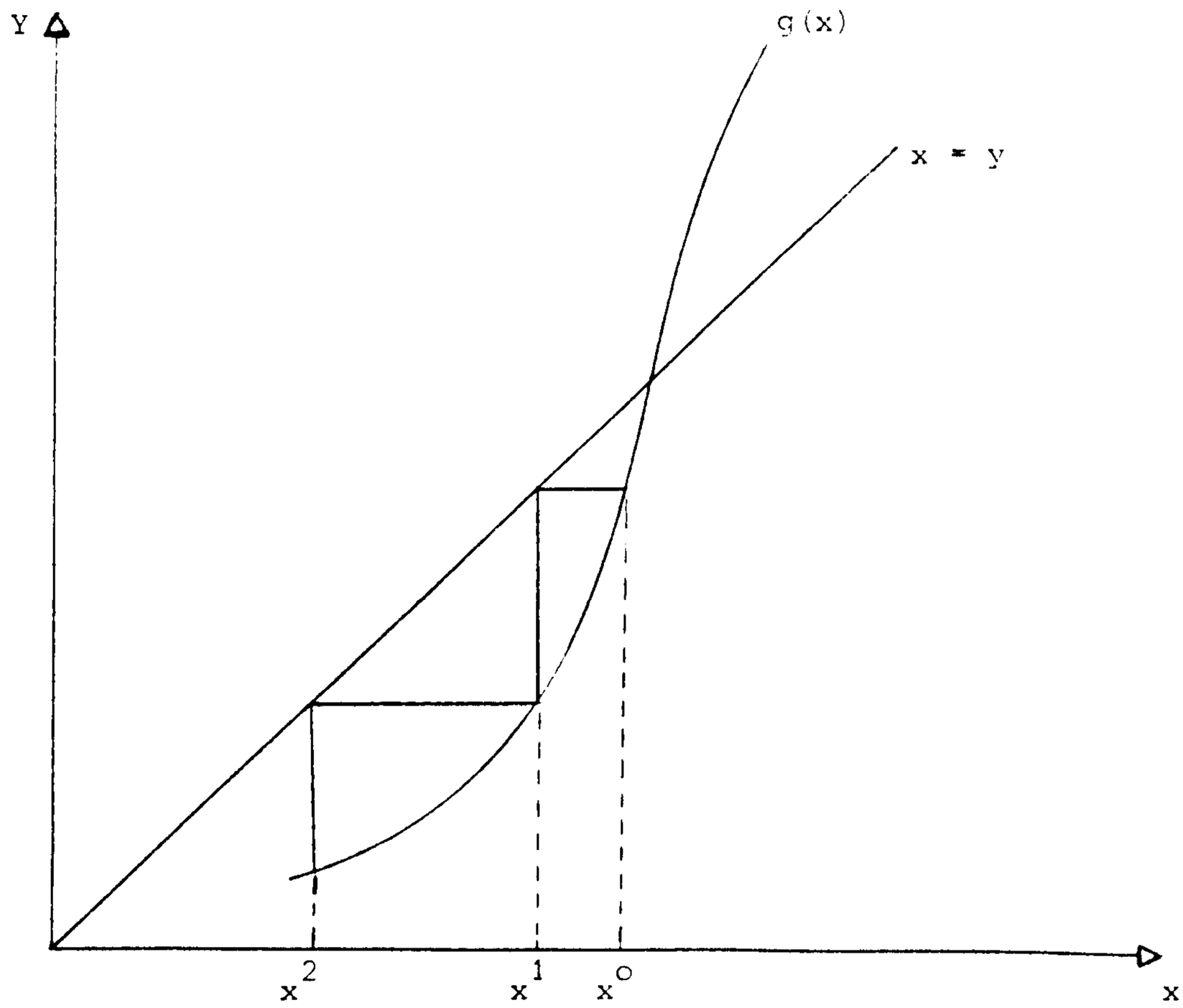

the system of non-linear phase equilibrium equations is written as

$$\bar{F}(\underline{\bar{x}}) = \underline{\bar{x}} - \underline{\bar{x}} * \frac{\bar{F}_{iL}}{\bar{F}_{iV}} \qquad (\bar{g}(\underline{\bar{x}}) = \underline{\bar{x}} * \frac{\bar{F}_{iL}}{\bar{F}_{iV}}$$

. . . . . Eq 6-10

where

$$\underline{\bar{x}} = (\underline{x}_1, \underline{x}_2, \ldots\ldots, \underline{x}_n)^T$$

$$\bar{F}_{iL} = (F_{1L}, F_{2L}, \ldots\ldots, F_{nL})^T,$$

$$\bar{F}_{iV} = (F_{1V}, F_{2V}, \ldots\ldots, F_{nV})^T$$

$$F_{iL} = F_{iL}(\underline{x}_1, \underline{x}_2, \ldots\ldots, \underline{x}_n),$$

$$F_{iV} = F_{iV}(\underline{x}_1, \underline{x}_2, \ldots\ldots, \underline{x}_n)$$

and the correspondence to the physical variables

$$\begin{array}{lll} \underline{x}_1 = K_1 & F_{1L} = f_{1L} & F_{1V} = f_{1V} \\ \underline{x}_2 = K_2 & F_{2L} = f_{2L} & F_{2V} = f_{2V} \\ \vdots & \vdots & \vdots \\ \underline{x}_n = K_n & F_{nL} = f_{nL} & F_{nV} = f_{nV} \end{array}$$

Figure 6-4 gives a flowchart of the isothermal flash calculation solved by the Successive Substitution Method.

(ii) The second approach involves the use of second order Newton methods with minimum number of iteration variables. To solve the phase equilibrium problem, the following steps should be taken

- An array $\underline{\bar{x}} = (\underline{x}_1, \underline{x}_2, \ldots\ldots, \underline{x}_n)^T$ should be selected whose elements are the variables to be iterated.
- An array $\bar{F} = (F_1, F_2, \ldots\ldots, F_n)^T$ of multi-variable functions of the iteration variables should be defined where $F_i = F_i(\underline{x}_1, \underline{x}_2, \ldots\ldots, \underline{x}_n)$. The

number of the functions is equal to the number of the iteration variables.

- An array $\bar{h} = (h_1, h_2, \ldots\ldots, h_m)^T$ of functions should be defined where $h_i = h_i(\underline{x}_1, \underline{x}_2, \ldots\ldots, \underline{x}_n)$. These functions are the defining functions and are used to calculate the remaining variables $\bar{\underline{Y}}_i(\bar{\underline{Y}}_i = (\underline{Y}_1, \underline{Y}_2, \ldots\ldots, \underline{Y}_m))$ using the assumed values of the iteration variables. m is the number of the variables that are calculated directly using the defining equations. n + m is the total number of unknowns in the problem.

- An array of values $\bar{\underline{x}}^* = (\underline{x}_1^*, \underline{x}_2^*, \ldots\ldots, \underline{x}_n^*)^T$ should be found which satisfies the equations

$$F_i(\underline{x}_1, \underline{x}_2, \ldots\ldots, \underline{x}_n) = 0 \quad i = n$$

The sequence to achieve solution can be summarised in a four step process:

1. Assume an array $\bar{\underline{x}}^o = (\underline{x}_1^o, \underline{x}_2^o, \ldots\ldots, \underline{x}_n^o)^T$ of starting values for the iteration variables.
2. Use the defining equations to calculate the dependent variables.
3. Use the values ($\bar{\underline{x}}^o$) to calculate the values of the functions F_i (error equations). The closer the elements of the array ($\bar{\underline{x}}^o$) are to the elements of ($\bar{\underline{x}}^*$), the closer the values of $F(\bar{\underline{x}}^o)$ are to zero.
4. Use a correction step method to update the values ($\bar{\underline{x}}^o$) in the direction of the solution.

Figure 6-5 gives the flowchart for the solution of the isothermal flash calculation using a second order Newton method. Undoubtedly the Newton method is much more robust than the SSM method, although it requires more complex arithmetic. Given the importance of the critical point region on gas miscibility and to ensure the convergence of the algorithm to near critical conditions, a second order Newton method was selected to build up the computer model.

The model which can predict the phase behaviour and physical properties of mixtures of injected gases and hydrocarbons at near critical conditions and can follow the miscibility path, was built on a modification of an already existing simulator which has been written to predict the pressure drop for a two phase flow in a vertical lift process[3]. The reformulation of Flashman

was found to be necessary to increase the robustness of the model and achieve solution at near critical conditions.

6.3.2 Iteration Method Used in this Study

The Iteration Method used in this study is the Minimum Variable Iteration Method. This method reduces the dimension of the correction step by eliminating as many unknowns as possible. The decomposition of the total system of equations into a minimum number of equations that have to be solved simultaneously is achieved in this study by inspection of the system of equations. Only some of the unknown variables are included in the iterative process and are called independent variables. The rest of the

FIGURE 6-4

FLOW CHART FOR THE SOLUTION OF THE ISOTHERMAL FLASH CALCULATION BY A SUCCESSIVE SUBSTITUTION METHOD (SSM)

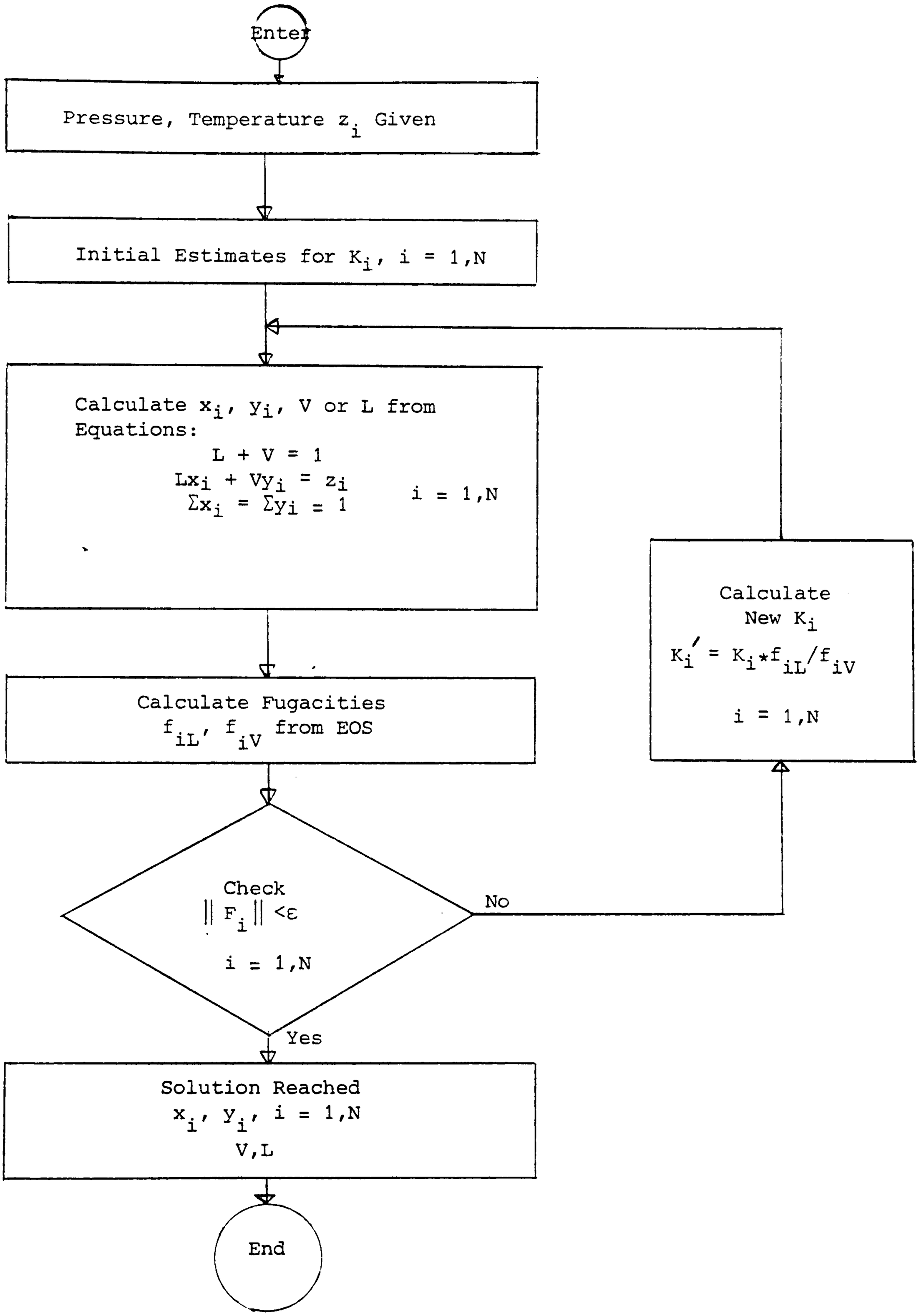

FIGURE 6-5

FLOWCHART FOR THE ALGORITHM OF AN ISOTHERMAL FLASH CALCULATION USING SECOND ORDER NEWTON METHOD

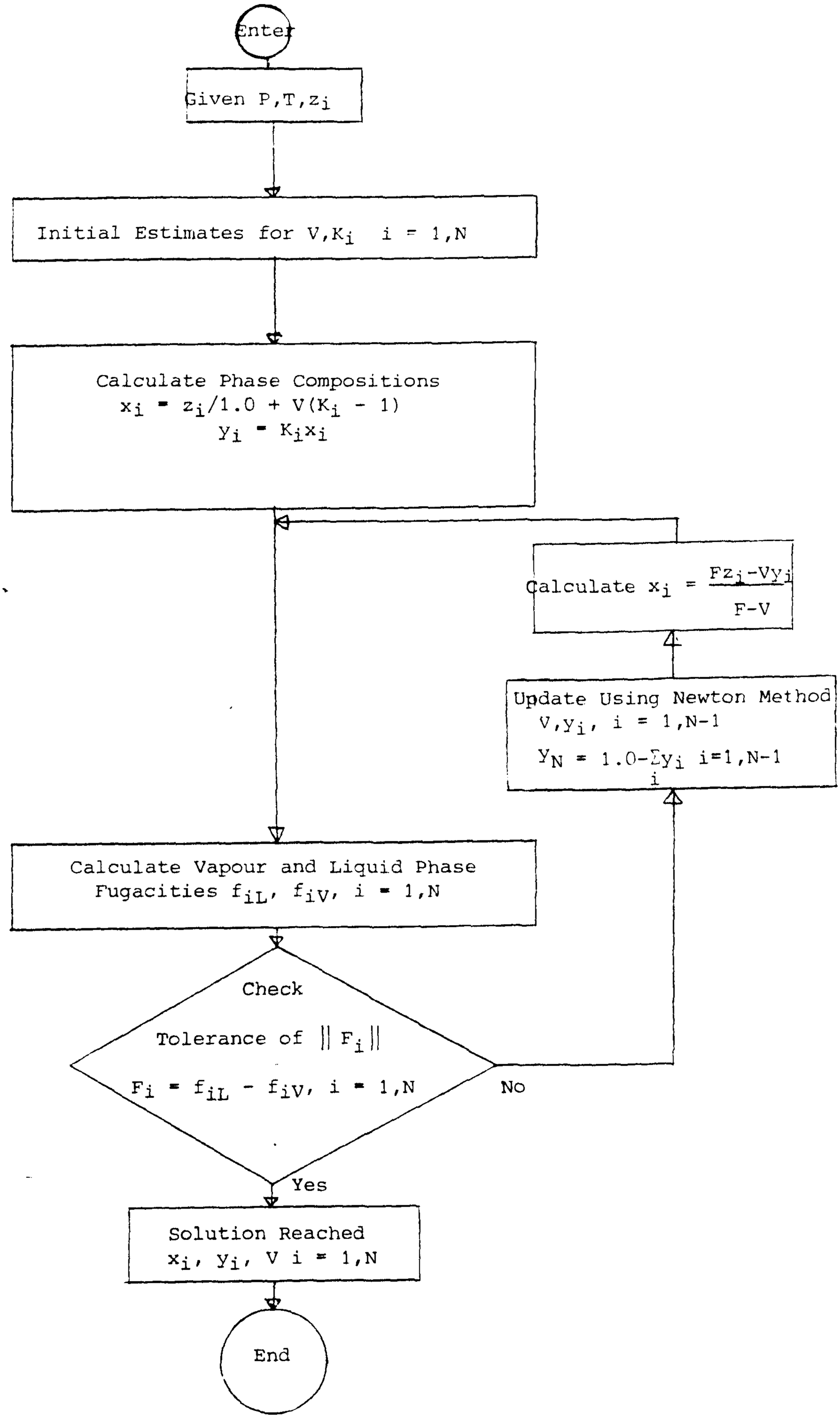

variables are the dependent variables and they are determined from the independent variables using the defining equations.

An equal number of defining equations and dependent variables is required. The remaining equations, equal in number to the number of iteration variables, are called the error equations. By reducing the number of variables to a minimum, the computational cost for each iteration is reduced drastically.

6.3.3 Isothermal Flash Calculation

A mixture of F moles of overall composition z_i, i = 1,N is brought at pressure P and temperature T in equilibrium. Two phases are going to be formed; L moles will form a liquid phase of composition x_i, i = 1,N and V moles will form a vapour phase of composition y_i, i = 1,N. The total number of unknown variables is 4N + 2 (L,V,N liquid phase fugacities, N vapour phase fugacities, N liquid compositions, N vapour compositions).

In the model, only n(n = N) variables are treated as independent variables, either the vapour molar fraction V and the N-1 vapour phase compositions or

the liquid molar fraction L and N-1 liquid phase compositions. The former applies when the mixture is characterised as predominantly vapour and the latter when predominantly liquid.

6.3.4 Mixture Predominantly Liquid

Mathematical Formulation of the Problem

With respect to the general mathematical formulation of the problem (6.3.1), there is the following correspondence between the generalised variables and the physical variables.

$\bar{x} = (x_1, x_2, \ldots\ldots, x_n)^T$ where $n = N$

$x_1 = V$

$x_2 = y_2$

$x_3 = y_3$

$\vdots$

$x_N = y_N$

$F = (F_1, F_2, \ldots\ldots, F_n)^T$ where $F_i = f_{iL} - f_{iV}$ $i = 1, N$

$\bar{h} = (h_1, h_2, \ldots\ldots, h_m)^T$ where $m = 3N + 2$

$$h_1 = 1 - \sum_{i=2}^{N} y_i$$

$h_2 = F - V$

$$h_3 = \frac{Fz_1 - Vy_1}{F - V}$$

$\vdots$

$$h_{N+2} = \frac{Fz_N - Vy_N}{F - V}$$

$h_{N+3} = f_{1L}$

$\vdots$

$h_{2N+2} = f_{NL}$

$h_{2N+3} = f_{1V}$

$\vdots$

$h_{3N+2} = f_{NV}$

$$\bar{Y} = (Y_1, Y_2, \ldots\ldots, Y_m)^T,$$

$$Y_i = h_i(\bar{x}) \qquad \text{where} \qquad m = 3N + 2$$

$$Y_1 = y_1$$

$$Y_2 = L$$

$$Y_3 = x_1$$

$$\vdots$$

$$Y_{N+2} = x_N$$

$$Y_{N+3} = f_{1L}$$

$$\vdots$$

$$Y_{2N+2} = f_{NL}$$

$$Y_{2N+3} = f_{1V}$$

$$\vdots$$

$$Y_{3N+2} = f_{NV}$$

Initial Estimates of Iteration Variables

The iteration starts with V = 0 and the N-1 vapour phase compositions determined previously by the bubble point calculation. The reason that a saturation condition calculation preceeds a flash calculation, is because:

(i) As it will be discussed later, the existing equations and correlations to obtain initial values for the phase compositions are very poor and these poor estimates sometimes slow down or even fail the Newton type iteration methods.

(ii) The saturation conditions calculated beforehand allow the operator to know if at the conditions of the flash, the mixture is in the two phase region, or if it lies on the single phase area outside the phase envelope and hence a possible answer to the flash problem will be a trivial solution.

Defining Equations

The total hydrocarbon mole balance is used to calculate L

$$L = F - V \quad \ldots\ldots\ldots\ldots\ldots\ldots \quad \text{Eq 6-11}$$

The restrictive equation on the vapour phase compositions is used to calculate the composition of the first component in the vapour phase y_1

$$Y_1 = 1 - \sum_{i=2}^{N} y_i \quad \ldots\ldots\ldots\ldots\ldots\ldots \quad \text{Eq 6-12}$$

The component balance equations are used to calculate the liquid mole fractions using the assumed vapour mole fractions and vapour molar fraction V.

$$x_i = \frac{Fz_i - Vy_i}{F - V} \quad \ldots\ldots\ldots\ldots\ldots\ldots \quad \text{Eq 6-13}$$

The equation of state is used to calculate the liquid and vapour compressibility factors.

Equations 5-19, 5-24, 5-26 are used to calculate the liquid and vapour phase fugacity coefficients ϕ_i and then the fugacities of the two phases.

Error Equations

The N thermodynamic phase equilibria equations are used in the form

$$F_i = f_{iL} - f_{iV} \quad 1 \leq i \leq N \quad \ldots\ldots\ldots\ldots\ldots\ldots \quad \text{Eq 6-14}$$

$$f_{iL} = f_{iL}(x_j), \qquad f_{iV} = f_{iV}(Y_j) \qquad j = 1,N$$

If the Euclidean norm of the residuals F_i's is less than a specified error tolerance, it is assumed that the values for the iteration variables used for that iteration are the solutions to the problem and the iterative sequence ends. If not, the iteration variables are updated using a correction step which utilises the information gained by the previous step.

6.3.5 Mixture Predominantly Vapour

Mathematical Formulation of the Problem

As far as the general mathematical formulation of the problem (6.3.1) is concerned, the following correspondence between the generalised mathematical variables and the physical variables can be asserted.

$\bar{\underline{x}} = (\underline{x}_1, \underline{x}_2, \ldots\ldots, \underline{x}_n)^T$ where $n = N$

$\underline{x}_1 = L$

$\underline{x}_2 = x_2$

$\vdots$

$\underline{x}_N = x_N$

$\bar{F} = (F_1, F_2, \ldots\ldots, F_n)^T$ where $F_i = f_{iL} - f_{iV}$ $i=1,N$

$\bar{h} = (h_1, h_2, \ldots\ldots, h_m)^T$ where $m = 3N + 2$

$$h_1 = 1 - \sum_{i=2}^{N} x_i$$

$$h_2 = F - L$$

$$h_3 = \frac{Fz_1 - Lx_1}{F - L}$$

$\vdots$

$$h_{N+2} = \frac{Fz_N - Lx_N}{F - L}$$

$$h_{N+3} = f_{1L}$$
$$\vdots$$
$$h_{2N+2} = f_{NL}$$

$$h_{2N+3} = f_{1V}$$
$$\vdots$$
$$h_{3N+2} = f_{NV}$$

$\bar{Y} = (Y_1, Y_2, \ldots, Y_m)^T$, $Y_i = h_i(\bar{x})$

where $m = 3N + 2$

$$Y_1 = x_1$$

$$Y_2 = V$$

$$Y_3 = y_1$$
$$\vdots$$
$$Y_{N+2} = y_N$$

$$Y_{N+3} = f_{1L}$$
$$\vdots$$
$$Y_{2N+2} = f_{NL}$$

$$Y_{2N+3} = f_{1V}$$
$$\vdots$$
$$Y_{3N+2} = f_{NV}$$

Initial Estimates of Iteration Variables

The iteration starts with L = 0 and N-1 liquid phase compositions determined previously by the dew point calculation.

Defining Equations

The total hydrocarbon mole balance is used to calculate V

$$V = F - L$$

The restrictive equation on the liquid phase compositions is used to calculate the composition of the first component in the liquid phase x_1.

$$x_1 = 1 - \sum_{i=2}^{N} x_i$$

The component balance equations are used to calculate the vapour mole fractions using the assumed liquid mole fractions x_i and liquid molar fraction L.

$$y_i = \frac{Fz_i - Lx_i}{F - L} \qquad i = 1,N$$

The equation of state is used to calculate the liquid and vapour compressibility factors. Equations 5-19, 5-24, 5-26 are used to calculate the liquid and vapour phase fugacity coefficients ϕ_i and then the fugacities of the two phases.

Error Equations

The Euclidean norm of the residuals of the thermodynamic phase equilibria equations

$$F_i = f_{iL} - f_{iV} \qquad 1 \leq i \leq N$$

where

$$f_{iL} = f_{iL}(x_j)$$

$$f_{iV} = f_{iV}(y_j) \qquad j = 1,N$$

should be less than a specified tolerance.

6.3.6 Bubble Point Calculation

The total number of variables in this case is 3N + 1 (P or T,N vapour compositions, N vapour phase fugacities and N liquid phase fugacities). Although according to the minimum variable iteration method only N of the variables should be iterated, in the model N + 1 variables are treated as independent; the N compositions of the

vapour phase and either the saturation pressure or the saturation temperature (n = N + 1). The reason the Nth composition of the vapour is treated as an extra iteration variable and is not calculated from the restrictive equation on the phase mole fractions

$$y_N = 1 - \sum_{i=1}^{N-1} y_i$$

is that experience showed that the robustness of the method increased considerably in the former case. The explanation is that in the latter case the Nth composition as being calculated from the summation of the N - 1 compositions accumulates the deviations of these N-1 iteration variables from the solution and therefore does not follow the same rate of convergence.

Mathematical Formulation of the Problem

As far as the mathematical formulation of the problem is concerned (6.3.1), the following correspondence between the generalised mathematical variables and the physical variables can be asserted:

$\bar{\underline{x}} = (\underline{x}_1, \underline{x}_2, \ldots, \underline{x}_n)^T$ where $n = N + 1$

$\underline{x}_1 = P$ or T

$\underline{x}_2 = y_1$

$\underline{x}_3 = y_2$

$\vdots$

$\underline{x}_{N+1} = y_N$

$\bar{F} = (F_1, F_2, \ldots, F_n)^T$ where $F_i = f_{iL} - f_{iV} \quad i=1,N$

$$F_{N+1} = 1 - \sum_{i=1}^{N} y_i$$

$\bar{h} = (h_1, h_2, \ldots, h_m)^T$ where $m = 2N$

$h_1 = f_{1L}(z_i,P,T)$

$h_2 = f_{2L}(z_i,P,T)$

$\vdots$

$h_N = f_{NL}(z_i,P,T) \quad i=1,N$

$h_{N+1} = f_{1V}(y_i,P,T)$

$\vdots$

$h_{2N} = f_{NV}(y_i,P,T)$

$\bar{Y} = (Y_1, Y_2, \ldots, Y_m)^T,$

$\underline{Y_i} = h_i(\bar{x})$ $\quad m = 2N$

$Y_1 = f_{1L}$

$Y_2 = f_{2L}$

$\vdots$

$Y_N = f_{NL}$

$Y_{N+1} = f_{1V}$

$\vdots$

$Y_{2N} = f_{NV}$

Initial Estimates of Iteration Variables

The iteration starts with an assumption for the saturation pressure or temperature given to the program by the operator. The Antoine equation for predicting the vapour pressure of mixtures as the sum of the pure component vapour pressures

$$P_{start} = \sum_{i=1}^{N} \left(\exp\left[A_i - \frac{B_i}{T+C_i}\right] * 2.3026\right) * z_i \qquad \text{Eq 6-15}$$

was used initially to generate the starting value for the bubble point pressure. Experience has shown that these estimates are generally very poor for complex hydrocarbon mixtures and sometimes convergence could not be achieved. In the case that the bubble point temperature has to be calculated the re-arranged Antoine

equation has been tried to provide the starting temperature[3], and this method has also been proved poor. A first estimation for the liquid phase compositions can be taken using the component K-values calculated by the empirical Wilson Equation[4]

$$K_i = \exp\left\{5.37(1 + \omega_i)(1 - 1/T_{ri})\right\}/P_{ri} \qquad 1 \leq i \leq N \qquad \text{Eq 6-16}$$

This equation comes from Hoffman's et al generalised equation[5]

$$\log K_i P = A(P) * F_i(T) + Y(P) \quad . \; . \; . \; . \; . \; . \; . \qquad \text{Eq 6-17}$$

where

$$F_i(T) = \frac{1/T_{ci} - 1/T}{1/T_{bi} - 1/T_{ci}} \log (P_{ci}/P_a), \; P_a = \text{atmospheric pressure}$$

and

$Y(P)$ is the pressure dependent intercept.

These K values are used to flash the overall fluid mixture at the system temperature and an estimated saturation pressure.

Defining Equations

The compressibility factors Z_L and Z_V are calculated by solving the equation of state and the corresponding expression that gives the fugacity coefficients is used to calculate the liquid and vapour fugacities.

Error Equations (N + 1)

The residual of the restrictive equation on the vapour phase mole fractions, plus N equations representing the residual of the thermodynamic phase equilibria expressions are used as error equations.

$$F_i = f_{iL} - f_{iV} \qquad 1 \leq i \leq N$$

$$F_{N+1} = 1 - \sum_{i=1}^{N} y_i \qquad \text{. . . . . Eq 6-18}$$

where

$$f_{iL} = f_{iL}(z_j, P \text{ or } T)$$

$$f_{iV} = f_{iV}(y_j, P \text{ or } T) \qquad j = 1,N$$

Fussel is using a different equation as the F_{n+1} equation[8]

$$F_{n+1} = P_s - \sum_{j=1}^{N} f_{jL}/\Phi_{jV} \qquad \text{. . . . . Eq 6-19}$$

Equation 6-19 was tried in the model but the rate of convergence it was giving was slower than the rate of convergence when Equation 6-18 was used.

6.3.7 Dew Point Calculation

Mathematical Formulation of the Problem

As far as the mathematical formulation of the problem is concerned (6.3.1), the following correspondence between the generalised mathematical variables and the physical variables can be asserted:

$\bar{\underline{x}} = (\underline{x}_1, \underline{x}_2, \ldots, \underline{x}_n)^T$ where $n = N + 1$

$\underline{x}_1 = P$ or T

$\underline{x}_2 = x_1$

$\underline{x}_3 = x_2$

$\underline{x}_{n+1} = y_N$

$\bar{F} = (F_1, F_2, \ldots, F_n)^T$ where $F_i = f_{iL} - f_{iV}$ $\quad i=1,N$

$$F_{N+1} = 1 - \sum_{i=1}^{N} x_i$$

$h = (h_1, h_2, \ldots, h_m)^T$ where $m = 2N$

$$h_1 = f_{1L}(x_i, P, T)$$
$$h_2 = f_{2L}(x_i, P, T)$$
$$\vdots \qquad i=1,N$$
$$h_N = f_{NL}(x_i, P, T)$$
$$h_{N+1} = f_{1V}(z_i, P, T)$$
$$\vdots$$
$$h_{2N} = f_{NV}(z_i, P, T)$$

$\bar{Y} = (Y_1, Y_2, \ldots, Y_m)^T$, $m = 2N$

$Y_i = h_i(\bar{x})$

$$Y_1 = f_{1L}$$
$$Y_2 = f_{2L}$$
$$\vdots$$
$$Y_N = f_{NL}$$
$$Y_{N+1} = f_{1V}$$
$$\vdots$$
$$Y_{2N} = f_{NV}$$

Initial Estimates of Iteration Variables

The same method for the calculation of the initial estimates of the independent variables with the bubble point calculation is followed.

Defining Equations

They are the same as with the bubble point calculation.

Error Equations (N+1)

The residual of the restrictive equation on the liquid phase mole fractions is used as the F_{N+1} equation

$$F_{N+1} = 1 - \sum_{i=1}^{N} x_i$$

6.3.8 Ternary Phase Envelope Calculation

A type of calculation very useful for the design of a gas miscible flooding in a reservoir, is the construction of the phase envelopes of mixtures of the injection gas and reservoir fluid at any ratio, on a ternary diagram at the temperature of the reservoir and the pressure of the injection.

This representation, although it simplifies the complexities of the multicomponent phase equilibrium into that of the three components' system, gives useful visual conception of the mass transfer between the phases of the reservoir fluid and of the advancing injection gas. It can also determine, with a fair degree of accuracy, the miscibility path and gives indication of the minimum miscibility pressure required for a particular application. More extended discussion on the advantages and disadvantages of the ternary representation has been expounded in Chapter 4.

The construction of the phase envelope in a ternary diagram is another option of the simulation model VLE. The components of the multicomponent mixture are grouped into three pseudocomponents (usually injection gas, intermediates and heavy components) with overall mole fractions z_G, z_I, z_H in such a way that each individual component belongs to one and only one pseudocomponent. This option starts with an isothermal flash calculation for a mixture whose composition lies on the side of the triangle (Fig 6-6), where the mole fraction of the intermediates is zero, at the

FIGURE 6-6

TERNARY PHASE ENVELOPE CALCULATION

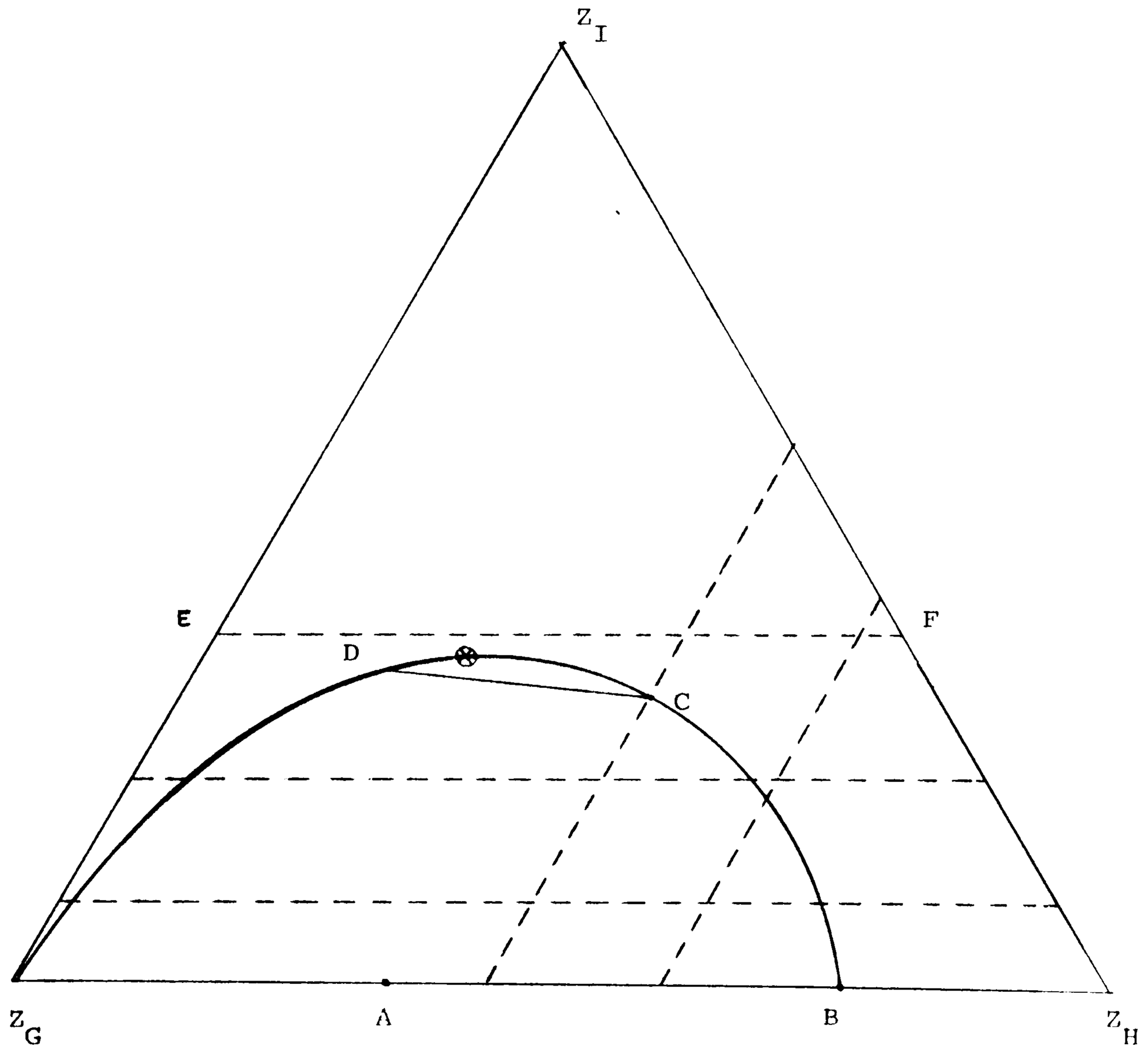

specified temperature and pressure. The vapour and liquid compositions in equilibrium are determined on the same side of the triangle (z_I = 0.0) (Fig 6-6) and they define the two points where the phase envelope intersects that side. The program then performs a series of bubble point calculations at the same T and P, starting from the liquid mixture of composition B and following the saturation curve towards the critical point. The mole fraction of the one of three pseudocomponents is specified and determines the calculation step, the mole fraction of the second pseudocomponent is an independent variable and the mole fraction of the third component is a dependent one calculated from the restrictive equation on the mole fractions and the other two. In other words, the problem is to find for each mixture comprising of a specified mole fraction of one component, the mole fraction of the other component so that the mixture can be saturated at the specified T and P, and determine the composition of the vapour phase in equilibrium with the liquid.

Mathematical Formulation of the Problem

As far as the mathematical formulation of the problem is concerned (6.3.1), the following correspondence between the generalised mathematical variables and the physical variables can be asserted:

$\bar{\underline{x}} = (\underline{x}_1, \underline{x}_2, \ldots, \underline{x}_n)^T$ where $n = N$

$\underline{x}_1 = z_H$

$\underline{x}_2 = y_2$

$\vdots$

$\underline{x}_N = y_N$

$\bar{F} = (F_1, F_2, \ldots, F_n)^T$ where $F_i = f_{iL} - f_{iV}$ $i=1,N$

and $f_{iL} = f(z_H)$, $f_{iV} = f(Y_j)$

$j = 1,N$

$\bar{h} = (h_1, h_2, \ldots, h_m)^T$ where $m = 2N + 2 + \ell$

$$h_1 = 1.0 - (z_I + z_H)$$

$$h_2 = 1 - \sum_{i=2}^{N} Y_i$$

$h_3 = f_{1L}$

$h_4 = f_{2L}$

$\vdots$ $\quad i = 1,N$

$h_{N+2} = f_{NL}$

$h_{N+3} = f_{1V}$

$\vdots$ $\quad i = 1,N$

$h_{2N+2} = f_{NV}$

$h_{2N+3} = z_H * x_j$

$h_{2N+4} = z_H * x_{j+1}$

$\vdots$

$h_{2N+2+\ell} = z_H * x_N$

$x_j, \ldots, x_N$ are the mole fractions of the components grouped in the heavy pseudocomponent in the original reservoir fluid, j-2 the number of the components of the intermediate and ℓ the number of the components in the heavy pseudocomponent

$\bar{Y} = (Y_1, Y_2, \ldots, Y_m)$ where $m = 2N + 2 + \ell$

$Y_1 = z_G$

$Y_2 = x_1$

$Y_3 = f_{1L}$

$\vdots$

$Y_{N+2} = f_{NL}$

$Y_{N+3} = f_{1V}$

$Y_{2N+2} = f_{NV}$

$$Y_{2N+3} = x_j$$

$$Y_{2N+4} = x_{j+1}$$

$$\vdots$$

$$Y_{2N+2+\ell} = x_N$$

Initial Estimates of the Iteration Variables

The iteration starts with the vapour phase compositions of the isothermal flash calculation as initial estimates for the vapour phase mole fractions of the second problem. The mole fraction z_I of the intermediate component (z_I = 0.0 at start) is specified at the begining of each calculation. Big steps of the z_I can cause problems to the calculation (non convergence) and uncertainty on the drawing of the phase envelope. The initial estimate for the iteration variable z_H is the mole fraction of the heavy component of the liquid phase of the previous calculation.

Defining Equations

The restrictive equation on the vapour phase compositions is used to calculate the composition of the first component in the vapour phase y_1

$$y_1 = 1 - \sum_{i=2}^{N} y_i$$

The restrictive equation on the three pseudocomponents mole fractions is used to determine the mole fraction of the injection gas z_G:

$$z_G = 1.0 - (z_I + z_H) \quad \ldots\ldots\ldots\ldots \quad \text{Eq 6-20}$$

The compressibility factors Z_L and Z_V are calculated by solving

the equation of state and its expression that gives the fugacity coefficient is used to calculate the liquid and vapour fugacities.

Error Equations

The N thermodynamic phase equilibria equations

$$F_i = f_{iL} - f_{iV}, \quad 1 \leq i \leq N$$

Extrapolation Technique

After the three first calculations have been performed, the quadratic extrapolation technique is used to speed up the calculations by providing initial values for the next problem, very close to the answer. This technique is explained in detail in section 6.4.2.

Increments of the z_I

The program decides itself about the size of the next increment of the specified variable z_I, according to the ease with which the previous problem was solved, (ie the number of iterations required and the number of times the Jacobian had to be recalculated). The user has specified from the begining the upper and lower limits of the increments.

Change in Iteration Variables

Sometimes depending on the shape of the phase envelope and particularly on the position of the critical point, a change in the choice of the

independent variable z_H has to be considered. After the saturated liquid C (Figure 6-6) has been determined in equilibrium with the vapour D, the next increment of the z_I may determine a line EF

which does not intersect the phase envelope at any point. This means that there is not a mixture having z_I mole fraction and being saturated at the specified pressure and temperature. In such a case, the algorithm fails to converge and returns back to the previous solution. To complete the phase envelope, z_H is now specified before each calculation and z_I becomes the independent variable. When the K-value of the injection gas comes very close to unity (≤ 1.005), then the calculations terminate and the bubble and dew point curves, as they have been determined by the liquid and vapour phase compositions in equilibrium on the ternary diagram, close using interpolation. The liquid and vapour phases of all calculations, expressed as three component mixtures are stored in a file, which can be called later to plot the phase envelope.

6.4 ITERATIVE UPDATING TECHNIQUE

6.4.1 Updating Technique used in this Study

The purpose of the correction step is to obtain improved estimates of the iteration variables that in turn will reduce the residuals calculated by the selected error equations. The correction step reduces to a matrix problem with an order equal to the number of the iterative variables. The problem consists of finding an array of values of $\underline{\bar{x}}_i$, denoted by $(\underline{\bar{x}}^*)$ which satisfies the equations

$$F_i(\underline{x}_1, \underline{x}_2, \ldots, \underline{x}_n) = 0 \quad i = 1,n \quad \ldots \quad \text{Eq 6-21}$$

where $F_i(\underline{x}_1, \underline{x}_2, \ldots, \underline{x}_n)$ is an array of non-linear multi-variable functions.

If $\underline{\bar{x}}^{(k)}$ is the vector of values of the iteration variables at the k-th iteration, an array $\Delta\underline{\bar{x}}^{(k)}$ is required which will provide the updated values for the iteration variables at the (k+1)th iteration.

$$\underline{\bar{x}}^{(k+1)} = \underline{\bar{x}}^{(k)} + \Delta\underline{\bar{x}}^{(k)} \quad \ldots \quad \text{Eq 6-22}$$

The whole philosophy of the iterative methods is based on the replacement of the non-linear functions F at each point, by linear ones L which approximate as closely as possible the functions F. The linear equations are then solved and their roots are used as the new approximations to the roots of the functions F. If these values do not reduce to zero the residual of the error equations, new linear functions are chosen until the F's and L's have the same roots. The basic form of iteration is therefore the solution of a sequence of linearised problems by a standard method. The

selection of the linear functions at each step is what makes the difference between the various iteration methods.

For this study, a quasi-Newton method is used. In Newton's method the linear function L, which approximates the function F, is obtained by truncating the Taylor series expansion of the non-linear function after the first order term.

$$L(\underline{\bar{x}}) = F(\underline{\bar{x}}^o) + F'(\underline{\bar{x}}^o)(\underline{\bar{x}} - \underline{\bar{x}}^o) \quad \ldots\ldots\ldots \quad \text{Eq 6-23}$$

In the graphic representation of the Newton method, a non-linear function F of one variable $\underline{x}$ is approximated by the linear function L tangent to F at any point (Fig 6-7). Obviously the root $\underline{\bar{x}}^1$ of the linear function does not coincide with the root of the non-linear function $\underline{\bar{x}}^*$. The updated value $\underline{\bar{x}}^1$ is given by the equation

$$\underline{\bar{x}}^1 = \underline{\bar{x}}^o + \frac{F(\underline{\bar{x}}^o)}{F'(\underline{\bar{x}}^o)} \quad \ldots\ldots\ldots\ldots\ldots\ldots \quad \text{Eq 6-24}$$

$\underline{\bar{x}}^1$ is used as the value of the independent variable for the new iteration. $\underline{\bar{x}}^1$ should be closer to the solution $\underline{\bar{x}}^*$ than the value $\underline{\bar{x}}^o$ of the previous iteration. In the case that the function F close to the solution has a point of inflexion or a turning point, then the value $\underline{\bar{x}}^1$ for the next iteration provided by the Newton method may be further from the solution than the value of the previous iteration $\underline{\bar{x}}^o$ (Fig 6-8). In that case a step size control has to be used to reduce the size of the step and ensure final convergence. The full Newton step with step size control is given by the equation

FIGURE 6-7

GRAPHICAL REPRESENTATION OF NEWTON-RAPHSON METHOD

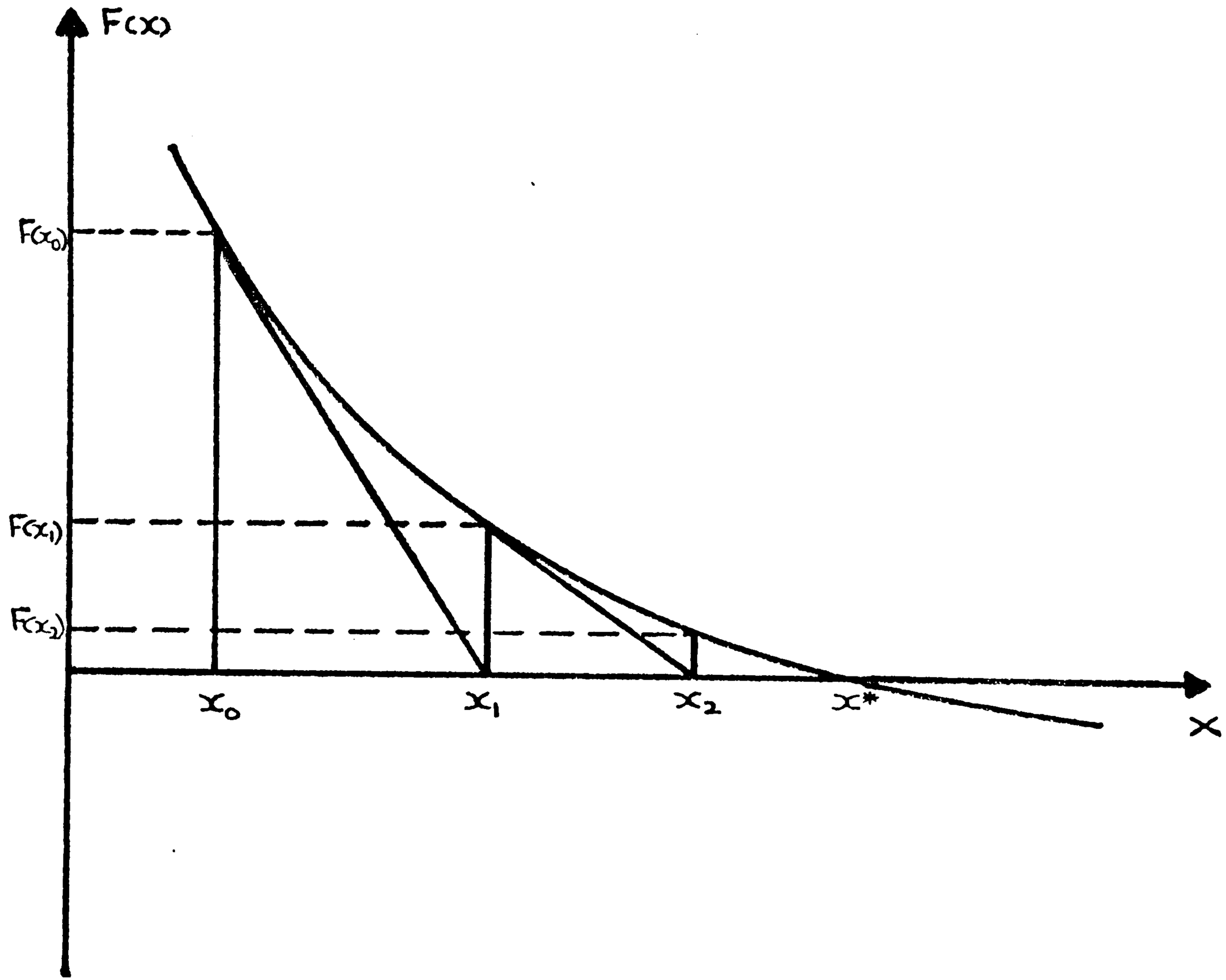

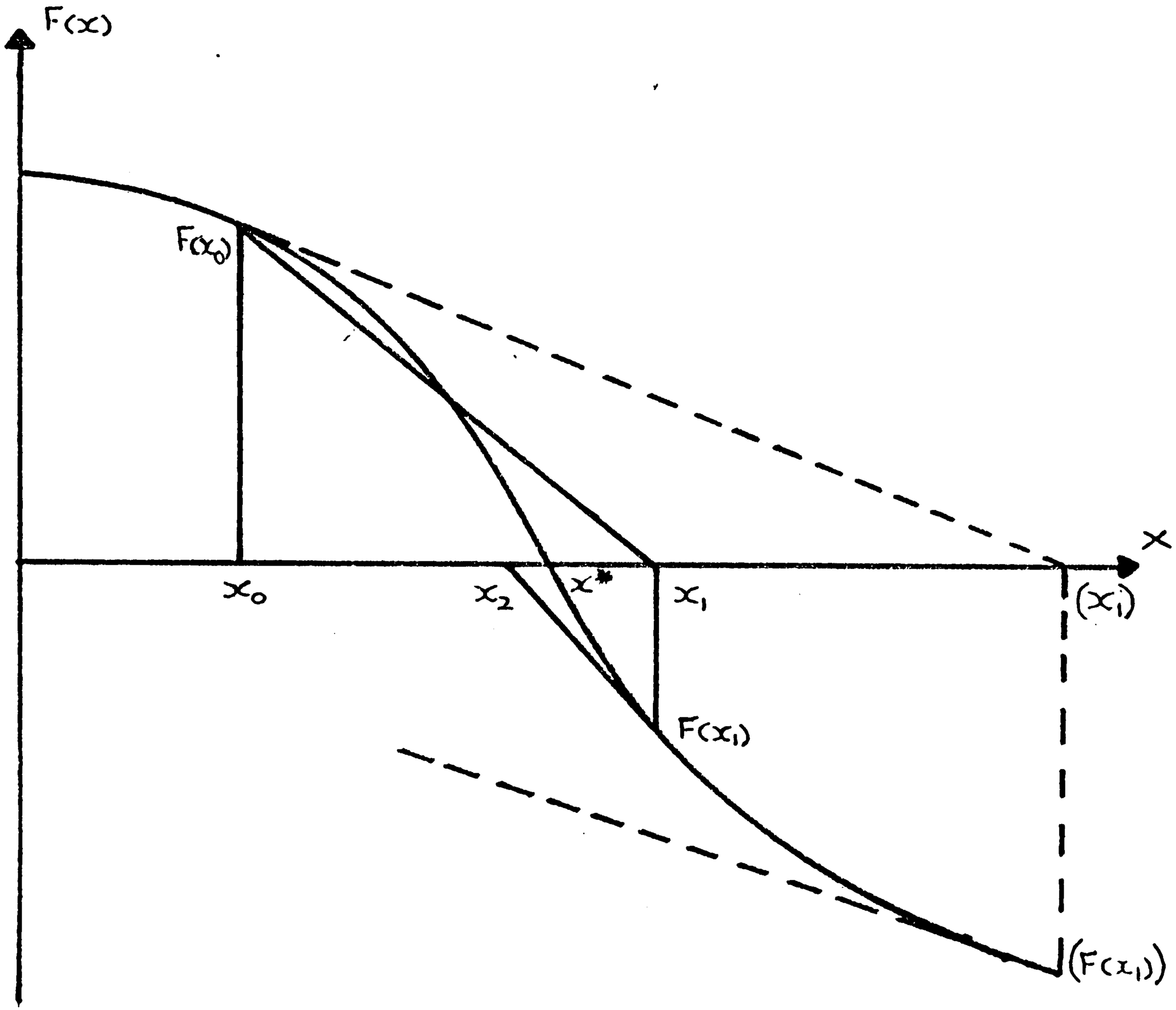

USE OF STEPSIZE CONTROL

FIGURE 6-8

$$\underline{\bar{x}}^1 = \underline{\bar{x}}^0 + \alpha \frac{F(\underline{\bar{x}}^0)}{F'(\underline{\bar{x}}^0)} \quad \ldots\ldots\ldots\ldots\ldots \quad \text{Eq 6-25}$$

with α chosen such that

$$||F(\underline{\bar{x}}^1)|| < ||F(\underline{\bar{x}}^0)||$$

Equation (6-22) can be written:

$$\underline{\bar{x}}^1 = \underline{\bar{x}}^0 + \alpha\Delta\underline{\bar{x}}^0, \quad \Delta\underline{\bar{x}}^0 = F(\underline{\bar{x}}^0)/F'(\underline{\bar{x}}^0) \quad \ldots\ldots \quad \text{Eq 6-26}$$

Although Newton's method converges quadratically towards the solution and convergence rate when close to the solution is very fast indeed, the full Newton step has several disadvantages:

(i) The non-linear functions F should be analytically differentiable.

(ii) n^2 function evaluations are required per step, where n is the number of the linear functions F.

(iii) The Jacobian matrix should be inverted.

(iv) The algorithm may diverge if the starting values for the iteration variables are very poor.

The items (i) - (iii) contribute to long computer time and high algebraic complexity, whereas item (iv) is dealing with the robustness of the algorithm. To overcome these problems a modification of the Newton method was used:

- With regard to item (i), analytical differentiation has been replaced with numerical differentiation avoiding the complex algebra.
- With regard to item (iii), Broyden's rank-one updating formula[8] is used to approximate the inverse Jacobian for the next iteration using the information collected from previous steps. In that way the need for

calculating and inverting the Jacobian at each cycle is eliminated.

- As far as item (iv) is concerned, a three point continuation method is used to provide improved initial estimates for the next calculations when successive slightly different problems are being solved. The continuation method used in the study will be discussed later.

Before Broyden's method is discussed, the underlying principle of his updating technique will be illustrated with the use of two non-linear equations in two variables $F_1(x_1,x_2)$ and $F_2(x_1,x_2)$. Figure 6-9 provides a visualisation of the geometry of the problem where the $F_1(x_1,x_2)$ and $F_2(x_1,x_2)$ are represented by two surfaces intersecting each other at the point (x_1^*,x_2^*) on the coordinate plane. The point (x_1^*,x_2^*) corresponds to the solution of the system of the equations. Suppose an initial estimate of the solution is denoted by (x_1^o,x_2^o). A linear approximation L_1^o to F_1^o is constructed which is defined by its gradients in the coordinate directions and a point through which it passes. If analytical differentiation is used and thereby the elements of the Jacobian are calculated precisely, the full Newton method is used. The gradients which define the plane L_1^o can be approximations to the gradients of the Jacobian at the point (x_1^o, x_2^o). That can be done by differentiating numerically the function $F_1(x_1,x_2)$ at the point (x_1^o,x_2^o). The plane L_1^o intersects the x_1,x_2 coordinate plane and in conjunction with the intersection of the corresponding approximation L_2^o to the function $F_2(x_1,x_2)$, the estimation for the next iteration (x_1^1,x_2^1) is obtained. The functions are re-evaluated at the new point yielding F_1^1 and F_2^2

(Figure 6-10). The step from (x_1^0, x_2^0) to (x_1^1, x_2^1) defines a direction vector $\bar{P}_o = \Delta\bar{x}^o$ (Fig 6-11). The important point is that the information about the rate of change of the functions F_1 and F_2 in the direction $\bar{p}_o$ has been gained from the function evaluations at (x_1^0, x_2^0) and (x_1^1, x_2^1). The method follows Broyden's suggestion that the next approximation to the Jacobian at (x_1^1, x_2^1) should satisfy the condition that the gradient of the approximating hyperplane in the direction of the previous step p_o, should be the slope of the chord (F_1^0, x_1^0, x_2^0) to (F_1^1, x_1^1, x_2^1) for the function F_1 and of the chord (F_2^0, x_1^0, x_2^0) to (F_2^1, x_1^1, x_2^1) for the function F_2. For the second gradient needed to define the new hyperplane, Broyden suggested that since no new information on function behaviour has been obtained, the gradient of the approximation hyperplane in a direction q_o orthogonal to p_o, should remain unchanged. In accordance with that suggestion the updating technique consists of rotating the hyperplanes L_1^o and L_2^o about an axis co-linear with its gradient in the q_o direction and jacking up the plane until it passes through the new points (F_1^1, x_1^1, x_2^1) and (F_2^1, x_1^1, x_2^1) (Fig 6-12).

The equations:

$$\Delta\underline{\bar{x}}^k = - H^k \bar{F}^k$$

$$\underline{\bar{x}}^{k+1} = \underline{\bar{x}}^k + \alpha\Delta\underline{\bar{x}}^k$$

$$\underline{Y}^k = \bar{F}^{k+1} - \bar{F}^k$$

$$\bar{P}^k = \Delta\underline{\bar{x}}^k$$

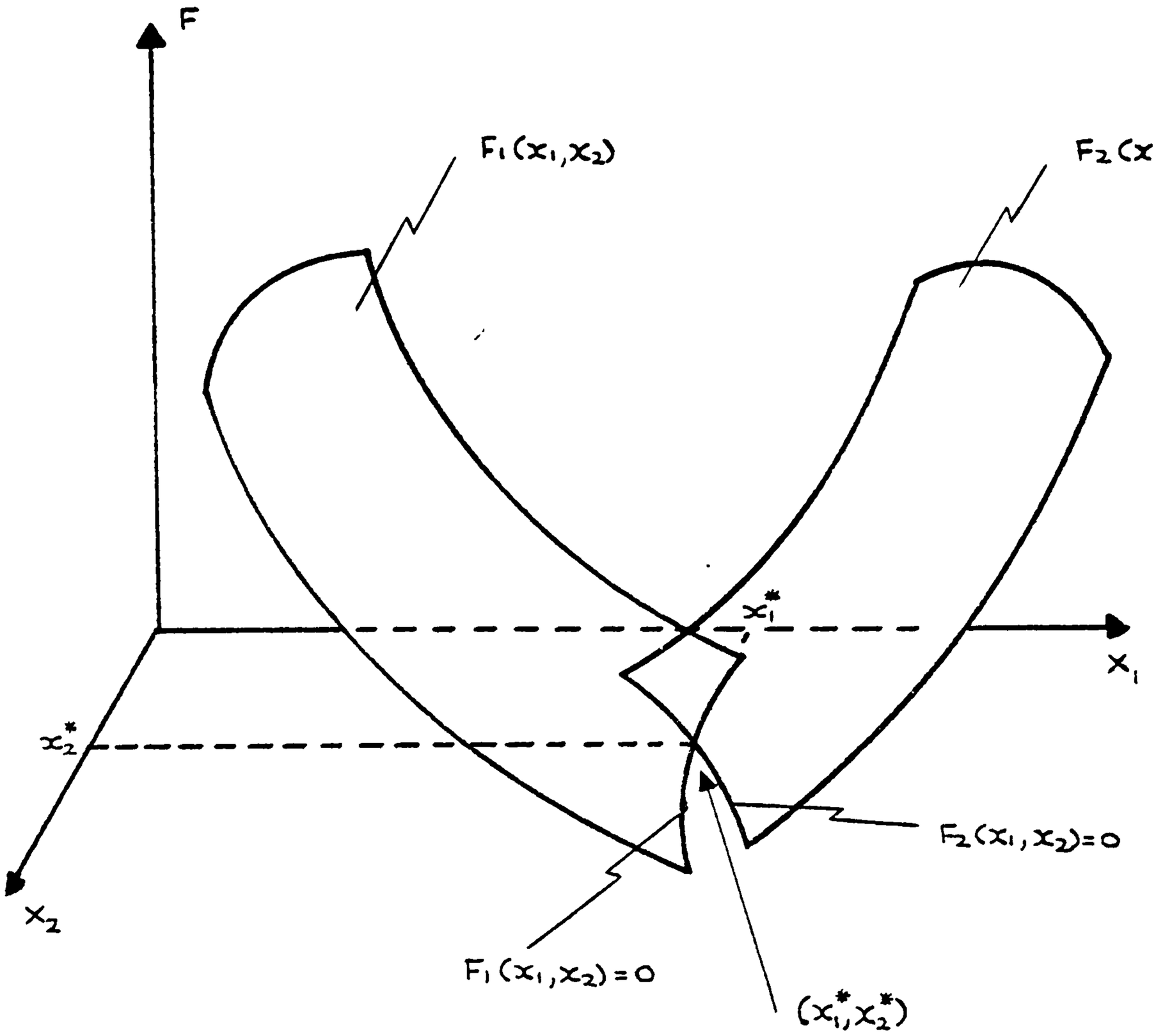

FIGURE 6-9

THREE DIMENSIONAL REPRESENTATION OF TWO NON LINEAR EQUATIONS IN TWO VARIABLES

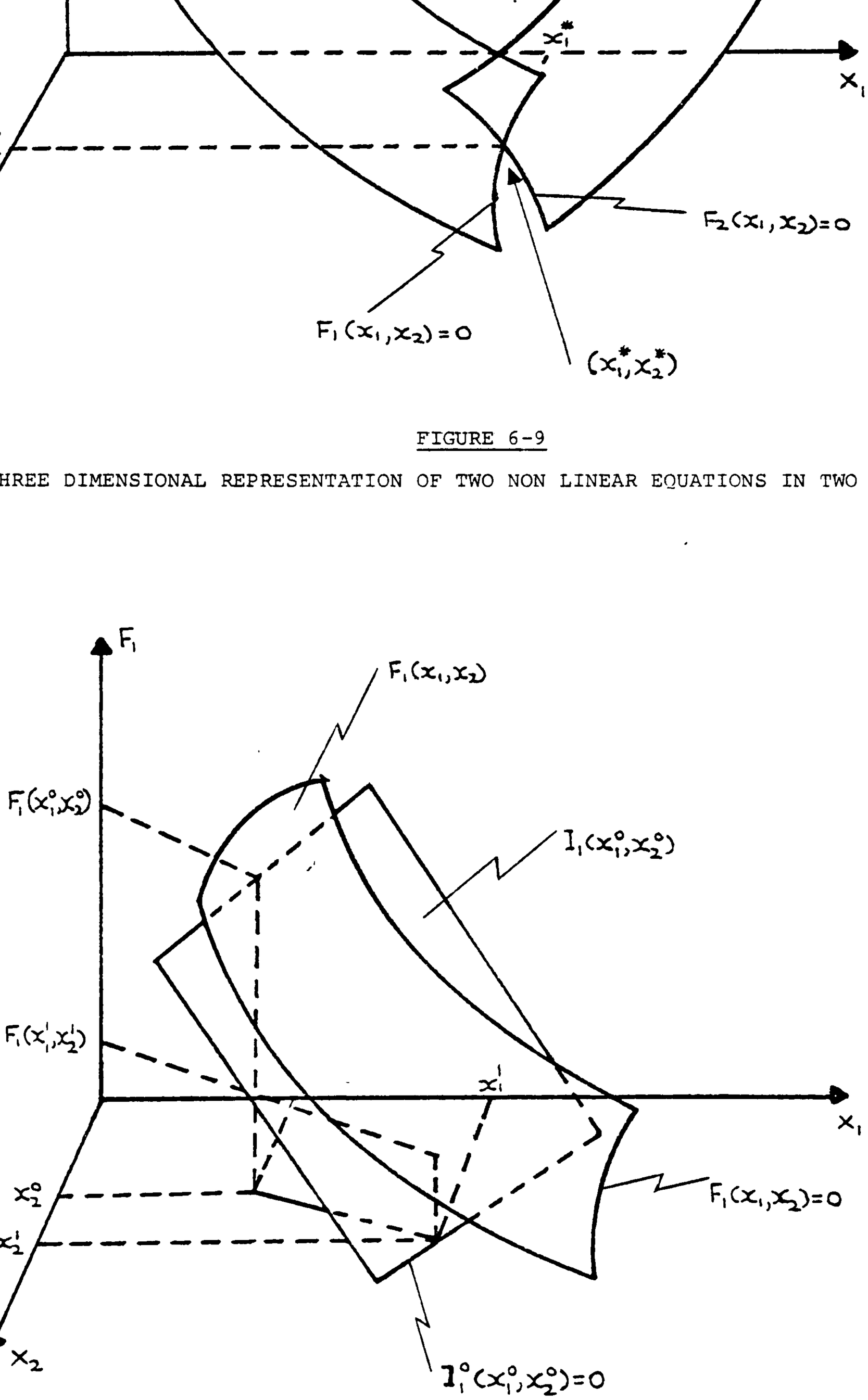

HYPERPLANE APPROXIMATING NON-LINEAR FUNCTION

FIGURE 6-10

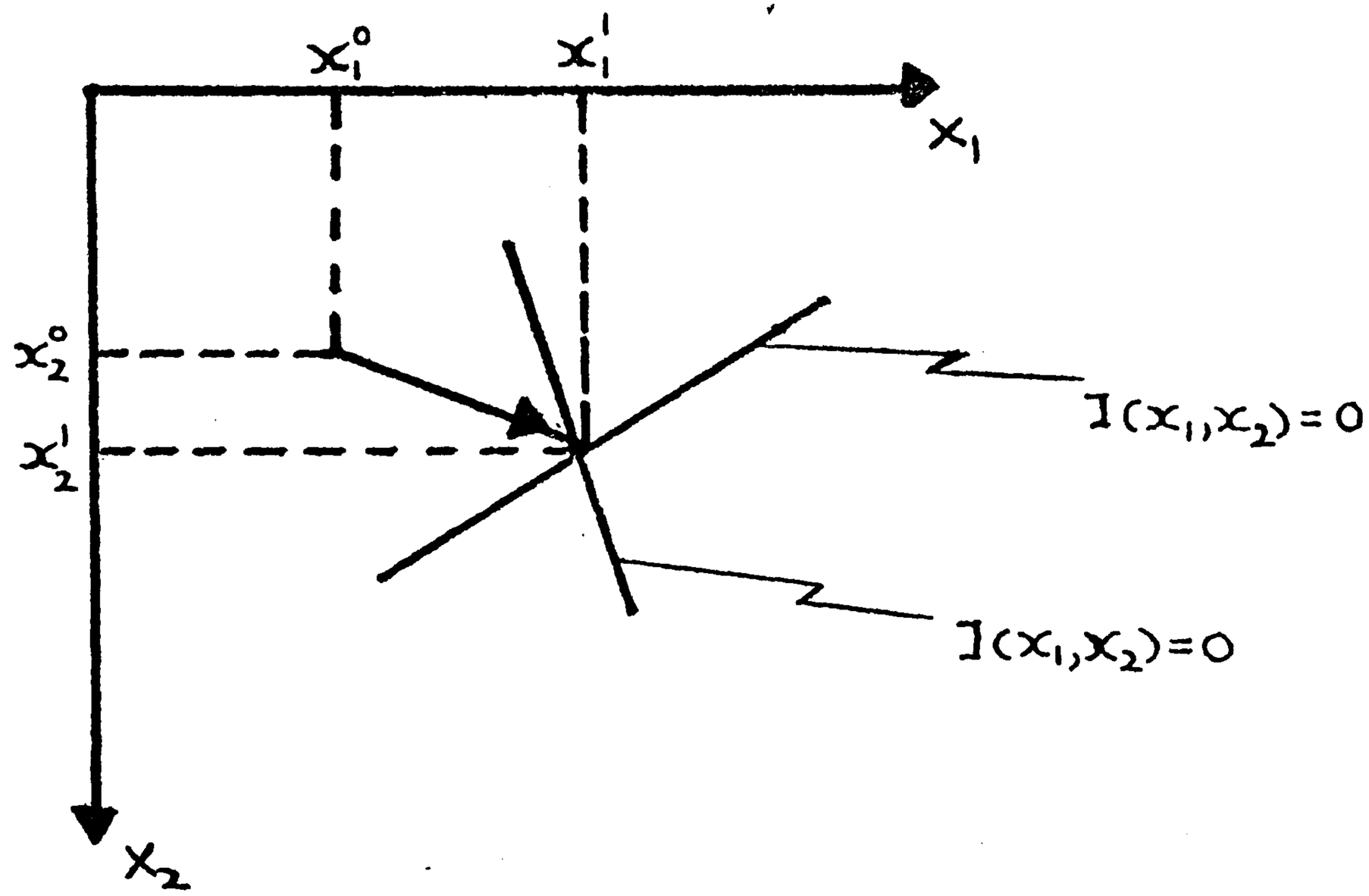

DIRECTION OF THE APPROACH TO THE SOLUTION

FIGURE 6-11

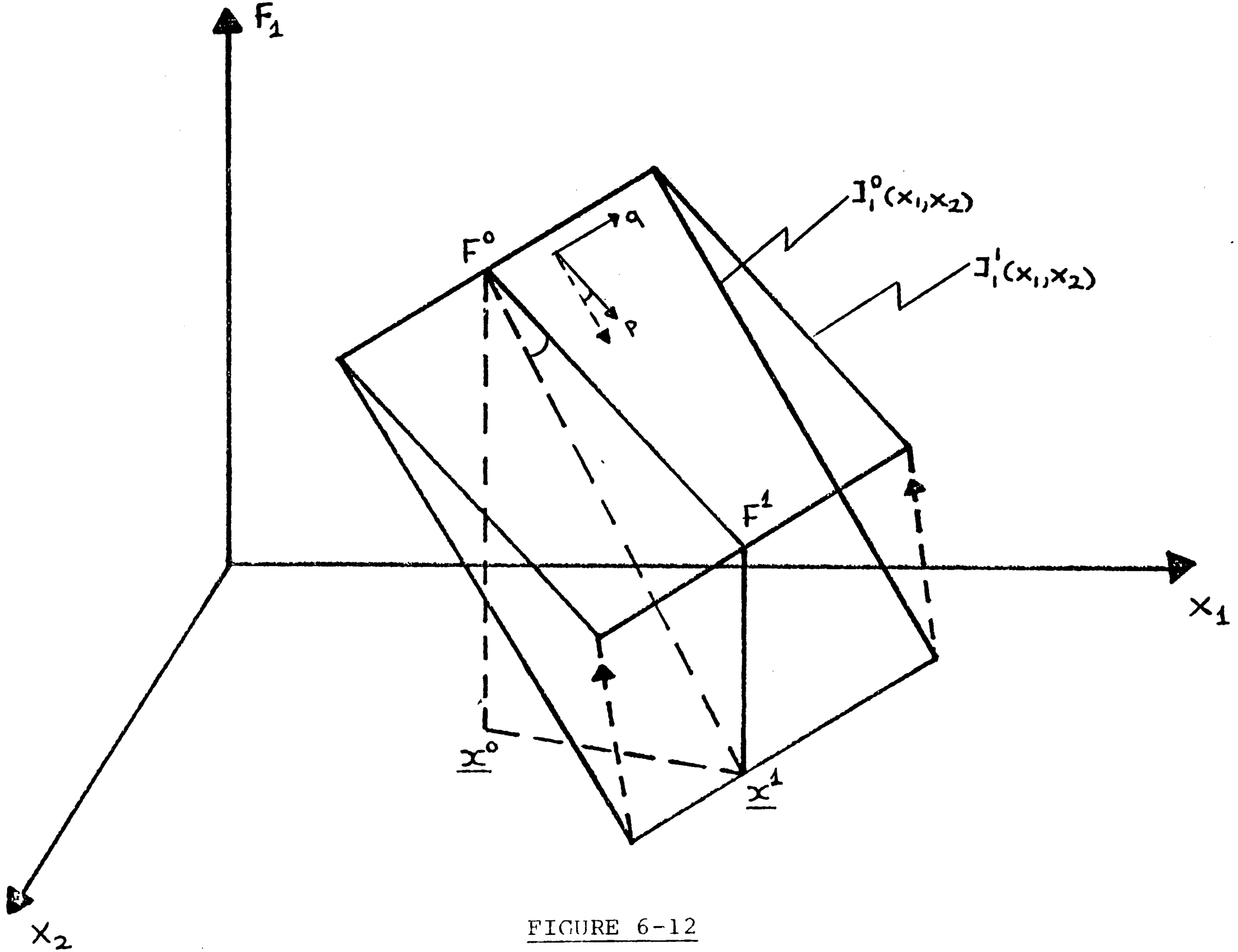

FIGURE 6-12

GEOMETRIC INTERPRETATION OF BROYDEN'S UPDATE FORMULA

$$H^{k+1} = \frac{H^k - (H^k \bar{Y}^k - \bar{P}^k)^T H^k}{(\bar{P}^k)^T H^k \bar{Y}^k} \qquad \text{Eq 6-27}$$

where k is the number of iterations, express in mathematical terms the previously described conditions and are used in the model to update the approximation to the inverse Jacobian H^k for the next iteration, H^{k+1}, without having to recalculate it from the beginning and to have to invert it at each cycle. In that way the number of the function evaluations needed per calculation is n instead of nxn for the full Newton step and therefore the reduction to the computer cost required is quite considerable. A second order method using this updating scheme is called quasi-Newton method and the final convergence is super-linear rather than quadratic. The solution techniques used in the model can be summarised in the following steps:

(1) Obtain an initial estimate for the vector of the iteration variables $\bar{x}^o$

(2) Obtain an initial approximation to the iteration matrix

(3) Compute a vector of function values $\bar{F}^o$

(4) Calculate $\Delta\bar{x}^o$

(5) Calculate the vector of the iteration variables for the second iteration $\bar{x}^1$

(6) Compute the vector of the new function values $\bar{F}^1$

(7) If $||F^1||$ is not less than $||F^o||$ use step-size control and return to step 6.

(8) Test for convergence $||F_i|| \leq$ tolerance, i = 1,n

(9) Update the iteration matrix to calculate H^1

(10) Return to step (4)

6.4.2 Extrapolation Technique to Improve Initial Estimates

In some of the phase behaviour problems, solutions are required as functions of a specified parameter p, in a succession of calculations. This may be written symbolically as

$$\underline{x}^* = f(p) \quad \ldots\ldots\ldots\ldots\ldots\ldots \quad \text{Eq 6-28}$$

where the function f represents the mapping of the solution and parameter space and p is any parameter entering the basic problem as a constant. For example, the bubble point pressure of a mixture may be required at different temperatures in order to construct a P-T diagram. Thus the solution P_{SAT} is required at different values of the parameter T. When the solution of the basic problem shows a continuous variation with some parameter, the latter is denoted a continuation parameter.

For miscible gas flooding design, the construction of the whole phase envelope (on a P-Z) diagram) of mixtures of reservoir oil and injection gas is very useful. In this case the bubble point pressure or the dew point pressure of the mixture has to be calculated as a function of different overall mole fractions of the injection gas, x_{inj}.

$$P_{SAT} = f(x_{inj})$$

The mole fractions of the unknown phase can also be considered as functions of the same parameter viz

$$y_i = f_i(x_{inj}) \quad i = 1,N$$

Figure 6-13 illustrates the bubble point pressure of North Sea STO and CO_2 mixtures as a function of the CO_2 overall mole fraction.

The ternary phase envelope is also used for the design of a gas miscible flooding process in a reservoir (Chapter 4). The problems associated with the evaluation of this phase envelope are a series of calculations of the mole fraction of the heavy pseudocomponent z_{HSAT} for a sequence of specified mole fractions of the intermediate pseudocomponent z_I, which defines a mixture of saturation pressure equal to the given pressure (6.2.7) (Fig 6-14).

In this case:

$$z_{H_{SAT}} = f(\bar{z}_I) \quad \ldots\ldots\ldots\ldots\ldots \quad \text{Eq 6-29}$$

Very often for a given mixture of composition z_i, i = 1,N at temperature T, isothermal flash calculations are required for a series of pressures. In this case the vapour or liquid molar fraction and the compositions of the unknown phase can be regarded as functions of a single continuation parameter, in this case pressure viz

$$V \text{ or } L = f(P)$$

$$x_i \text{ or } y_i = f_i(P)$$

In these cases where more than one calculation is associated within the same problem and the iteration variables can be expressed as functions of a single continuation parameter, an extrapolation technique can be used to provide very good initial estimates for the iteration variables for the next calculation. The need for good initial estimates is even more important as the

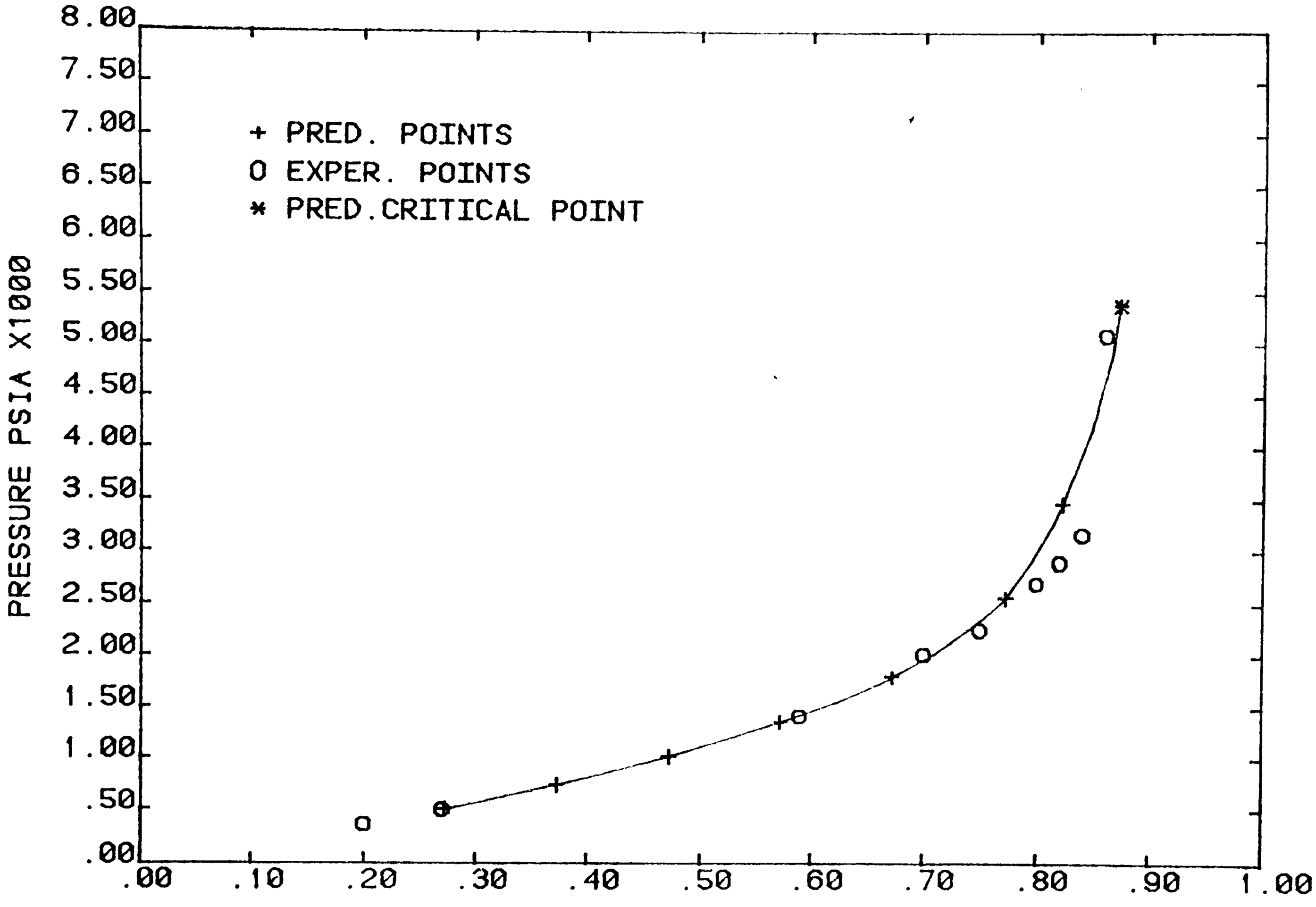

FIGURE 6-13

BUBBLE POINT CURVE FOR A CRUDE OIL CO_2 MIXTURE

FIGURE 6-14

THE TERNARY PHASE ENVELOPE CALCULATION AS A SUCCESSION OF SIMILAR PROBLEMS

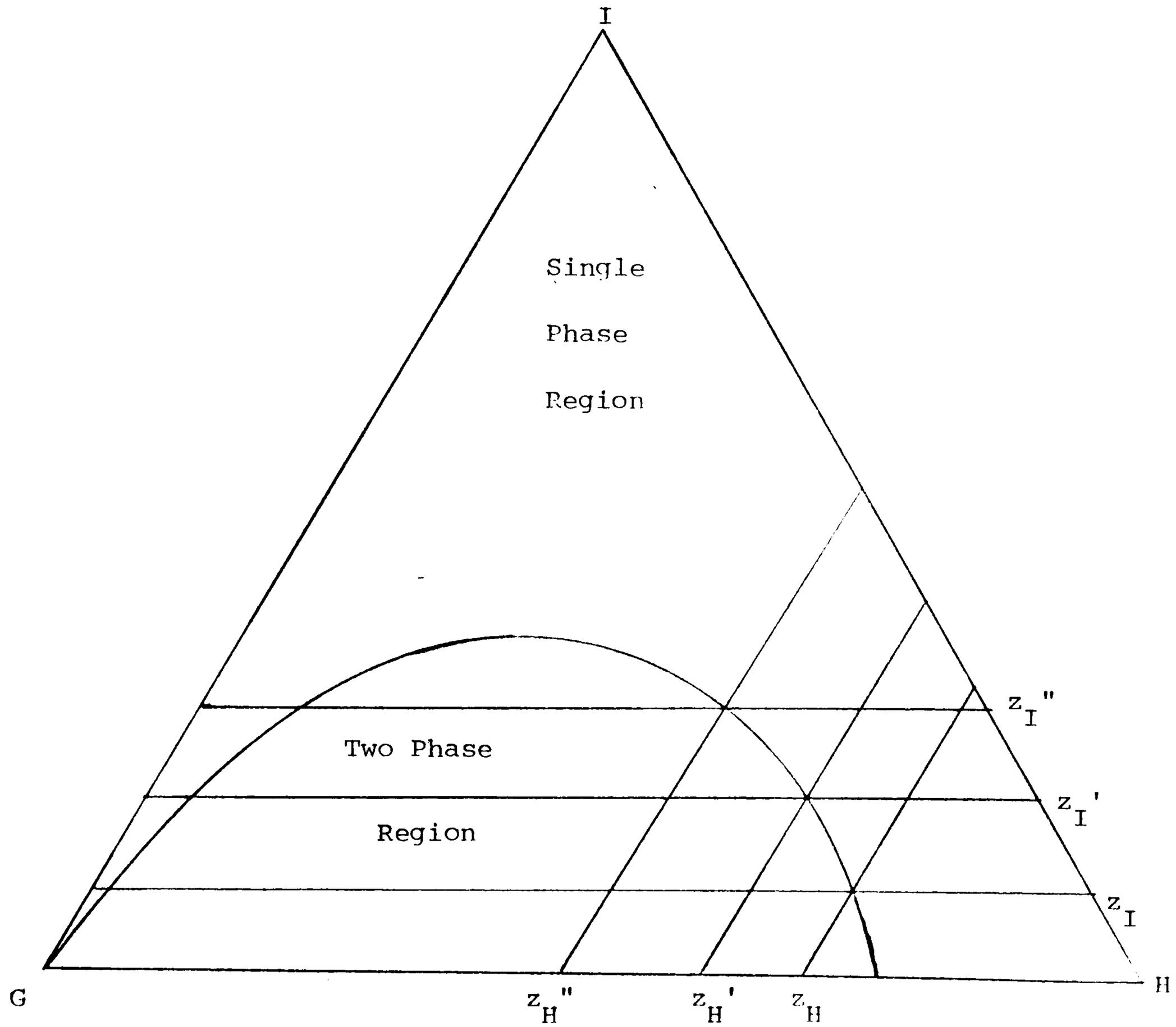

overall composition approaches the critical, the injection gas composition is relatively high in the mixture and the two fluids are nearly miscible. In this region of the phase diagram very small changes in composition cause very significant and radical changes in the phase properties.

Poor initial estimates for calculations around the critical point can be responsible for non-convergence or convergence on a trivial solution which usually is the case when all K-values are equal to unity before the critical point has been approached[18].

These problems can be resolved by selecting a naturally occurring continuation parameter and approaching the very difficult problems through a sequence of calculations in which the continuation parameter is progressively changed along a path until the desired terminal value is reached.

A continuation method is available in the model which projects the answers of previous calculations to give a prediction of the solution at the new value of the continuation parameter. This provides improved initial estimates for the independent variables for the new calculation. The extrapolation method uses a combination of quadratic and linear continuation using the converged answers for each iteration variable for the last three values of the continuation parameter. The initial estimates for the next run are defined as the extrapolation of the quadratic curves or the lines, to the new value of the continuation parameter. If the fitted quadratic does not have a function value at the new parameter, then a two-point linear extrapolation is used instead (Fig 6-15).

Continuation drastically improved the computation in reducing in most cases by more than 60%, the number of iterations required to achieve convergence[7]. Table 6-1 indicates the total number of iterations required for a complete bubble point curve calculation for a mixture of synthetic oil and carbon dioxide[7]. The total number of the components in the mixture is 12 and the saturation pressure curve was calculated at 18 different compositions ranging from 0% CO_2 up to 81% CO_2 which corresponds to the critical composition. It also presents the number of iterations required for bubble point calculation for two different compositions of the synthetic oil - CO_2 mixture.

Using the extrapolation technique and the step by step approach to the critical region, the final calculation for the critical point itself usually requires only one or two iterations. Table 6-2 gives the Euclidean norms for the same synthetic mixture with and without extrapolation. Table 6-3 demonstrates how closer to the actual values the extrapolated initial estimates of the vapour phase0 CO_2 compositions are compared with the results of the previous calculation.

Figure 6-16 shows the application of the continuation method, for the calculation of the saturation pressure of the same mixture at 40% mole fraction CO_2 overall composition. S is the actual bubble point pressure for that composition, E is the estimated value by the extrapolation method and P is the value of the saturation pressure of the previous calculation. Mehra et al[9] underlined the net saving in computer time achieved when an extrapolation method is used. Tables 6-4 and 6-5 give the composition of the hydrocarbon mixture they used and the number of iterations needed

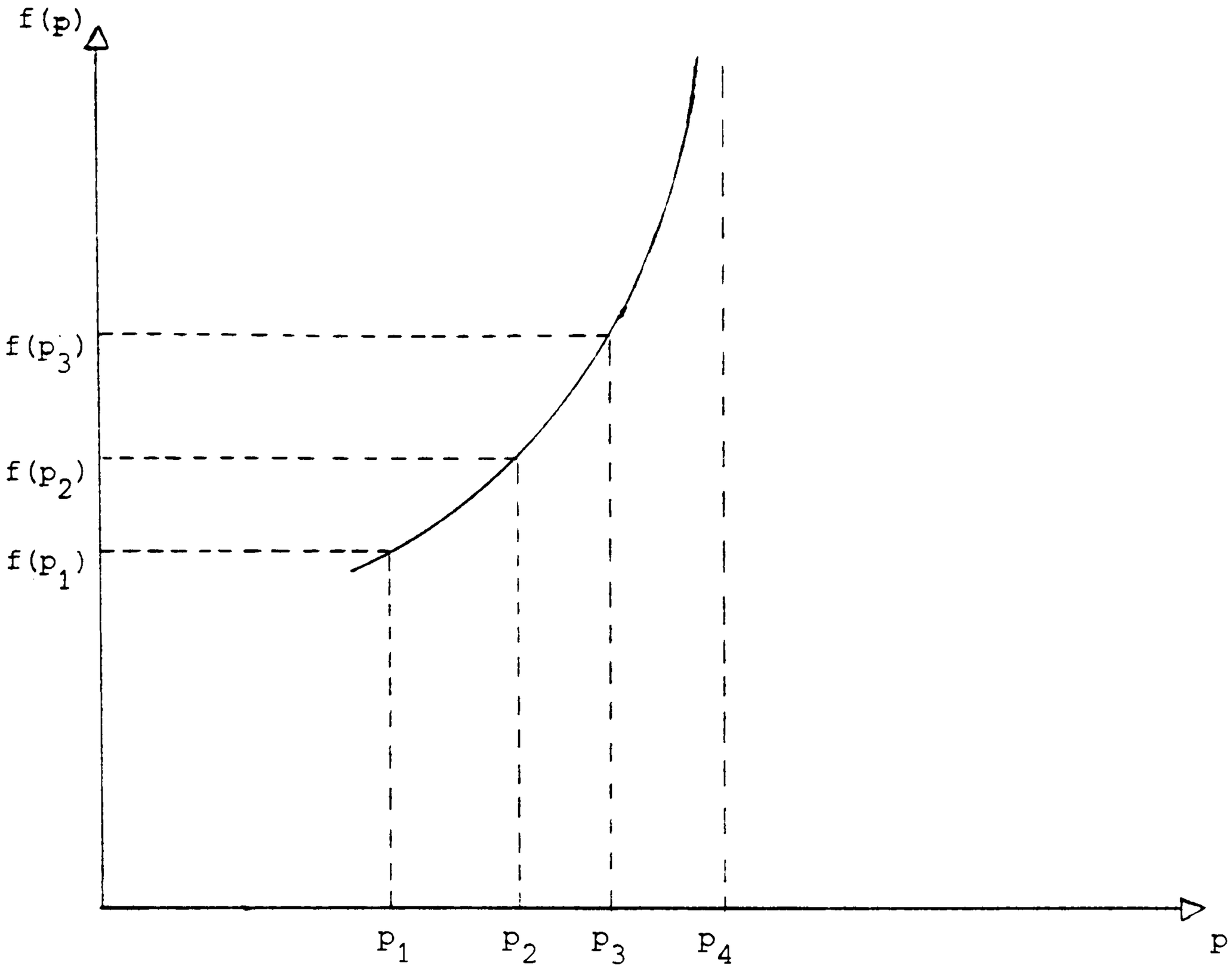

FIGURE 6-15

QUADRATIC CURVE DOES NOT INTERSECT THE LINE $x = P_1$

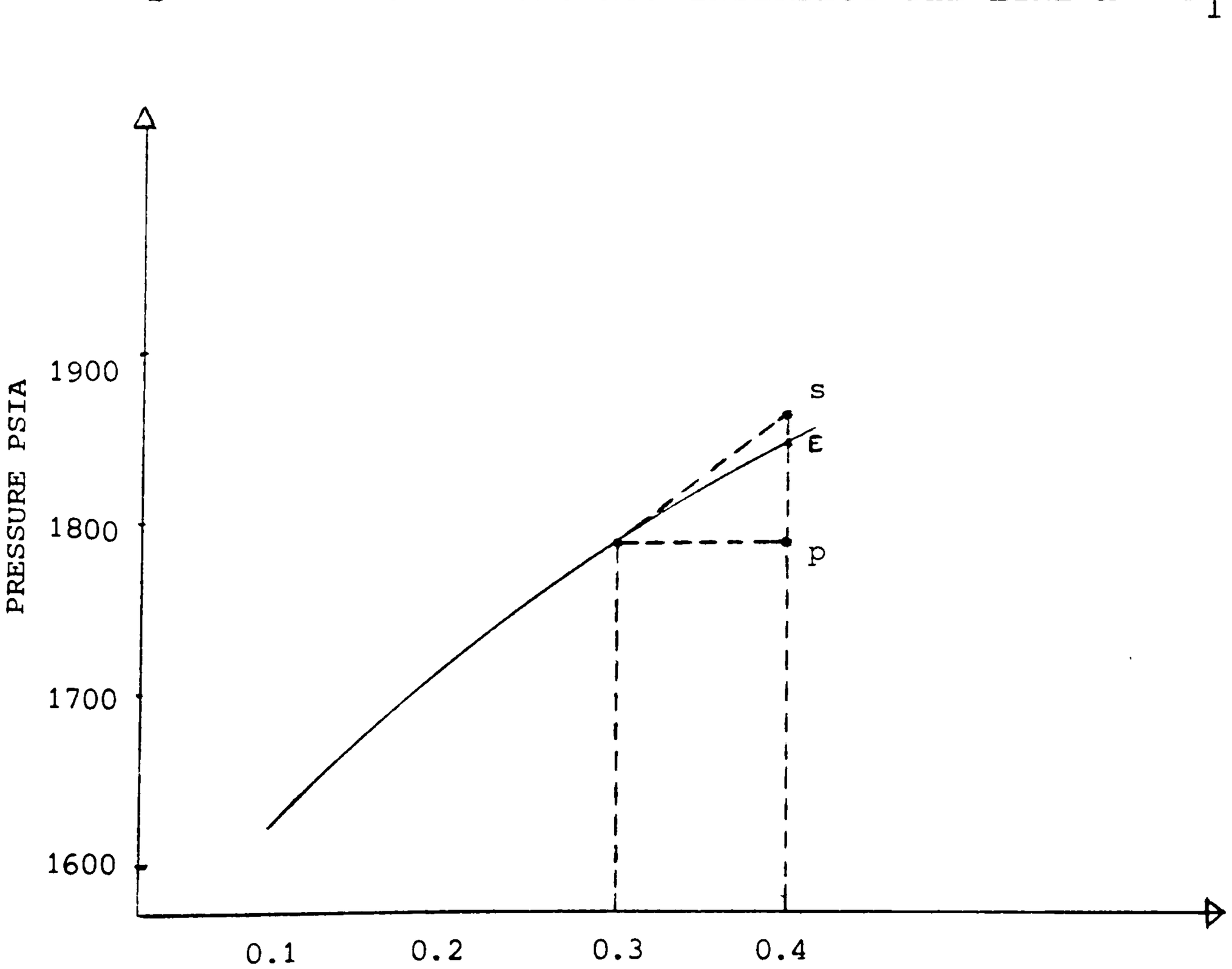

FIGURE 6-16 USE OF THE CONTINUATION TECHNIQUE FOR THE CALCULATION OF THE BUBBLE POINT CURVE OF CO_2-SYNTHETIC OIL MIXTURE

for different phase behaviour calculations with and without extrapolation.

6.4.3 Stability Analysis of the Equation of State Based Phase Behaviour Predictions

The conditions for equilibrium of two multicomponent phases as they were defined in Chapter 5, include material balance equilibria and thermodynamic equilibria. First material balance must be preserved, second there must be no driving force to cause a net movement of any component from one phase to any other phase. This condition is expressed by the equality of the chemical potentials. There is also a third condition based on the second thermodynamic law which ensures the stability of the predicted phases. This condition requires that the predicted system in equilibrium has the lowest possible Gibbs energy at the temperature and pressure of the test. If the Gibbs energy of a predicted equilibrium state is greater than that of another state which also satisfies the first two conditions, the state with the greater Gibbs energy is not stable and there is a lower internal energy accessible to the mixture by separating into two or more phases[10].

In most of the phase behaviour predictions, the material balance and equality of chemical potentials used as the only criteria for solution of phase equilibrium problems, provide the right answer. But, as Baker et al state[11], equality of chemical potentials is necessary but not sufficient for minimisation of the Gibbs energy function. The iterative solution techniques may lead to a trivial situation where both phases present, have the same properties, and which always satisfy the first two requirements but not

necessarily the third. The single phase molar Gibbs free energy of mixing ΔG is related to fugacities as follows[12]:

$$\Delta G = RT \left[\sum_{i=1}^{N} z_i \ell n f_i - \sum_{i=1}^{N} z_i \ell n f_i^{o} \right] \quad \ldots\ldots \quad \text{Eq 6-30}$$

where f_i^{o} is the fugacity of pure component i at the temperature and pressure of the mixture. In a closed system of π phases and N components, the Gibbs free energy is given by[9]:

$$\frac{G}{RT} = \sum_{i}^{\pi} \sum_{j}^{N} n_{ij} \ell n f_{ij} + \frac{G_m^{o}}{RT} \quad \ldots\ldots\ldots\ldots \quad \text{Eq 6-31}$$

where n_{ij} are the moles of component j in phase i and G_m^{o} is the molar Gibbs energy of component i in the standard state.

Figure 6-17[11] shows the Gibbs energy (g-surface) diagram versus composition for a mixture of hypothetical components A and B. The solution of the phase behaviour problem mathematically, is to find the plane tangent to the g-surface with material balance restrictions and whose slope corresponds to the component chemical potentials. The points of tangency of the plane and the g-surface correspond to the compositions of the predicted phases. For a given feed composition, the liquid and vapour phase fractions can be determined by application of the lever rule. The Gibbs energy g_z is the molar sum of the phase Gibbs energies and lies on the tangent line at the feed composition. For multicomponent mixtures, the g-surface has to be considered as hypersurface and the tangent plane as a hyperplane. The two-phase Gibbs energy g_z is less than the Gibbs energy g_1 of the hypothetical homogeneous

FIGURE 6-17

GIBBS ENERGY DIAGRAM FOR A-B SYSTEM AT P_I [11]

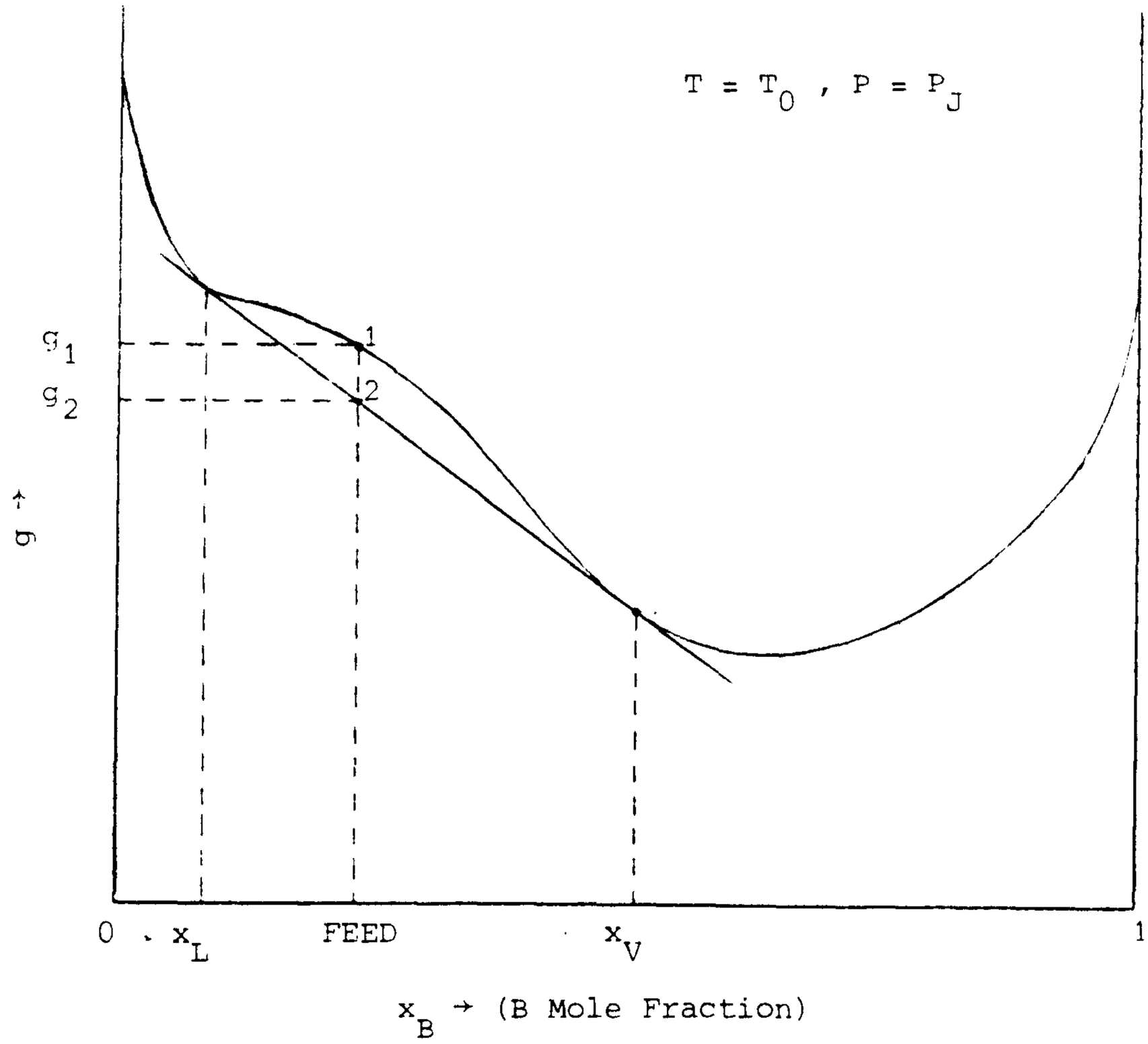

FIGURE 6-18

GIBBS ENERGY DIAGRAM FOR A-B SYSTEM AT P_2 [11]

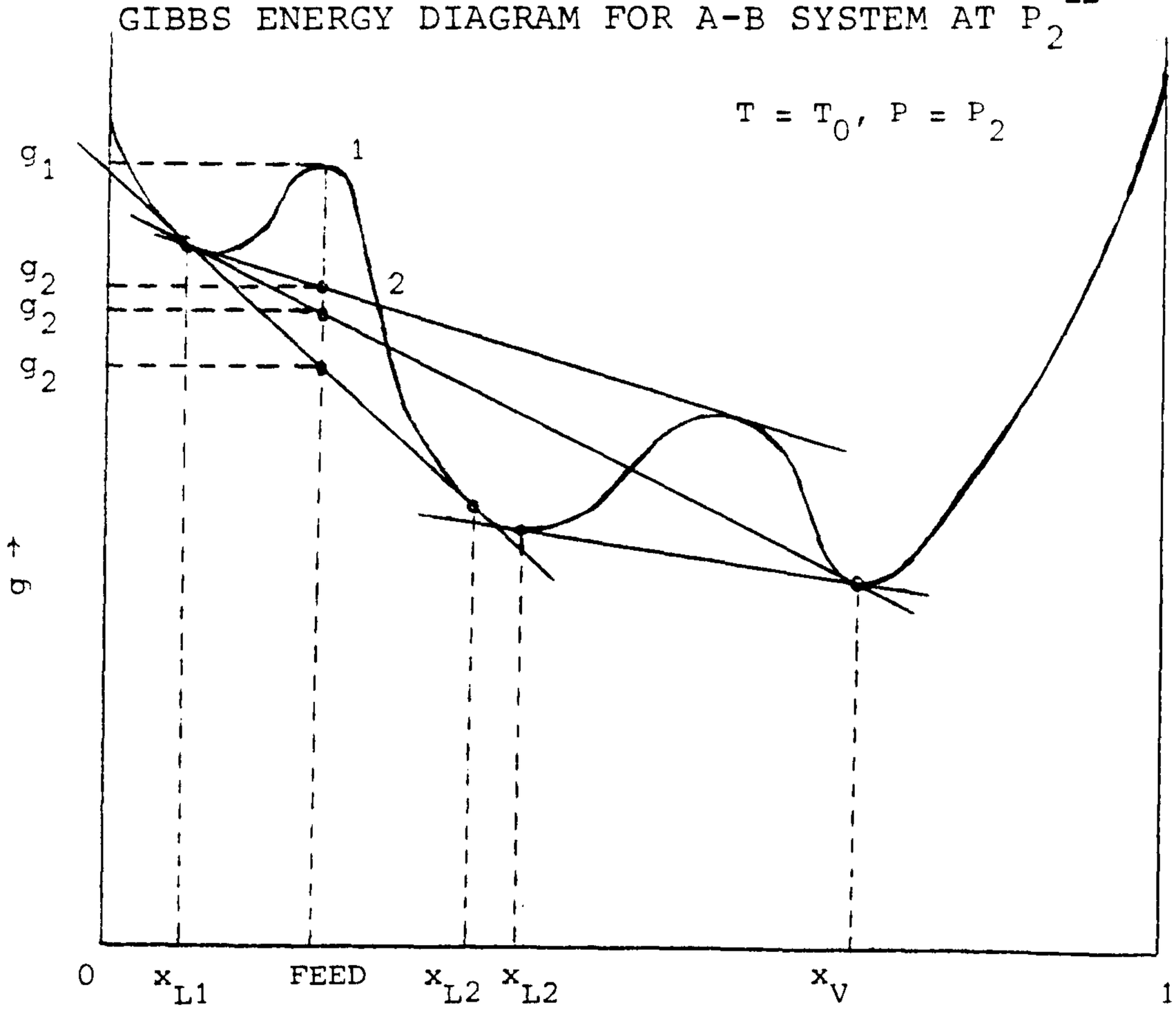

phase of this composition, indicating the two-phase system is more stable than a single phase one.

The general phase equilibria problem for a feed of N components consists of finding a stationary state that is an equilibrium state[11]. A stationary state is defined as any extremum or saddle point in the total Gibbs energy of a system. Although the stationary state satisfies material balance and chemical potential condition, it is not always an equilibrium state. Equilibrium state is defined as the stationary state that corresponds to the global minimum in the total Gibbs energy of the system. In other words, the stability check consists of determining whether the tangent hyperplane lies above the Gibbs surface at any composition. The tangent plane corresponding to the equilibrium state lies entirely below or tangent to the Gibbs energy surface. Figure 6-18[11] demonstrates both stationary and equilibrium states where in the former the tangent intersects the g-surface whereas in the latter the tangent lies entirely below the Gibbs energy curve.

The application of the stability check in this study is regarded as too complex to implement.

6.5 ALTERNATIVE SOLUTION TECHNIQUES SURVEYED FROM THE LITERATURE

Initial Estimates

Among the different investigators there are great differences as far as the solution techniques used to solve the system of the phase behaviour equations are concerned. A very important part of

the solution technique are the initial estimates given to the iteration variables. There are three conditions such estimates should meet:

(i) The estimates should be as close as possible to the solution in order to obtain a rapid convergence.

(ii) The estimates should assure that the calculations start in the two-phase region in order to avoid false single-phase solutions.

(iii) The composition estimates should have sufficient spread to avoid false solutions where all K-values become equal to one.

For saturation conditions determination, the pressure or temperature of the mixture has to be initially estimated. The available correlations usually based on data of pure components, provide very poor starting values and therefore it is widely accepted in the literature that the operator chooses the starting value, judging from his experience[13,14,15,16].

As far as the set of initial K-values for the iteration procedure is concerned, there are mainly two different approaches. The first one uses Wilson's equation or different variations of it. Li et al[12] are using the following equation

$$K_i = \frac{P_{ci}}{P} \exp\left[5.42\left(1 - T_{ci}/T\right]\right] \quad i = 1,N \quad \ldots \quad \text{Eq 6-32}$$

Whitson et al[17] proposed a reformulation of the Wilson equation to provide starting K-values over a wider range of pressures and temperatures

$$K_i = \left[\frac{P_{ci}}{P_k}\right]^{A-1} \exp\{5.37\, A(1+\omega_i)(1-1/T_{ri})\}/P_{r_i}$$

. . . . . Eq 6-33

where $A = A(p) = 1 - \left[\frac{P-P_a}{Pk-Pa}\right]^n$, n is an exponent which varies from 0.5 to 0.8, according to the mixtures whose K-values have to be predicted: P_K is the convergence pressure and P_a is the atmospheric pressure. Equation 6-33 for A = 1 ($p = p_a$) is reduced to the Wilson equation.

The alternative to the empirical formula approach is based on the fugacities of the components in the different phases calculated from the equations of state. Risnes et al[18] are suggesting to consider the mixture liquid at the temperature and pressure of the run. A gas phase is then assumed to be formed by evaporation from the liquid, but the evaporation rate for each component is assumed to be proportional to the fugacity of that component, if considered all in the liquid phase. They suggest that the evaporation should stop when only half of the liquid phase remains, or before the liquid phase has run out of any component. From the resulting compositions the fugacity coefficients are calculated for both phases where the K-value estimates are obtained.

Baker et al[11] propose a different method to provide initial estimates for the Minimum Variable Newton Raphson Method (MVNR), based on the calculation of the fugacities. The method can be summarised in the following five steps:

(i) A low starting pressure eg 1 psi is being chosen.

(ii) The fugacity coefficients Φ_{iL}, Φ_{iV} are calculated at

the assumed pressure using compositions determined in the previous iterations. For the very first iteration and for a bubble point calculation the fugacity coefficients of the components in the upper phase are assumed equal to 1

$$\Phi_{iV} = 1 \quad i = 1,N$$

For a dew point calculation, the fugacity coefficients of the unknown phase are calculated from the equation:

$$\Phi_{iL} = \Phi_i^{o} \exp[Z_L^{o}(P/P_{si} - 1)] \quad i = 1,N$$

. . . . . Eq 6-34

where Φ_i^{o} is the pure component fugacity coefficient evaluated at the pure component vapour pressure, Psi, which is calculated from the Clausius–Clapeyron equation:

$$P_{si} = P_{Ci} \exp\left[\frac{\Delta H_{vi}}{T_{Ci}}\left[1 - \frac{T_{Ci}}{T}\right]\right]$$

ΔH_{vi} = Heat of vapourisation

(iii) The composition of the unknown phase is calculated:

$$x_i = y_i(\Phi_{iV}/\Phi_{iL}) \quad \text{(Dew point calculation)}$$
$$y_i = x_i(\Phi_{iL}/\Phi_{iV}) \quad \text{(Bubble point calculation)} \qquad i = 1,N$$

if Σx_i or $\Sigma y_i < 1$, then the assumed pressure in step (i) is greater than the saturation pressure. If Σx_i or $\Sigma y_i > 1$, then the assumed pressure is too low.

(iv) The assumed pressure is corrected in the direction indicated in the previous step.

(v) The unknown phase composition calculated in step (iii) is corrected by normalisation and the method

returns to step (ii) for the new iteration.

Iteration is halted when the saturation pressure is localised within a reasonable range eg $\pm$ 20 psi. The resulting phase compositions and pressure are used as initial estimates for the MVNR solution.

The empirical formula Equation 6-33[17] has been tried in the model used for this study, instead of Wilson's equation. For some problems it was providing slightly better estimates, whereas for others the convergence rate was retarded due to poor starting values.

Risnes' method starts the iteration in the middle of the two-phase region where both L and V are equal to 0.5 and therefore does not cover satisfactorily the problems along the phase boundaries. The method has been reported to break down along the lower dew point curve[18]. Baker's method requires considerable calculation and for the first iteration is using rather arbitrary relations based on pure component's vapour pressure data.

Alternative Iteration Methods

An iteration method alternative to the MVNR method is the successive substitution method (SSM)[15,18,12,17]. This method is based on the concept of the equilibrium constants Ki. Values for the equilibrium constants are assumed and the resulting set of equations for each problem can easily be solved for the unknowns L, V, x_i, y_i. The liquid and vapour fugacities are then determined from the phase compositions using the EOS and new estimates for K values are obtained from the equation:

$$K_i = \Phi_{iL}/\Phi_{iV} = \frac{f_{iL}/(x_iP)}{f_{iV}/(y_iP)} = R_i \frac{y_i}{x_i} \quad \ldots\ldots \quad \text{Eq 6-36}$$

These K-values are used to calculate new compositions and the cycle is repeated until convergence is achieved. The method has been discussed in 6.3.1.

As the calculation approaches convergence, $\sum_{i=1}^{N} R_i$ approaches zero.

The criterion for acceptance of a solution is based on the fugacity ratios. To comply with other iteration methods, the following error norm is used:

$$\sum_{i=1}^{N} (R_i - 1)^2 < \epsilon \quad \ldots\ldots\ldots\ldots\ldots \quad \text{Eq 6-37}$$

As compared with the Newton type methods, the SSM has the advantage that an nxn matrix does not have to be calculated or updated at each step. The disadvantage is that the convergence rate of the SSM towards the solution is very slow and the number of iterations required compared with the Newton type methods is very large.

Nghiem et al[15] have revealed that the convergence of the SSM deteriorates as the critical point is approached and that after a few iterations the slope of each curve remains almost constant for a large number of iterations.

An improved successive substitution method was presented by Risnes et al[16]. A method similar to Aitken's accelerating formula is

used to speed up the convergence rate. The equilibrium constants are regarded as long products starting with the initial estimates K_i and then multiplied by the fugacity ratios R_i which approach unity as the number of iterations increases.

$$K_i = K_i^0 * R_i^1 * R_i^2 * R_i^3 * ....R_i^j \quad . . . . . \quad \text{Eq 6-38}$$

According to that method, the updated values for the iteration variables K_i for the j+1 iteration are given by the equation

$$K_i^{j+1} = K_i^j * R_i^{j(1/1-k)} \quad . . . . . \quad \text{Eq 6-39}$$

where the k in the exponent to the fugacity ratio is given by

$$k = \frac{\log R^{j+1}}{\log R^j} \approx \frac{\log R^j}{\log R^{j-1}} \approx \frac{R^j - 1}{R^{j-1} - 1} \quad . . . . \quad \text{Eq 6-40}$$

Sometimes the acceleration step fails to lead the solution to convergence, the fugacity ratios diverge from unity and in that case a single step of the Successive Substitution Method has to be taken. Each accelerated step should be followed by a single step, in order that the quotient k be determined.

Nghiem et al[15] are using the SSM method to start the iterations and they are proposing criteria to switch to a more fast and robust method when the convergence rate is detected to be very slow.

These criteria are:

$$\sum_{i=1}^{N} (R_i^{j+1} - 1)^2 \Big/ \sum_{i=1}^{N} (R_i^j - 1)^2 > \epsilon_R$$

$$|V^{j+1} - V^j| < \epsilon_V$$

$$\epsilon_L < \sum_{i=1}^{N} (R_i^j - 1)^2 < \epsilon_\mu$$

$$0 < V^{j+1} < 1 \qquad \text{. . . . . Eq 6-41}$$

where R_i^j are the fugacity ratios at the j iteration, ϵ_R, ϵ_V, ϵ_L, ϵ_μ tolerances usually taken as

$$\epsilon_V = 10^{-2},\ \epsilon_V = 10^{-3},\ \epsilon_L = 10^{-5},\ \text{and}\ \epsilon_R \text{ around } 0.6$$

When these criteria are satisfied, the convergence rate of the SSM is slow and the algorithm switches to Powell's method which combines Newton's method and the steepest descent method. Powell's algorithm computes the step $\Delta\bar{x}^N$ as follows[19]

$$\Delta\bar{x}^N = \theta^N \bar{\alpha}^N + [1 - \theta^N]\bar{b}^N \qquad \text{. . . . . Eq 6-42}$$

where θ is a scalar such that $0 \leq \theta^N < 1$ and defines the contribution of the Newton step $\bar{\alpha}^N$ and the steepest descent method step $\bar{b}^N$ to the correction step $\Delta\bar{x}^N$ taken at the Nth iteration. $\theta^N = 1$, corresponds to the full Newton's method and $\theta^N = 0$ corresponds to the steepest descent method. This method appears to have the divergence avoiding characteristic of the steepest descent method and the rapidly converging property of the Newton's method near the solution.

The disadvantage of this algorithm lies in the complexity of the method and the number of computations required. Fussel et al[8] are using the MVNR iteration method and the Newton method to update the independent variables. The Jacobian is calculated by an analytical differentiation of the defining equations at every iteration. This method requires nxn function evaluations and

matrix inversion at each step whereas a quasi Newton method requires only n function evaluations per step.

6.6 ADDITIONAL OPTIONS IN THE MODEL

6.6.1 Constant Volume Depletion Calculation

An additional option in the VLE program is the constant volume depletion calculation. Constant volume depletion studies are performed on gas condensate and volatile oil fluids to simulate reservoir depletion performance and compositional variation. Resulting data can be used in a variety of reservoir engineering calculations, among the most useful being material balance calculations, generating "black oil" PVT properties and more recently the tuning of empirical equations of state.

Consider the case of a gas condensate which has a saturation pressure PDEW at the temperature of the reservoir charged in a high pressure experimental cell. At dew point conditions a first drop of liquid will be formed and it will be in equilibrium with the saturated gas. At the second stage of the constant volume depletion experiment, mercury is withdrawn from the bottom of the cell, thereby lowering the pressure as the fluid expands. During this process a second phase develops, either retrograde liquid for gas condensates or solution gas for volatile oils. Mercury withdrawal is ceased when a predetermined pressure has been reached. The new volume is measured together with the liquid phase volume. Mercury is then re-injected into the cell at constant pressure while simultaneously withdrawing an equivalent volume of gas. When the initial cell volume is reached, the mercury injection is ceased. The withdrawn gas is analysed using

gas chromatography to determine compositions y_i. The same procedure is repeated several times until a low pressure is reached. The remaining liquid is removed, separated and analysed using gas chromatography. Measured liquid compositions should check with material balance derived compositions.

Predictions for the gas compositions and densities as well as for the liquid compositions and densities for the different stages of the constant volume depletion, can be made by using the COVODE routine of the phase behaviour simulator VLE. The volume and moles of gas displaced, the volume and moles of liquid formed and the cumulative moles and volumes of gas and liquid are calculated too.

Calculations

With the assumption of one mole initial fluid charged in the cell (F = 1), the VLE's dew point option predicts the dew point pressure PDEW, the liquid phase compositions of the first liquid drop and the density of the gas at saturation conditions d_1. The molecular weight of the gas at the dew point is calculated from the gas composition

$$MW_P = \sum_i^N y_i MW_i \quad \ldots\ldots\ldots\ldots\ldots\ldots \quad \text{Eq 6-43}$$

where y_i are the mole fractions of the N components. The mass of the gas at the dew point M_1 is

$$M_1 = F*MW_P = 1*MW_P \quad \ldots\ldots\ldots\ldots\ldots \quad \text{Eq 6-44}$$

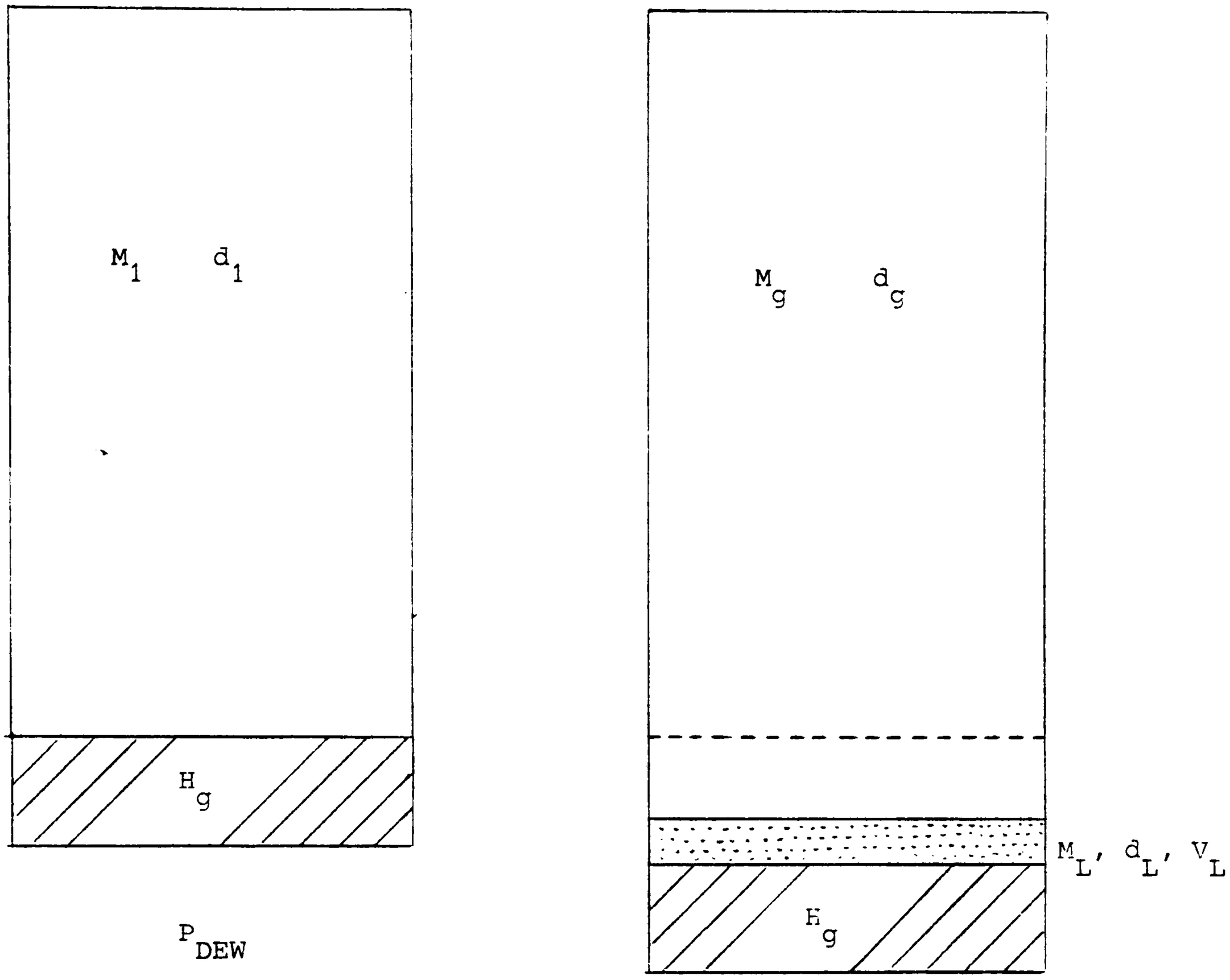

FIGURE 6-19

SCHEMATIC REPRESENTATION OF CONSTANT VOLUME DEPLETION

The volume which one mole of gas occupies at saturation conditions should be

$$V_{SAT} = M_1/d_1 \quad \ldots\ldots\ldots\ldots\ldots\ldots \quad \text{Eq 6-45}$$

When the pressure has been decreased to P_1, two phases are present in the cell. A gas phase of mass M_G, density d_G and volume V_G and a liquid one of mass M_L, density d_L and volume V_L (Fig 6-19). At pressure P_1 the volume that the mixture occupies is

$$V_{mix} = V_G + V_L \quad \ldots\ldots\ldots\ldots\ldots\ldots \quad \text{Eq 6-46}$$

The volume of gas that has to be displaced at pressure P_1 so that the cell volume will become again V_{sat} is

$$V_{dis} = (V_G + V_L) - V_{SAT}$$

or

$$\frac{M_{dis}}{dg} = \frac{M_G}{d_G} + \frac{M_L}{dL} - \frac{M}{d}$$

or the mass of the gas to be displaced

$$M_{dis} = \left[\frac{M_G}{d_G} + \frac{M_L}{d_L} - \frac{M}{d}\right] d_G \quad \ldots\ldots\ldots\ldots \quad \text{Eq 6-47}$$

If MW_G is the molecular weight of the vapour phase at P_1, then the moles of gas that have to be displaced are

$$N_{MOLES}^{DISPL} = \left[\frac{M_G}{d_G} + \frac{M_L}{d_L} - \frac{M}{d}\right] d_G/MW_G \quad \ldots\ldots\ldots\ldots \quad \text{Eq 6-48}$$

The number of moles of gas remaining in the cell are

$$N_{MOLES}^{REM} = V * F - N_{MOLES}^{DISPL} \quad \ldots\ldots\ldots\ldots \quad \text{Eq 6-49}$$

where

V = molar vapour fraction

The number of moles of liquid in the cell are

$$N_{MOLES}^{LIQ} = (1 - V) * F \quad \ldots\ldots\ldots\ldots\ldots \quad \text{Eq 6-50}$$

For the new overall composition of the mixture in the cell, after N_{MOLES}^{DISPL} have been displaced, the component material balance equation is used:

$$F * Z_i = N_{MOLES}^{REM} * y_i + N_{MOLES}^{LIQ} * x_i \quad \ldots\ldots \quad \text{Eq 6-51}$$

the new feed for the next stage calculation is now

$$F = N_{MOLES}^{REM} + N_{MOLES}^{LIQ} \quad \ldots\ldots\ldots\ldots\ldots \quad \text{Eq 6-52}$$

After calculations for three different pressures have been performed, the quadratic fit continuation technique is used to provide initial estimates for the vapour molar fraction and the liquid phase compositions for the next pressure step. The continuation parameter in this case is the pressure.

6.6.2 Differential Vapourisation

Another option of the VLE program is the differential vapourisation option. This process is useful for the study and characterisation of the crude oils and particularly their volatility. The high pressure and temperature single phase crude oils are allowed to expand. A gas phase consisting of the more volatile components is formed on top and after equilibrium has

been established, is displaced out of the container. The new single phase fluid, poorer now in light hydrocarbons is allowed to expand further. The same procedure is repeated until stock tank oil conditions have been reached. At each step the liquid and gas volumes are measured as well as the displaced gas composition. The differential vapourisation gives a good idea of the ease with which a crude oil can be stripped of its light components.

The simulation of the differential vapourisation consists of a series of isothermal flash calculations at different pressures. The overall composition of the mixture that is flashed at each step is the liquid phase composition of the previous step. The program calculates the liquid and vapour mole fractions, volumes and densities at each step and determines the overall composition for the next step. After the first three calculations, the continuation method is used to speed up the calculations providing initial estimates very close to the actual solutions.

6.6.3 Optimisation of the Binary Interaction Coefficient

This option of the VLE calculates the optimised binary interaction coefficient for any binary mixture and for each one of the three available equations of state, using experimental phase equilibrium data for the particular binary.

For this option, the interaction coefficient is the only iteration variable. A number of criteria have been proposed in the literature for the evaluation of the binary interaction parameter. The binary coefficients were optimised by matching:

(i) Experimental K-values[20,21]

(ii) Experimental bubble point pressures[22,23,24,25]

(iii) Experimental bubble point vapour composition[22,23]

(iv) Experimental flash volumes[24]

(v) Experimental flash vapour and liquid compositions[26,27]

In the model there are three different methods available. The interaction parameters can be optimised by matching:

(i) Experimental bubble point pressures

(ii) Experimental K-values at bubble point conditions

(iii) Both the experimental saturation pressure and the vapour phase compositions at saturation conditions

There is no assurance that the binary coefficients obtained by different methods will be identical and therefore there is the problem which method will yield the most desirable results. Table 6-6 shows the results of a bubble point calculation using VLE and the Peng-Robinson EOS with an interaction parameter k_{ij} = - 0.0066 for the binary methane-propane at 310°K. The interaction parameter was calculated with the first method and therefore predicts the bubble point pressure precisely. The predicted vapour phase mole fractions are slightly different from the experimental ones.

In the first method, iteration starts with an estimated value for the binary coefficient and using one out of the three equations of state available in the model, the bubble point pressure of the mixture is predicted and compared to the experimental value. The new estimate for the interaction parameter is provided by a Newton-type iteration method. The calculation continues until predicted and experimental values coincide.

In the second method, the fugacity coefficients of the two phases at saturation conditions are determined and hence the component

K-values at the particular pressure and temperature conditions. The ratio of the K-values of the two components K_1/K_2 is compared with the experimental value. If the residual

$\phi = (K_1/K_2)_{PR} - (K_1/K_2)_{EXP}$ is less than a specified tolerance the iteration sequence stops. . If not, the binary coefficient is updated using the correction step provided by the Newton-type method and the calculation is repeated until convergence.

In the third method, the interaction parameter is iterated until an objective function is minimised. The objective function contains the differences between the experimental and calculated values of both the saturation pressure and the vapour phase composition at saturation conditions.

The third method appears to be more accurate to provide values for the interaction parameter that match both the pressure and composition for a binary mixture at saturation conditions..

Table 6-7 shows the results of the same bubble point calculation using $k_{ij} = 0.047$. This time the interaction parameter was calculated with the second method and therefore the match on the experimental vapour phase mole fractions is excellent. The predicted bubble point pressure is a few psi higher than the experimental one.

Table 6-8 shows the results of the same bubble point calculation using $k_{ij} = 0.045$. The interaction parameter was calculated with the third method and the match on both the experimental bubble point pressure and vapour mole fractions is excellent.

TABLE 6-1

NUMBER OF ITERATIONS FOR A SYNTHETIC MIXTURE

	No extrapolation	Extrapolation
Total no iterations bubble point curve 18 points	100	46
No iterations for bubble point 30% CO_2 - 70% oil	5	2
No iterations for critical point 82% CO_2 - 18% oil	5	1

TABLE 6-2

EUCLIDEAN NORMS FOR THE CO_2-SYNTHETIC OIL MIXTURE

(1) USING BROYDEN'S METHOD TO UPDATE THE MATRIX

(2) RECALCULATING THE MATRIX AT EACH STEP

	No Iteration	Broyden's Method No Extrapolation	Broyden's Method Extrapolation	Recalculating the Matrix
	1	0.4784	0.000502	0.4784
Euclidean Norms	2	0.04629	0.0000033	0.0017855
for Bubble Point	3	0.00697		0.0000032
30% CO_2 - 70% Oil	4	0.000397		
	5	0.0000257		

TABLE 6-3

EXTRAPOLATED INITIAL ESTIMATES

Synthetic oil CO_2 mixture calculation steps	Extrap initial estimates CO_2 mole fraction	Non extrap initial estimates CO_2 mole fraction	Actual CO_2 mole fraction next step
30% CO_2-40% CO_2	0.5358	0.4176	0.5329
40% CO_2- 50% CO_2	0.6393	0.5329	0.6356
50% CO_2-60% CO_2	0.7298	0.6356	0.7241

TABLE 6-4

COMPOSITION OF HYDROCARBON SYSTEM USED BY MEHRA ET AL[9]

Component	Mole Fraction
Ethane	0.39842
Propane	0.29313
n-Butane	0.20006
n-Pentane	0.07143
n-Hexane	0.03696

TABLE 6-5

TWO-PHASE VLE, FIVE COMPONENT SYSTEM OF TABLE 6-4

NUMBER OF ITERATIONS

		w Extrapolation			w/o Extrapolation	
P, kPa	Vapour Fraction	ACSS	Newton	CPU, sec	Total	CPU, sec
4033	1.00000	3	-	0.412	3	0.347
4201	0.99982	6	2	0.539	8	0.525
4369	0.98813	-	2	0.146	8	0.519
4537	0.97267	-	2	0.159	8	0.528
4705	0.95209	-	2	0.162	9	0.552
4873	0.92431	-	2	0.146	9	0.254
5041	0.88597	-	2	0.143	9	0.592
5209	0.75932	-	2	0.143	10	0.684
5377	0.81490	-	3	0.197	10	0.682
5411	0.92549	-	2	0.135	12	0.737
5445	1.0000	14	-	0.782	14	0.782

TABLE 6-6

METHANE - PROPANE MIXTURE, T = 310°K

k_{ij} = -0.0066 PENG-ROBINSON EOS

	Experimental	Predicted
PBUB (psi)	200	200
C_1 vapour mole fraction	0.0521	0.0457
C_3 vapour mole fraction	0.9479	0.9543

TABLE 6-7

METHANE - PROPANE MIXTURE, T = 310°K

k_{ij} = 0.047 PENG-ROBINSON EOS

	Experimental	Predicted
PBUB (psi)	200	201.77
C_1 vapour mole fraction	0.0521	0.0519
C_3 vapour mole fraction	0.9479	0.9481

TABLE 6-8

METHANE - PROPANE MIXTURE, T = 310°K

k_{ij} = 0.045 PENG-ROBINSON EOS

	Experimental	Predicted
PBUB (psi)	200	201.8
C_1 vapour mole fraction	0.0521	0.0521
C_3 vapour mole fraction	0.9479	0.9479

LIST OF REFERENCES

1. Fussel, L and Fussell, D.D.:
Paper SPE No 6891, 1977.

2. Commander, R.J.:
PhD Dissertation submitted in the Department of Chemical Engineering Heriot-Watt University, October 1975.

3. McGlashan, R.S.:
PhD Dissertation submitted in the Department of Petroleum Engineering Heriot-Watt University, August 1980.

4. Wilson, G.:
Paper No 15c presented at the A.I.Ch.E. 65th National Meeting, Cleveland, Ohio, May 4-7, 1969.

5. Hoffman, A.E.:
Trans. AIME (1953) 198, 1-10.

6. Broyden, C.G.:
Mathematics of Computation, Vol 19 pp 577-593, 1963.

7. Varotsis, N, Todd, A.C. and Stewart, G.:
Paper presented at the European Symposium on Enhanced Oil Recovery, Bournemouth, Seoptember 21-23, 1981.

8. Fussell, D.D. and Yanosik, J.L.:
SPEJ, June 1978.

9. Mehra, R.K., Heidemann, R.A. and Aziz, K.:
"Computation of Multiphase Equilibrium for Compositional Simulation", 1981.

10. Heidemann, R., Khalil, A.:
A.I.Ch.E. Jounal Vol 26, No 5 pp 769-778.

11. Baker, L., Pierce, A. and Lucks, K.:
SPE/DOE paper No 9806, 1981.

12. Li, Y.K., Nghieu, L.X.:
SPE paper No 11198, 1982.

13. Mott, R.E.:
Lecture presented at North Sea Condensate Reservoirs and their Development, London, October 1982.

14. Fussell, L.L.:
SPE paper No 6722, 1977.

15. Nghiem, L.X. and Aziz, K.:
SPE paper No 8285, 1979.

16. Coats, K.:
SPE paper No 8284, 1979.

17. Whitson, C.H. and Torp, S.B.:
SPE paper No 10067, 1981.

18. Risnes, R., Dalen, V. and Jensen, J.I.:
Paper presented at European Symposium on EOR, Bournemouth, September 21-23, 1981.

19. Powell, M.J.D.:
"A Hybrid Method for Nonlinear Equations" Numerical methods for Nonlinear Algebraic Equations, P. Rabinowitz, Editor Gordon and Breach, London 1970.

20. Orye, R.V.:
Ind. Eng. Chem. Process Des. Dev., 8: 579-588, 1969.

21. Zudkevitch, D. and Joffe, J.:
A.I.Ch.E.J., 16 pp 112-119, 1970.

22. Kato, M., Chung, W.K. and Lu, B.C.Y.:
Chem. Eng. Sci., 31, pp 733-736, 1976.

23. Huron, M.J., Dutair, G.N. and Vidal, J.:
Fluid Phase Equilibria, 1 pp 247-265, 1977/1978.

24. Graboski, M.S. and Danbert, T.E.:
Ind. Eng. Chem Process Des. Dev., 17 pp 448-454, 1978.

25. Plockner, V., Knapp, H. and Prausnitz, J.:
Ind. Eng. Chem. Process Des. Dev., 17 pp 324-332.

26. Evelein, K.A. and Moore, R.G.:
Ind.eng. Chem. Process Des. Dev., 18 pp 618-624, 1979.

27. Paunovic, R., Javanovic, S. and Mihajlov, A.:
Fluid Phase Equilibria, 6, (1981), pp 141-148.

CHAPTER 7

TREATMENT OF THE C_{7+} FRACTIONS

7.1 INTRODUCTION

7.2 THE CHARACTERISATION OF HEPTANES PLUS OR UNDEFINED FRACTIONS FOR EQUATION OF STATE TREATMENT

7.3 EXTENDED ANALYSIS OF THE C_{7+} FRACTION USING STATISTICAL METHODS

7.4 METHODS OF REDUCING MULTI-COMPONENT RESERVOIR FLUID DESCRIPTION TO A SMALLER NUMBER OF PSEUDOCOMPONENTS

7.5 TUNING THE EOS BASED MODEL

7.1 INTRODUCTION

The equations of state, being functions of the composition as well as of temperature and pressure, require a reasonably good compositional characterisation of the reservoir fluid. In a standard PVT report the compositional analysis of the reservoir fluid is generally reported as a series of pure components from methane through to hexane (or nonane), with the remaining components grouped together as heptanes plus, or decanes plus pseudocomponent. Usually a single heptanes plus fraction lumps together all components with higher carbon number than six. Measured molecular weight and gravity of a C_{7+} fraction usually describe the multiplicity of components making up a fraction. Sometimes a partial component analysis is available from chromatography and/or distillation studies. In this case, the mole fraction of several single carbon number groups, ie hydrocarbons are lumped together and represented as a single "component", reported normal boiling points, gravities and molecular weights may be measured but this is more often the exception than the rule.

In order to use the equation of state based model to predict the phase or the volumetric behaviour of mixtures, the critical temperature, the critical pressure and the acentric factors should be supplied for both the defined and undefined fractions in the mixture. The proper characterisation of the heavy fractions is necessary in order to adequately predict reservoir performance, liquid recoveries, performance of surface processing equipment, etc. It is also important for the study of the phase behaviour in a gas miscible displacement where components even higher than

eicosanes are transferred into the vapour phase[1] and it is the transfer of such heavy components which determines the conditions in which miscibility can be achieved.

7.2 THE CHARACTERISATION OF HEPTANES PLUS OR UNDEFINED FRACTIONS FOR EQUATION OF STATE TREATMENT

The heavy fractions typically include paraffins, aromatics and napthenes. Due to the lack of information about the chemical nature of the components included in a specific cut, either correlations are used to find the aromatic and napthenic content, or properties of a normal alkane are given to the fraction. The correlations use macroscopic properties of the group of components such as weight averaged molecular weight, boiling point, specific gravity, which are all easily measured in the laboratory.

Several schemes have been proposed for determining the paraffinic-napthenic-aromatic (PNA) content of the pseudocomponents. Peng and Robinson[2] proposed in 1978, a procedure for characterising heavy fractions. Assuming that each cut characterised by its carbon number consists of a paraffin P, a napthene N and an aromatic component A, the PNA content can be obtained by solving the following system of equations:

$$\sum_{i=1}^{3} x_i = 1$$

$$\sum_{i=1}^{3} x_i M_i T_{Bi} = M*WABP$$

$$\sum_{i=1}^{3} x_i M_i = M \qquad \text{Eq 7-1}$$

where the subscript i represents P, N and A, WABP and M is the weight average boiling point and the average molecular weight of the pseudocomponent respectively. The normal boiling point temperatures for the n-alkanes, the n-alkyl-cyclohexanes and the n-alkyl-benzenes can be obtained for each of the three hydrocarbon groups from the equation[32]

$$\ell n T_B = \sum_{i=1}^{6} C_i (n-6)^{i-1} \quad \ldots\ldots\ldots\ldots \quad \text{Eq 7-2}$$

where C_i are coefficients for each component and n is the hydrocarbon number. The above set of linear equations can be solved directly for the three unknowns x_p, x_N and x_A. To avoid negative values for the PNA contents, some constraints have to be used to keep the aromatic and napthenic fractions within certain limits. The procedures and equations are based on the requirement that each heavy fraction represents a single carbon number. Napthenes and aromatics are given carbon numbers one less than paraffins. The critical parameters and acentric factors for the "pure components" which constitute the cuts of the heptanes plus fraction are calculated according to the following equations

$$P_{Ci} = \frac{14.026n + \gamma i}{(0.227n + \beta_i)^2} \quad \ldots\ldots\ldots\ldots \quad \text{Eq 7-3}$$

where n = hydrocarbon number, β, γ coefficients for each hydrocarbon group.

$$T_{Ci} = S * T_{Bi}\left[1 + \frac{3 \log P_{Ci}}{7(1 + \omega_i)}\right]$$

where $S = 0.996704 + 0.00043155n$ and $\omega_i = fn + g$ where f, g are

coefficients for each component.

Having obtained the critical properties and acentric factors for each "pure component" the overall parameters for each cut are calculated using the following equations:

$$T_c = \Sigma x_i T_{ci}$$

$$P_c = \Sigma x_i P_{ci}$$

$$\omega = -\log_{10}\left[\frac{\Sigma x_i P_{ci}^{10-(1+\omega_i)}}{P_c}\right] - 1$$

Whitson[3] indicated various limitations of the method. These limitations include the maximum carbon number of the SCN that can be used, as well as the validity of the specific gravities, boiling points and acentric factors estimated by the correlations.

Another method reported in GPA RR13[4], follows the Lin and Hopke approach of breaking the pseudocomponents into PNA fractions but uses the normal boiling point as a correlating parameter. Cavett's[5], equations are then used to predict the critical properties of the individual fractions.

Bergman in 1976[6,7], presented a PNA approach to calculate the critical properties of the heavy pseudocomponents. The basic difference of his method from the Peng-Robinson method is that it assumes all three constituents have the same boiling point, but different properties otherwise. Bergman suggests that his method gives satisfactory results for fractions up to C_{15} and he

recommends the use of Cavett's correlation if the pseudocomponents are greater then C_{15}.

Cavett's correlations, proposed in 1962, calculate the critical pressure and critical temperature of the heavy fractions using the mean average, the cubic average and the molar average boiling point temperatures. In practice, the average boiling point temperature are approximated to the normal average boiling point temperature. The correlations for obtaining the critical properties are as follows:

$$T_C = a_0 + a_1(BP) + a_2(BP)^2 + a_3(API)(BP) + a_4(BP)^3 + a_5*(API)(BP)^2 + a_6(API)^2(BP)^2$$

$$\log P_C = b_0 + b_1(BP) + b_2(BP)^2 + b_3(BP)^3 + b_4(API)(BP) + b_5(API)(BP)^2 + b_6(API)^2(BP) + b_7(API)^2(BP)^2$$

. . . . . Eq 7-4

where

$$API = \frac{141.5}{S.G} - 131.5$$

T_C = critical temperature (°R)

P_C = critical pressure (psia)

BP = normal boiling point (°F)

S.G = specific gravity

The constants a_0 to a_6 and b_0 to b_7 are tabulated in Table 7-1. For the calculation of the acentric factor Edmister's equation is used.

$$\omega_i = 3/7\left[\frac{\log\left[\frac{P_{ci}}{14.69}\right]}{\frac{T_{ci}}{T_{Bi}} - 1.0}\right] - 1.0 \quad \text{. . . . . Eq 7-5}$$

The BP and specific gravity required for each pseudocomponent are usually calculated from Bergman's empirically fitted equations[7]

$$S.G = MW*(8.597*10^{-3} + 5.647*10^{-6}*(BP) - 8.303*10^{-8}*(BP)^2 + 1.513*10^{-10}*(BP)^3 - 8.742*10^{-14}(BP)^4)$$

. . . . . Eq 7-6

$$MW = 54.389 + 0.17566*(BP) + 1.2102*(BP/100)^2 + 0.22885*(BP/100)^3$$

where

S.G = density (g/cm^3 at 60°F) and

BP = normal boiling point (°F)

If only one out of these parameters S.G., MW, BP is known, the other two can be calculated from the equations.

The above correlations were built into a program designed to simulate tray to tray distillation up to pressures of 1000 psia. Although these correlations have been widely adapted, they include limitations. Bergman's correlations were tried during this study for various runs of North Sea crude oils and injection gas mixtures. Experience showed that the correlation which provides the specific gravity of a pseudocomponent as a function of the boiling point does not apply for heavy fractions whose boiling point is higher than 850°F. Table 7-2 illustrates the values of the SG obtained for different values of BP from Eq 7-6. For values

of BP higher than 850°F the value of the specific gravity becomes negative.

7.3 EXTENDED ANALYSIS OF THE C+ FRACTION USING STATISTICAL METHODS

Whitson[8] and Lohrenz et al[9] have used probability functions to analyse the molar distribution of hydrocarbon mixtures whose heavy components are given as C+ fraction. Condensate systems' and volatile oils' compositional characterisation usually exhibits an exponential distribution. Other systems, particularly heavier ones, show more of a left skewed distribution (Fig 7-1)[7]. Whitson in 1980, has chosen the three parameter gamma function to describe the molar composition of the heavy ends of reservoir fluids. The probability density is given by

$$P(X) = \frac{(X-n)^{a-1}\exp[-(X-n)/\beta]}{\beta^{a}\Gamma(a)} \quad \ldots\ldots\ldots \quad \text{Eq 7-7}$$

where a, β, n are parameters defining the distribution. The variable X in this equation is the average molecular weight of the hydrocarbon fraction. For alpha equal to unity the distribution is exponential, whilst increasing values of alpha yield left skewed distributions.

Whitson's approach to estimate the physical properties of the hydrocarbon fractions from C_7 to C_{45} is based on Watson's characterisation factor K_i[10]. The equation proposed for relating an approximation K_{C+} to Watson's characterisation factor K_i, specific gravity and molecular weight is

$$K_{C+} = 4.5579 * MW_{+}^{0.15178} * SG_{+}^{-0.84573} \quad \ldots\ldots \quad \text{Eq 7-8}$$

FIGURE 7-1

EXPONENTIAL AND LEFT SKEWED MOLAR DISTRIBUTION FOR DIFFERENT VALUES OF THE GAMMA FUNCTION PARAMETER

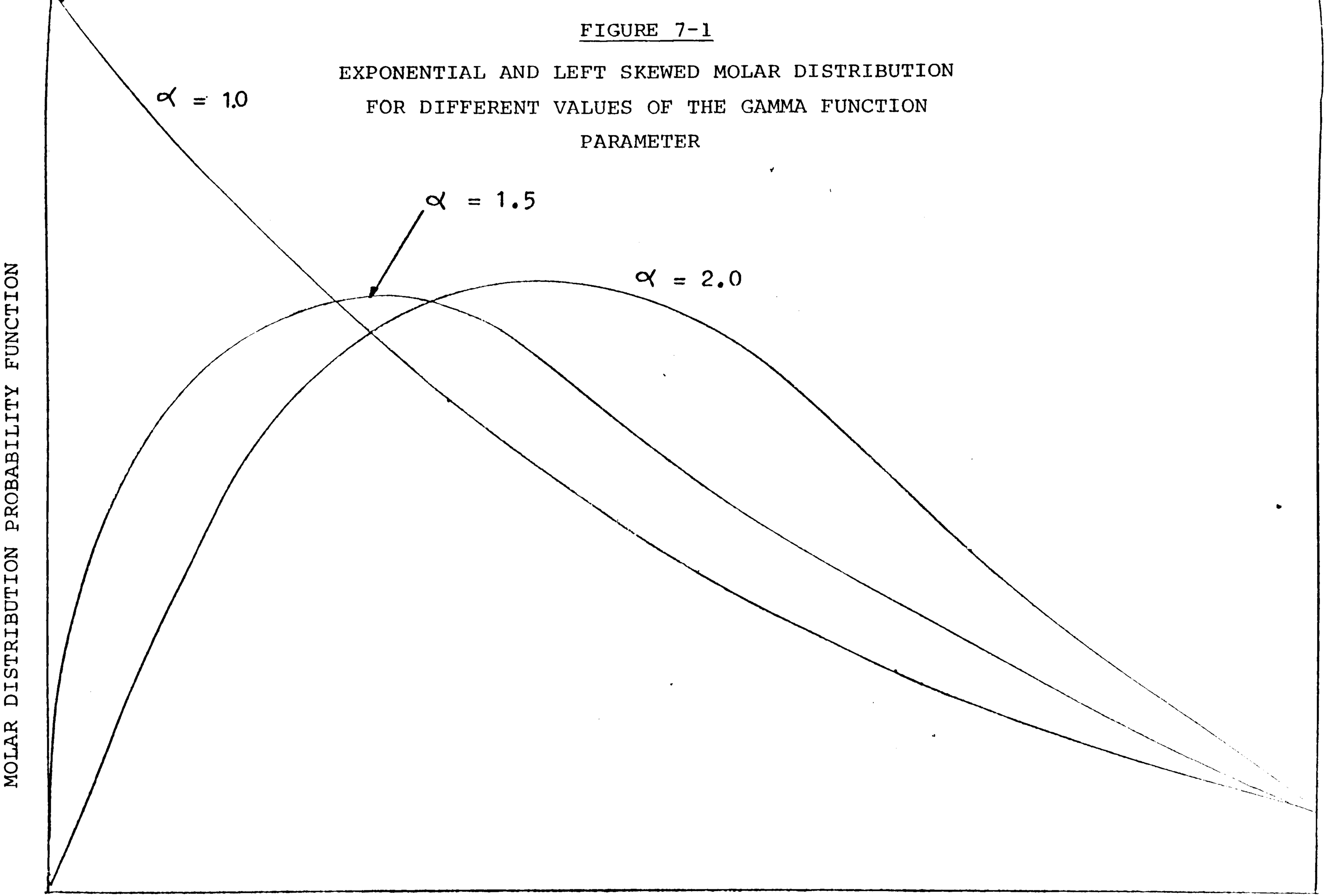

The Whitson procedure begins by assuming an average K_{C7+} for the plus fraction and estimated SG and MW of the lumped cut is used to calculate the characterisation factor. The characterisation factors then of the single carbon number groups are estimated using the following correlations developed by Haaland[11,3]

$$K_{CN}/K_{C7+} = -0.011*C_N + 1.101 \quad \text{for } C_N = 6\text{-}11$$

$$K_{CN}/K_{C7+} = 0.0025*C_N + 0.9525 \quad \text{for } C_N = 11\text{-}19$$

$$K_{CN}/K_{C7+} = 0.0014*C_N + 0.9734 \quad \text{for } C_N = 19\text{-}24$$

$$K_{CN}/K_{C7+} = 1.007 \quad \text{for } C_N = 24\text{-}\infty$$

where C_N is the single carbon number of the group. Since Equation 7-8 is only valid up to a boiling point of 730°K the K_{C7+} is usually calculated using C_{7+} molecular weight and specific gravity.

The specific gravities of the single carbon number groups are calculated from Eq 7-8. Later, Whitson suggested the use of the Hariu-Sage[12] equation for that calculation. The overall specific gravity of the cut is then calculated using the SG's of the SCN groups,

$$SG_{7+} = \sum_{i=n}^{N+} fw_i SG_i \quad \text{Eq 7-10}$$

where f_{wi} is the weight fraction.

If the calculated specific gravity does not compare favourably with the measured value, then the procedure is repeated until these two values match.

Lohrenz et al in 1964[13] introduced an exponential distribution of individual C_{7+} components which passes through the hexane mole fraction X_{C6} and tails off to extremely small or heavy hydrocarbons well beyond the equivalent to the average molecular weight of the C_{7+} fraction, to characterise the heavy fraction. The assumption that the individual C_{7+} components are normal paraffins is used for the estimations of the critical properties. Mathematically the mole fraction of each hydrocarbon C_i is determined as follows

$$x_{Ci} = x_{C6}e^{A(i-6)^2 + B(i-6)} \quad \ldots\ldots\ldots \quad \text{Eq 7-11}$$

where i is the carbon number of each group and ranges from 7 to 40. The constants A and B are determined such that

$$x_{C7+} = \sum_{i=7}^{40} x_{Ci} \quad \text{and}$$

$$x_{C7+}M_{C7+} = \sum_{i=7}^{40} (x_{Ci}*M_{Ci}) \quad \ldots\ldots\ldots \quad \text{Eq 7-12}$$

using an iterative method. This characterisation of the heavy end is usually used with the Lohrenz method of calculating the viscosity of multicomponent hydrocarbon mixtures.

7.4 METHODS OF REDUCING MULTI-COMPONENT RESERVOIR FLUID DESCRIPTIONS TO A SMALLER NUMBER OF PSEUDOCOMPONENTS

Phase behaviour simulators using an equation of state to describe the equilibrium of multicomponent fluid mixtures are expensive to run because of the large number of iterative calculations and large computer storage space required. For these reasons the

number of components used in describing a fluid mixture must be kept to a minimum. Some authors suggest that as few as two hydrocarbon components[14] or as many as 50 may be required to simulate various processes, such as thermal recovery or miscible gas injection. For most situations a compromise can be found between using a single plus fraction or individual SCN groups to achieve the accuracy required for a particular problem. The heavy components must be grouped together so that the predicted phase behaviour is not altered significantly and the important features of the process remain intact.

In the past the lumping of reservoir fluid components has been primarily based upon the true boiling point analysis. The components boiling within a range are combined together. Lee et al[15] observed that the closeness of the physico-chemical properties of the components are reflected by the slopes of the curves when these properties are plotted against the weight-averaged boiling point curve. Fractions with similar slope are combined into pseudocomponents. The disadvantages of this method are the requirement of a large amount of experimental data and the lack of a wider theoretical basis.

Hong[16] suggested a simple method based on trial and error for reducing a multi-component characterisation of a reservoir fluid to a smaller number of pseudocomponents. Using the Peng-Robinson equation of state and a compositional reservoir simulation program, he tested his theory predicting pressure composition diagrams for reservoir fluid systems using initially a small number of pseudo-components. The number of components is then systematically increased until a good match between calculated and

experimental data is achieved. No significant loss of accuracy was reported in several tests of the method compared with laboratory or field results. The drawback of the method is that depending on the conditions of the test, it may be proved quite time consuming.

Mehra et al[17] presented a statistical approach to properly combine the reservoir components based upon the minimisation of the errors introduced in the predicted phase saturations. The reservoir components according to this method should be grouped together so as to minimise the errors introduced in the prediction of the saturation conditions. The objective function

$$|(\Delta S) - (\Delta S)^*| = \text{minimum} \quad \ldots\ldots\ldots\ldots \quad \text{Eq 7-13}$$

which comes as the difference between the relation which gives the variation in the phase saturation due to small perturbations in the composition when the system is represented by all its N components

$$(\Delta S) = \sum_{i}^{N}\left[\frac{\partial S}{\partial n_i}\right]\Delta n_i \quad \ldots\ldots\ldots\ldots \quad \text{Eq 7-14}$$

and the one which comes when the mixture is represented by ℓ pseudocomponents $\ell \leq N$

$$(\Delta S^*) = \sum_{j}^{\ell}\left[\frac{\partial S}{\partial x_j}\right]\Delta x_j \quad \ldots\ldots\ldots\ldots \quad \text{Eq 7-15}$$

has to be minimised.

Lee and Kesler mixing rules are suggested for the calculation of the properties of the pseudocomponents. The above method requires

a considerable amount of calculations before the necessary information about the lumping of the pseudocomponents is obtained. Another disadvantage is that the optimal lumping scheme strongly depends on the conditions of the process (temperature, pressure, reservoir fluids). Considering only one thermodynamic function, the phase saturation is being suggested, whose errors in prediction should be minimised to determine the lumping scheme, adequate information has not been collected so that the particular scheme can be used for the same process but for different conditions. Therefore, for different conditions the mixture's characterisation would have to change and consequently the optimisation routine has to be repeated several times.

Whitson[6] presented together with his lumped fraction split-up method, a scheme of regrouping the Single Carbon Number (SCN) cuts determined by his method. To estimate the number of pseudocomponents, Whitson suggests using Sturge's rule,

$$\text{No of pseudos} = \text{INTEGER}\{1.0 + 3.3\log(N - n)\} - 1 \quad \ldots\ldots \quad \text{Eq 7-16}$$

where N is the carbon number of the highest hydrocarbon fraction and n is the number of the first hydrocarbon fraction in the plus fraction. The molecular weight separating the pseudocomponents can then be calculated using the equation:

$$MW_i = MW_n \{\exp[(1/NG)\ln(MW_N/MW_n)]\}^i \quad \ldots\ldots \quad \text{Eq 7-17}$$

where NG is the number of the pseudocomponents, MW_N, MW_n are the molecular weights of the last and the first SCN group and $i = 1,2, \ldots NG$ The pseudocritical properties of the groups are averaged from the SCN properties of the relative mole fraction of

each SCN to the mole fraction of the group or they are calculated from relations developed between molar weight and mean average boiling points and pseudocritical and critical properties[18].

Coats in 1982[14] presented a 2-component black oil model to be used for simulation of gas condensates depletion and cycling. The multicomponent condensate fluid is reduced to a pseudo 2-component mixture of surface gas and oil. An equation of state compositional simulator has to be used in the beginning to match laboratory PVT data such as dew-point, differential expansion results and separator data using the multi-component gas-condensate reservoir fluid description. The program then flashes the original reservoir fluid composition through the desired surface separator combination and the separator gas and separator oil multi-component compositions obtained are taken as the two pseudocomponents. With some oversimplification this method is the basis of the "black oil" treatment which has been used for many years and is different from other pseudoisation methods in that each pseudocomponent includes some of each component present in the original reservoir fluid description. An essential condition for this 2-component method to give fairly accurate results compared with full compositional model results, is that the injected or cycling lean gas should be the surface separation gas defined as the one of the two pseudocomponents. For "dry" gas cycling above the dew point, the method was reported[19] to work satisfactorily since the undersaturated reservoir fluid is of uniform composition. However, for "dry" gas cycling below the dew-point, the results are not so accurate because the K-values significantly depend on composition and that

composition dependence cannot be obtained from volumetric test data alone, like the black-oil treatment[20].

7.5 TUNING OF THE EOS BASED MODEL

The calculation of the phase behaviour and of the physical properties of multicomponent hydrocarbon mixtures using an EOS based method, requires the selection of appropriate values for the characteristic parameters of the equation of state in order that the predictions match the experimental results. These parameters may be divided into two groups. The first covers values which characterise the heavy fractions like critical temperature, critical pressure and acentric factor. Results indicate that relatively small differences in critical properties and acentric factor can result in significant differences in EOS predictions[6,7,14,21,22,23,24]. The second group includes the binary interaction coefficients of CO_2-hydrocarbons and/or CH_4-hydrocarbons and/or N_2-hydrocarbons.

For the purposes of this study the numerical simulator VLE can use two different methods for the treatment of the pseudocomponents. Either Cavett's method to provide the critical temperature, critical pressure and acentric factor of the heavy ends, or a PNA analysis of the lumped fraction based on the GPA RR13 method can be used. Experience has proved the first method far more accurate and therefore is the method which has been used for all the phase behaviour predictions throughout this study. In many cases Cavett's correlations were found to be inadequate to provide the critical properties of the pseudos to match the experimental data and therefore correction factors P_{CMOD}, T_{CMOD} can be selected by

the operator to adjust the values of the critical pressure and of the critical temperature of the lumped components.

The VLE model is used to support and rationalise the experimental programme and as such information is exchanged in both directions. For the multicomponent mixtures studied in the laboratory, an extended chromatographic analysis is available which provides the molecular composition as a function of the boiling point. The components within a certain boiling point range are grouped as pseudocomponents whose average molecular weights can also be calculated approximately from the weight fractions. The specific gravities which are also required for Cavett's correlations are chosen from Katz-Firoozabadi's tabulated generalised properties of petroleum hexane plus groups[25] (Table 7-3). As far as the second group of parameters is concerned, the calculations begin with a table of default values for the interaction parameters of CO_2, N_2, C_1 and hydrocarbons[29] which are subjected to alteration during the matching process. The two groups of parameters are altered separately to match two sets of experimental values. These two sets are selected according to the problem to be solved but usually are the saturation pressure on the one hand and the liquid phase density either at saturation conditions or at stock-tank conditions, on the other. The reason why the saturation pressure was chosen is due to the fact that it is a property, easily measured in the laboratory and characteristic of the particular mixture. The liquid density was chosen because the equations of state, by being originally derived for gas mixtures, usually overestimate the liquid volumes (and underestimate the liquid densities), especially at near ambient conditions.

To tune the simulator to match the experimental data, first the binary coefficients are altered to achieve a predicted value for the saturation pressure very close to the experimental one. By increasing the k_{ij} of CO_2 and hydrocarbons, CH_4 and hydrocarbons, and N_2 and hydrocarbons, the calculated values are increasing. At the same time, the differences in the predicted phase volumes are negligible. After the saturation conditions have been matched the critical properties of the pseudocomponents are altered by adjusting the values of the correction factors until the predicted densities are in acceptable agreement with the reported values. During this stage the saturation conditions change very slightly. Obviously if the parameter adjustment is made for separator conditions the calculated density at saturation pressure will be different from the experimental value[26]. The Peng-Robinson EOS was used by VLE to predict the saturation pressure as a function of CO_2 mole fraction, for a synthetic mixture which consisted of CO_2-nC_6-C_{12}. Figure 7-2 shows the predicted curve using the default value 0.1 for the CO_2-hydrocarbon binary coefficient together with the calculated bubble point curve using k_{ij} = 0.11 compared with the experimental values.

Whitson[3] notices that saturation pressures may be over-estimated if coefficients matched at one temperature are used to estimate saturation pressure at a lower temperature. Varotsis et al presented generalised correlations for the binary coefficients as functions of reduced pressure, temperature and molecular size[30].

Symeonides, having matched the liquid density for a volatile oil at saturation conditions predicted, using VLE and the Peng-Robinson EOS, a much lower density than the measured one[27].

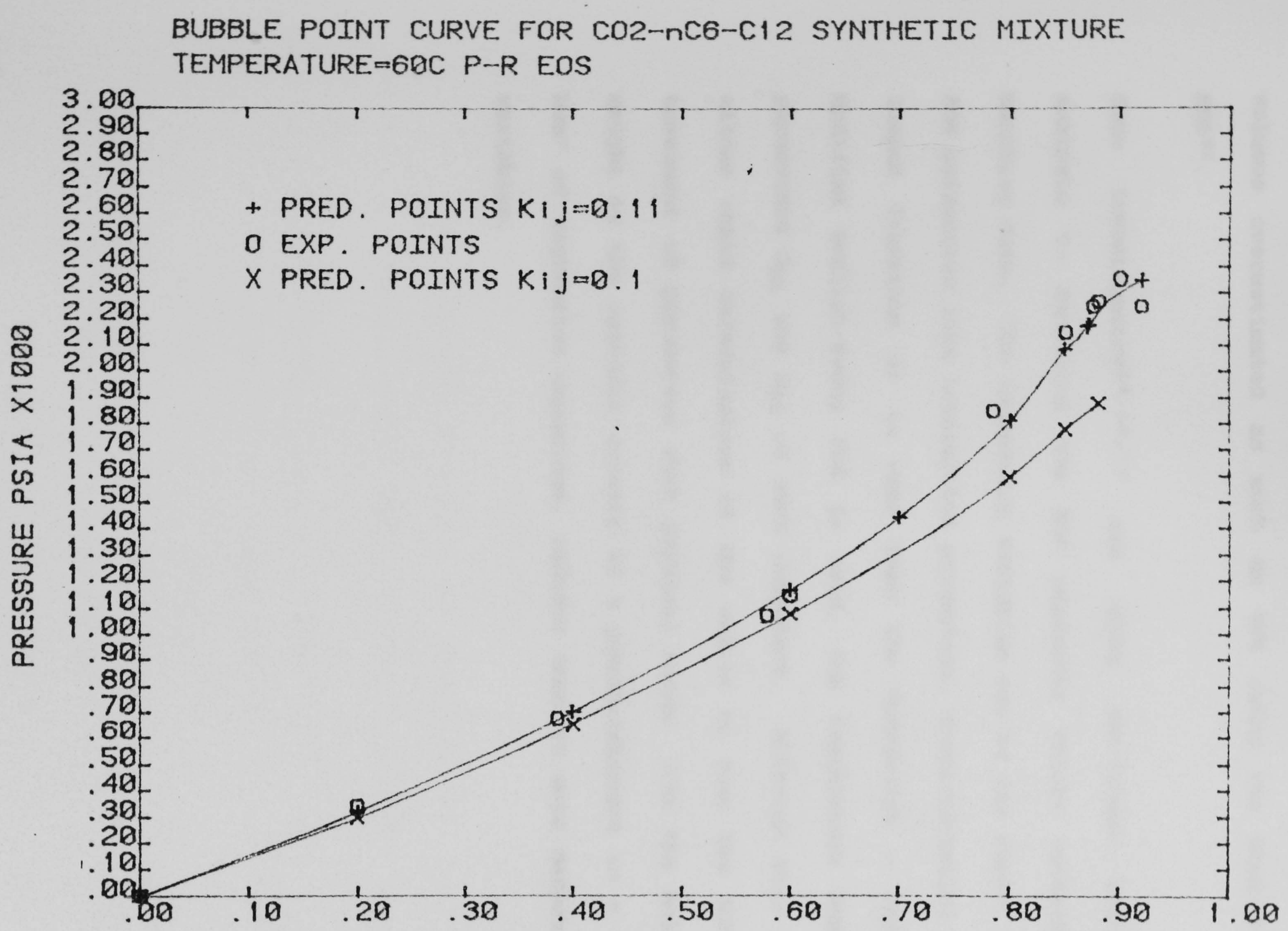
BUBBLE POINT CURVE FOR CO2-nC6-C12 SYNTHETIC MIXTURE
TEMPERATURE=60C P-R EOS
+ PRED. POINTS Kij=0.11
O EXP. POINTS
X PRED. POINTS Kij=0.1
PRESSURE PSIA X1000
3.00
2.90
2.80
2.70
2.60
2.50
2.40
2.30
2.20
2.10
2.00
1.90
1.80
1.70
1.60
1.50
1.40
1.30
1.20
1.10
1.00
.90
.80
.70
.60
.50
.40
.30
.20
.10
.00
.00
.10
.20
.30
.40
.50
.60
.70
.80
.90
1.00
MOLE FRACTION CARBON DIOXIDE

FIGURE 7-2

Whitson et al in gas condensate studies found the predicted liquid volumes overestimated as much as 45% using the Peng-Robinson EOS[31].

Some investigators[28,19,17] are using non-linear regression analysis to determine the EOS parameter values necessary in matching data. The regression variables can be any subset of the EOS parameters like interaction parameters, characteristics of the lumped fractions or in case that the Zudkevitch - Joffe or Modified Redlich-Kwong EOS is used, the temperature dependent parameters Ω_{ai} and Ω_{bi} of each component. Although this method allows rapid determination of the values to tune the EOS, the treatment of parameters with physical sense, like the molecular weight or the specific gravity of a pseudocomponent in a "black box" of regression equations, reduces them to mere mathematical variables.

TABLE 7-1

CONSTANTS FOR T_C, P_C USING CAVETT'S METHOD

	a	b
0	768.017	2.824
1	1.713	0.441×10^{-3}
2	-0.108×10^{-2}	-0.304×10^{-5}
3	-0.892×10^{-2}	-0.208×10^{-4}
4	0.388×10^{-6}	0.151×10^{-6}
5	0.530×10^{-5}	0.110×10^{-7}
6	0.327×10^{-7}	-0.482×10^{-7}
7		0.139×10^{-9}

TABLE 7-2

SPECIFIC GRAVITIES AS FUNCTIONS OF BOILING POINT USING BERGMAN'S EQUATION

BP(°F)	SG
300	$MW*6.19*10^{-3}$
400	$MW*5.02*10^{-3}$
600	$MW*3.445*10^{-3}$
700	$MW*2.77*10^{-3}$
800	$MW*1.63*10^{-3}$
900	$MW*(-6.33*10^{-4})$
1000	$MW*(-5.906*10^{-3})$

TABLE 7-3

GENERALIZED PROPERTIES OF PETROLEUM HEXANE[25] PLUS GROUPS.

Hydrocarbon Group	Boiling Range °C	Boiling Range °F	Average Boiling Pt. °C	Average Boiling Pt. °F	Density g/ml	Molecular Weight
C_6	36.5-69.2	97.9-156.7	63.9	147	0.685	84
C_7	69.2-98.9	156.7-210.1	91.9	197.5	0.722	96
C_8	98.9-126.1	210.1-259.1	116.7	242	0.745	107
C_9	126.1-151.3	259.1-304.4	142.2	288	0.764	121
C_{10}	151.3-174.6	304.4-346.4	165.8	330.5	0.778	134
C_{11}	174.6-196.4	346.4-385.5	187.2	369	0.789	147
C_{12}	196.4-216.8	385.5-422.2	208.3	407	0.800	161
C_{13}	216.8-235.9	422.2-456.7	227.2	441	0.811	175
C_{14}	235.9-253.9	456.7-489.2	246.4	475.5	0.822	190
C_{15}	253.9-271.1	489.2-520	266	511	0.832	206
C_{16}	271.1-287.3	520-547	283	542	0.839	222
C_{17}	287-303	547-577	300	572	0.847	237
C_{18}	303-317	577-603	313	595	0.852	251
C_{19}	317-331	603-628	325	617	0.857	263
C_{20}	331-344	628-652	338	640.5	0.862	275
C_{21}	344-357	652-675	351	664	0.867	291
C_{22}	357-369	675-696	363	686	0.872	305
C_{23}	369-381	696-717	375	707	0.877	318
C_{24}	381-392	717-737	386	727	0.881	331
C_{25}	392-402	737-756	397	747	0.885	345
C_{26}	402-413	706-775	408	766	0.889	359
C_{27}	413-423	775-793	419	784	0.893	374
C_{28}	423-432	793-810	429	802	0.896	388
C_{29}	432-441	810-826	438	817	0.899	402
C_{30}	441-450	826-842	446	834	0.902	416
C_{31}	450-459	842-857	455	850	0.906	430
C_{32}	459-468	857-874	463	866	0.909	444
C_{33}	468-476	874-888	471	881	0.912	458
C_{34}	476-483	888-901	478	895	0.914	472
C_{35}	483-491	901-915	486	908	0.917	486
C_{36}			493	922	0.919	500
C_{37}			500	934	0.922	514
C_{38}			508	947	0.924	528
C_{39}			515	959	0.926	542
C_{40}			522	972	0.928	556
C_{41}			528	982	0.930	570
C_{42}			534	993	0.931	584
C_{43}			540	1004	0.933	598
C_{44}			547	1017	0.935	612
C_{45}			553	1027	0.937	626

LIST OF REFERENCES

1. Orr, F.M. and Taber, J.J.:
Displacement of Oil by Carbon Dioxide,
Annual report for DOE/US, November 1981.

2. Robinson, D.B. and Peng, D.-Y.:
"The Characterisation of the Heptanes and Heavier Fractions"
Research Report 28, GPA Tulsa (1978).

3. Whitson, C.H.:
"Effect of Physical Properties Estimation on Equation of State Predictions", SPE paper No 11120, 1982.

4. Erbar, J.H.:
Prediction of Absorber Oil K-values and Enthalpies,
Gas Processors Ass, Tulsa, GPA, RR13, 1977.

5. Cavett, R.H.:
Physical Data for Distillation Calculations - Vapour Liquid Equilibrium, Proc 27th Meeting, API,
San Francisco (1962) 351-366.

6. Bergman, D.F.:
Predicting the Phase Behaviour of Natural Gas in Pipelines,
PhD Dissertation, U of Michigan, Ann Arbor (1976).

7. Bergman, D.F., Tek, M.R. and Katz, D.L:
Retrograte Condensation in Natural Gas Pipelines,
Project PR 26-69 of the Pipelines Research Committee,
AGA (Jan 1977).

8. Whitson, C.H.:
Characterising Hydrocarbon Plus Fractions, EUR No 183,
presented at European Offshore Petroleum Conference and Exhibition, London, Oct 1980.

9. Lohrenz, J., Bray, B., Clark, C.:
Calculating Viscosities of Reservoir Fluids from their Compositions, JPT, October 1964.

10. Watson, K.M., Nelson, E.F. and Murphy, G.B.:
Characterisation of Petroleum Fractions,
Ind Eng Chem Vol 27 (1935) 1460-1464.

11. Haaland, S.:
Characterisation of North Sea Crude Oils and Petroleum Fractions, MS Thesis, Norwegian Institute of Technology, University of Trondheim, Norway.

12. Hariu, O.H. and Sage, R.C.:
Crude Split Figured by Computer,
Hydro Proc (April 1969) 143-148.

13. Lohrenz, J. and Bray, B.C.:
The Calculation of Bubble Points of Reservoir Fluids from their Compositions, SPE paper 792, May 1964.

14. Coats, K.:
Simulation of Gas Condensate Reservoir Performance,
SPE paper No 10521, 1982.

15. Lee, S.T., Jacoby, R.H., Chen, W.H. and Culham, W.E.:
Experimental and Theoretical Studies on the Fluid Properties
Required for Stimulation of Thermal Processes,
Soc Pet Eng J, October 1982 pp 535-550.

16. Hong, K.C.:
Lumped Component Characterisation of Crude Oils for
Compositional Simulation, SPE/DOE No 10691.

17. Mehra, R.K., Heidemann, R.A. and Aziz, K.:
A Statistical Approach for Combining Reservoir Fluids into
Pseudocomponents for Compositional Model Studies,
SPE paper No 11201, 1982.

18. Smith, R.L. and Watson, K.M.:
Boiling Points and Critical Properties of Hydrocarbon
Mixtures, Ind Eng Chem, Vol 29 (1937) 1408-1414.

19. Mott, R.E.:
Modelling of Condensate Reservoirs, Seminar on North Sea
Condensate Reservoirs and their Development,
London, October 1982.

20. Fussell, D.D. and Yarborough, L.:
The Effect of Phase Data on Liquid Recovery During
Cycling of a Gas Condensate Reservoir,
SPE paper No 3373, March 1971.

21. Hughes, D.S., Matthews, J.D. and Mott, R.E.:
Theoretical Aspects of Calculating the Performance of
CO_2 as an EOR Process in North Sea Reservoirs,
1st European Symposium on EOR, Bournemouth, Sept 21-23,
1981.

22. Mott, R.E.:
Calculating PVT Behaviour in Gas Condensate Reservoirs,
Oil Recovery Projects Division, Atomic Energy Establishment,
Winfrith April 1982.

23. Rowe, A.M.:
Internally Consistent Correlations for Predicting
Phase Compositions for Use in Reservoir Compositional
Simulators, SPE paper 7475, October 1-3, 1978.

24. Standing, M.B.:
Volumetric and Phase Behaviour of Oil Field Hydrocarbon
Systems, Soc Pet Engnrs, Dallas (1977) 124.

25. Katz, D.L. and Firoozabadi, A.:
Predicting Phase Behaviour of Condensate-Crude
Oil Systems Using Methane Interaction Coefficients.

26. Conrand, P.G., Gravier, J.F.:
Peng-Robinson EOS Checks validity of PVT experiments
Oil and Gas Journal, April, 21, 1980.

27. Symeonides, P.:
Generation of a PVT Report from a Vapour Liquid Equilibria Model, M Eng Project, Heriot-Watt University, 1982.

28. Coats, K.H. and Smart, G.T.:
Application of a Regression Based EOS PVT Program to Laboratory Data.

29. McGlashan, R.S.:
A Compositional Phase Equilibrium Model Applied to Pressure Drop Prediction in North Sea Oil Wells, PhD Dissertation, Heriot-Watt University, 1980.

30. Varotsis, N., Stewart, G., Todd, A.C. and Clancy, M.:
An Experimental and Theoretical Study of the Phase Behaviour of North Sea Reservoir Fluids with Special Reference to Miscibility with the Injection Gases CO_2, N_2 and CH_4, to be presented at the 1984 SPE EOR Symposium to be held April 15-18, 1984 in Tulsa US.

31. Whitson, C.H. and Torp, S.B.:
Evaluating Constant Volume Depletion Data, SPE paper No 10067, 1981.

32. API Research Project 44, Selected values of Physical and Thermodynamic Properties of Hydrocarbons and Related Compounds, Texas University, Texas 1972.

CHAPTER 8

THE PHASE BEHAVIOUR SIMULATION MODEL

8.1 GENERAL

The mathematical models and algorithms presented earlier have been formulated into a computer program called VLE. This section contains a detailed description of the structure of the program, its options and its main subroutines. The program is written in FORTRAN IV language and is implemented as a conversational timeshare package using a visual display unit linked to a Honeywell 66/6000 computer.

8.2 THE MAIN PROGRAM

The user of the program is guided through the data input and calculation options by a question and answer sequence at the visual display unit. A full description of the user dependent input parameter is given in Appendix I. The available modes of calculation are:

(i) Bubble point calculation (pressure or temperature)

(ii) Bubble point curve calculation (P–Z diagram)

(iii) Dew point calculation (pressure or temperature)

(iv) Dew point curve calculation (P–Z diagram)

(v) Isothermal flash calculation

(vi) Successive isothermal flash calculations

(vii) Ternary phase envelope calculation

(viii) Constant volume depletion

(ix) Differential vapourisation

(x) Binary interaction parameter optimisation

Figures 8–1, 8–2, 8–3, 8–4, 8–5, 8–6 give general flow charts of the dew and bubble–point and isothermal flash calculations, the

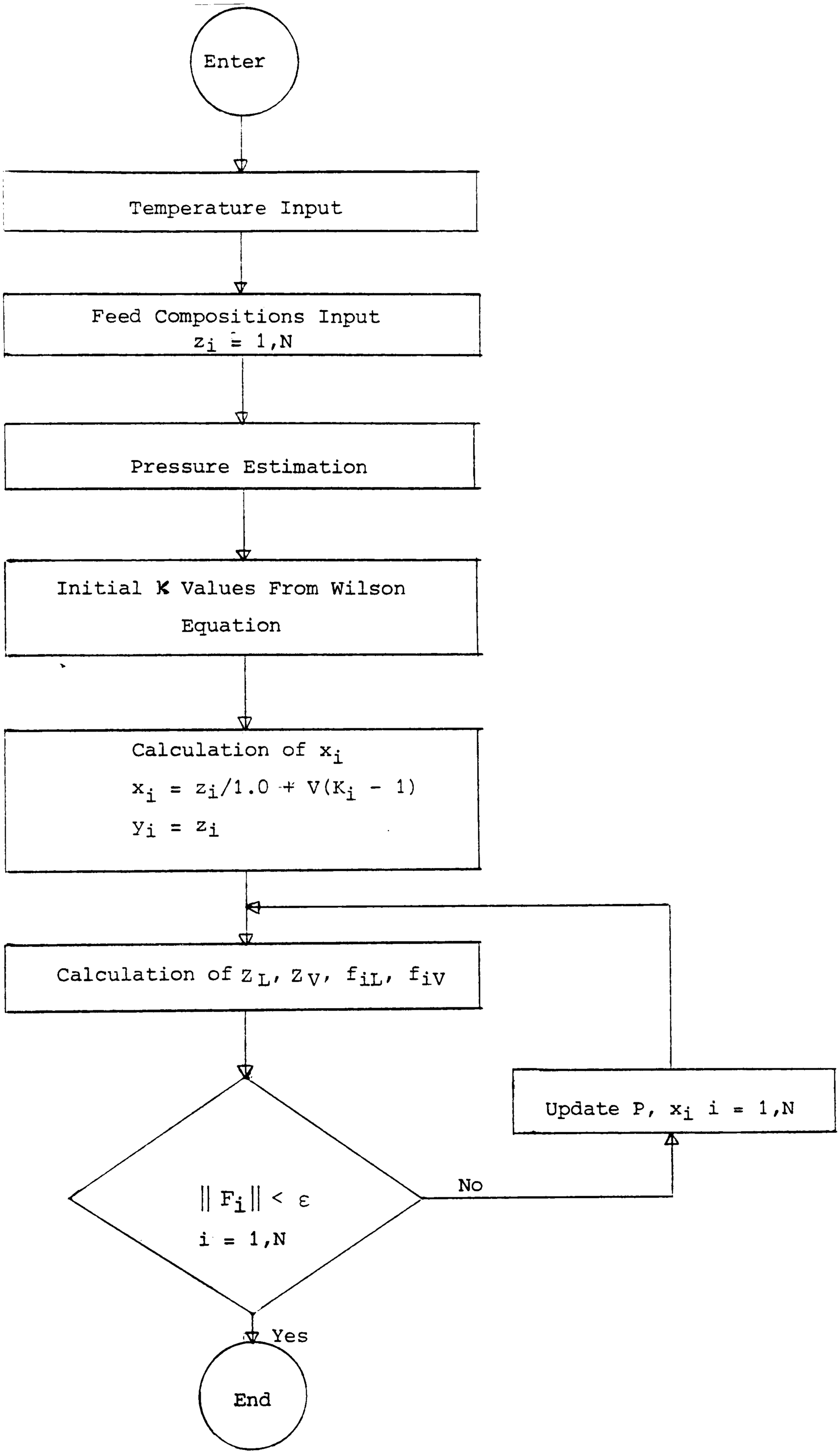

FIGURE 8-1

DEW-POINT CALCULATION - FLOW CHART

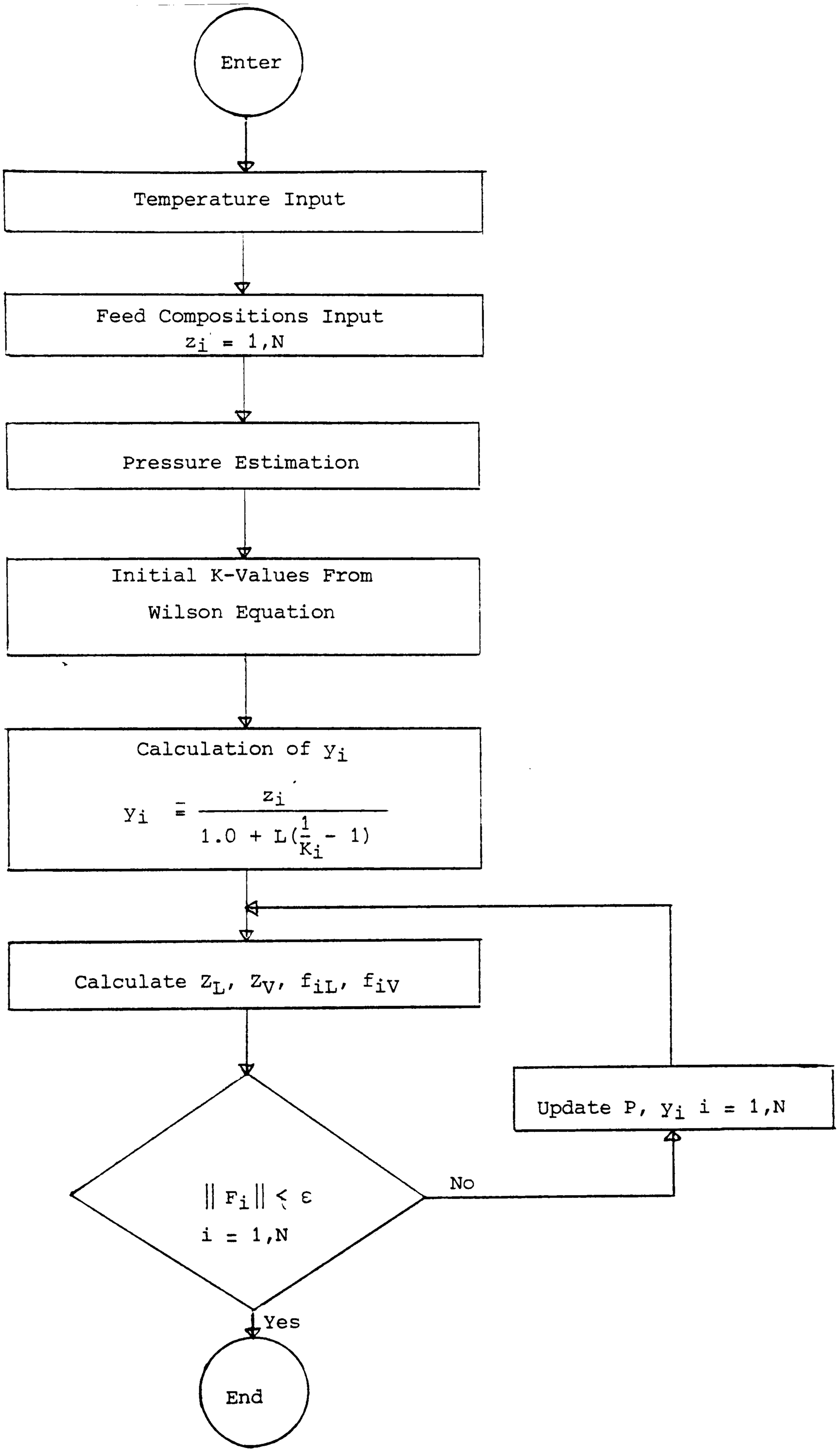

FIGURE 8-2

BUBBLE POINT CALCULATION FLOW CHART

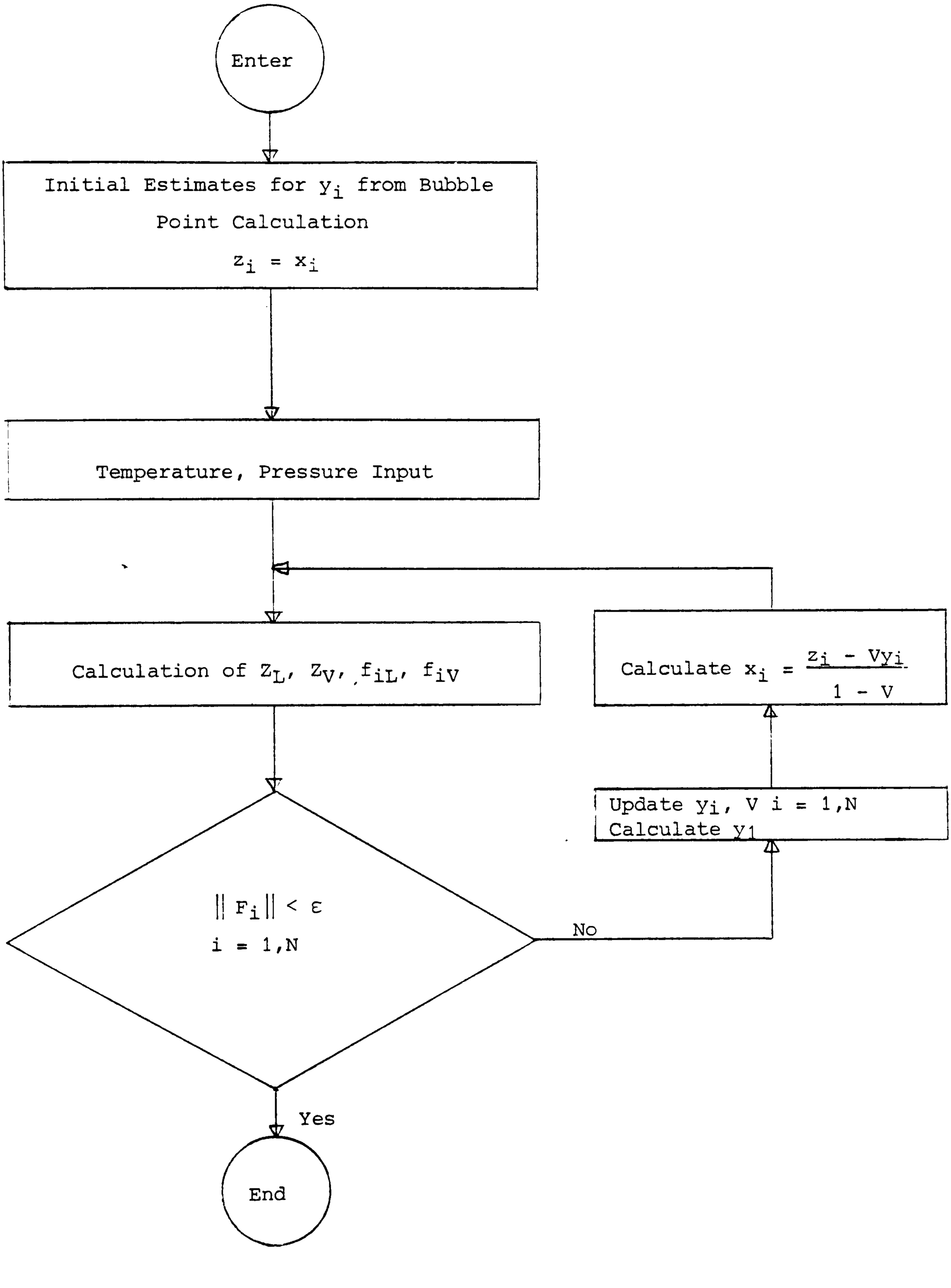

FIGURE 8-3

ISOTHERMAL FLASH CALCULATION MIXTURE PREDOMINANTLY LIQUID
FLOW CHART

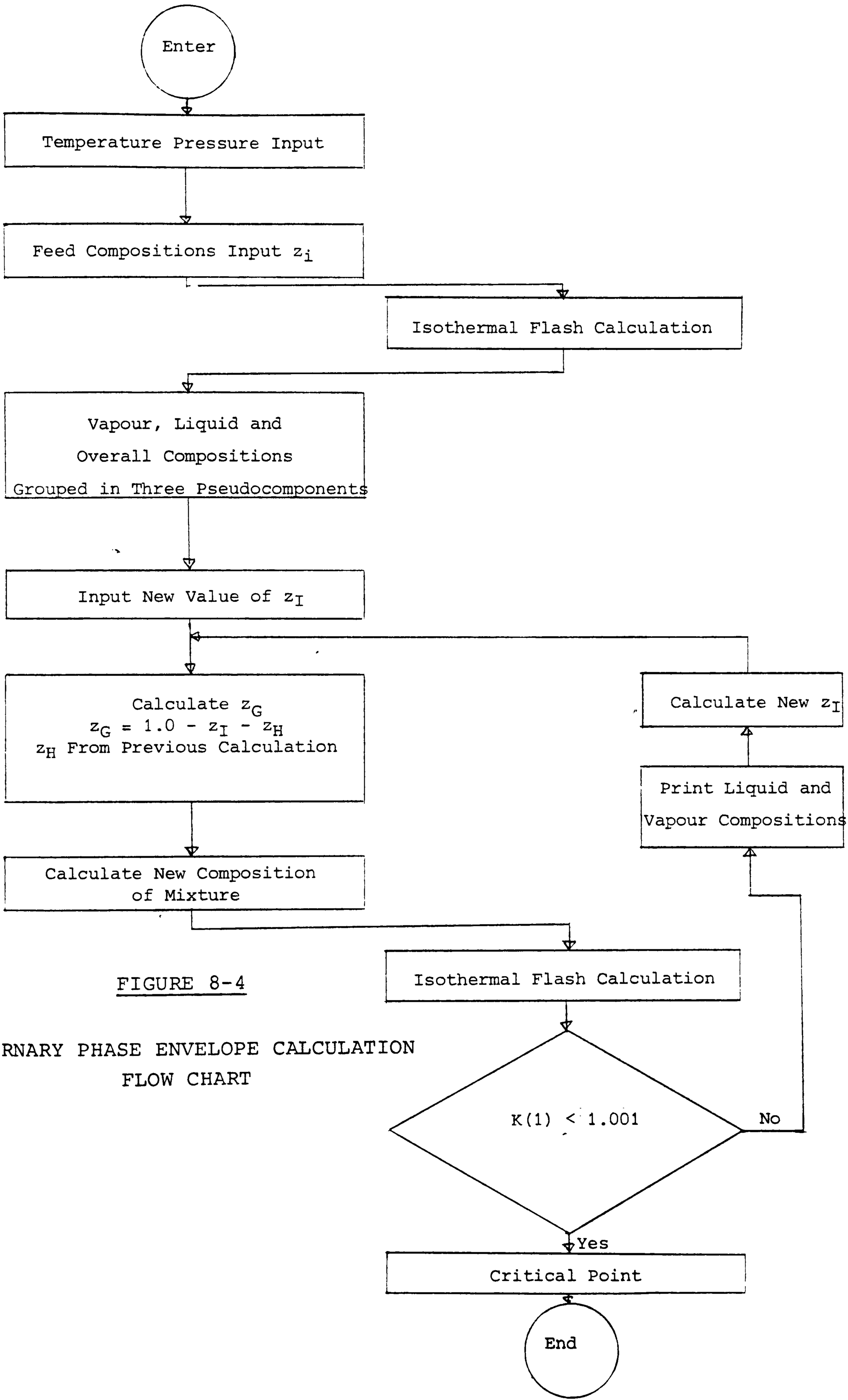

FIGURE 8-4

TERNARY PHASE ENVELOPE CALCULATION
FLOW CHART

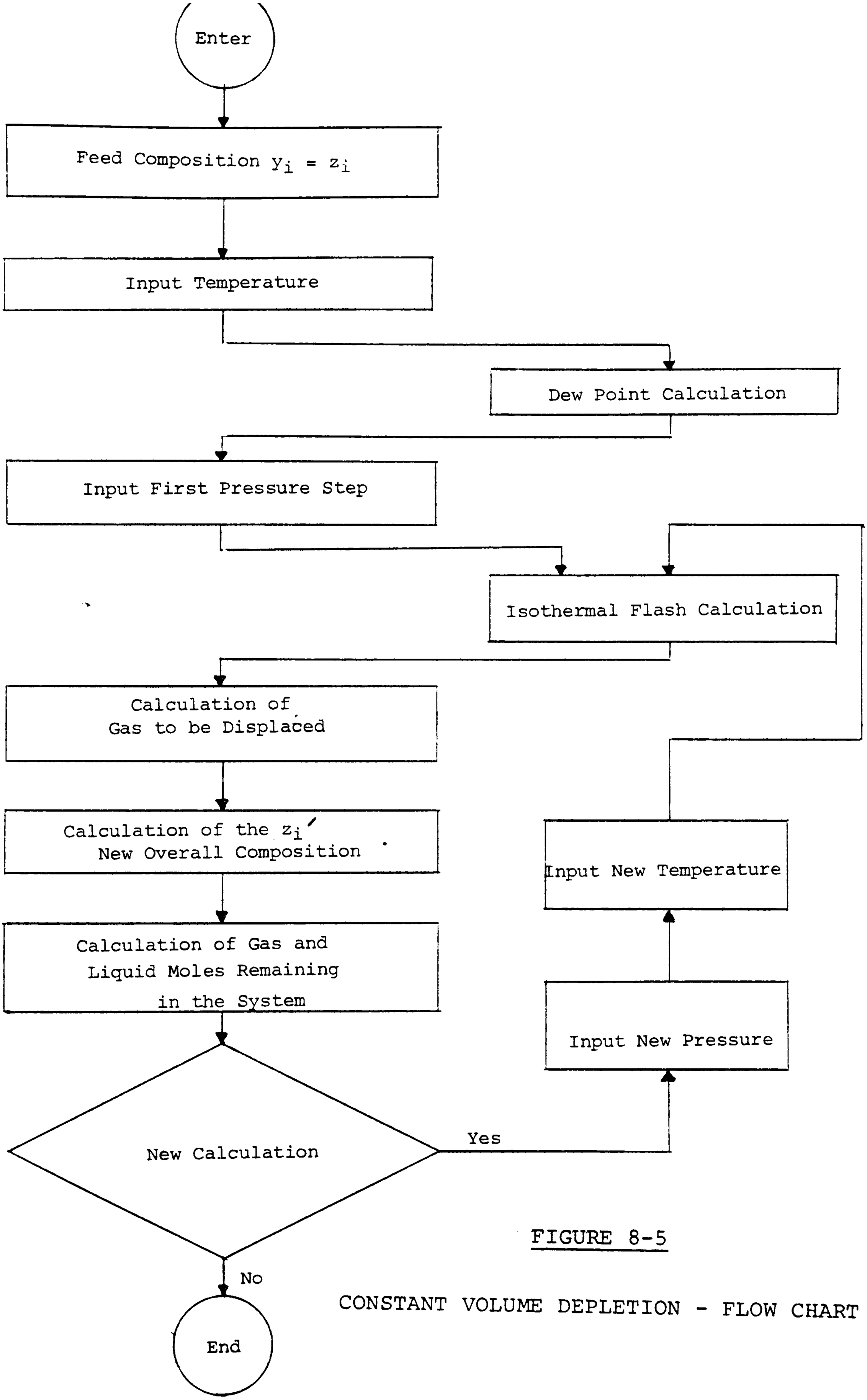

FIGURE 8-5

CONSTANT VOLUME DEPLETION - FLOW CHART

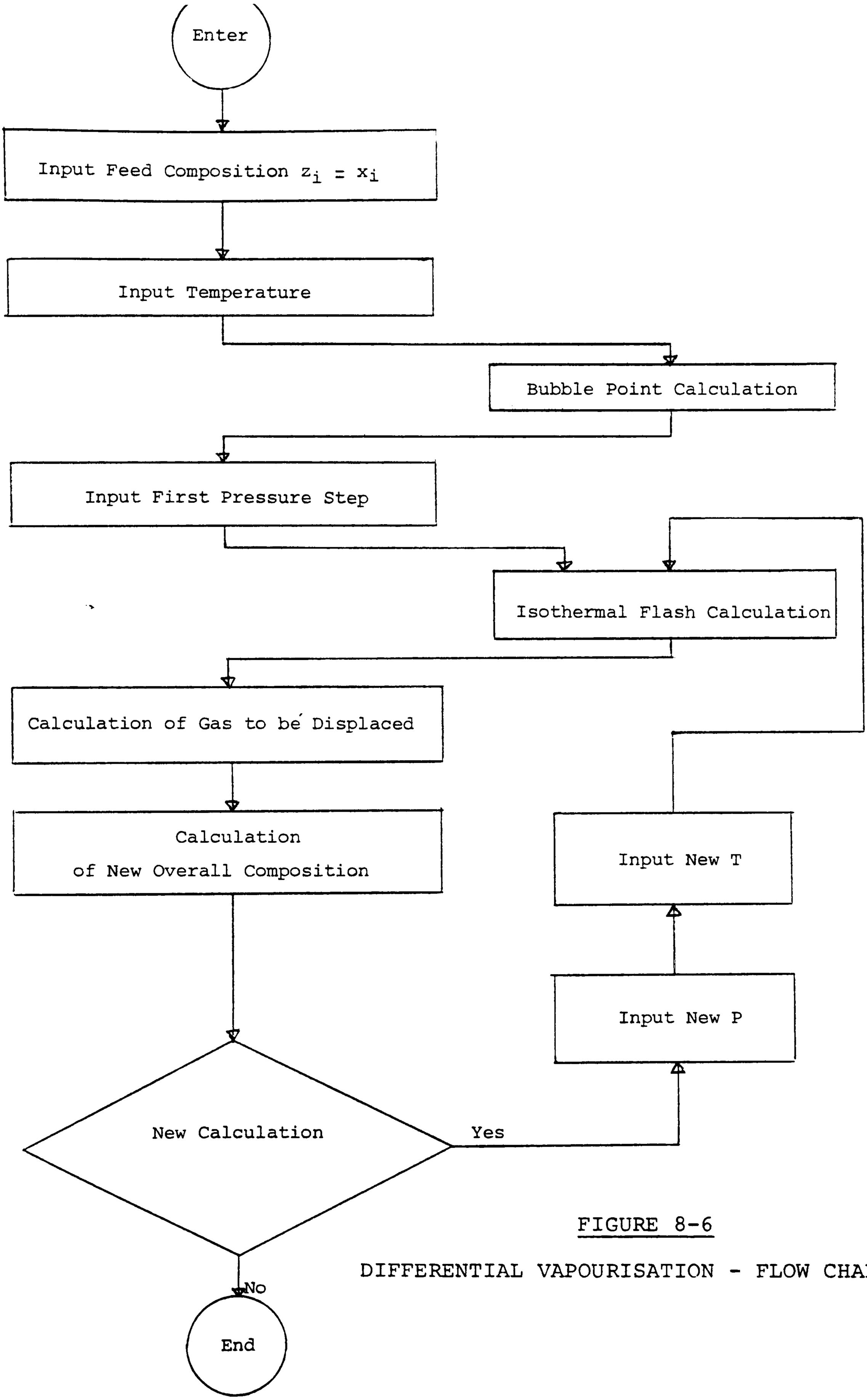

FIGURE 8-6

DIFFERENTIAL VAPOURISATION - FLOW CHART

ternary phase envelope calculation, the constant volume depletion and the differential vapourisation calculation.

8.3 THE DRIVING SUBROUTINES FOR EQUILIBRIUM CALCULATIONS

The driving subroutines for the equilibrium calculations are:

- CDEWPT for the dew-point calculation
- CBUBPT for the bubble-point calculation
- CILF for the isothermal flash calculation

Each driving subroutine calls the quasi-Newton method contained in subroutine SONEM2 to solve the system of non-linear algebraic equations. Figure 8-7 gives the flow chart of CDEWPT. The CBUBPT routine has a similar flow chart and Figure 8-8 demonstrates the flow chart of the isothermal flash calculation driving routine CILF.

8.3 SUBROUTINES FOR EVALUATING THE ALGEBRAIC EQUATIONS

These subroutines return the function evaluations of the algebraic equations which model the various equilibrium calculations that are solved by the quasi-Newton method implemented in subroutine SONEM2. The subroutines for evaluating the algebraic equations are:

- DEWPT for the dew-point calculation
- FBUB for the bubble-point calculation
- ISFL for the isothermal flash calculation

Figure 8-9 gives the flowchart of DEWPT. The FBUB routine has a similar flowchart and Figure 8-10 gives the flowchart of ISFL.

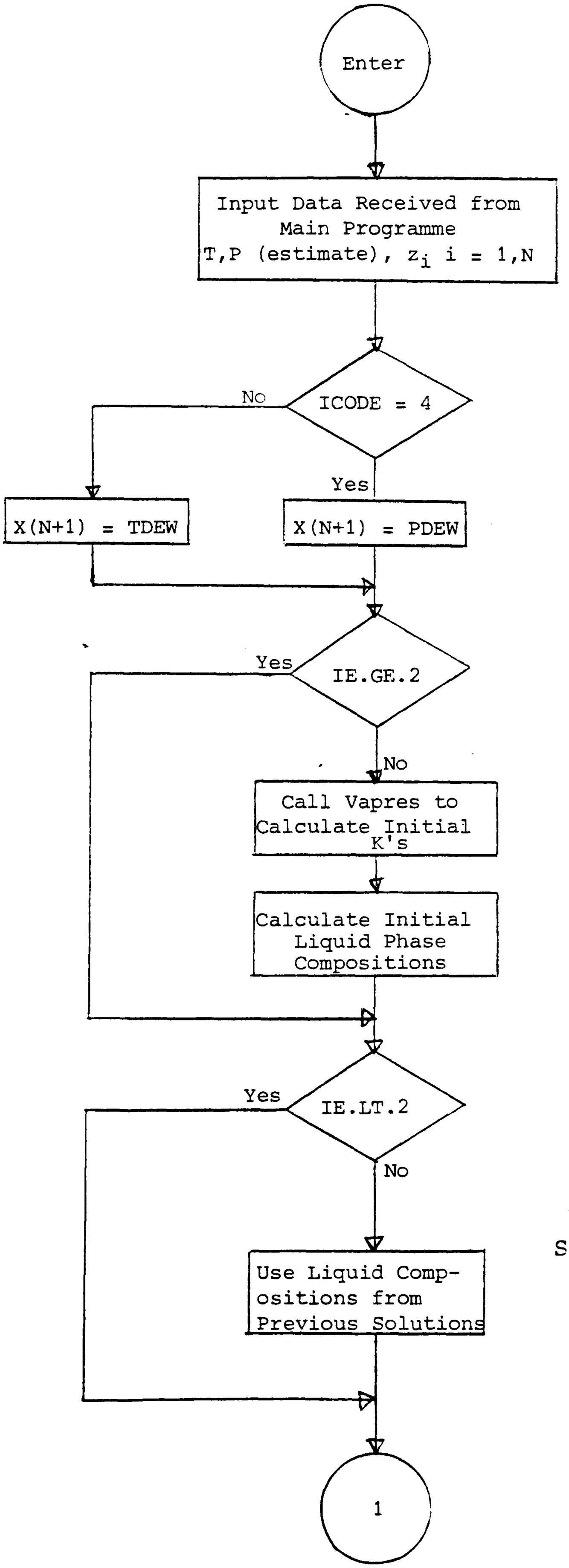

FIGURE 8-7 contd

SUBROUTINE CDEWPT

FLOW CHART

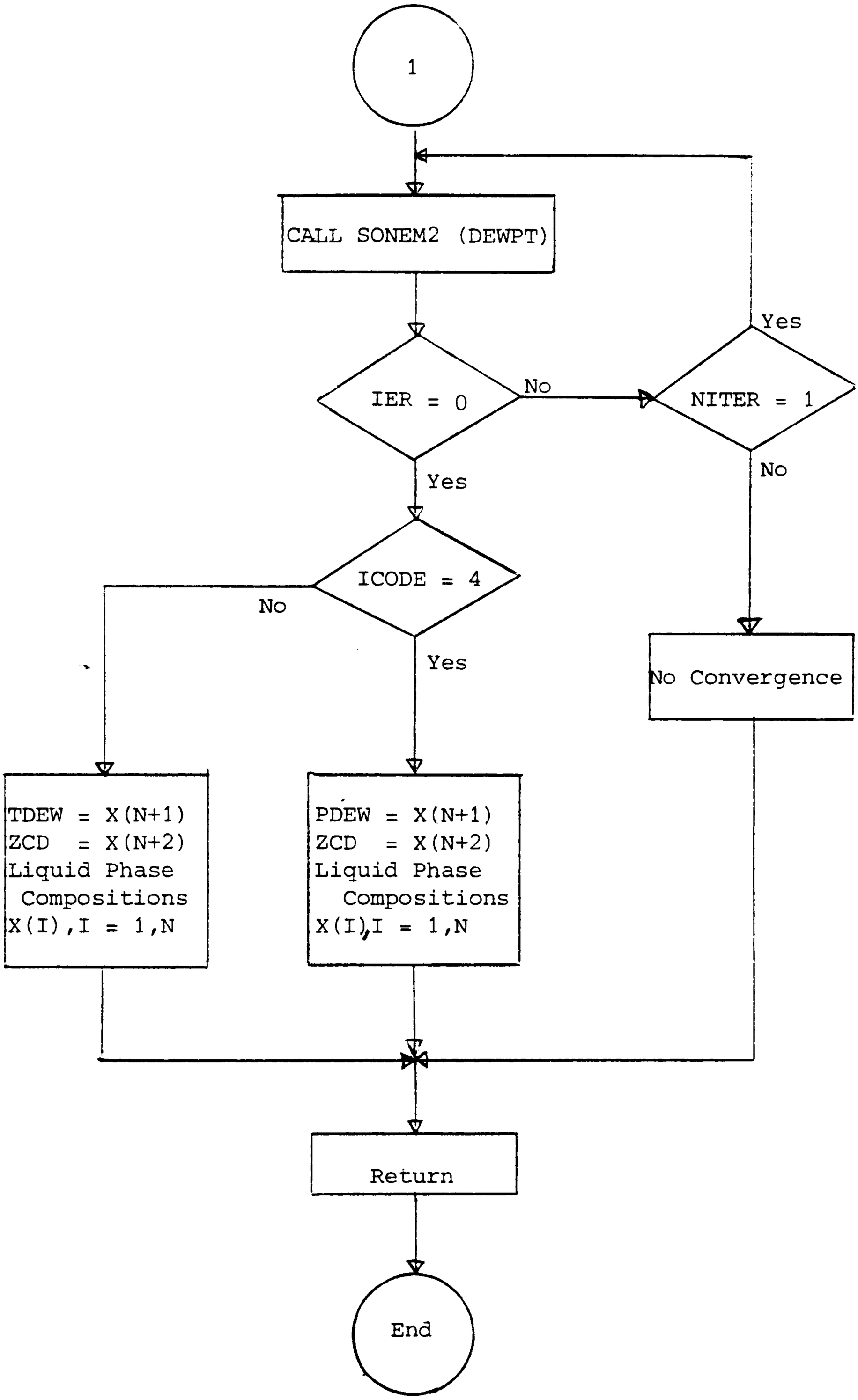

FIGURE 8-7

SUBROUTINE CDEWPT FLOW CHART

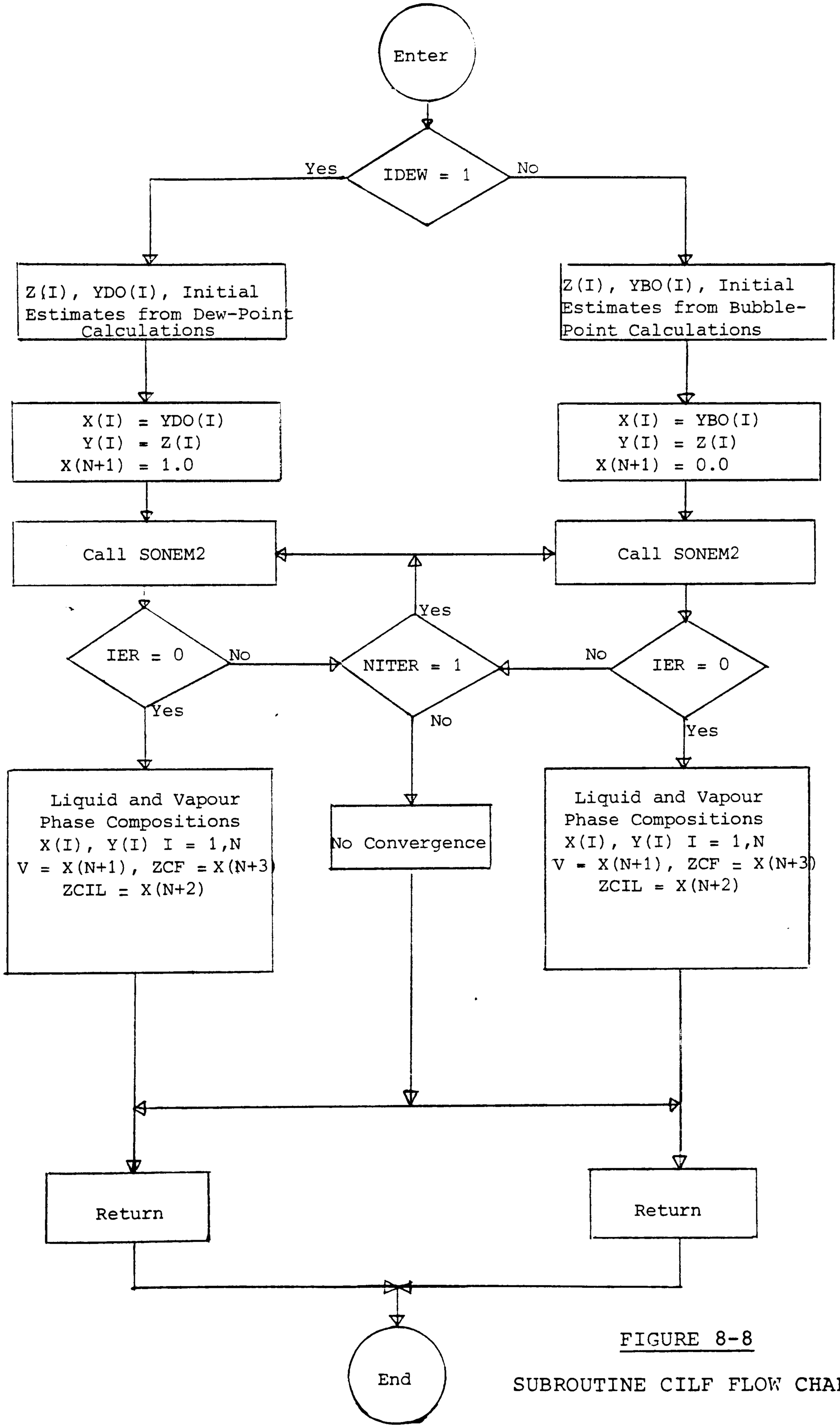

FIGURE 8-8

SUBROUTINE CILF FLOW CHART

FIGURE 8-9

SUBROUTINE DEWPT FLOW CHART

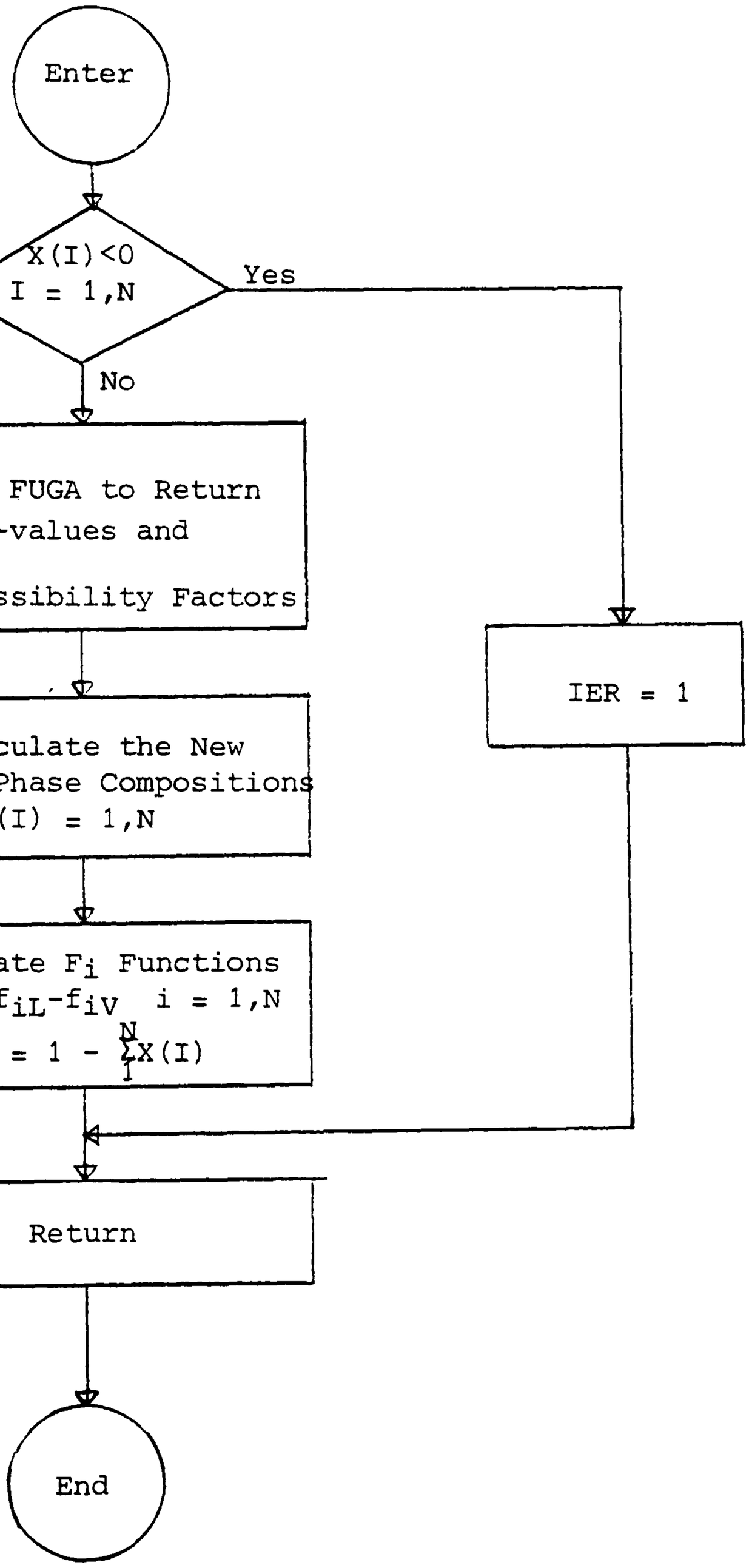

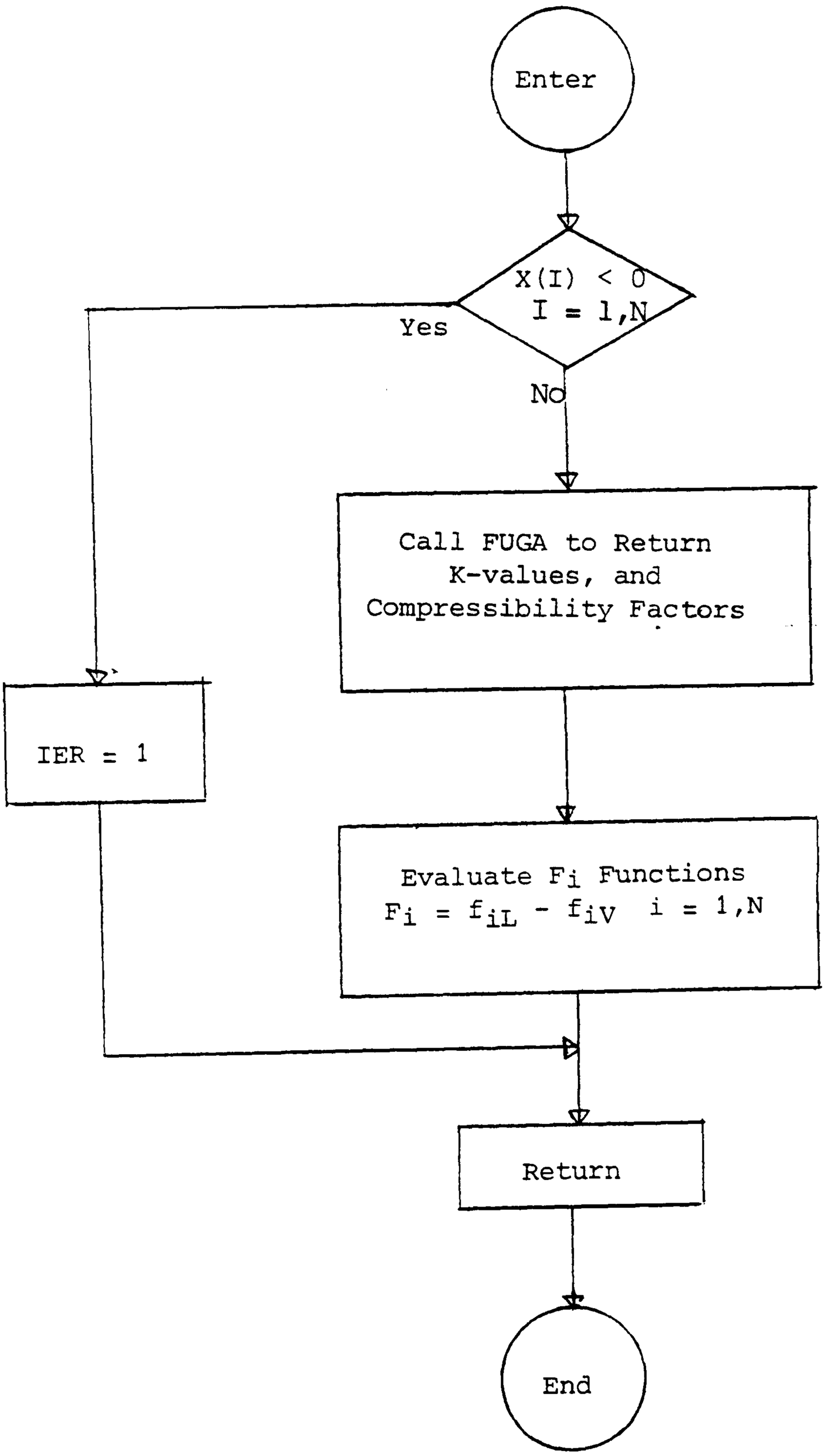

FIGURE 8-10

SUBROUTINE ISFL FLOW CHART

8.5 SUBROUTINES USED TO SOLVE THE ALGEBRAIC EQUATIONS

The subroutines in this section include and solve the system of the non-linear algebraic equations using a quasi-Newton method and Broyden's rank-one updating formula. Subroutine SONEM2 implements the Broyden's n-dimensional quasi-Newton method. The routine operates on a function subroutine FX which returns the function values F_i for each set of independent variable values x_i. Subroutine STEP updates the values of the iteration variables at each step and evaluates the function values F_i at the new step by the call of a function subroutine FX. The iteration matrix, H, is then updated using Broyden's rank-one update formula. Figure 8-11 gives the flowchart of subroutine STEP.

8.6 SUBROUTINES USED FOR THE EVALUATION OF THE CHOSEN EQUATION OF STATE

Subroutine FUGA calls the specific subroutines to calculate the parameters of the chosen equation of state, returning the phase fugacities and compressibility factors to FUGA. The specific subroutines are:

- PENG for the Peng-Robinson EOS
- SRKEQU for the Soave-Redlich-Kwong EOS
- RKEQU for the Modified Redlich-Kwong EOS

The equation of state is solved by an analytical method. Figure 8-12 and 8-13 give the flowcharts of the subroutines FUGA and PENG respectively.

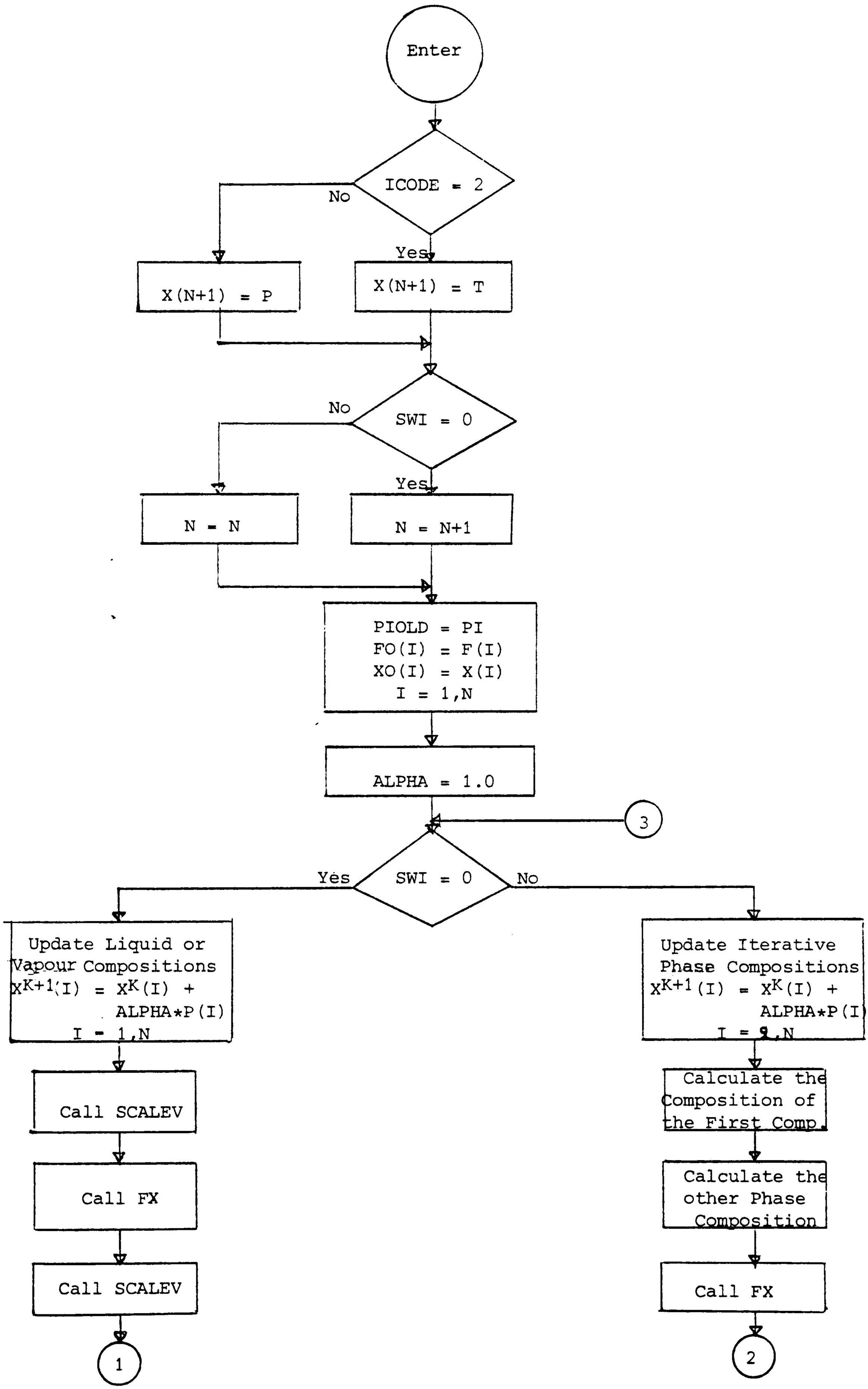

FIGURE 8-11 contd

SUBROUTINE STEP FLOW CHART

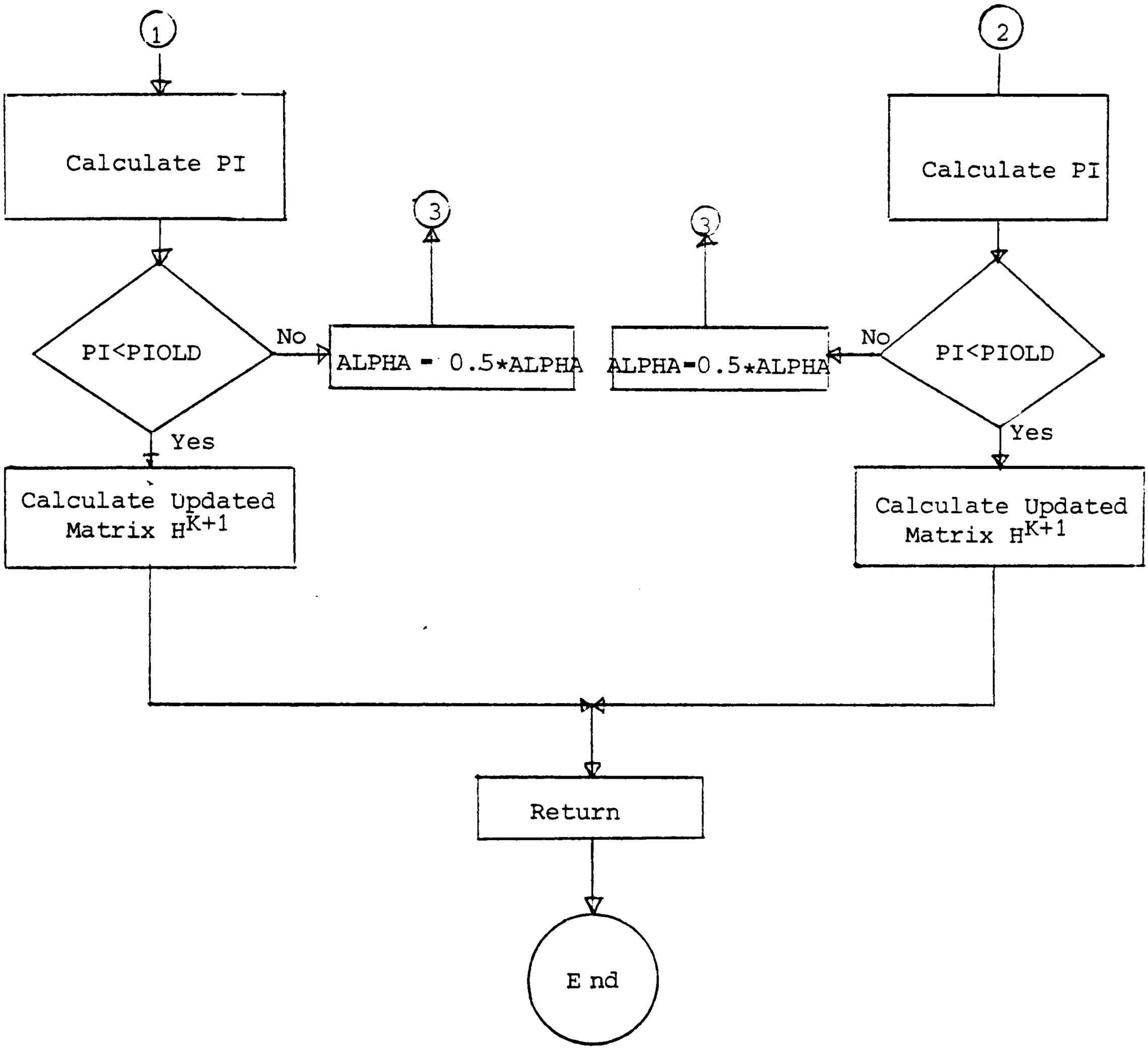

FIGURE 8-11

SUBROUTINE STEP FLOW CHART

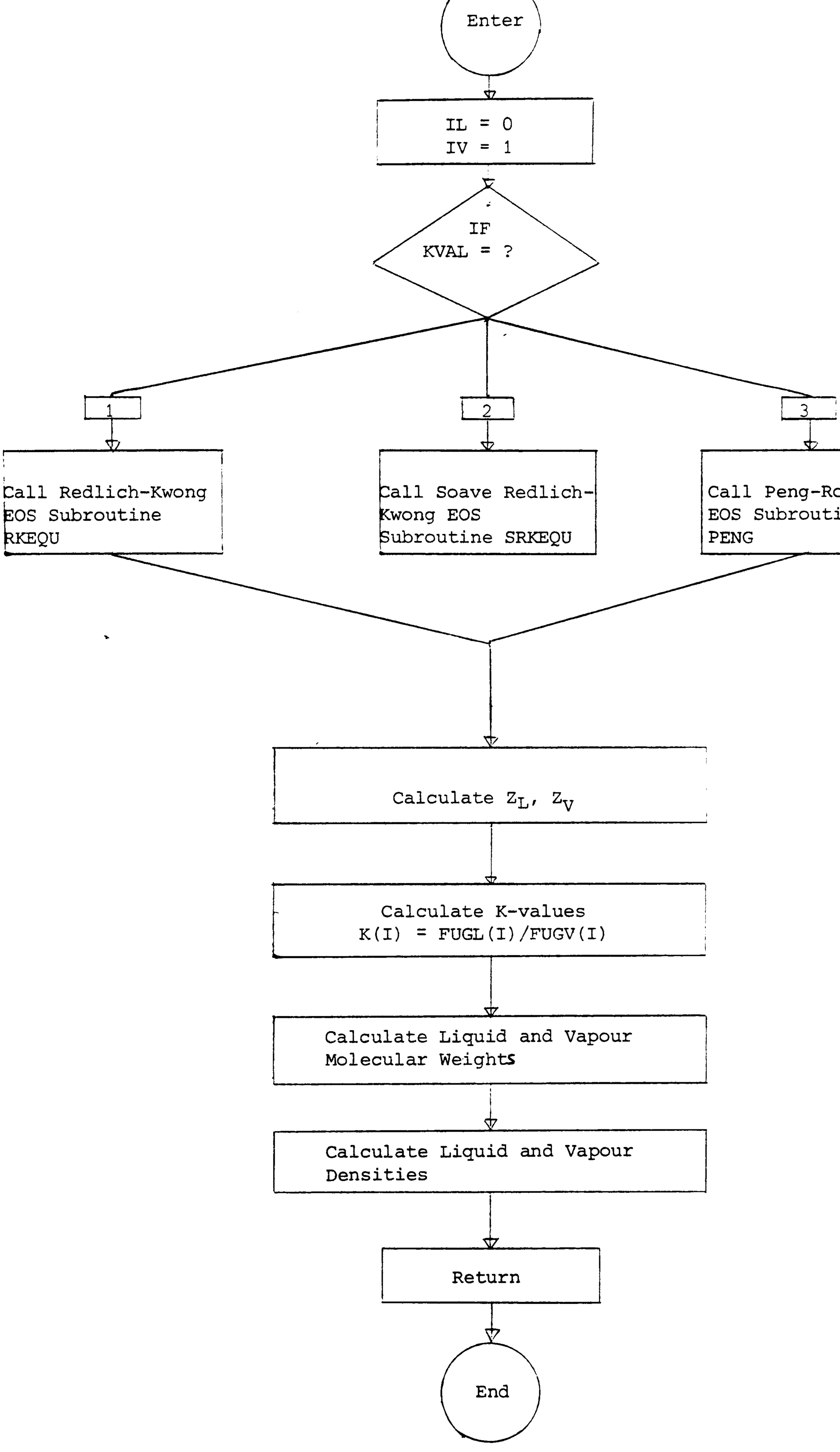

FIGURE 8-12 SUBROUTINE FUGA FLOW CHART

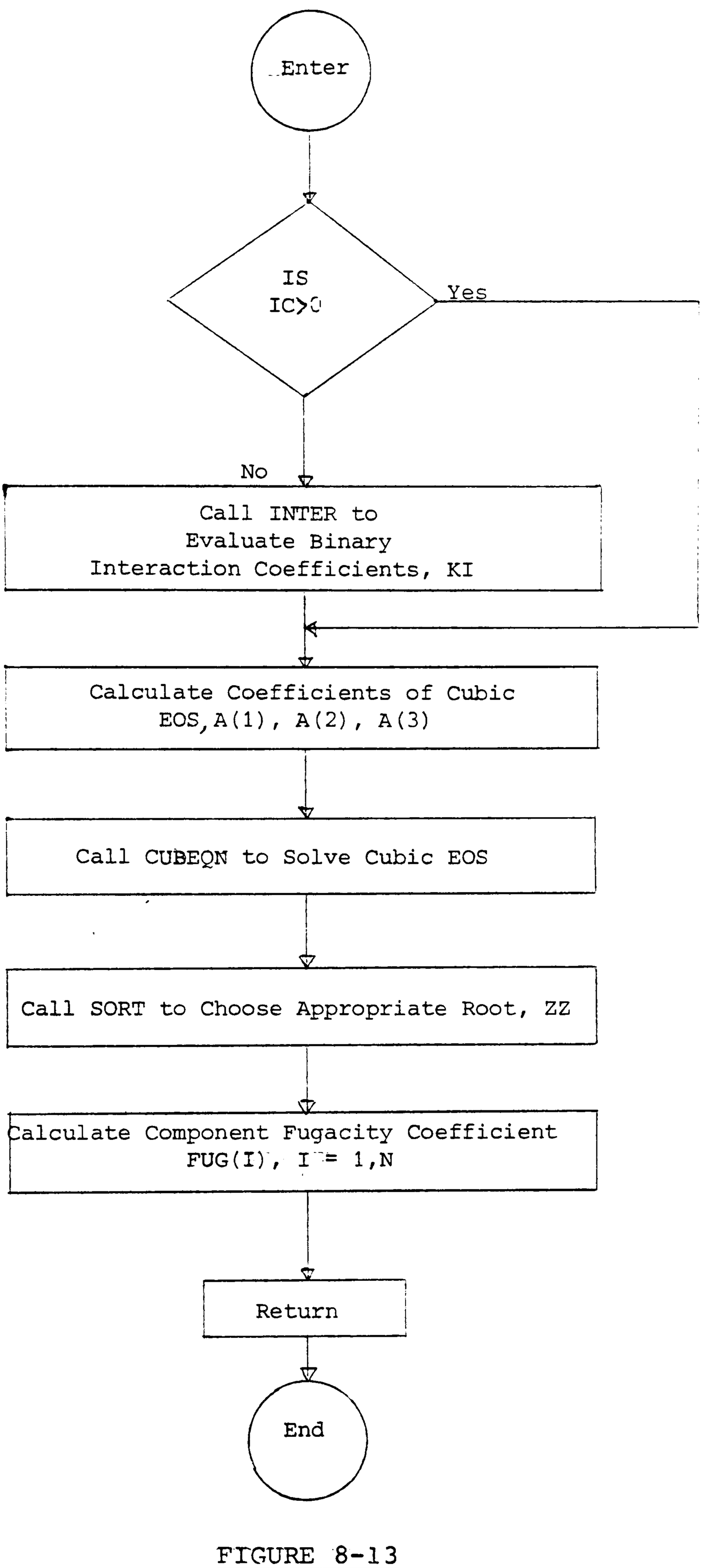

FIGURE 8-13

SUBROUTINE PENG FLOWCHART

CHAPTER 9

EVALUATION OF THE COMPUTER PROGRAM TO SIMULATE HYDROCARBON VAPOUR - LIQUID EQUILIBRIUM CALCULATIONS

9.1 INTRODUCTION

In this chapter, the VLE program described in chapter 8 is used to perform vapour-liquid equilibrium calculations on various types of reservoir fluid systems. The program is also used to simulate the phase behaviour of mixtures of injection gases and hydrocarbons in place, during a miscible flooding in comparison with published data. Later on in this work, the model will be tested against own experimental data.

9.2 BINARY SYSTEMS

The prediction of the phase behaviour of binary mixtures in comparison with published experimental data, and particularly of mixtures which have CO_2, methane or N_2, as one of their components, gives a very good idea as to the selection of the interaction parameters needed to be used with the equation of state, for the particular pair of components.

9.2.1 CO_2 - N Butane Mixture

The experimental data for this binary system have been reported by Olds et al[1]. The phase envelopes were calculated at 100°F and 220°F. The VLE's bubble and dew-point options were used with all three available equations of state. Figure 9-1 shows the predictions of the saturation pressure against CO_2 mole fraction using the Modified Redlich-Kwong EOS at 100°F in comparison with the experimental results. Figure 9-2 shows the predictions for the same phase envelope using the MSRK EOS and Figure 9-3 gives the graphic respresentation of the calculations for the same mixture at two different temperatures, 100°F and 220°F using the P-R

FIGURE 9-1

PHASE ENVELOPE FOR CO2-nBUTANE MIXTURE
TEMPERATURE=100F R-K EOS

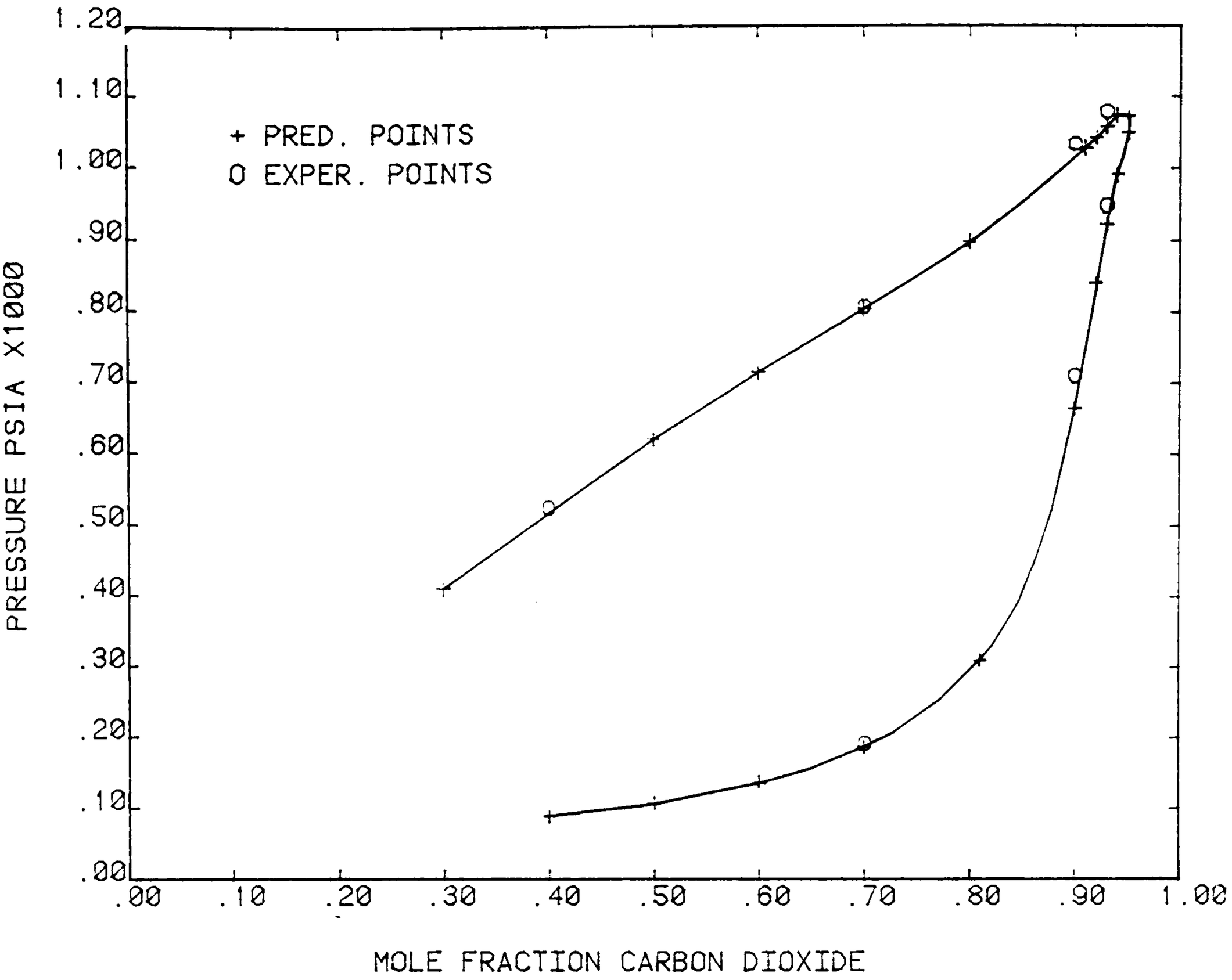

FIGURE 9-2

PHASE ENVELOPE FOR CO2-nBUTANE MIXTURE
TEMPERATURE=100 F MOD.S-R-K EOS

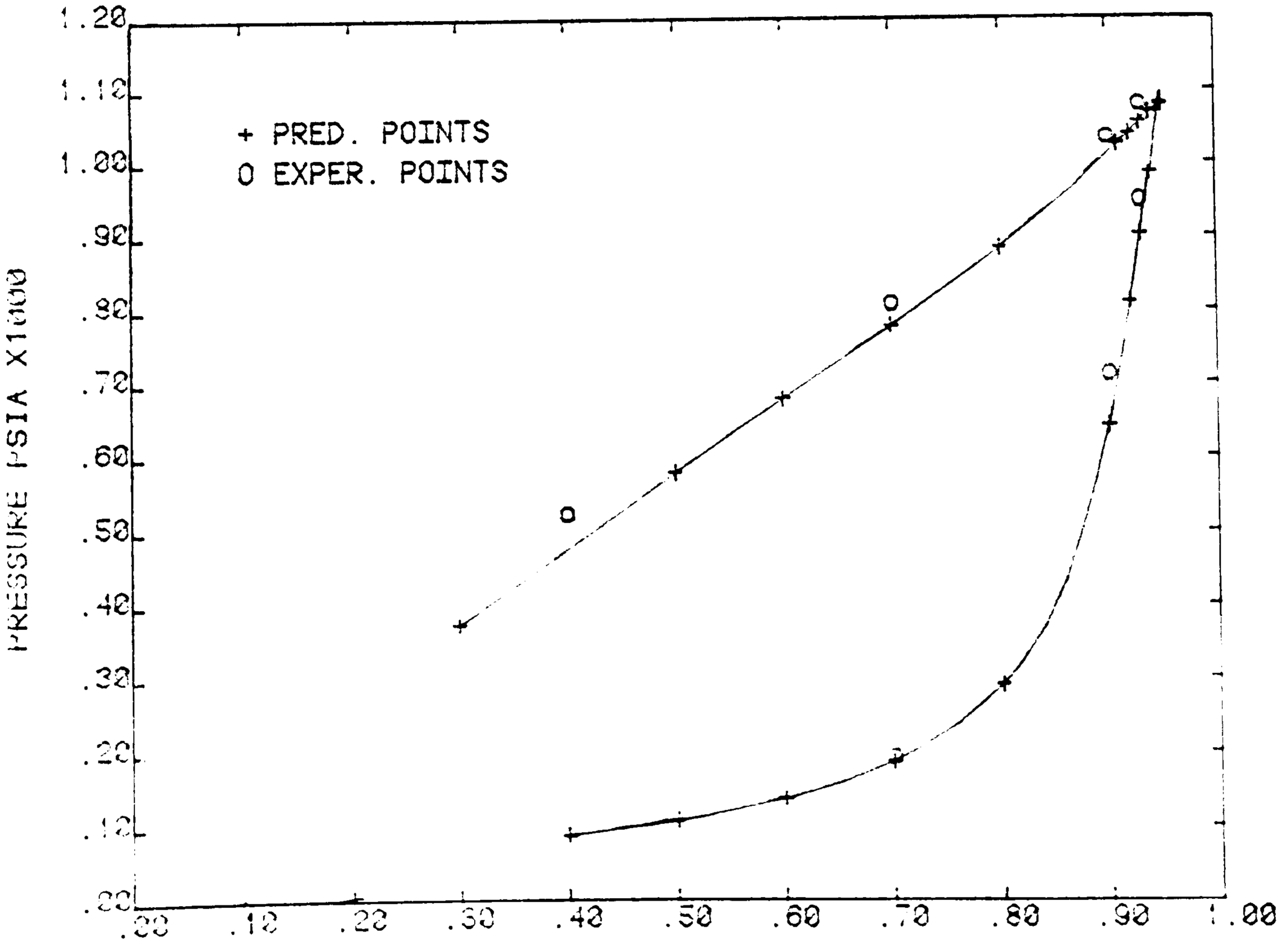

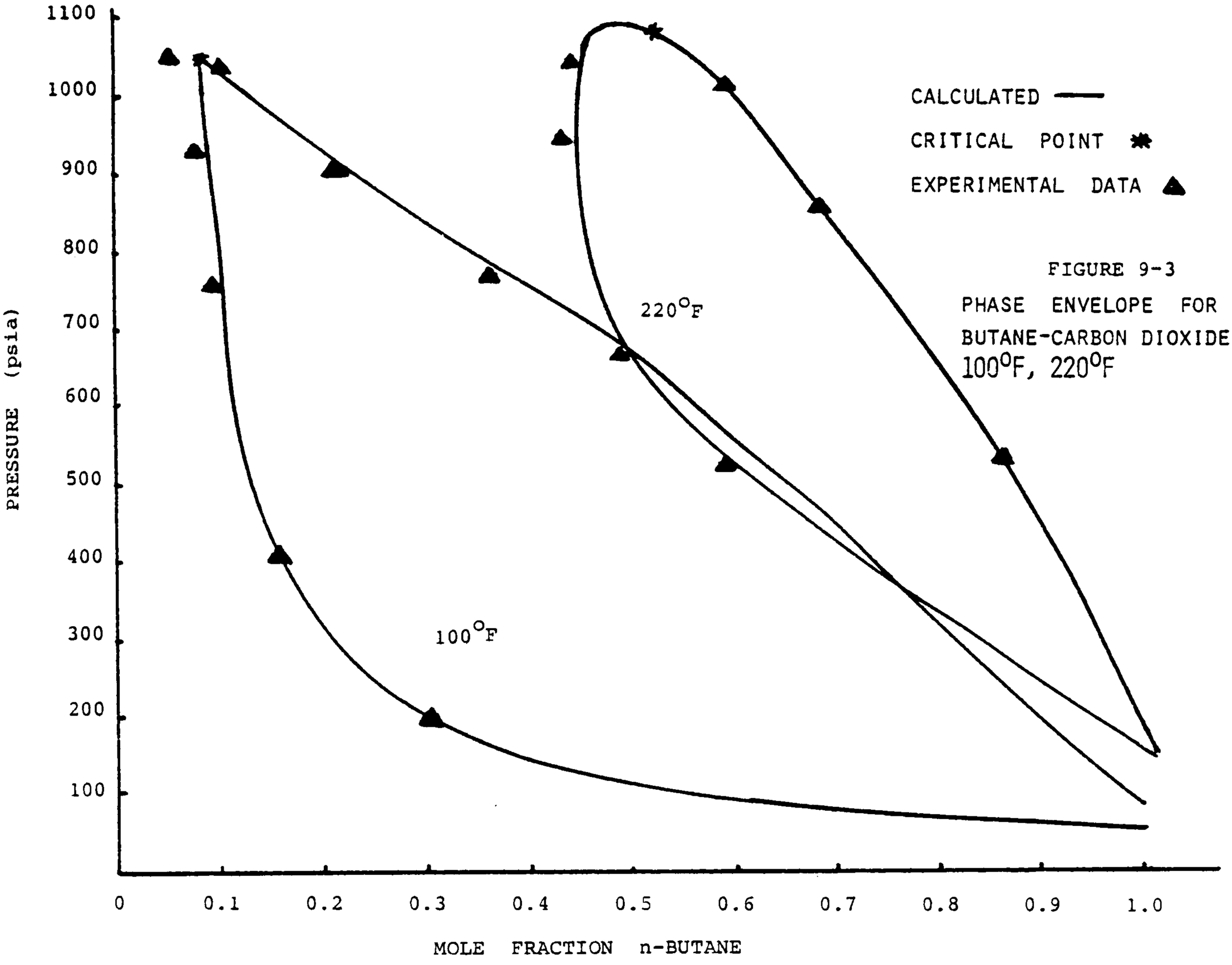

FIGURE 9-3

PHASE ENVELOPE FOR N-BUTANE-CARBON DIOXIDE AT 100°F, 220°F

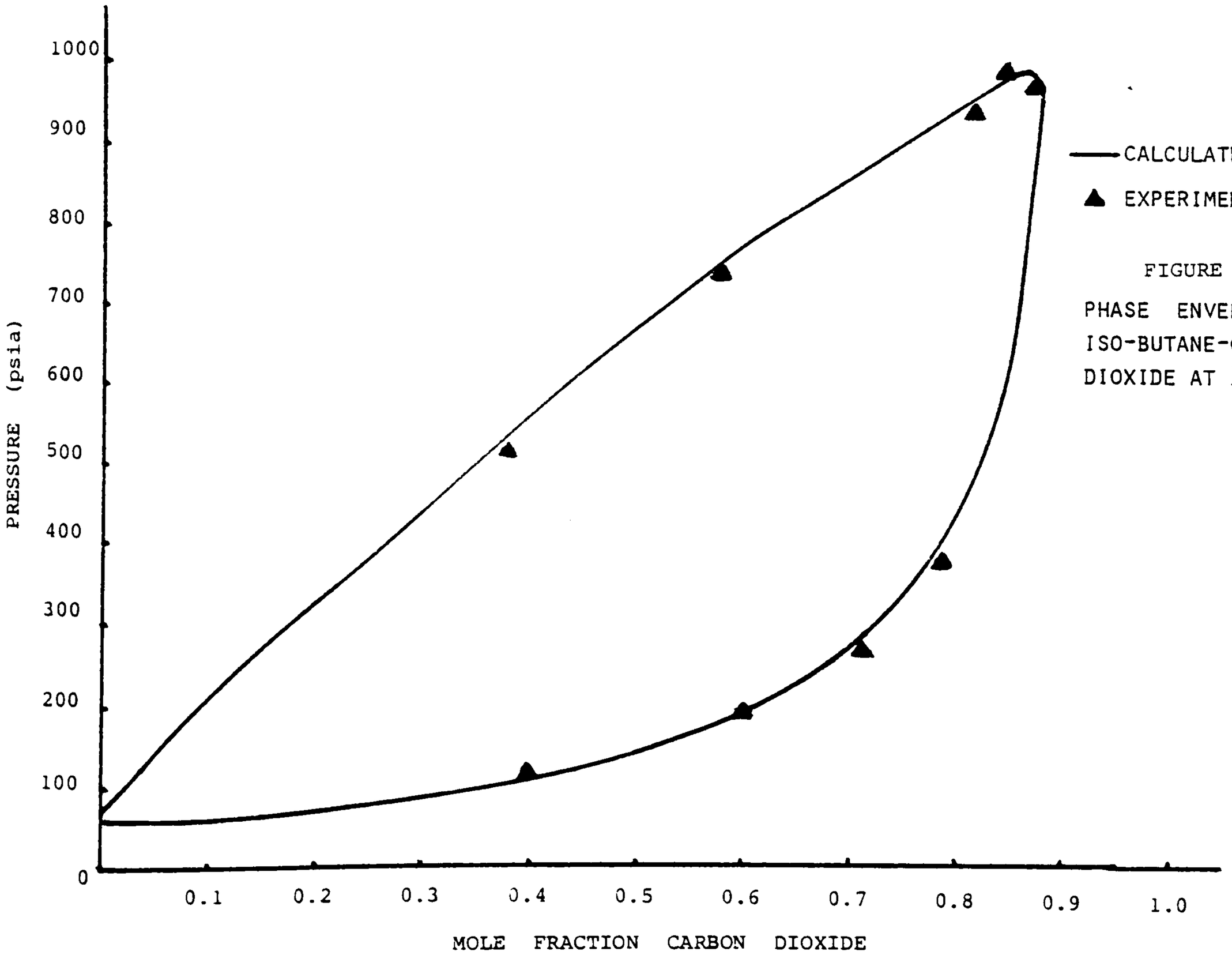

FIGURE 9-4

PHASE ENVELOPE FOR ISO-BUTANE-CARBON DIOXIDE AT 100°F

equation of state. Although the agreement between predicted and measured data is very good for all three EOS, the R-K seems to match perfectly the published measurements.

9.2.2 CO_2 - Isobutane Mixture

The phase behaviour of this mixture has been measured by Besserer and Robinson[2] and theoretical predictions have been reported by Peng and Robinson. The phase envelope was calculated at 100°F and is illustrated in Figure 9-4, as saturation pressure against CO_2 mole fraction. The fitting of the predicted phase boundaries to the experimental data is almost perfect. A binary coefficient of 0.105 was used with the MSRK equation of state as the interaction parameter for the mixture.

9.3 TERNARY MIXTURES CO_2 - N BUTANE - DECANE MIXTURE

The experimental data for this ternary mixture has been published by Metcalfe and Yarborough. The phase envelopes (z-z diagrams) were calculated for two different pressures 1700 psia and 1500 psia at 160°F. Figure 9-5 shows the ternary representations of the two phase envelopes.

9.4 MULTICOMPONENT SYNTHETIC MIXTURES

9.4.1 Eleven Components Synthetic Oil - CO_2 Mixture

This mixture has been studied by Metcalfe and Yarborough[3]. The composition of this oil is given in Table 9-1. The saturation pressure curve as a function of CO_2 mole fraction was calculated at 150°F. Figures 9-6 and 9-7 present the experimentally obtained pressure-composition data and the predicted data derived using the MRK and the MSRK equations of state. The MRK equation of state

seems to fit perfectly the dew-point curve and the critical point. The maximum deviation between the predicted and the experimental points is 3.6%. The interaction coefficient used for CO_2-hydrocarbons is 0.1 and for methane and hydrocarbons heavier than hexane, varies between 0.04 - 0.05.

9.5 RESERVOIR FLUID MIXTURES

9.5.1 Rangely Field Oil-Injection Gases 1 & 2

Rangely field in Colorado, US, was discovered in 1933 and waterflooding was initiated in 1958. It is an almost "dead oil" like a lot of the reservoir oils before the beginning of the tertiary recovery. The experimental data on the phase behaviour of the oil and two different injection gases were published by Graue et al[4]. The compositions of the Rangely oil and of the two injection gases are given in Table 9-2. The bubble point curve calculated as a function of the injected gas fraction in the mixture using the Peng-Robinson equation of state, is plotted in Figure 9-8. The maximum observed deviation between the predicted and the experimental points is 3.5% and occurs at the critical composition. The study has been carried out at a temperature of 160°F.

9.5.2 Reservoir Oil - CO_2 Mixture

This reservoir oil has been studied by Simon et al[5] and its composition is given in Table 9-3. The C_{7+} cut has been divided into three pseudocomponents and the bubble point curve was calculated at 255°F using the MRK equation of state. Figure 9-9 presents the pressure-composition phase envelope and, once again,

FIGURE 9-5

PHASE ENVELOPES FOR THE CO_2-NC_4-C_{10} TERNARY PRESSURE 1500, 1700 PSIA
TEMPERATURE 160°F

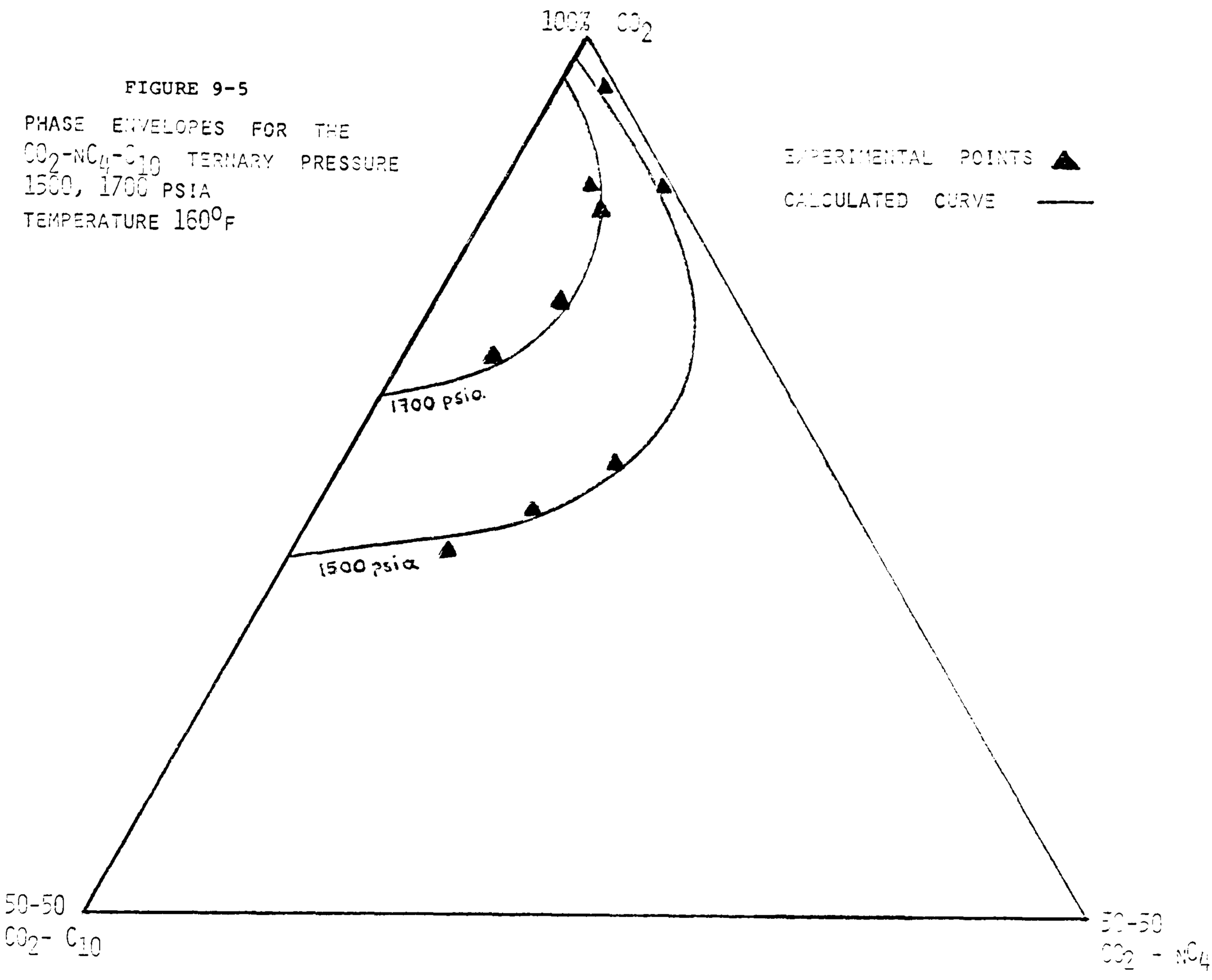

FIGURE 9-6

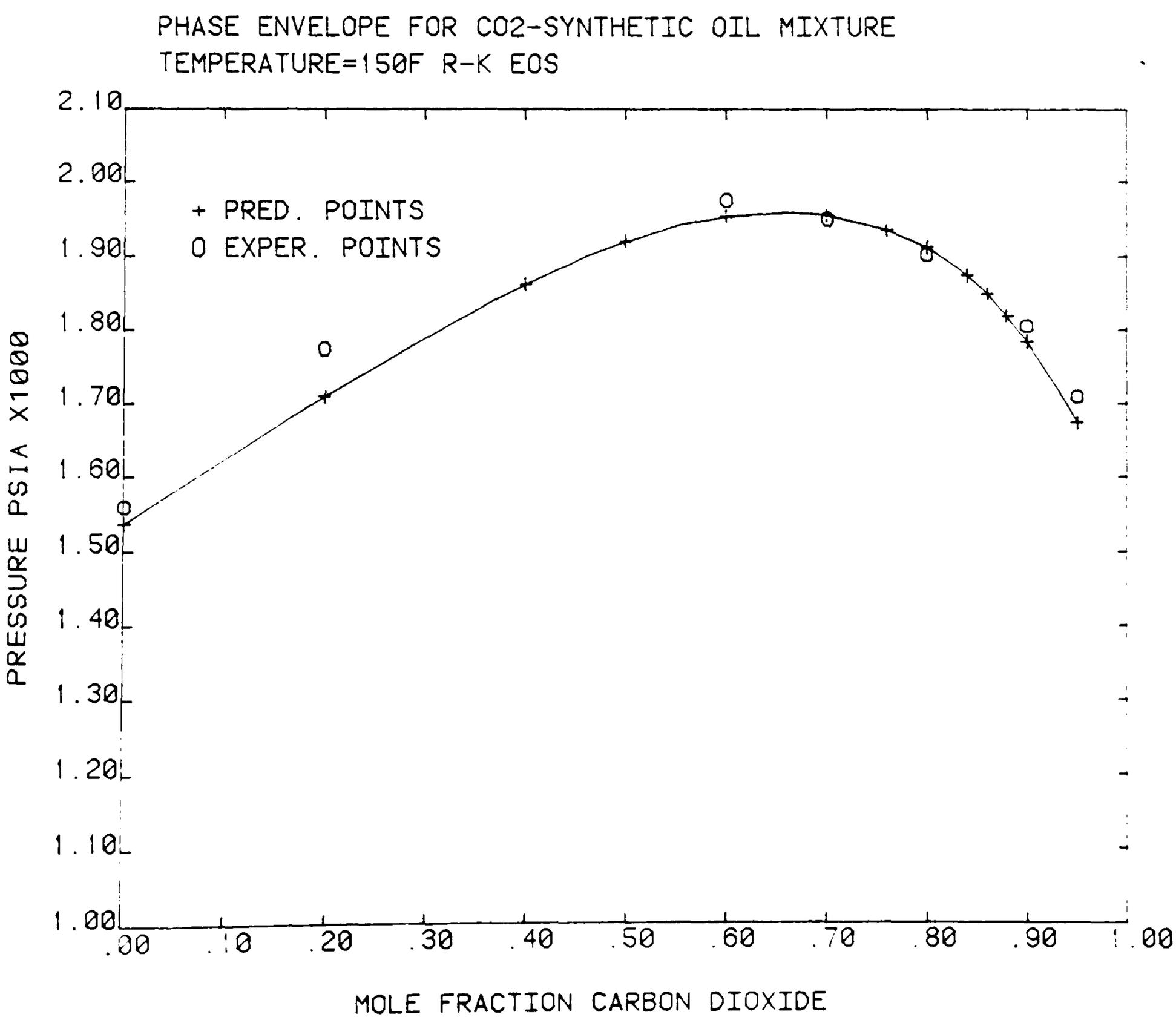

FIGURE 9-7

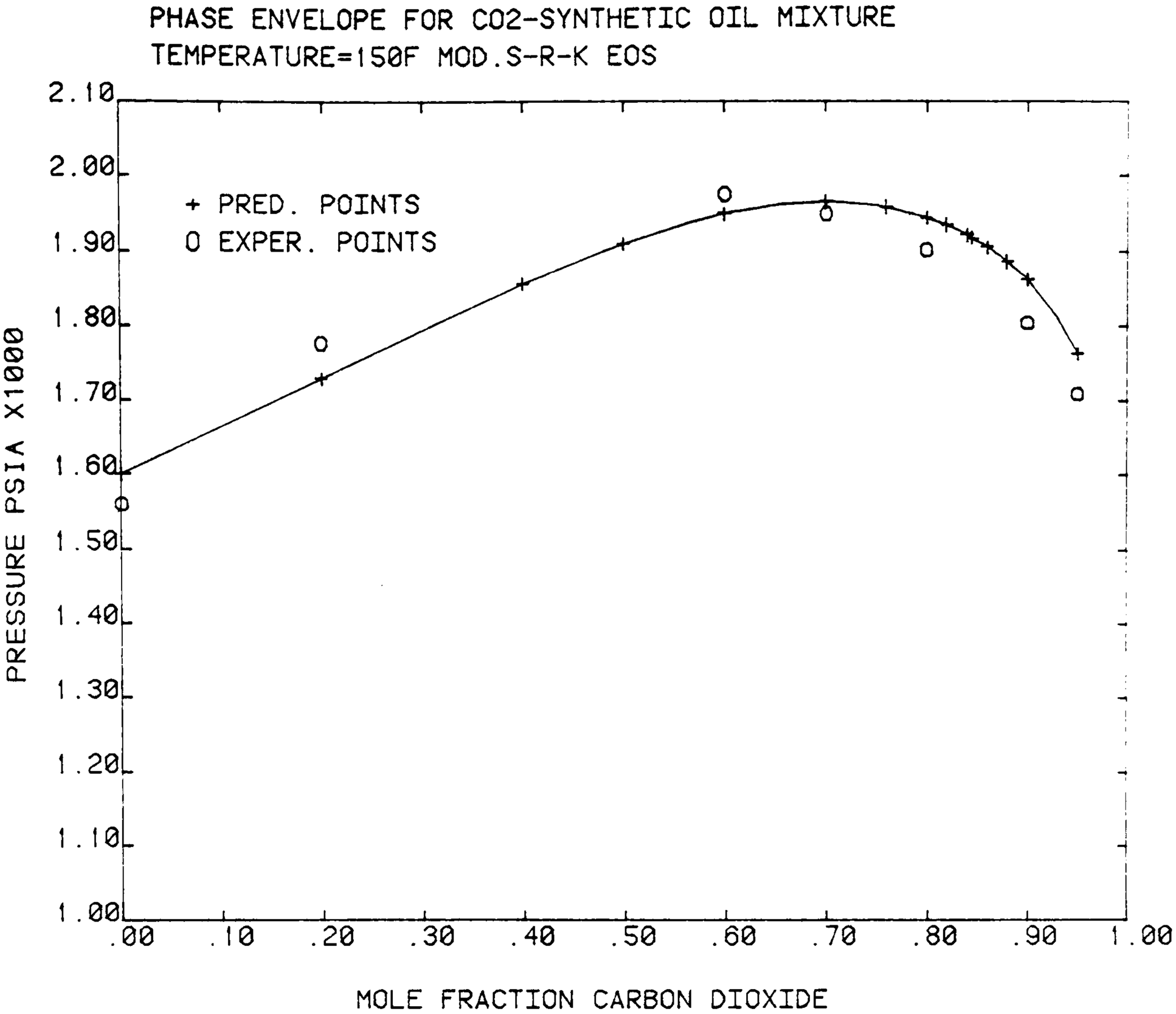

FIGURE 9-8

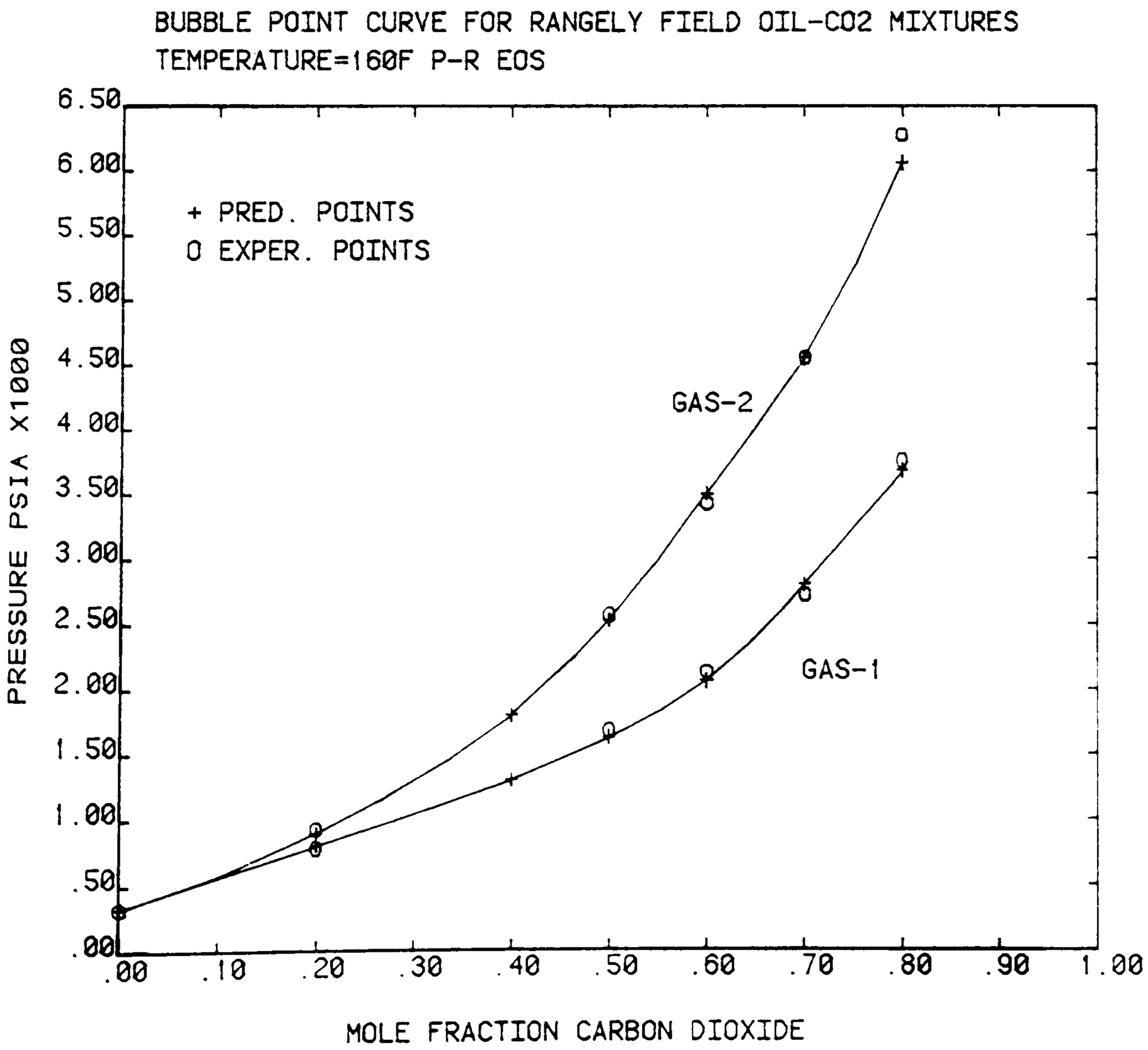

FIGURE 9-9

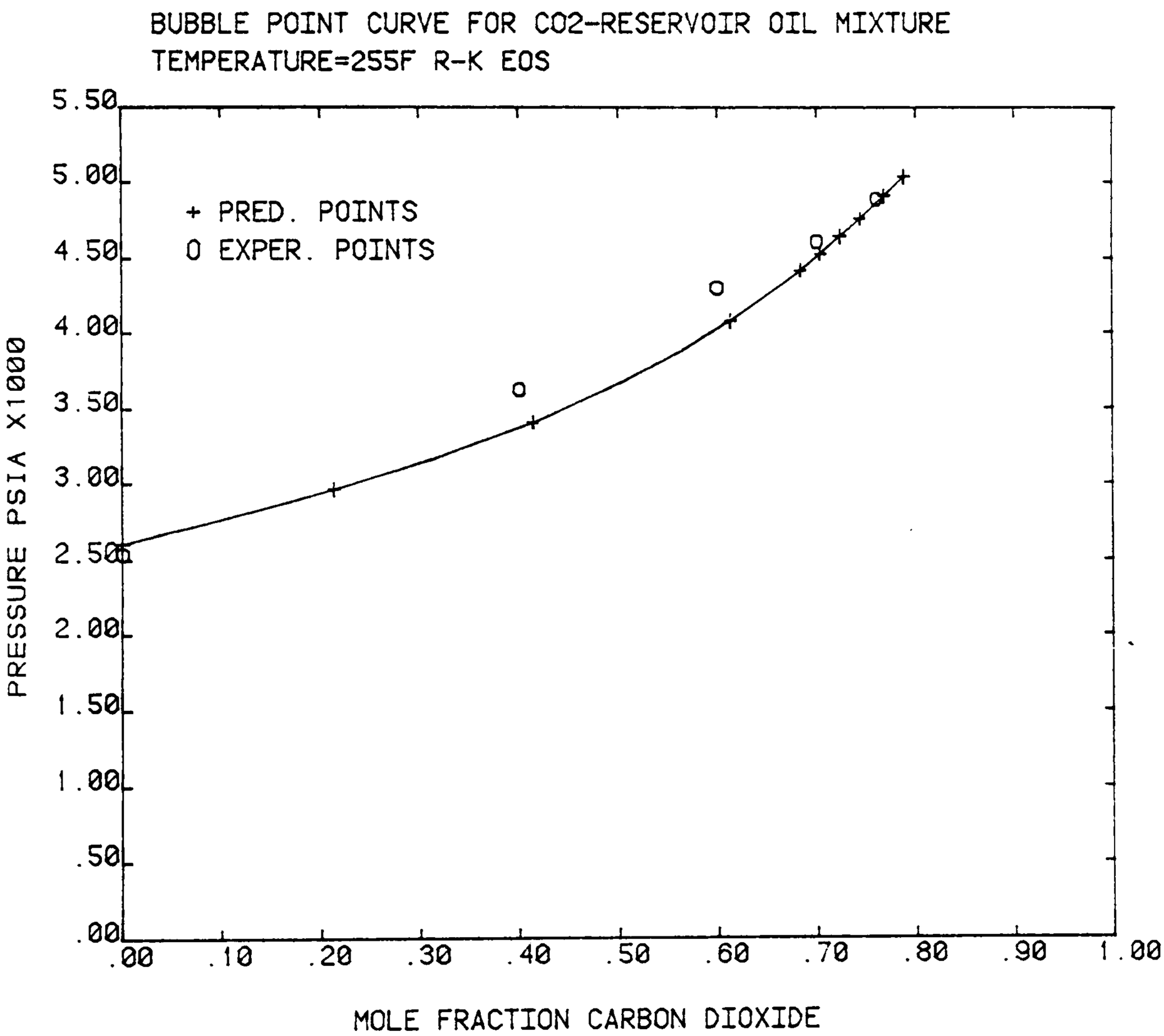
BUBBLE POINT CURVE FOR CO2-RESERVOIR OIL MIXTURE
TEMPERATURE=255F R-K EOS
+ PRED. POINTS
O EXPER. POINTS
PRESSURE PSIA X1000
5.50
5.00
4.50
4.00
3.50
3.00
2.50
2.00
1.50
1.00
.50
.00
.00
.10
.20
.30
.40
.50
.60
.70
.80
.90
1.00
MOLE FRACTION CARBON DIOXIDE

in the near critical region the fit of the predicted curve is almost perfect.

9.5.3 Differential Vapourisation of a Reservoir Oil

The composition of this oil was obtained from a laboratory report by FLOPETROL and is given in Table 9-4. It is considered to be a volatile oil. The compositions of the liberated gas phases at each stage of the process are listed in Table 9-5. Figure 9-10 shows the plot of the predicted and reported values of the oil density as a function of pressure during the differential vapourisation. Figure 9-11 gives the graphic representation of the gas gravity at each pressure step at 305°F. The equation of state used in this study was that of Peng-Robinson. The computer model was tuned at the saturation conditions and Figure 9-10 reconfirms the fact that although the predicted liquid densities at high pressures match precisely the laboratory values, at low pressures the liquid volumes are slightly over-estimated.

9.5.4 Constant Volume Depletion Study of a Gas Condensate

A North Sea gas condensate was selected and the VLE was tuned to match the dew-point pressure of the fluid at the temperature of the reservoir, which was the only available data. The composition of the gas condensate is given in Table 9-6. The constant volume depletion routine of the VLE was used to simulate the depletion of the reservoir at 237°F. The liquid drop out at any stage of the depletion process as a function of pressure passes through a maximum at about 4000 psia and reaches to a final 13.5% in the hypothetical case of depletion until exhaustion (Fig 9-12). The

FIGURE 9-10

DIFFERENTIAL VAPOURISATION
OF RESERVOIR FLUID AT 305 F.

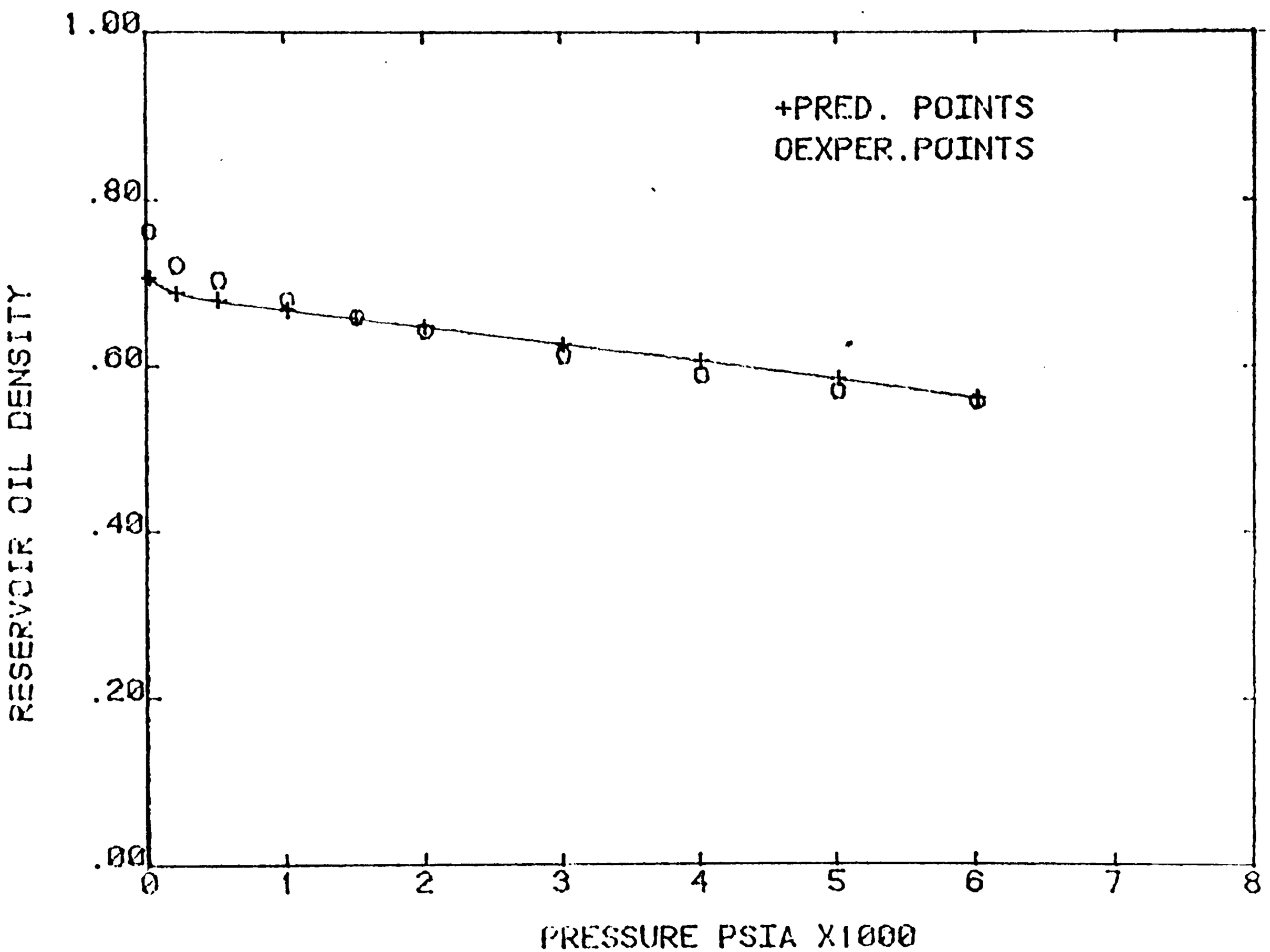

FIGURE 9-11

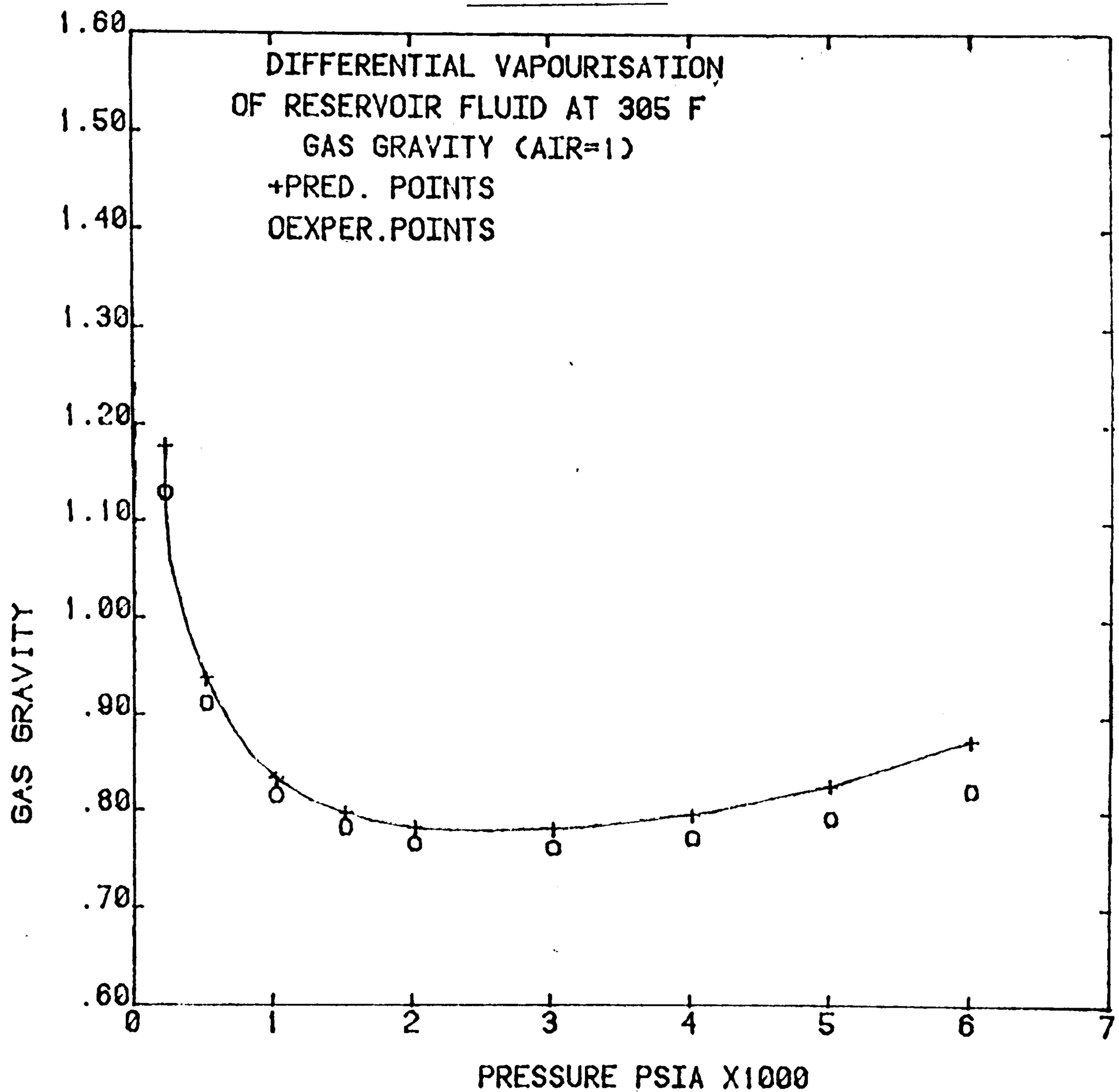
DIFFERENTIAL VAPOURISATION
OF RESERVOIR FLUID AT 305 F
GAS GRAVITY (AIR=1)
+PRED. POINTS
OEXPER.POINTS
GAS GRAVITY
1.60
1.50
1.40
1.30
1.20
1.10
1.00
.90
.80
.70
.60
0
1
2
3
4
5
6
7
PRESSURE PSIA X1000

FIGURE 9-12

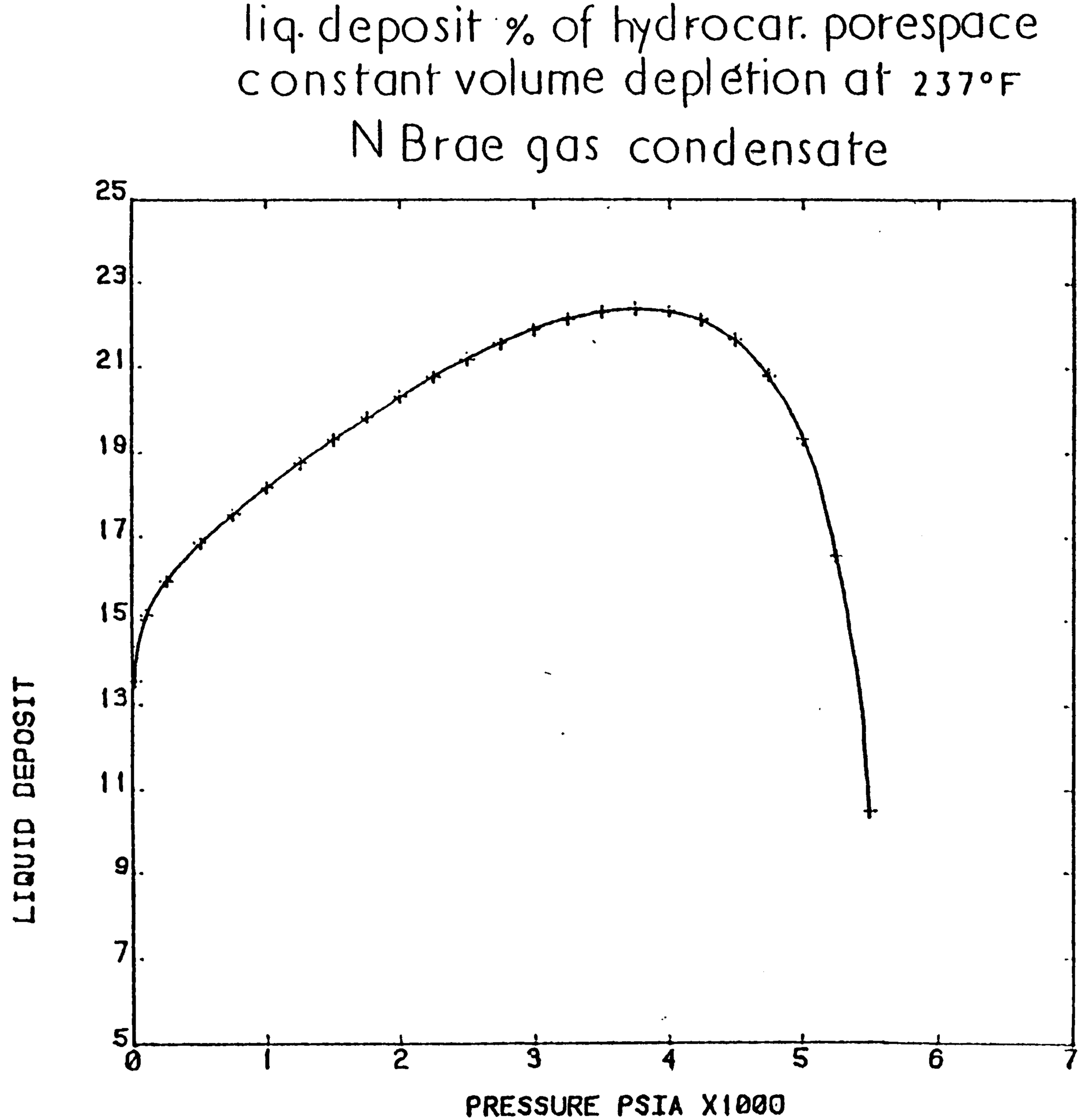
liq. deposit % of hydrocar. porespace
constant volume depletion at 237°F
N Brae gas condensate
LIQUID DEPOSIT
25
23
21
19
17
15
13
11
9
7
5
0
1
2
3
4
5
6
7
PRESSURE PSIA X1000

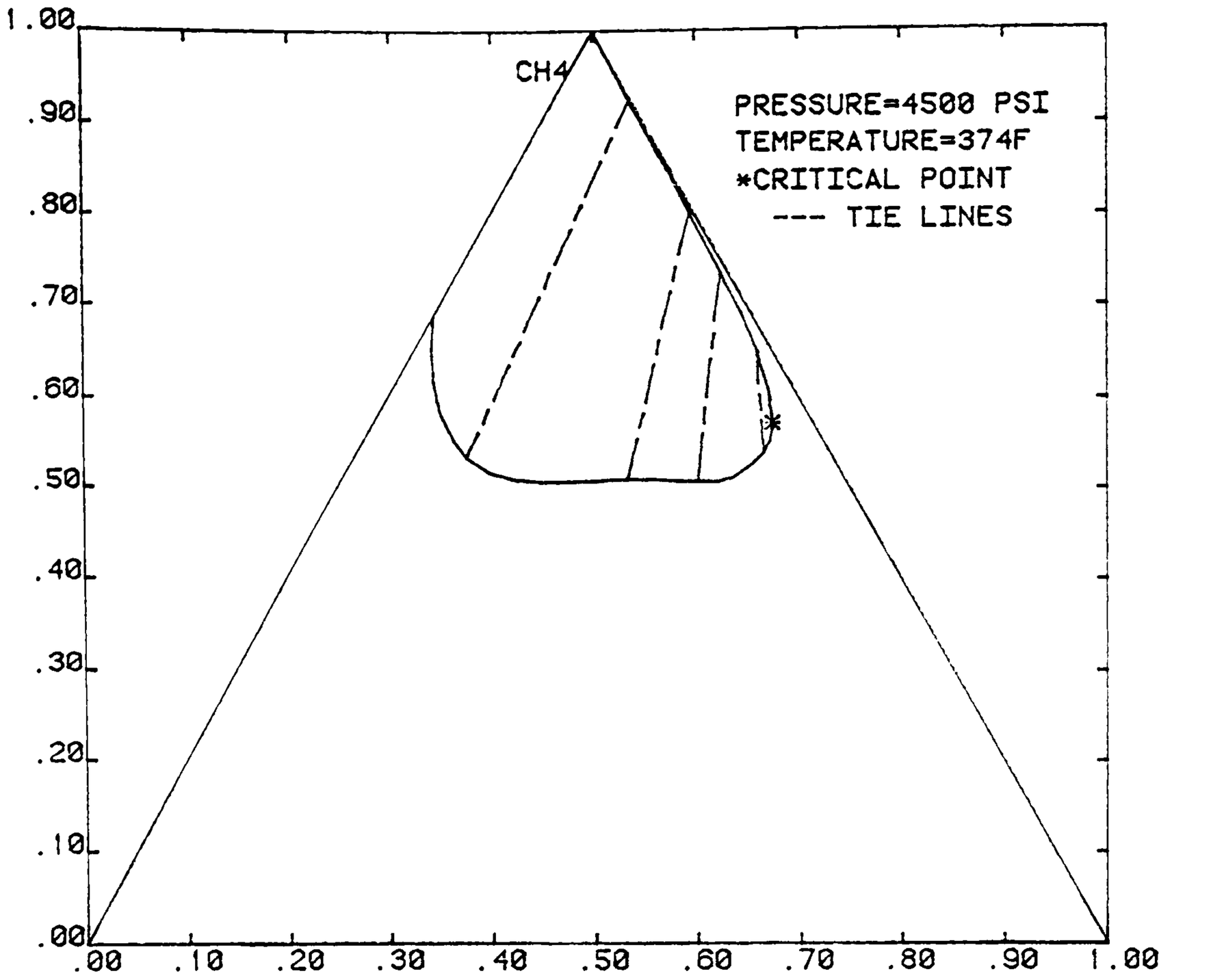

TERNARY DIAGRAM FOR FLOPETROL RESERVOIR OIL

FIGURE 9-13

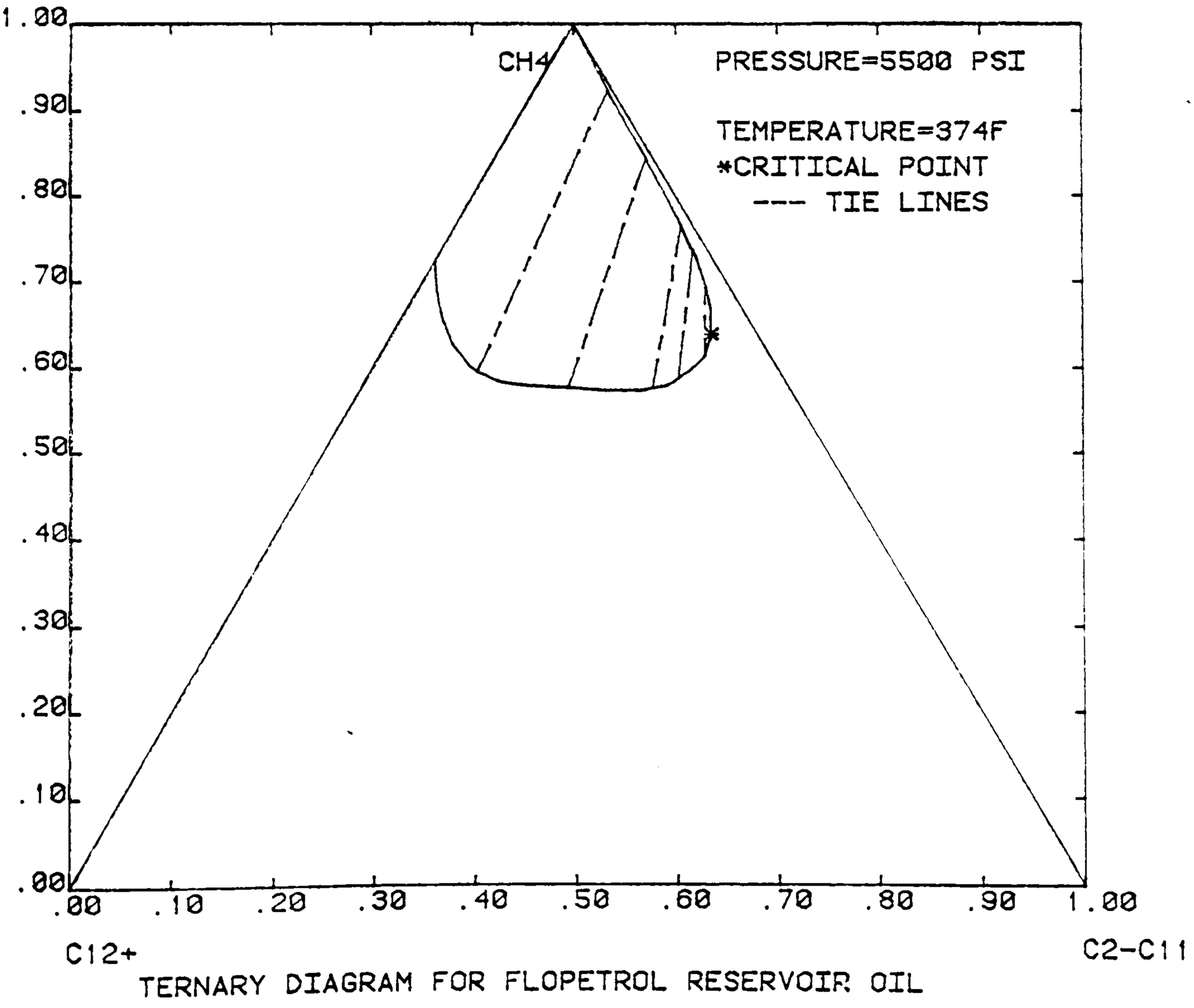

TERNARY DIAGRAM FOR FLOPETROL RESERVOIR OIL

FIGURE 9-14

molecular composition of the liquid remaining at the end of depletion at 237°F is given in Table 9–7. The P–R EOS was used.

9.5.5 Ternary Representation of the Phase Envelope of a Reservoir Fluid

For this application the reservoir oil used at 9.5.3 was selected. The three pseudocomponents chosen to represent the fluid on a ternary diagram were CH_4, $C_2 - C_{11}$ and C_{12+}. The phase envelope was studied at 374°F and at 4500 psia and 5500 psia. The correction coefficients used for the critical temperature and the critical pressure were $Tc_{MOD} = 0.9$ and $Pc_{MOD} = 1.4$. Figure 9–13 and Figure 9–14 show the phase envelopes for the two pressures, a few equilibrium lines and the critical points. VLE was run with the Peng-Robinson EOS.

TABLE 9–1

FLUID COMPOSITIONS AND PROPERTIES[3]

Component	Composition–Mole Percent
C_1	35
C_2	3
C_3	4
C_4	6
C_5	4
C_6	3
C_7	5
C_8	5
C_{10}	30
C_{14}	5

TABLE 9–2

RANGELY FIELD OIL AND INJECTION GAS PROPERTIES[4]

	COMPOSITION, MOLE FRACTION		
Component	Reservoir Oil	Injection Gas 1	Injection Gas 2
N_2	0.00338	0.00081	0.09658
CO_2	0.00245	0.95016	0.85757
C_1	0.04067	0.04892	0.04563
C_2	0.03106	0.00009	0.00014
C_3	0.04816	0.00002	0.00004
iC_4	0.02088	–	0.00003
nC_4	0.03582	–	–
iC_5	0.02448	–	0.00001
nC_5	0.03067	–	–
C_6	0.05512	–	–
C_{7+}	0.70671	–	–
	1.00000	1.00000	1.00000
Mole wt	177.05	42.63	41.19

C_{7+} properties (1 atm)

Mole wt	227.94
Gravity °API	32.75

TABLE 9–3

RESERVOIR OIL COMPOSITION[5]

ORIGINAL MIXTURE	OIL B
TEMPERATURE, °F	255
PRESSURE, psia	2554
PHASE	Liquid
PHASE MOL FRACTION	1.00
COMPONENT	
CO_2	.0133
C_1	.3870
C_2	.0431
C_3	.0315
C_4	.0295
C_5	.0269
C_6	.0271
C_{7+}	.4389
Bubble Point, psia	2554
Mol Wt, gm/gm-mol	120.3
Density, gm/cc	0.648
Viscosity, centipoise	–

C_{7+} properties of Oil B;

mol wt = 239.1

sp gr @ 60°F = 0.8496

°API = 35.05

TABLE 9-4

FLOPETROL CRUDE-OIL SYSTEM

MOLECULAR COMPOSITION OF RESERVOIR FLUID

Methane	59.75
Nitrogen	0.65
Carbon dioxide	1.03
Hydrogen sulphide	-
Ethane	8.25
Propane	4.11
i-Butane	0.83
n-Butane	1.92
i-Pentane	0.78
n-Pentane	1.50
Hexanes	1.24
Heptanes	1.46
Octanes	1.72
Nonanes	1.37
Decanes	0.98
Undecanes	0.62
Dodecanes plus	13.79
TOTAL	100.00

Molecular weight of Dodecanes plus in reservoir fluid: 324

Specific gravity of dodecanes plus : 0.88

Reservoir temperature : 462.82°K

Bubble point pressure : 6370.0 psig

Bubble point oil density : 0.554 gr/cc

TABLE 9-5

DIFFERENTIAL VAPOURISATION OF RESERVOIR FLUID AT 308.6°K

MOLECULAR COMPOSITION OF LIBERATED GASES (MOLE PERCENT)

Pressure (psia)	6015.000	3015.000	1015.000	215.000
Methane	0.7920219E 00	0.7906523E 00	0.7192187E 00	0.4638340E 00
Nitrogen	0.9749349E-02	0.8842506E-02	0.5551756E-02	0.1898967E-02
Carbon Dioxide	0.1087244E-01	0.1234224E-01	0.1642225E-01	0.2080230E-01
Ethane	0.8404165E-01	0.9425825E-01	0.1298099E 00	0.1959765E 00
Propane	0.3668416E-01	0.4050497E-01	0.6005767E-01	0.1263887E 00
Iso-Butane	0.5773425E-02	0.6323091E-02	0.9808671E-02	0.2643815E-01
N-Butane	0.1262464E-01	0.1360482E-01	0.2101994E-01	0.5880610E-01
Iso-Pentane	0.4537988E-02	0.4562153E-02	0.6536666E-02	0.1901735E-01
N-Pentane	0.8411913E-02	0.8316668E-02	0.1175356E-01	0.3445523E-01
N-Hexane	0.5962583E-02	0.5332515E-02	0.6688629E-02	0.1929357E-01
N-Heptane	0.6095631E-02	0.4881380E-02	0.5328359E-02	0.1458337E-01
N-Octane	0.6228052E-02	0.4416528E-02	0.4131855E-02	0.1050681E-01
N-Nonane	0.4309945E-02	0.2686053E-02	0.2132681E-02	0.4974755E-02
N-Decane	0.2719957E-02	0.1493655E-02	0.1005165E-02	0.2137530E-02
N-Undecane	0.1504425E-02	0.7205350E-03	0.4075211E-03	0.7855716E-03
Pseudocompon 1	0.8461932E-02	0.1062351E-02	0.1266068E-03	0.1010854E-03
TOTAL	1.000	1.000	1.000	1.000
Molecular Weight	25.3578	22.6490	24.1821	34.1090
Gas Gravity	0.87531	0.78181	0.83473	1.17739

TABLE 9-6

GAS CONDENSATE SYSTEM

MOLECULAR COMPOSITION OF RESERVOIR FLUID

Methane	68.20
Nitrogen	0.60
Carbon dioxide	8.14
Hydrogen sulphide	-
Ethane	7.58
Propane	3.56
i-Butane	0.97
n-Butane	1.84
i-Pentane	0.48
n-Pentane	0.73
n-Hexane	0.81
n-Heptane	1.15
n-Octane	1.01
n-Nonane	1.22
Decane plus	3.71
TOTAL	100.00

Molecular weight of Decane plus in reservoir fluid: 181.0

Specific gravity of Decane plus : 0.8275

Reservoir temperature : 387.16°K

Separator temperature : 110°F

Separator pressure : 550 psia

TABLE 9-7

MOLECULAR COMPOSITION OF REMAINING LIQUID AT END OF DEPLETION STUDY AT 237.22 F

ATMOSPHERIC PRESSURE

Components	Mole Percent
Methane	0.1242302E-02
Nitrogen	0.5140588E-05
Carbon Dioxide	0.4768396E-03
Ethane	0.6626407E-03
Propane	0.1004337E-02
Iso-Butane	0.1302094E-02
N-Butane	0.3718381E-02
Iso-Pentane	0.2877065E-02
N-Pentane	0.5721302E-02
N-Hexane	0.1881836E-01
N-Heptane	0.5768508E-01
N-Octane	0.8523917E-01
N-Nonane	0.1414125E 00
Pseudocompon 1	0.4128531E 00
TOTAL	1.0000
Gravity	0.64391
Molecular Weight	159.34

LIST OF REFERENCES

1. Olds, Reamer, Sage and Lacey:
"Phase Equilibria in Hydrocarbon Systems N Butane-CO_2 System", Ind. & Engin. Chemistry, 1949, p 475.

2. Besserer, G. and Robinson, D.:
"Equilibrium Phase Properties of i-Buthane-CO_2 system", J. Ch. Eng. Data, Vol. 18, No 3, 1973 p 298.

3. Metcalfe, R.S. and Yarborough, L.:
"Effect of Phase Equilibria on the CO_2 Displacement Mechanism", SPE paper No 7061.

4. Graue, D.J. and Zana, E.:
"Study of a Possible CO_2 Flood in the Rangely Field, Colorado", SPE paper No 7060, 1978.

5. Simon, R., Rosman, A. and Zana, E.:
"Phase Behaviour Properties of CO_2-Reservoir Oil Systems" SPE paper No 6387.

PART II

LABORATORY EXPERIMENTS ON THE PHASE BEHAVIOUR OF INJECTION GAS-HYDROCARBON SYSTEMS

CHAPTER 10

DESIGN OF THE EXPERIMENTAL APPARATUS - EXPERIMENTAL TECHNIQUES

10.1 INTRODUCTION

Laboratory experiments most often performed to investigate the efficiency and the controlling mechanisms of a miscible gas enhanced oil recovery project fall into three general categories[1]:

(i) High pressure and temperature volumetric and vapour-liquid equilibrium experiments.

(ii) Slim tube experiments.

(iii) Core displacements.

These three different types of experiments offer different information about the potential application of a gas injection scheme.

Equilibrium phase behaviour and fluid property measurements provide direct evidence concerning the physical behaviour of mixtures of injection gases and crude oils. The information obtained from these experiments include, solubility data of the injection gas into the reservoir fluid phase, swelling of the latter as a result of the mixing, the number and kind of phases present, the densities and viscosities of these phases which together with relative permeabilities control the rates at which the phases move under the imposed pressure gradient and the distribution of hydrocarbons and inorganic gases throughout the reservoir. This data determines the degree of efficiency of the injected media to recover the oil which has been left behind in the reservoir.

Slim tube experiments provide information on the prediction of the minimum operating pressure required for miscibility within the reservoir, they provide a method for mixing injection gas and oil

in a flowing multiple contact process but they are not intended to simulate fluid mobility properties[2].

Core displacements give some evidence of the problems concerning the flow of the phases inside the reservoir rock, such as viscous fingering, gravity segregation channelling or by-passing of oil due to core heterogeneities and provide some insight in the residual oil saturation of the swept zones and on the effect the flooding has on the core permeability. Although these experiments appear to simulate closer than any other experiments the conditions prevailing in the reservoir, usually they are used to give evidence on the displacement mechanisms rather than be used as measurements designed for scale-up calculations for particular reservoirs.

The study in this thesis is focused on PVT vapour-liquid equilibrium experiments and the aim of the experimental work is to measure the ranges of phase compositions and properties likely to exist in a miscible gas flooding process, to understand how such composition variations effect displacement efficiency and to investigate in general, the phase behaviour of mixtures of reservoir fluids and injection gases at conditions as close as possible, to those prevailing in a reservoir during the displacement process.

10.2 TYPES OF EXPERIMENTS PERFORMED IN THIS STUDY

The various types of experiments required to back up the numerical simulator's predictions for the study of the phase equilibria occurring in a gas miscible displacement are:

(i) Volumetric experiments. Saturation pressures (bubble

or dew point pressures) are measured by the change of the compressibility of the phases in a PVT cell, as the pressure changes and the measurement is reconfirmed by visual observation where possible.

(ii) Vapour-liquid equilibrium experiments. A mixture of injection gas and reservoir fluid of a certain overall composition is equilibrated and the phase volumes, densities and compositions are measured. In multiple contact experiments, which simulate the enrichment of the phases by components present in the other phase, volumes of the phases in equilibrium are brought in contact with either fresh reservoir oil (upper phase) or injection gas (lower phase). Figure 10-1 shows schematically the series of experiments to simulate the process by which the injection gas strips hydrocarbons from the reservoir fluid phase (Figure 10-1a) as well as the process by which the injection gas condenses into the oil phase (Figure 10-1b). In the former a certain volume of injection gas contacts successively fresh reservoir oil, such that it becomes richer and richer in hydrocarbons and the two phase compositions approach each other. In the latter a certain volume of reservoir fluid is brought in successive contacts with fresh injection gas.

10.3 DESIGN OF THE HIGH PRESSURE EQUIPMENT

To meet the requirements for the type of experiments which were just described, a high pressure experimental facility was designed

FIGURE 10-1a

MULTIPLE CONTACTS SIMULATING MASS TRANSFER NEAR THE INJECTION WELL

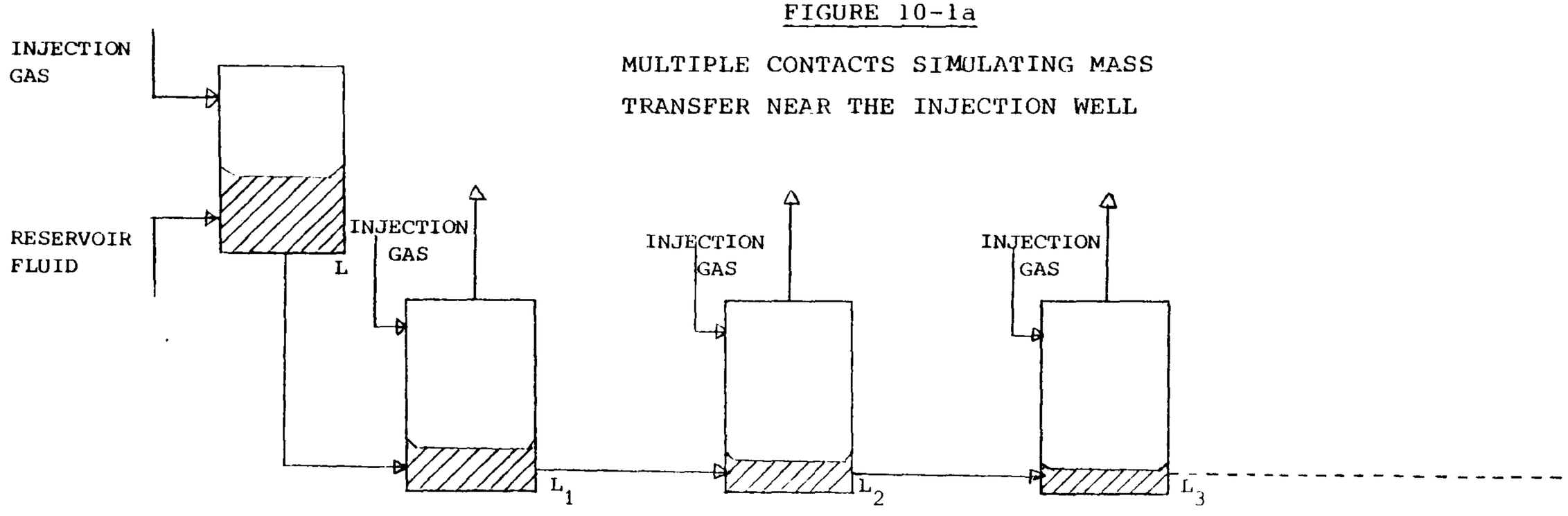

FIGURE 10-1b

MULTIPLE CONTACTS SIMULATING MASS TRANSFER OF FORWARD CONTACTS

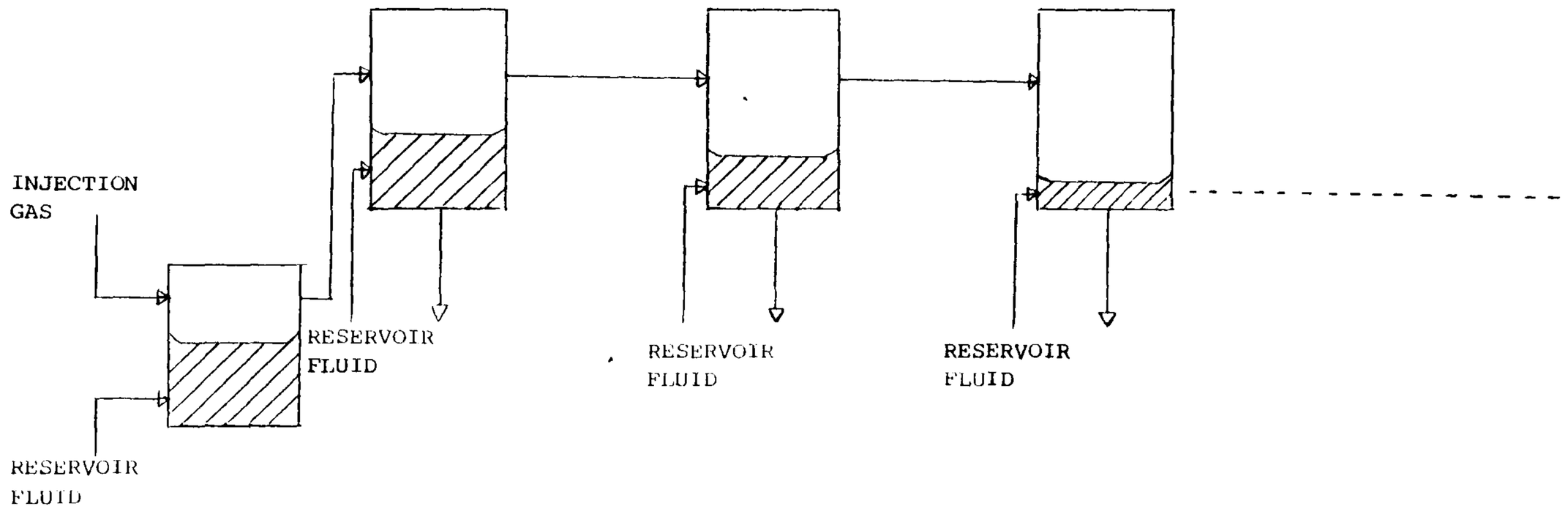

and built. It consists of the following three main groups of units:

(a) A pressure application system together with pressure measurement and temperature control systems.

(b) A high temperature air bath with high pressure equilibrium cells and apparatus to measure density and composition of resulting phases.

(c) Mixing vessels and other auxiliary vessels and apparatus.

A process flow scheme of the equilibrium phase behaviour apparatus is presented in Figure 10-2. The three main groups of equipment consist of:

(a) <u>Pressure Application and Measurement System</u>

1. Mercury pump A
2. Mercury pump B
3. Pressure transducer
4. Pressure gauge
5. Vacuum gauge

(b) <u>Air Bath-Measuring Devices</u>

6. High pressure windowed cell A
7. High pressure windowed cell B
8. High pressure and temperature densitometer
9. Sampling trap
10. High temperature direct sampling system

(c) <u>Auxiliary Devices</u>

11. Auxiliary high pressure cylinder
12. Auxiliary high pressure cylinder

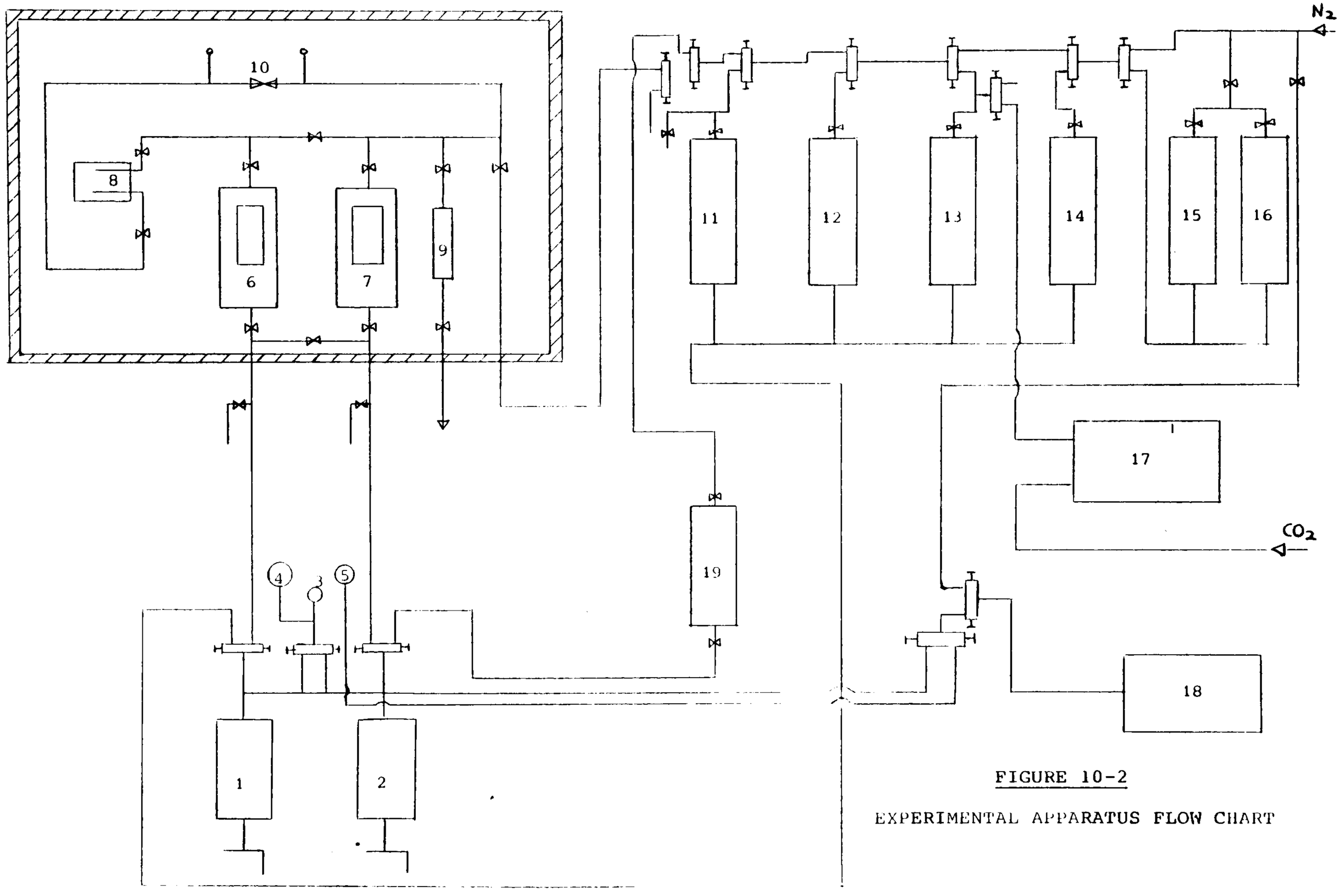

FIGURE 10-2

EXPERIMENTAL APPARATUS FLOW CHART

13. CO_2 storing high pressure cylinder

14. Auxiliary high pressure cylinder

15. Naptha container

16. Acetone container

17. Gas intensifier

18. Vacuum system

19. Rocking/mixing cell for storing reservoir fluids equipped with heating jacket to warm up heavy crudes.

The principal units of each main group of apparatus are:

(i) Double cylinder mercury pump

(ii) Pressure and temperature measurement and control system

(iii) Temperature controlled air bath

(iv) High pressure windowed equilibrium cells

(v) High pressure and temperature densitometer

(vi) Blow down sampling system

(vii) High temperature direct sampling system

(viii) Gas chromatograph

These units are described in more detail below.

10.3.1 The Double Cylinder Mercury Pump

A motorised double cylinder Ruska positive displacement pump is used to pressurise the fluids in the system. Transfer of phases from one cell to the other, or from an auxiliary cylinder to the cells, can be achieved with the pump maintaining the pressure constant throughout the transfer. The continuous discharge is accomplished by charging one of the cylinders of the pump while the other is discharging. When the two cylinders are running in

parallel they can either both charge, discharge or the one can charge and the other discharge at the same rate. Different displacement rates are available ranging from 2.50cc/h to 560cc/h per cylinder, using a gear system.

Each positive displacement pump works on the principle of volume displacement of mercury. A plunger of uniform diameter is forced into the mercury filled cylinder by a measuring screw. The volume displaced by the movement of the plunger is expressed on a linear scale calibrated in cubic centimeters. The double cylinder pump can be either hand-operated or motor-operated.

The pumps are rated to 8000 psi and tested at 12,000 psi and the capacity of each cylinder is 250cc. Small bore stainless steel tubing (1/8" OD) was used in most of the high pressure flow lines to minimise the dead volumes and consequently the liquid hold up.

10.3.2 The Pressure and Temperature Measurement and Control Systems

The apparatus, as shown in Figure 10-2, is equipped with a pressure transducer and a pressure gauge. They can both monitor the pressure of every loop of the system connected with either of the pump cylinders. While the transducer provides the accurate reading, the pressure gauge is used as an additional safety check for the pressure not to exceed a maximum set limit. A strain gauge 10V DC transducer, provides 0-200mV output, whose signal is received by a signal conditioner which conditions it to a required output depending on the selected range. The pressure range of the transducer used is 0-10,000 psi. To ensure that the pressure of the system does not exceed the allowed limit, bursting discs are

connected to the lines very close to the pumps. The bursting discs used were limited to 8,500 psi. In the event of a burst disc the mercury would return to the mercury reservoir through a bypassing line.

Platinum film, high stability, 100 Ohm resistance thermocouples are connected to the devices whose function requires accurate temperature control. These are the two equilibrium cells, density cell, air bath and the rocking cell.

10.3.3 Temperature Controlled Air Bath

The heart of the experimental system which consists of the two high pressure windowed cells is contained inside an air circulating bath. The air bath, especially designed for the project, consists of a stainless steel inner shell which is sealed to prevent any mercury vapours contaminating the laboratory. The stainless steel shell is covered with insulation material to minimise the heat losses and the exterior of the air bath is covered with aluminium plates.

A hole in the bottom of the air bath which is connected with a rubber hose to an oil trap, was incorporated to collect any possible mercury spillage from the oven. In case that the mercury vapour concentration inside the oven becomes too high, a flap valve was designed which can be opened to allow the vapours to be extracted by the laboratory ventilation system. On the door of the air bath, exactly opposite of the cell windows, two bulletproof glass windows are mounted to allow observation of the phases in the cells without disturbing the temperature control and exposing the operator to possible hazards by opening the door.

The door of the air bath was specially designed to incorporate a movable viewing system which allows the mounting of boroscopes, to locate the position of the interfaces inside the cells, and allow viewing through a television monitor system. The position of the interface enables phase volumes to be determined. Plate 1 shows the oil-mercury interface as it can be seen on the television screen.

Valves mounted inside the oven as well as the top and bottom valves of the cells can be operated from outside the air bath using long stems. An electrically driven fan circulates the air through the electrical heaters and all around the oven. The air bath was tested up to temperatures of 130°C and the temperature during operation is controlled to $\pm$0.1°C. Plate 2 shows a general view of the experimental apparatus including the air bath, the double cylinder mercury pump and the viewing system.

10.3.4 High Pressure Windowed Cells

Two Ruska high pressure equilibrium cells are mounted on a single rotating plate inside the temperature controlled air bath. Each cell is made from stainless steel and has two windows mounted opposite each other to allow viewing with transmitted light. The exposed window surface is approximately 2 1/2" long and 1/4" wide. A light source is placed behind the back window of each cell so that the vapour-liquid interfaces can be discerned in transmitted light. An external light source is also used to provide sufficient light at the front window to be reflected on the mercury phase, so that the mercury-bottom phase interface can be clearly observed from outside. Each cell has ports on either end

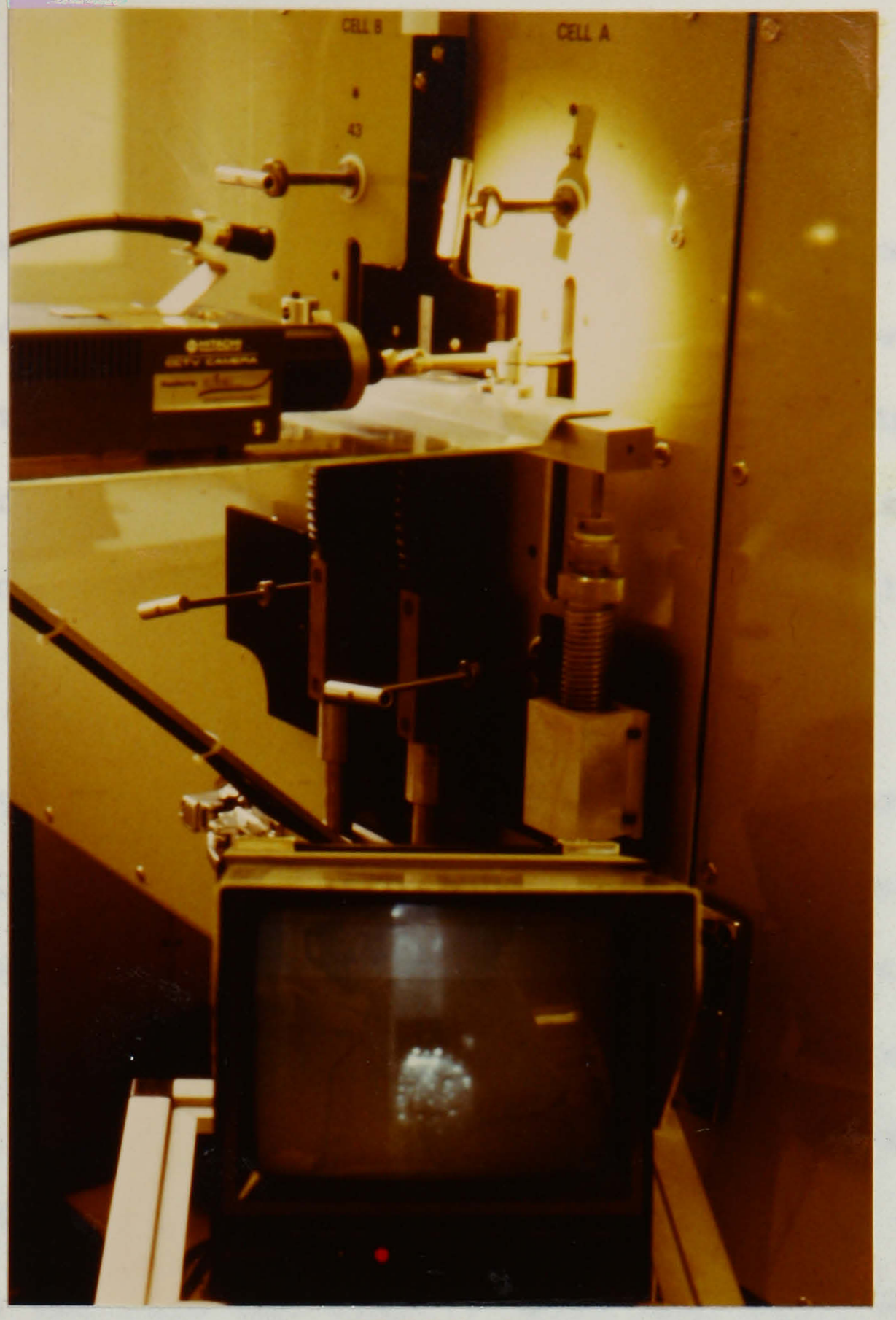

PLATE 1

VIEWING SYSTEM ALLOWING OBSERVATION OF PHASE BEHAVIOUR

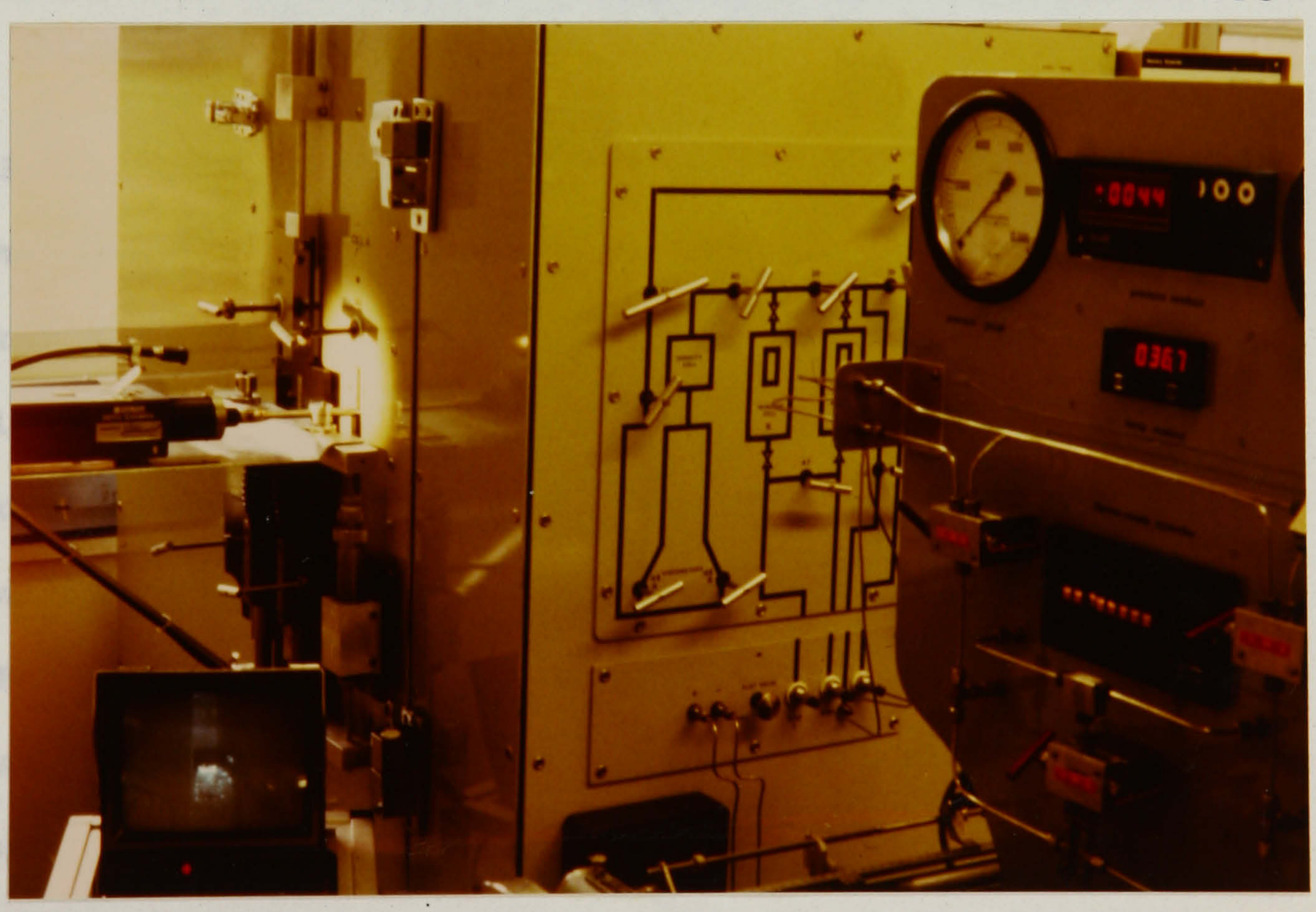

PLATE 2

GENERAL VIEW OF THE AIRBATH, THE MERCURY PUMPS AND THE CONTROL BOARD

as well as side traps for extraction of gases or fluids. The cell window frames are designed with clamping and balancing screws, to reduce strain on the glass, while ensuring positive sealing at high pressures and temperatures. Each cell has a volume of approximately 190cc, is rated at 10,000 psi and tested at 15,000 psi.

The single rotating plate upon which the cells are mounted allows the cells to be fully inverted. The windows are positioned so that in the inverted and normal position the whole length of the cell can be observed. Each cell was found to have a dead volume (volume between the top of the window and the top valve) of approximately 4cc. Plate 3 shows the two high pressure equilibrium cells mounted inside the air bath and Plate 4 shows the vapour-liquid interface after equilibrium has been established in one of the cells.

10.3.5 High Pressure and Temperature Densitometer

Inside the air bath a PAAR DMA 512 remote cell for density measurements under high pressure and temperature is installed. The density determination is based on measuring the period of oscillation of a vibrating V-shaped tube through which the sample fluid flows continuously. The sample tube is made of stainless steel with a wall thickness of about 0.3 mm and an inside diameter of 2.4 mm. The system is excited by two magnetic dynamic converters in connection with an electronic control and amplifier circuit, which guarantees a constant amplitude of the oscillator tube, even under extreme measurement conditions. The maximum operating temperature is 150°C and the maximum operating pressure is 6000 psi.

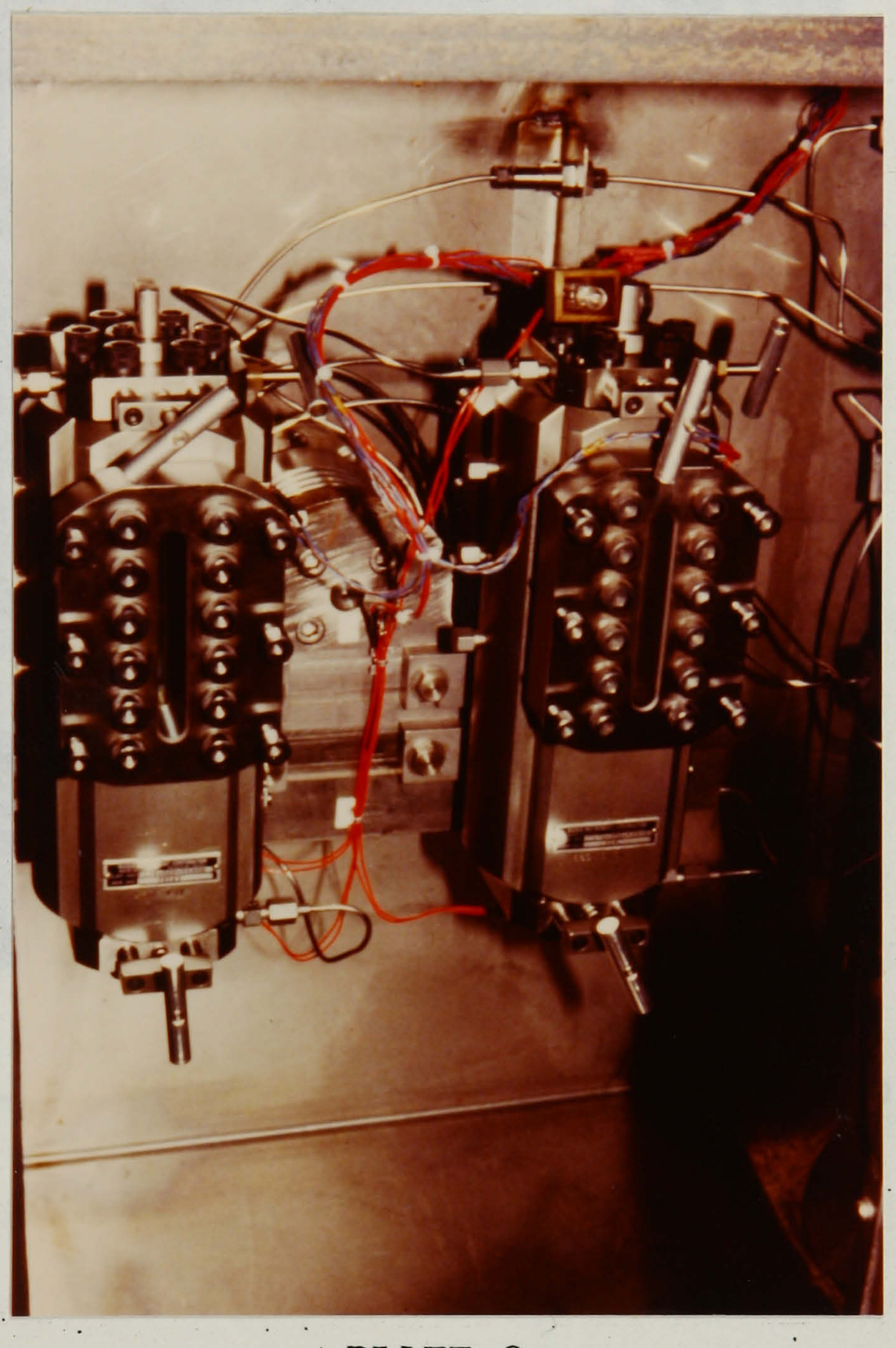

PLATE 3

THE EQUILIBRIUM CELLS MOUNTED INSIDE THE AIRBATH

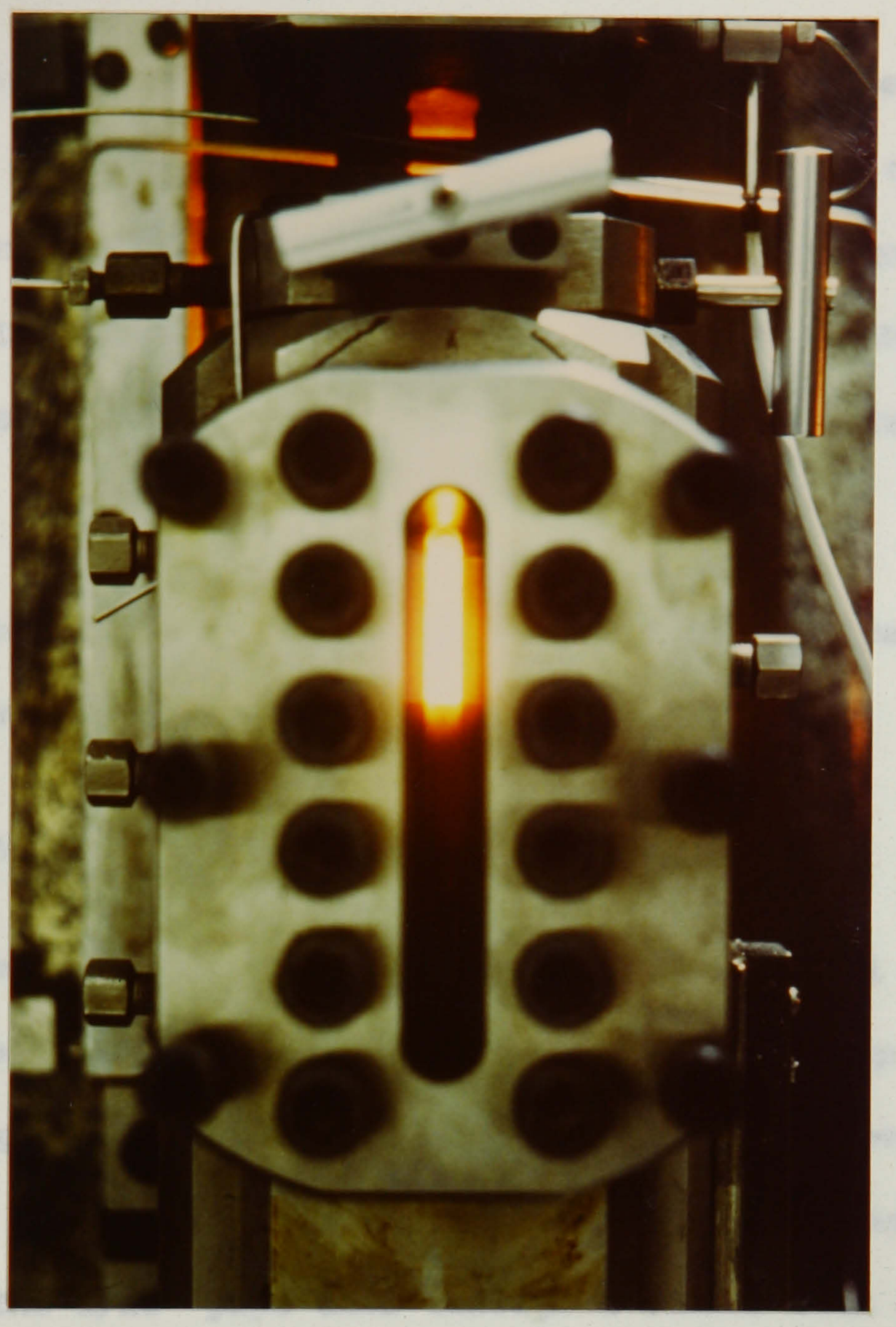

PLATE 4

VAPOUR-LIQUID EQUILIBRIUM IN THE WINDOWED CELL

The electronics had to be taken apart from the density cell and were put in a box on the top of the air bath as they cannot operate under high temperature. The period of oscillation signal is transmitted to a DMA 45 low pressure densitometer where either the period or the density of the mixture can be read directly from the digital read out.

The DMA 45 densitometer can be also used as an external cell for density measurements of mixtures under room conditions.

10.3.6 Blow Down Sampling System

As each one of the phases is being transferred from one cell to the other, a volume of about 4cc is trapped in a sampling loop. The sampling loop (Fig 10-3) consists of a piece of 1/4" OD pipe which passes through a cracking valve and ends outside the oven in a 1/16" OD pipe. The 1/16" pipe ends through a rubber seal into a pyrex centrifuge tube. The centrifuge tube has a glass branch which is connected with an elastic tube to a gas meter. The line passes through a six port external loop VALCO gas sampling valve, mounted in the side of the gas chromatograph. An ice bath is used to cool down the tube and the elastic pipe and to avoid liquid condensation in the gas metering system. The gas meter was designed and made in the Department and consists of a long high precision glass bore and a Teflon plug which seals on the bore with a mercury seal and can move up and down. The mercury seal minimises the friction between the plug and the bore of the tube. The gas phase as it enters the gas meter from the bottom hole, displaces the plug upwards. The displacement of the plug can be converted to gas volume using a calibration chart.

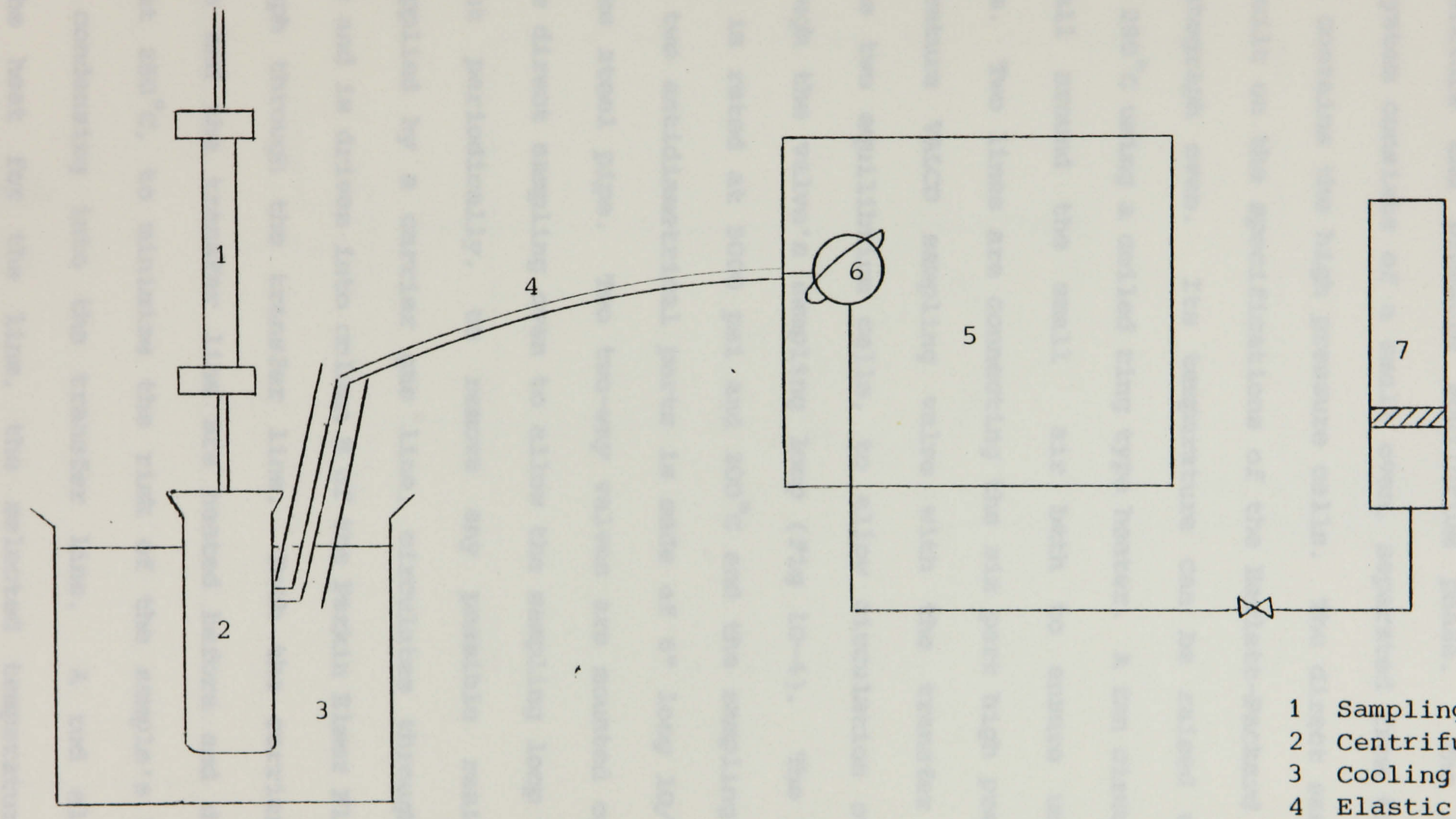

1 Sampling Trap
2 Centrifuge Tube
3 Cooling Water
4 Elastic Tube
5 Gas Chromatograph
6 VALCO Valve
7 Gas Meter

FIGURE 10-3

BLOW DOWN SAMPLING SYSTEM

10.3.7 The High Temperature Direct Sampling System

This system allows direct sampling of a few microlitres from a high temperature and pressure equilbrium phase. The direct sampling system consists of a small oven, separated from the air bath which contains the high pressure cells. The direct sampling oven was built on the specifications of the Hewlett-Packard 5880A gas chromatograph oven. Its temperature can be raised within minutes to 280°C using a coiled ring type heater. A fan circulates the air all around the small air bath to ensure uniform temperature. Two lines are connecting the six port high pressure and temperature VALCO sampling valve with the transfer loop between the two equilibrium cells, to allow circulation of the phase through the valve's sampling loop (Fig 10-4). The VALCO valve used is rated at 5000 psi and 300°C and the sampling loop connecting two antidiametrical ports is made of 6" long 10/1000" ID stainless steel pipe. Two two-way valves are mounted on the side of the direct sampling oven to allow the sampling loop to be flashed out periodically, to remove any possible residues. Helium, supplied by a carrier gas line, circulates through the VALCO valve and is driven into column B of the Perkin Elmer F17 gas chromatograph through the transfer line. Both the carrier gas supply line and the transfer line are heated before and during sampling, at 250°C, to minimise the risk of the sample's heavy components condensing into the transfer line. A rod element provides the heat for the line, the selected temperature is controlled automatically and the lines are insulated.

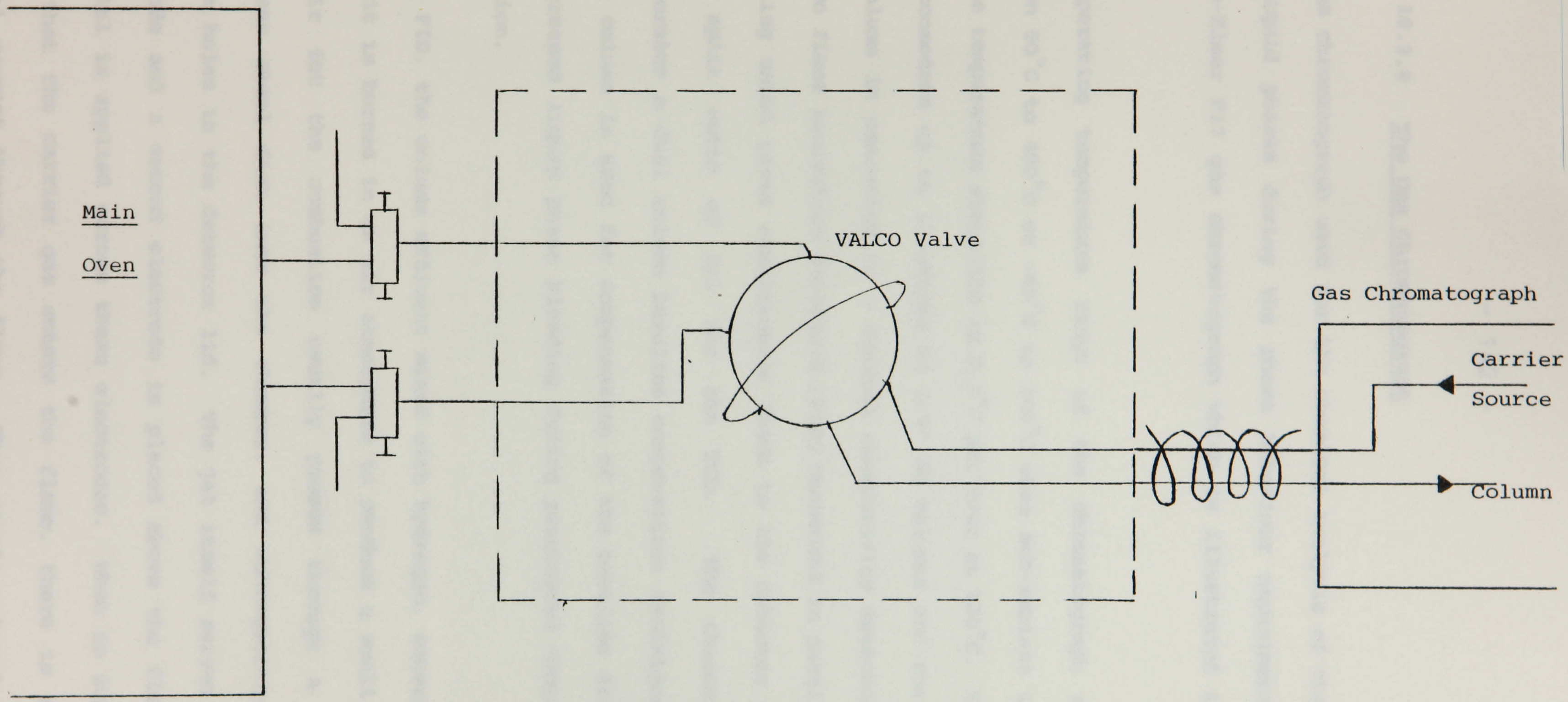

FIGURE 10-4

DIRECT SAMPLING SYSTEM

10.3.8 The Gas Chromatograph

The gas chromatograph used for the chemical analysis of the vapour and liquid phases during the phase behaviour experiments is a Perkin-Elmer F17 gas chromatograph which is illustrated in Plate 5.

The operating temperature range of the chromatograph oven is between 50°C to 450°C or -65°C to 350°C when sub-ambient is used, and the temperature stability is 0.1°C per hour at 100°C. The oven can accomodate up to 12 metres of 1/8" OD columns and the end of the column is connected to a thermal conductivity detector (TCD) and two flame ionisation detectors (FID) connected in parallel. A splitting union gives simultaneous feeds to the detector systems at a split ratio of 9/1 for the TCD. The chromatograph incorporates a dual column baseline compensation technique. The second column is used for compensation of the baseline drift due to increased liquid phase bleeding during programmed temperature operation.

In the FID, the column effluent mixed with hydrogen, enters a jet where it is burned in an air atmosphere to produce a small flame. The air for the combustion usually passes through a porous stainless steel disk into the chamber, and subsequently vents through holes in the detector lid. The jet itself serves as one electrode and a second electrode is placed above the flame. A potential is applied across these electrodes. When no substance other that the carrier gas enters the flame, there is a small residual current through the flame. When sample molecules enter the flame, ionisation occurs yielding a current flow which, after

PLATE 5

THE GAS CHROMATOGRAPH

proper amplification, is measured by an integrator and displayed on a strip chart recorder.

The FID is sensitive to all organic substances but insensitive to inorganic gases and water. It is a mass sensitive detector and its response is proportional to the total mass entering the detector per unit time. The TCD responds to all possible substances except the carrier gas and therefore is called universal detector. It consists of fine metallic wires mounted coaxially within a metal cylinder through which a gas flows. The wire is heated electrically and assumes a temperature which depends on the flow and thermal conductivity of the gas passing over it. When a foreign substance is introduced into the gas stream, the temperature of the wire and hence its resistance changes. The metal block also has a second channel in which a similar wire is mounted. This second channel is used as a reference and the composition of the gas flowing through this channel is kept unchanged. This means that the temperature and thus the resistance of the wire in the second, reference, channel remains constant. By incorporating the two wires into a Wheatstone bridge circuit, the change in resistance is converted into a small e.m.f. which can readily be recorded. The TCD is a concentration sensitive detector. The signal from the TCD is also measured by the integrator and displayed on a strip chart recorder.

A CO_2 cryogenic unit is used for sub-ambient temperatures and helium is used as carrier gas.

10.4 CALIBRATIONS

10.4.1 Volumetric Calibrations

Precise measurement of phase volumes and accurate metering of fluids into the high pressure cells requires careful volumetric calibration of the pumps, tubing and windowed cells which make up the PVT apparatus. First the volumetric delivery of each pump barrel was calibrated by comparing the actual volume of mercury removed from the pump at various pressures, to pump scale readings. Next, the expansion of the tubing manifold leading from the pumps to the cells was measured at various pressures by compressing mercury into it, at 20°C, 60°C, 75°C and 100°C. At the next stage the exact volumes of the high pressure windowed cells were measured at 20°C, 60°C, 75°C and 100°C as a function of pressure, by pumping predetermined volumes of mercury into the cells. Finally the readings of the length of the phases on the scale attached on the door of the air bath, were calibrated in terms of actual volume in the cell and the dead volumes of the two cells were measured as well. Volumetric calibration data were used to calculate the volumes of the phases in the cell from the position of the interfaces bounding it.

10.4.2 Densitometer Calibrations

The PAAR DMA 512 high pressure and temperature densitometer was calibrated at several temperatures and pressures. The stainless steel tube oscillates and the period of oscillation depends on the mass of the fluid within it, so that the density of the fluid can be calculated from the measured period of the oscillation.

At a given temperature and pressure the period of oscillation is given by

$$t^2 = A\rho + B \quad \ldots \quad \text{Eq 10-1}$$

where t is the period (milliseconds), ρ is the density (g/cc) and A and B are calibration constants which are determined experimentally. If periods t_1 and t_2 are measured corresponding to densities ρ_1 and ρ_2 the calibration constants are

$$A = \frac{t_1^2 - t_2^2}{\rho_1 - \rho_2}, \quad B = t_1^2 - A\rho_1 \quad \ldots \quad \text{Eq 10-2}$$

The constants A and B were found to depend on both temperature and pressure, so calibrations were made using two different components for which experimental density data was available over a wide range of pressure and temperature. Methane and decane were chosen for the calibration because they cover the range of densities which would be encountered during the phase behaviour experiments. Periods of oscillation of these two pure components were measured between 60°C and 110°C at pressures from atmospheric to 5000 psi.

Equation 10-2 was used to calculate the calibration constants. Least squares quadratic fits were made for the dependence of the slope A and intercept B on temperature at a reference pressure of 100 psig. Next, least square quadratic fit was made for the dependence of B on pressure.

The final form of the correlation developed for the calibration of the DMA 512 densitometer for measurements at elevated temperatures and pressures, gives density as

$$\rho = \frac{t^2 - B(T,P)}{A(T)} \quad \ldots\ldots\ldots\ldots \quad \text{Eq 10-3}$$

where t is the period of oscillation in milliseconds and

$$A(T) = 2.818367 + 0.013341\ T - 4.72276*10^{-5}T^2$$

$$B(T,P) = 16.136248 - 0.006853T + 6.534494*10^{-5}T^2 +$$

$$0.01685 - 7.135*10^{-6}(P-100) + 1.805*10^{-9}(P-100)^2$$

$$\ldots\ldots \quad \text{Eq 10-4}$$

10.5 COMPOSITIONAL CHARACTERISATION USING GAS CHROMATOGRAPHY

Gas chromatography is a very efficient method of physical separation, enabling a very small sample of fluid to be analysed into its components. The sample injected is vapourised in the injection block heater and swept by the carrier gas over a stationary phase. The components to be separated are distributed between two phases; one of them consititutes a stationary bed, the other is a fluid that percolates through or along the stationary bed. The chromatographic process occurs as a result of repeated sorption-desorption during the movement of the sample components along the stationary bed. The separation is due to differences in the distribution coefficients of the individual sample components. The retention time of a certain substance on a given stationary phase is characteristic of that substance and therefore retention data can be used for identification purposes. The whole process takes place in a column containing the stationary phase through which the moving phase is flowing. At the end of the column the individual components emerge more or less separated in time and are detected. During the whole process, the system is kept at

temperature sufficient to maintain the sample components in the vapour phase.

For the phase behaviour studies, the hydrocarbon characterisation is aimed at the analysis of the unknown mixtures by the identification and quantification of grouped carbon number rather than individual pure components, given the countless components present in a reservoir fluid. For the purposes of this study components with similar boiling points and therefore similar molecular weights are grouped together. Hydrocarbons with retention times between those of C_n and C_{n+1} were assumed to be C_{n+1}. The molecular weight of the normal alkane was used as an estimate of the molecular weight for each carbon number cut. the reason behind this is that the normal hydrocarbons are the components more easily identifiable in a crude oil sample. Even more detailed separations could have been obtained in a capillary column but the amount of data collected for each sample would be very large.

A technique was developed to enable the full compositional characterisation of mixtures of reservoir fluids and injection gases, using a single sample. During the single run the volatile inorganic gases, the light hydrocarbons and the heavy hydrocarbons up to C_{30}, can be identified and quantified in grouped carbon numbers. To identify the components of a sample injected in a particular column under particular conditions, retention time data has to be obtained, for all or at least some of the components of interest. This was achieved by injecting in the column reference mixtures made of these components, under the same conditions as the runs of the unknown composition mixtures, and recording the

retention times which are functions of the boiling point of the substances. Figure 10-5 gives the plot of the retention times as a function of the boiling point for the 10ft, 10% OV101 column at a temperature program from 20°C to 350°.

A second series of calibration tests involve the establishment of relative response factors (RRF). The RRF are the correction factors which divide raw peak areas measured by the integrator, to express the actual concentration of the individual components in the mixture. If the RRF is independent of sample size and the carbon number of the hydrocarbon, then the raw area of each peak should reflect the weight percent, for FID, or mole percent, for TCD, of the component in the sample.

A series of tests proved the RRF to be independent of the sample size, for sample sizes between 0.1µl up to 4µl, for the conditions set for the runs. The sample size was carefully measured and the repeatability of the run was guaranteed by the use of a Chaney adapter on the Hamilton syringes. A second series of tests investigated the variation of response factors with molecular size using both the TCD and FID detectors. These tests proved that the detectors responses depend on the molecular weight of the eluted components.

10.5.1 Calculation and Use of the Relative Response Factors

As already mentioned, the normalised peak area values are related to the concentration of the respective components in the sample. Mathematically speaking

$$A_i = RRF_i * C_i \quad i = 1,N \qquad \text{Eq 10-5}$$

FIGURE 10-5

PLOT OF N-ALKANE CARBON NUMBER VS RETENTION TIME

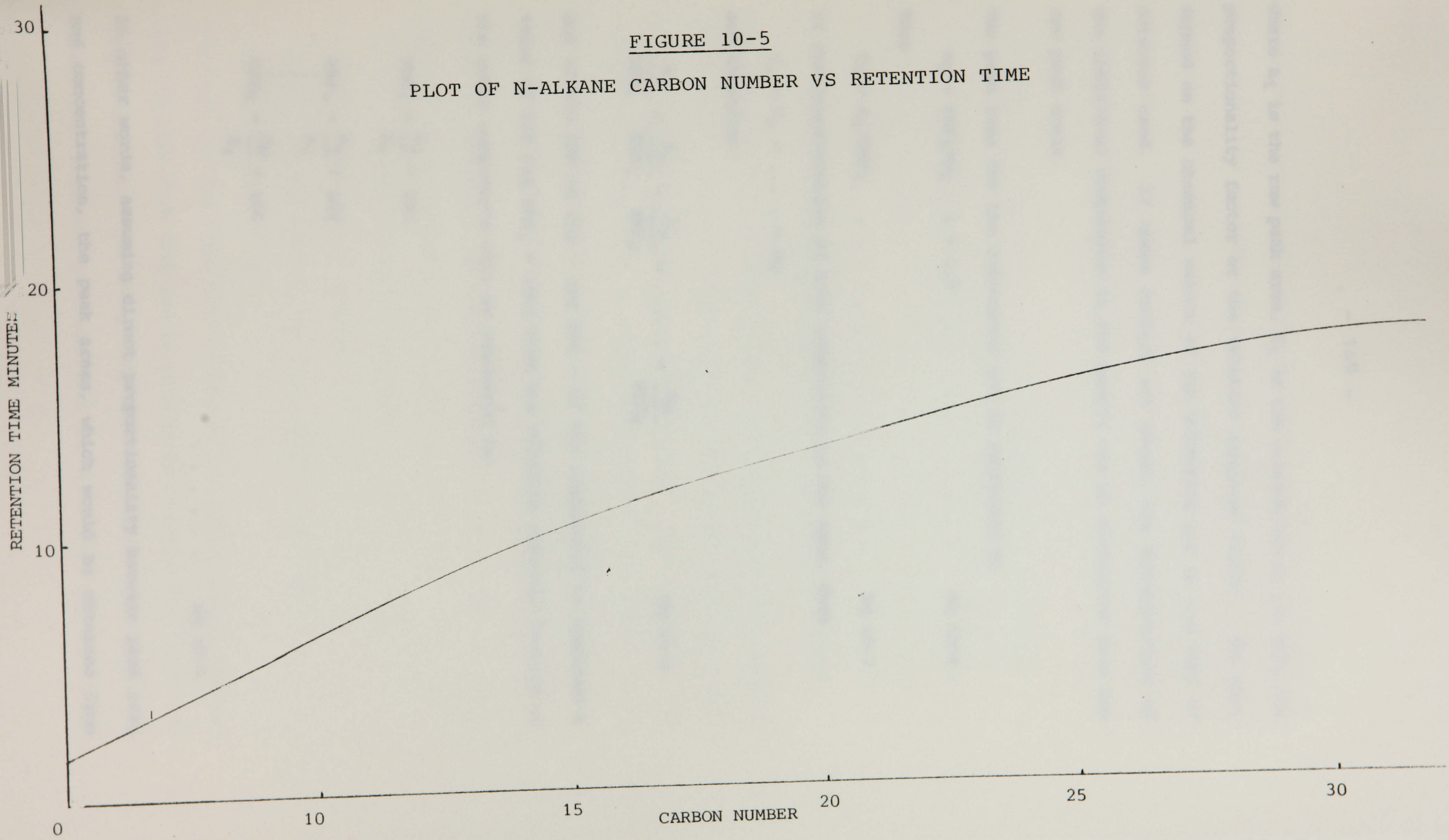

where A_i is the raw peak area, C_i is the concentration and RRF_i the proportionality factor or the relative response factor. The RRF_i depend on the chemical nature of the substance and on the type of detector used. If these factors are known, the concentration of the individual components in the sample can be calculated from the raw peak areas.

The peak area for the components can be expressed as

$$A_i = RRF_i * C_i \quad i = 1,N \quad \ldots\ldots\ldots\ldots \quad \text{Eq 10-6}$$

Thus

$$C_i = A_i / RRF_i \quad \ldots\ldots\ldots\ldots\ldots\ldots \quad \text{Eq 10-7}$$

If the concentration of both components is the same, then

$$C_1 = C_2 = \ldots\ldots = C_N$$

and therefore

$$\frac{A_1}{RRF_1} = \frac{A_2}{RRF_2} = \frac{A_3}{RRF_3} = \ldots\ldots = \frac{A_N}{RRF_N} \quad \ldots\ldots \quad \text{Eq 10-8}$$

and if the RRF of one - any one - of the components is assigned a value of 100 (eg $RRF_1 = 100$) then the relative response factors of the other components will be expressed as:

$$RRF_2 = \frac{A_2}{A_1} * 100$$

$$RRF_3 = \frac{A_3}{A_1} * 100$$

$$\vdots$$

$$RRF_N = \frac{A_N}{A_1} * 100$$

$\ldots\ldots$ Eq 10-9

In other words, assuming direct proportionality between peak area and concentration, the peak areas, which would be obtained from

having equal concentrations present, are calculated. To use the RRF_i, first the so called reduced peak area values (A_i/RRF_i) are established. Then, the concentrations of the individual components C_i are calculated as the ratio of their respective reduced peak areas and their sum

$$(A_1/RRF_1) + (A_2/RRF_2) + ... + (A_N/RRF_N) = \sum_{i=1}^{N} (A_i/RRF_i)$$

$$C_i = \frac{A_i/RRF_i}{\sum_{i=1}^{N} (A_i/RRF_i)} \qquad i = 1,N \quad . . . . . \quad \text{Eq 10-10}$$

10.5.2 Conditions for the Gas Chromatographic Analyses

Two 1/8" OD OV101 columns packed with 80/100 mesh size support coated with non-polar methyl silicone stationary phase were used in the Perkin Elmer F17 gas chromatograph. The length of the columns had to be 10 ft, a figure determined by the separation of CO_2, methane and ethane (the longer the column, the greater the differences in the retention times of the components).

Described below are the chromatographic techniques used for three types of samples analysed in this project

(i) Liquid hydrocarbon samples

(ii) Produced gas samples

(iii) Direct samples from high pressure and temperature phases

The first technique was used to analyse the liquid phases produced from the blow down sampling as well as to characterise liquids at room conditions. The second was used to analyse gas samples at atmospheric pressure, produced from the blow down system and the

third technique was used for the direct analysis of vapour and liquid phases sampled with the high temperature direct sampling system.

Separations of CO_2, N_2 and C_1–C_4 hydrocarbons present in high pressure samples, as well as heavy hydrocarbons like C_{30}, were performed in a single column without the use of column switching or backflush valves. It is important to avoid the use of valves in the oven, if possible, because the high temperature limit for valves currently available is much lower than the oven temperature required to elute the heavy hydrocarbons present in a crude oil[3]. The price paid for the simplicity of the analysis is that the separation of the light ends is not as efficient as could have been achieved with other columns at different conditions. Nevertheless the advantages of a single column analysis far outweigh the disadvantages.

10.5.3 Liquid Hydrocarbon Samples

To calibrate the response of the FID detector to mixtures of hydrocarbons having boiling points within the range of the analysis, a reference mixture consisting of normal alkanes from C_5 up to C_{30} was carefully prepared. The composition of this mixture simulates as close as possible a typical composition of a crude oil and is given in Table 10–1. A sample of 0.2 $\mu\ell$ was injected with a syringe through a septum, into the injection block of column B of the gas chromatograph. The FID's response to each component eluted from the column, was recorded as peak area counts by the electronic integrator. The RRF_i calculated for the normal alkanes between C_5 and C_{30} are given in Table 10-2. The RRF of C_{14}

was assumed 100. Typical chromatogram of such a run is shown in Figure 10-6. The conditions of the runs for the calibration tests as well as for any liquid hydrocarbon samples throughout this work are given in Table 10-3.

10.5.4 Estimation of the C_{30+} Fraction

A major difficulty encountered in the analysis of crude oil samples is the estimation of the fraction of the sample that has not eluted from the column at its maximum operating temperature. The maximum operating temperature for the Perkin Elmer F17 gas chromatograph does not allow components heavier than C_{30} to come out of the column and, hence, their signal to be detected. To calculate the non eluted weight fraction C_{30+}, a test method proposed by ASTM (1976)[3] was used. The method requires two runs to be performed for each sample, one in which a mixture of sample plus an internal standard, is injected (Run A) and another in which only the sample is injected (Run B). The internal standards are usually mixtures made up by equal parts of C_{14}, C_{15}, C_{16} and C_{17}. The volume ratio of the internal standard to the mixture, should be between 0.1 and 0.15. Typical result of such run is shown in Figure 10-7. Consider A_I be the area of the segment which contains the internal standard in the chromatogram for Run A, A the total area of run A, B_I the area of the internal standard segment of run B and B the total area of that run. Because the total areas of the two runs may not be the same due to small differences in injected sample volumes, the area of the segment which contains the internal standard A_I should be adjusted at the value which would have occurred had the volume injected in Run A been identical to that in Run B.

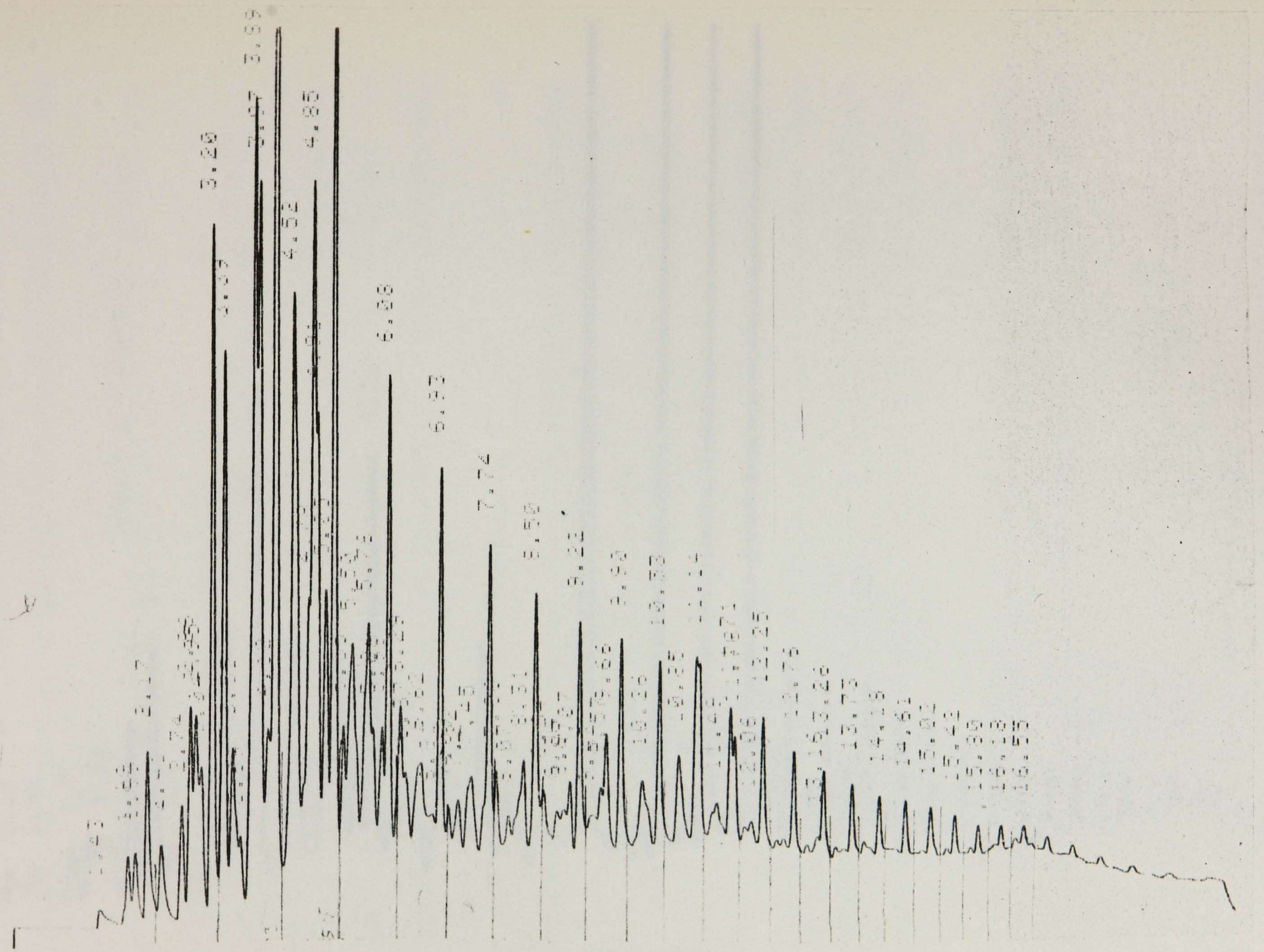

FIGURE 10-6

CHROMATOGRAM OF A CRUDE OIL

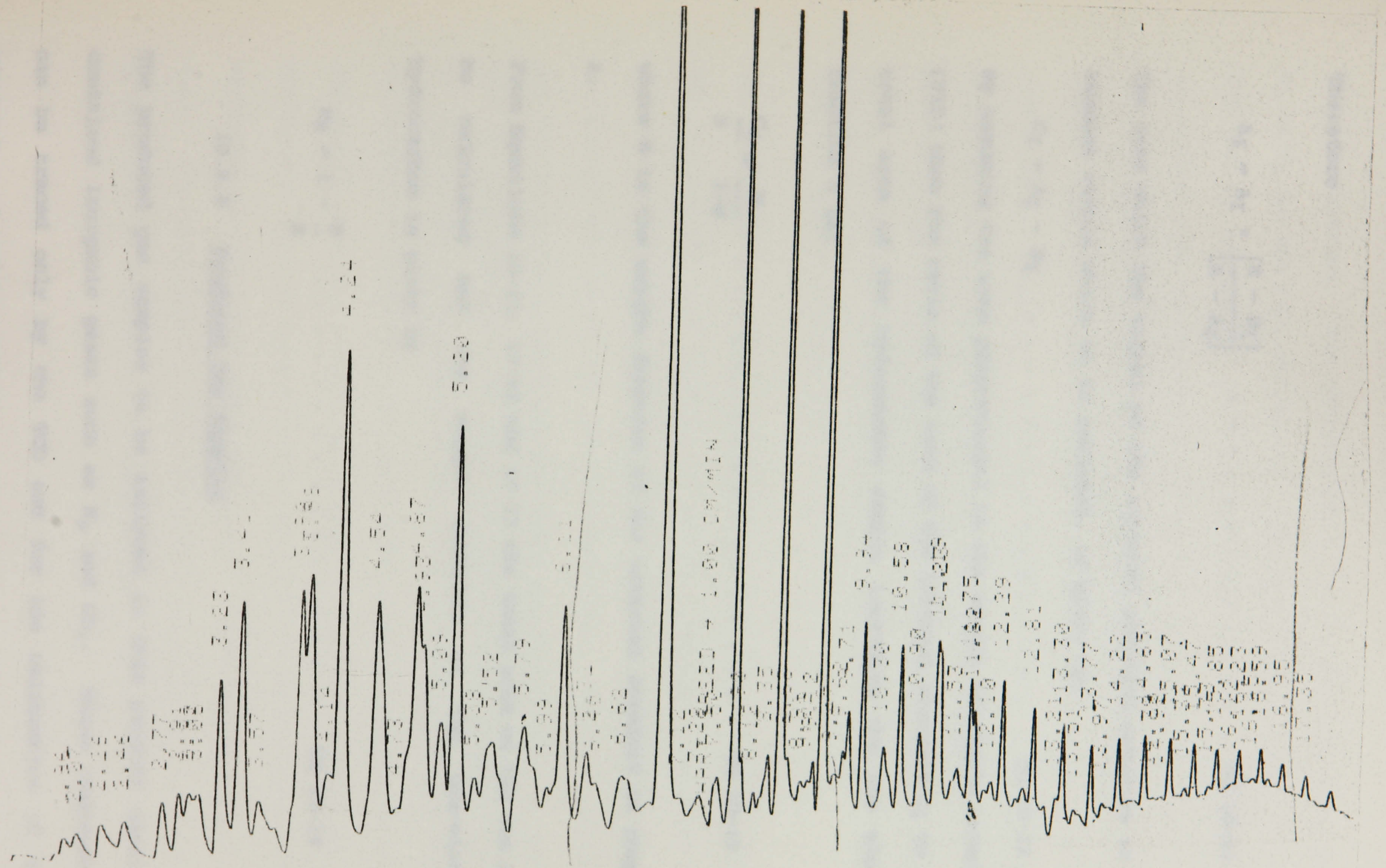

FIGURE 10-7

CHROMATOGRAM OF A CRUDE OIL INCLUDING INTERNAL STANDARD

Therefore

$$A_I = A_I * \left[\frac{B - B_I}{A - A_I}\right] \quad \text{. . . . . Eq 10-11}$$

The area which the signal of the internal standard occupies in the segment within which it is included, is given by:

$$C_I = A_I - B_I \quad \text{. . . . . Eq 10-12}$$

By assuming the area proportional to the weight of sample injected (FID) then the ratio of the area of the internal standard C_I to the total area of the hydrocarbon sample including the non eluted fraction S is:

$$\frac{C_i}{S} = \frac{W}{1-W} \quad \text{. . . . . Eq 10-13}$$

where W is the weight fraction of the internal standard in sample A.

From Equations 10-11, 10-12 and 10-13 the total area of the run can be calculated and the weight fraction of the non-eluted hydrocarbon is given by

$$W_H = 1 - \frac{B}{S} \quad \text{. . . . . Eq 10-14}$$

10.5.5 Produced Gas Samples

The produced gas samples to be analysed in this project usually contained inorganic gases such as N_2 and CO_2. These components can be traced only by the TCD and for the calibration of the thernmal conductivity detector's responses, a standard gas mixture was used. Table 10-4 gives the mole % composition of the gas

standard mixture. The establishment of the RRF_i for the alkanes C_1 to C_5 for the FID, follows the same procedure as before with the RRF for C_5 assumed as 113.3 so that the RRF_i of C_1–C_4 would be consistent with the previously determined response factors for the heavier hydrocarbons. These RRF_i are given in Table 10–5 and typical results of such run are given in Figure 10–8. Thermal conductivity detectors relative response data, can be used independently of the particular detector's characteristics[4]. The data tabulated by Dietz were used as RRF_i for the components C_1 up to C_5, N_2 and CO_2 for the thermal conductivity detector[5]. These RRF_i are listed in Table 10–6.

The conditions for the gas sample runs are shown in Table 10–3. The gas samples were injected in column A through a six port two position VALCO gas sampling valve, which is installed in the pneumatics section of the gas chromatograph. The two positions and the interport connections are shown in Figure 10–9. A sample loop of 100$\nu\ell$ was used. As gases are compressible, sampling has to be carried out at atmospheric pressure, and therefore the valve was allowed to bleed down to atmospheric pressure before injecting the sample into the carrier gas stream. First, the sample volume was purged, the gas sample supply was shut off and a plastic pipe connected to the valve exit port, was vented into a beaker of water. The achievement of the atmospheric equilibrium can be seen by watching the bubbles of the sample flow.

FIGURE 10-8

CHROMATOGRAM OF A C_1-C_5 MIXTURE - FID RESPONSE

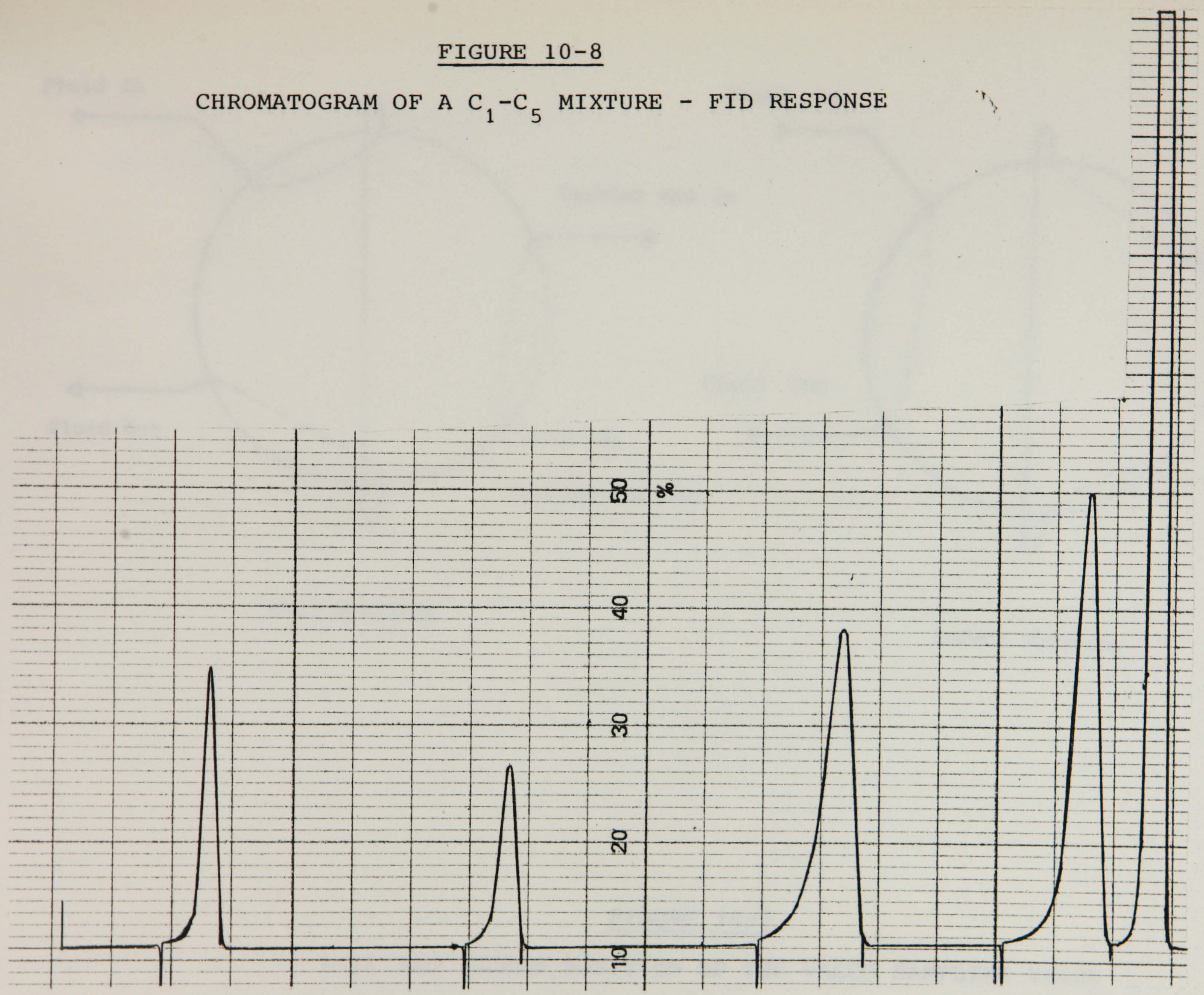

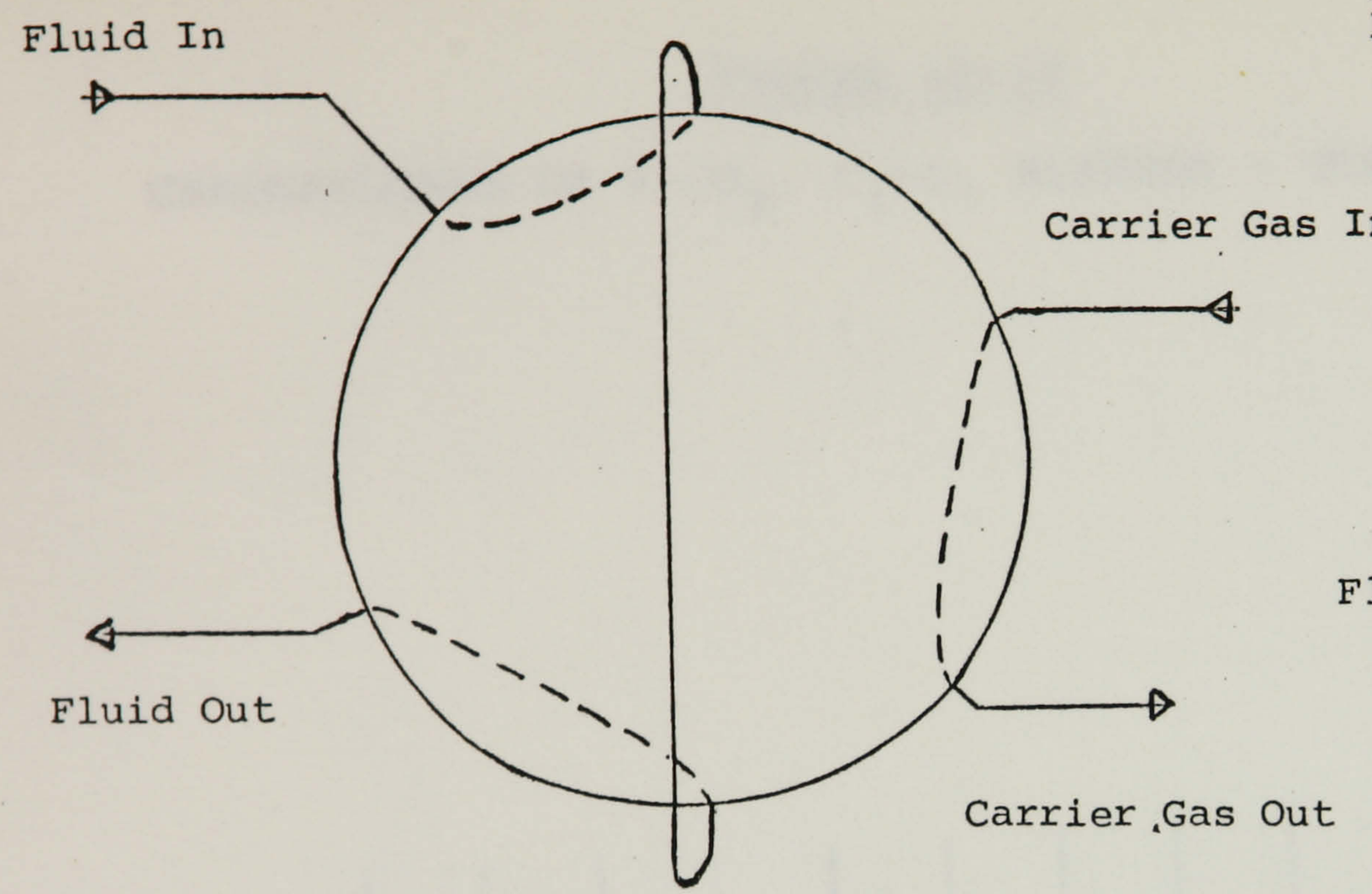

FILL POSITION

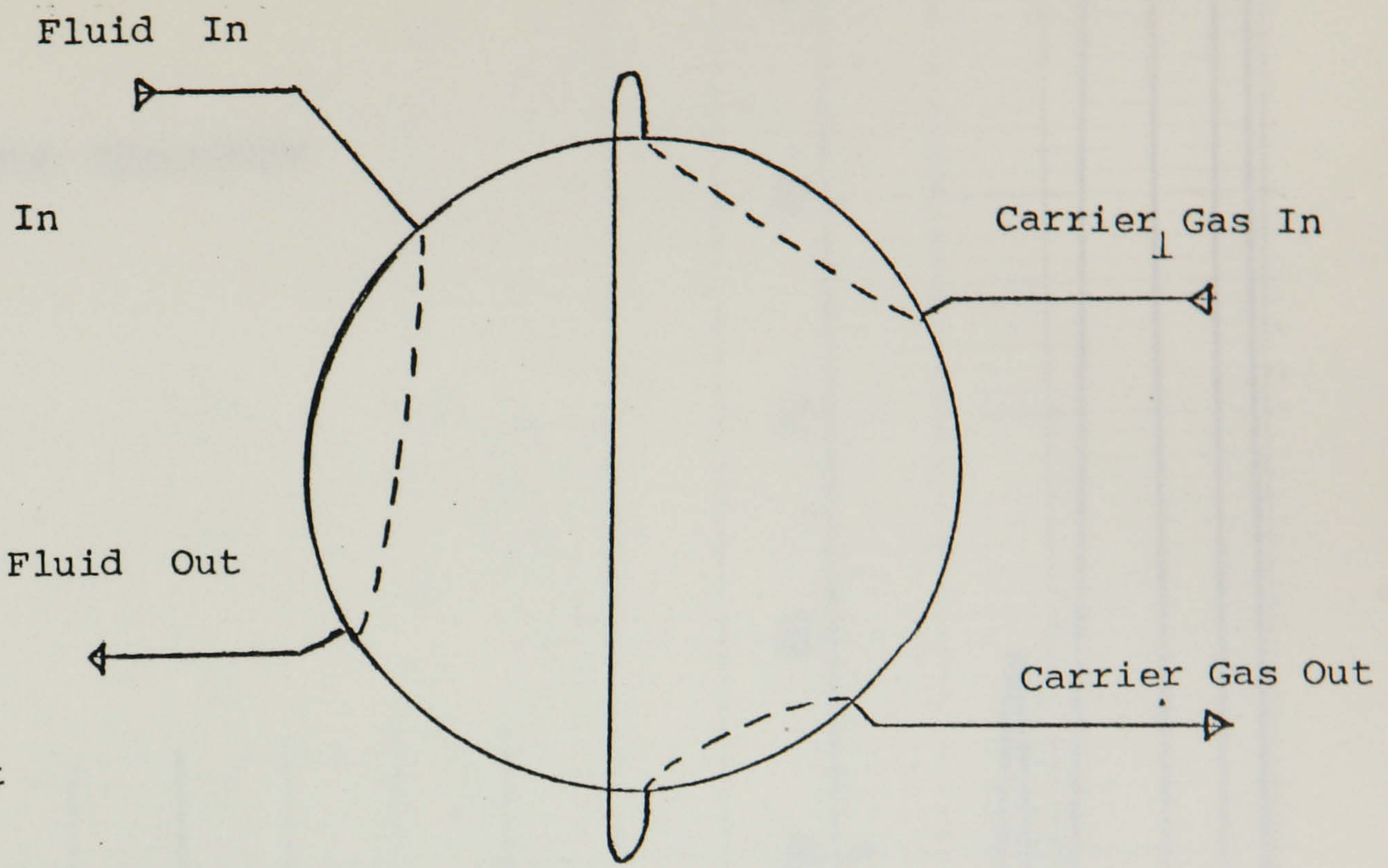

INJECT POSITION

FIGURE 10-9

FILL AND INJECT POSITION OF THE VALCO SAMPLING VALVE

FIGURE 10-10

CHROMATOGRAM OF A CO_2, C_1-C_5 MIXTURE - TCD RESPONSE

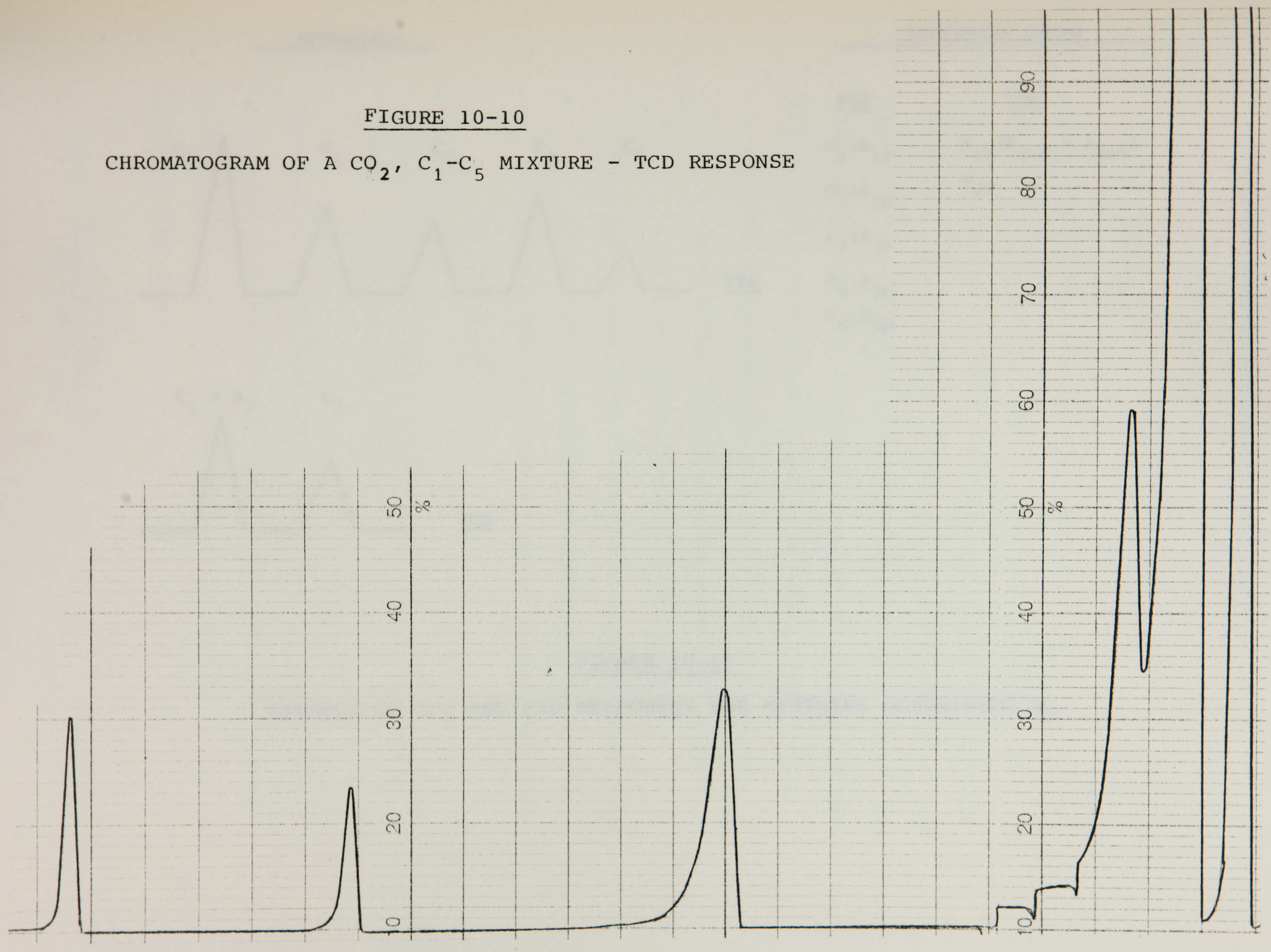

RESPONSES

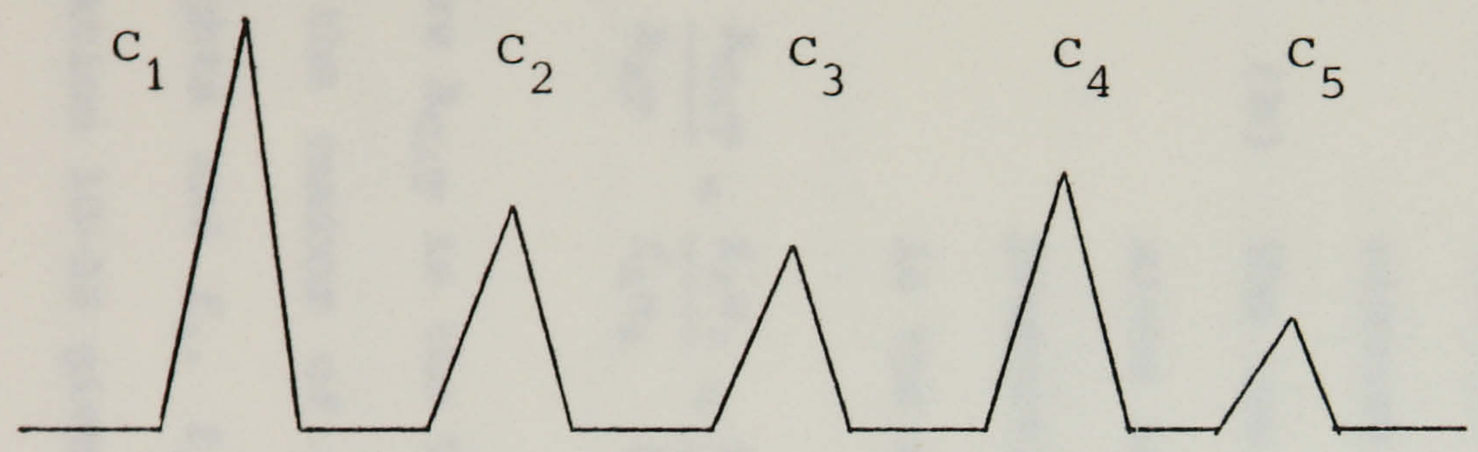

FID

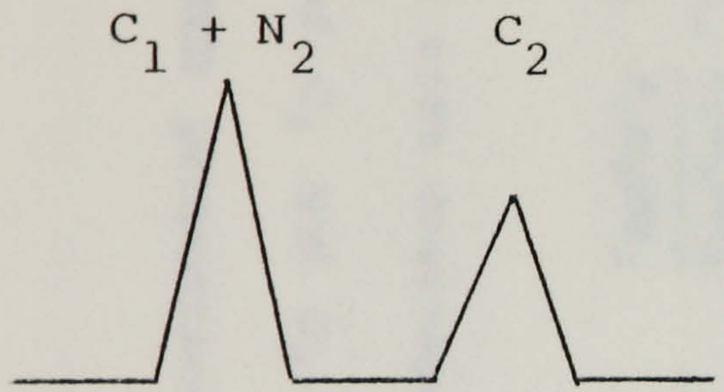

TCD

INTEGRATED AREAS

FID	TCD
$C_1 : A_{1F}$	$A_{1T}(A_{C1T} + A_{N1T})$
$C_2 : A_{2F}$	A_{2T}
$C_3 : A_{3F}$	
$C_4 : A_{4F}$	
$C_5 : A_{5F}$	

FIGURE 10-11

EXAMPLE OF TCD AND FID RESPONSES FOR MIXTURES CONTAINING N_2

10.5.6 Methods for Measuring the Concentration of N_2 and CO_2

(1) Nitrogen

At the conditions of the run (type and length of column, temperature programming etc), the TCD's responses give no resolution for the nitrogen and methane peaks and therefore they appear in a composite peak. To measure the concentration of both components in the sample, the responses from both FID and TCD detectors have to be considered. The method used is outlined briefly below. Consider the example presented in Figure 10-11.

(a) Using the previously established RRF_i for C_1 and C_2 the mass fractions of these two components in the mixture is calculated from the FID output.

(b) The raw peak areas of the thermal conductivity detector since it is a concentration sensitive detector, are proportional to the molar ratio of the two components in the mixture

$$\frac{A_{C_1T}}{A_{2T}} = \frac{f_1 n_1}{f_2 n_2} = \frac{f_1 m_1/MW_1}{f_2 m_2/MW_2} = \frac{f_1 m_1 MW_2}{f_2 m_2 MW_1} \quad \ldots\ldots\ldots \text{Eq 10-15}$$

where A_{C_1T} is the TCD peak area corresponding only to methane, n_1, n_2 the number of moles of C_1 and C_2, MW_1, MW_2 their molecular weights and f_1, f_2 the TCD proportionality factors of C_1, C_2. Equation 10-15 gives:

$$A_{C_1T} = \frac{A_{2T} * m_1 * MW_2 * f_1}{m_2 * MW_1 * f_2} \quad \ldots\ldots\ldots \text{Eq 10-16}$$

The raw peak area A_{N_1T} for nitrogen is calculated by

$$A_{N_1T} = A_{1T} - A_{C_1T} \quad \ldots\ldots\ldots\ldots\ldots \quad \text{Eq 10-17}$$

(c) The TCD raw peak areas for nitrogen and methane, A_{N_1T} and A_{C_1T} are proportional to the molar ratio of the two components in the mixture

$$\frac{A_{C_1T}/f_1}{A_{N_1T}/f_N} = \frac{m_1 MW_N}{m_N MW_1}$$

and therefore

$$m_N = \frac{A_{N_1T} * m_1 * MW_N * f_1}{A_{C_1T} * MW_1 * f_N} \quad \ldots\ldots\ldots \quad \text{Eq 10-18}$$

where m_N, MW_N, f_N are the mass fraction, molecular weight and thermal conductivity response of nitrogen. The mass fraction of nitrogen in the mixture is therefore calculated from Equation 10-18. In case that ethane is not contained in the mixture, the lightest alkane present is used instead.

(2) Carbon Dioxide

The second difficult separation is the one between CO_2 and ethane and for these components to be resolved, it was found that the initial oven temperature should be at -65°C and the length of the column at least 10ft. The maximum resolution between the CO_2 and C_2H_6 peaks achieved under these conditions, was about 90% (Figure 10-10).

If A_{CO_2T} is the raw peak area for the CO_2 detected by the TCD, then for the same reasons explained for nitrogen, the mass of CO_2 present in the sample is given by:

$$m_{CO_2} = \frac{A_{CO_2T} * m_1 * MW_{CO_2} * f_1}{A_{C_1T} * MW_1 * f_C} \quad \ldots\ldots\ldots \quad \text{Eq 10-19}$$

where f_C is the TCD relative response factor for the CO_2. In case that methane is not contained in the mixture, the lightest alkane present is used instead.

A much better separation between CO_2 - C_2H_6 and CH_4 - N_2 could have been achieved if a different column was used, such as a 6ft Porapak Q column[3], but given that all types of analysis had to be done using the same gas chromatograph and also that a Porapak column cannot stand temperatures as high as those required for the elution of the heavy hydrocarbons, a single column had to be used to analyse the whole range of components and therefore the OV101 packed column was chosen. Due to the fact that the silicone rubber liquid phase in the OV-101 column solidifies at temperatures around -65°, some tailing of the light end peaks occurs.

10.5.7 Direct Samples of High Pressure and Temperature Phases

A high pressure and temperature sample can contain the whole range of components including light, intermediate and heavy hydrocarbons as well as gases like CO_2 and N_2. In case CO_2 and N_2 are present in the sample, the signals from both FID and TCD should be recorded. The calibration and the calculation of the relative response factors follow the pattern described in the previous sections (10.5.5) and (10.5.6). The advantages of the direct sampling compared with the blow down method are:

(i) Negligible volumes of sample are required

(ii) The number of chromatographic runs required per phase is halved

(iii) The method is free of any measurements of volume (gas) or weight (liquid) where some errors can be made

(iv) The method avoids the problems of possible liquid coating on the sampling trap walls.

Various problems on the design and engineering of the direct sampling did not allow full advantage of the potential of the method to be taken during the course of this study, due to lack of time. A few runs only were made using standard mixtures with components ranging from C_5 to C_{20} which have given encouraging results. Table 10-7 shows the weight % composition of a typical compositional analysis of a calibration standard using the direct sampling in comparison to the mixture's actual composition. Table 10-3 gives the recommended conditions for the direct sampling runs.

10.6 REVIEW OF DIFFERENT EXPERIMENTAL SYSTEMS AND TECHNIQUES TO STUDY PHASE BEHAVIOUR

The measurements most commonly made determine saturation pressures for mixtures of reservoir fluid with injection gases usually CO_2[6,7,8,9,10,11]. In a typical experiment, gas and oil are charged in a single windowed cell mounted in an air[7.12,2] or water bath[13,14]. The saturation pressure, swelling factors and single phase densities and viscosities, as well as the volumes of the phases present in the system can be measured using simple experimental facilities. Single windowed cells used for these studies are Ruska cells[15], Jerguson Series cells[16,17,14] and cells similar to the one designed by Jacoby[7,18]. Huang and Tracht used

the latter for their work on CO_2-West Texas crude oil systems[7]. The cell is a varied volume cylinder, whose volume changes by means of a piston driven by high pressure hydraulic oil (Fig 10-12).

The cell operates to a maximum pressure of 20,000 psia and its maximum volume is 1 litre. The cell was enclosed in a thermostatically controlled air bath and narrow slit windows were located at the end of the cylinder bore, through which light was transmitted perpendicular to the cylinder, for observation and measurements. Sampling valves at the top and at the bottom of the cell, allow sampling of the gas and liquid phases. The system obviously cannot be used for multiple contact studies. Yarborough et al[18] have used the same cell in a slightly modified version.

Mercury pumps[15,3], hydraulic oil pumps[7], or rod cells[16] were used in different studies as pressure sources.

More detailed experimental data including measurement of phase compositions are time consuming, require more complicated designs and hence are less commonly performed. Phase composition data have been reported by Rathmell et al[19], Shelton et al[20], Simon et al[21], Graue et al[8], Gardner et al[22], Orr et al[1] etc.

Multiple contact experiments are needed to provide valuable information for the representation of the phase behaviour of injection gas-reservoir oil systems in terms of a small number of pseudocomponents. Such a representation is required if compositional simulations are to be performed for reservoir scale processes[1]. Multiple contact phase behaviour experimental data

for CO_2-crude oil systems have been reported by Gardner et al[22] and Orr et al[3,23].

The experimental facility used for the study in this thesis is similar to the one used by Orr at the New Mexico Petroleum Recovery Research Center. The main differences between the two systems, focus on the sampling techniques. The New Mexico research group, used a method which combined a VALCO six port sampling valve and syringes, able to withstand low pressures (250 psia). Before sampling, the sample groove in the Valco valve was cleaned and filled with CS_2 (Fig 10-13). The valve was then rotated to the vent position and a very small amount of sample vented to remove the CS_2 from the system. Then, with the valve in the load position, a large volume of the phase to be sampled was moved from one cell to the other. The sample was allowed to release pressure into the syringe and any hydrocarbons which condensed in the valve during blowdown, were displaced into the sample syringe with CS_2. The nose valve on the syringe was then closed, and the sample was injected immediately into the column. The same technique is being used by the Alabama University research group[24].

Yarborough et al[18] have used an Autoclave 30VM valve to trap the high pressure sample. As can be seen in Figure 10-14, just above the sample cavity the valve stem has a very loose fit in the valve body and as a result, the fluid is allowed to flow around the valve stem and through the valve when the sample cavity is closed. The stainless steel body of the valve allows it to be used at temperatures up to 350°F and pressures up to 10,000 psia.

FIGURE 10-12

EQUILIBRIUM CELL DESIGN BY JACOBY[18]

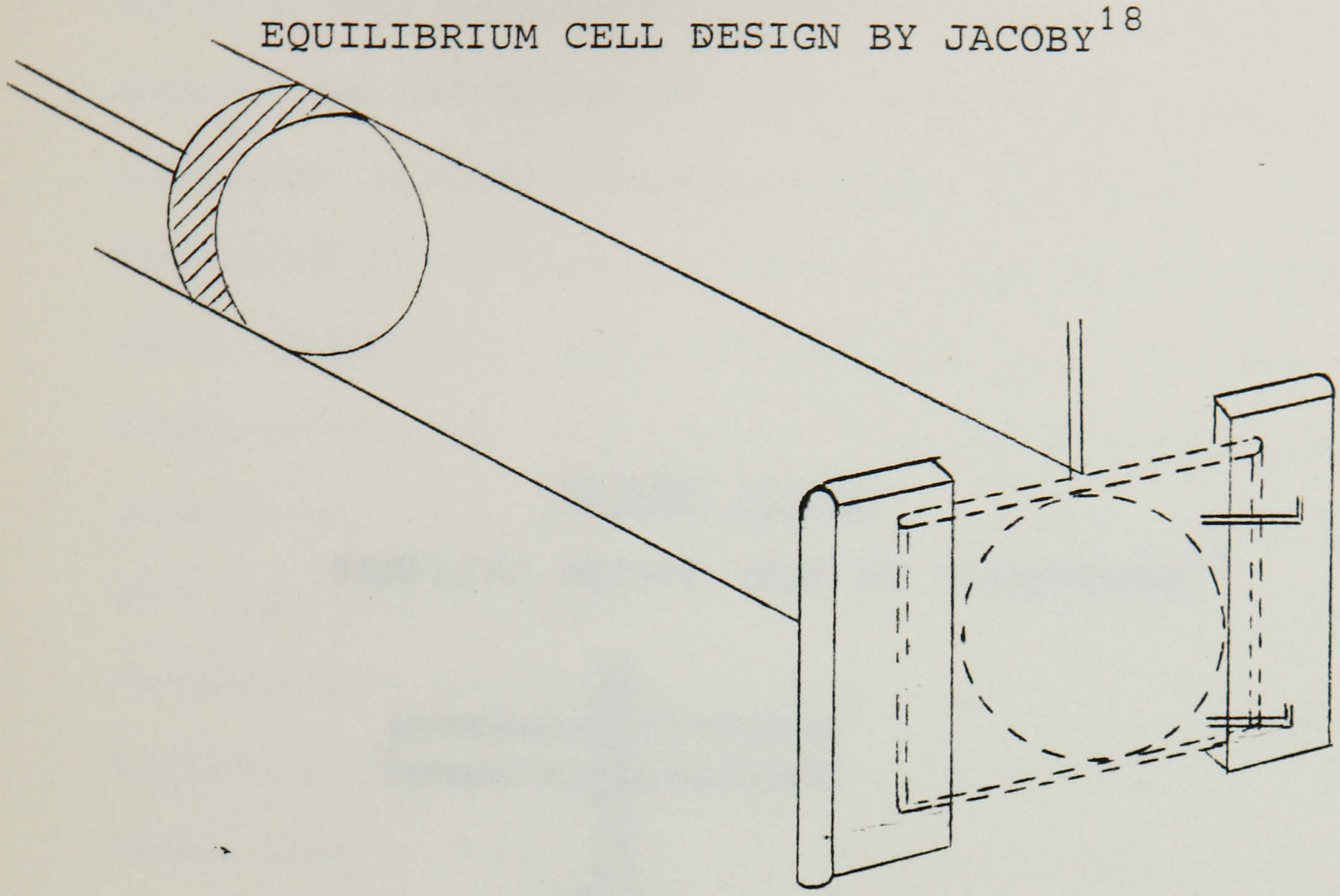

FIGURE 10-13

SAMPLING METHOD USED BY ORR[3,23]

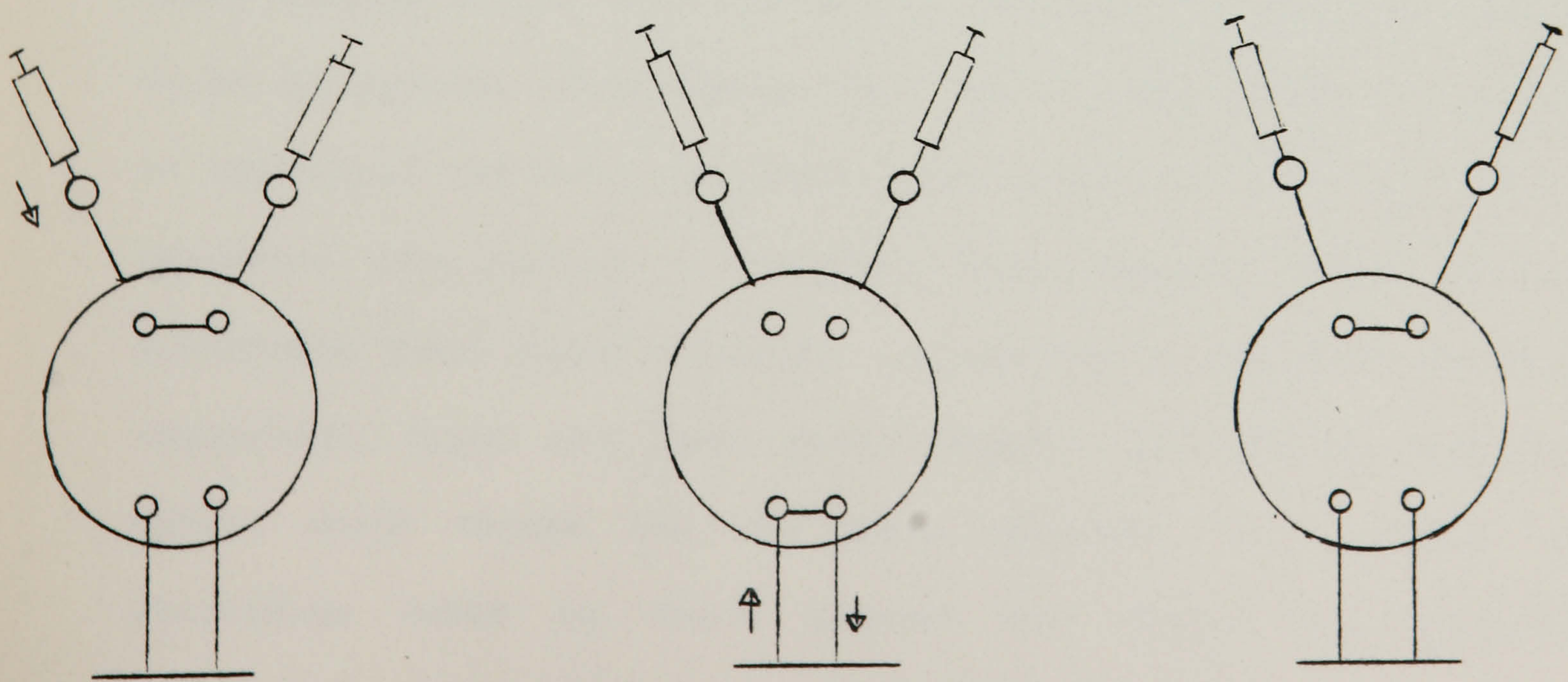

FIGURE 10-14

SAMPLING METHOD USED BY YARBOROUGH[18]

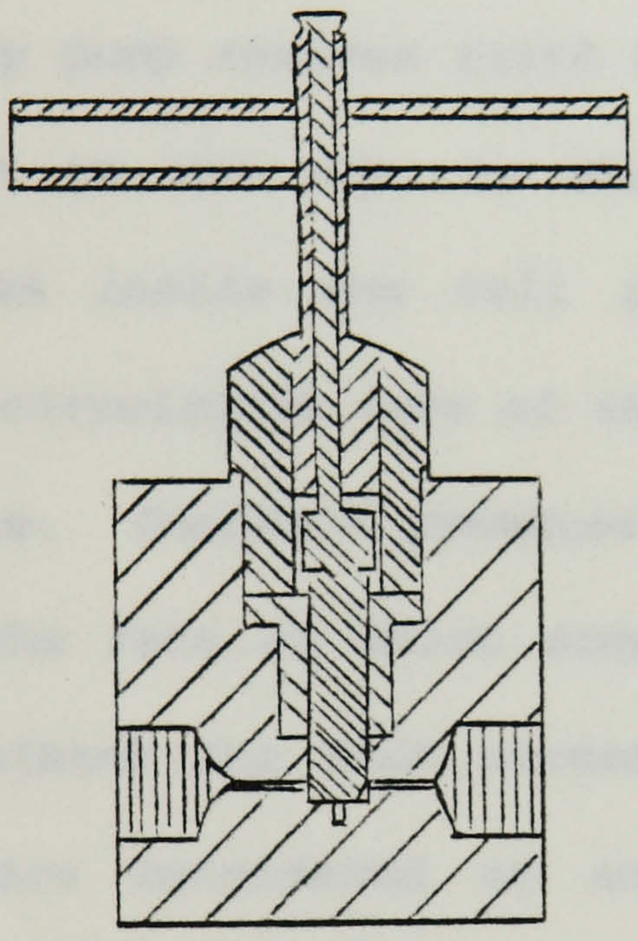

Orr et al have developed a new method to measure equilibrium phase compositions and densities[1]. The experimental technique called continuous multiple contact experiments, involves continuous circulation of the fluids in and out of the cell to ensure mixing, while samples are taken simultaneously from both the top and bottom of the cell (Fig 10-15). In a typical experiment a high pressure cell is filled with crude oil. A Ruska pump displaces CO_2 into the mixing vessel at a rate of 12cc/hr. A liquid chromatography pump removes fluid from the bottom of the cell and circulates it to the top, to mix the fluids within the cell. Teflon baffles inside the cell improve the mixing of the two phases. The circulation rate of 450cc/hr is large compared to the injection rate. Constant pressure is maintained in the cell, by controlling the rate at which samples are produced using a back pressure regulator for each stream. Although the phases during circulation are considered as not having any clear interface separating them, it is assumed that small volumes of the upper and lower phases in equilibrium, segregate to the top and to the bottom of the mixing cell respectively. Lower phase samples are drawn through a tube from the base of the cell and the lower phase to be circulated, is withdrawn from the annulus around that tube. At the top of the cell, the upper phase sample is withdrawn from a quiescent zone beneath a stainless steel umbrella around which, circulated lower phase descends. Downstream of the back pressure regulators, upper and lower phase samples flow through sampling valves which direct the two phase mixtures, to a series of centrifuge tubes in which liquids are caught and analysed afterwards. Gas samples are analysed on line by use of gas sampling valves with a cycle time of about ten minutes.

FIGURE 10-15

CONTINUOUS MULTIPLE CONTACT APPARATUS[1]

1 Densitometer
2 Multi Port Sampler
3 Gas Chromatograph
4 Wet Test Meter
5 Back Pressure Regulator
6 Mixing Vessel
7 Teflon Baffles

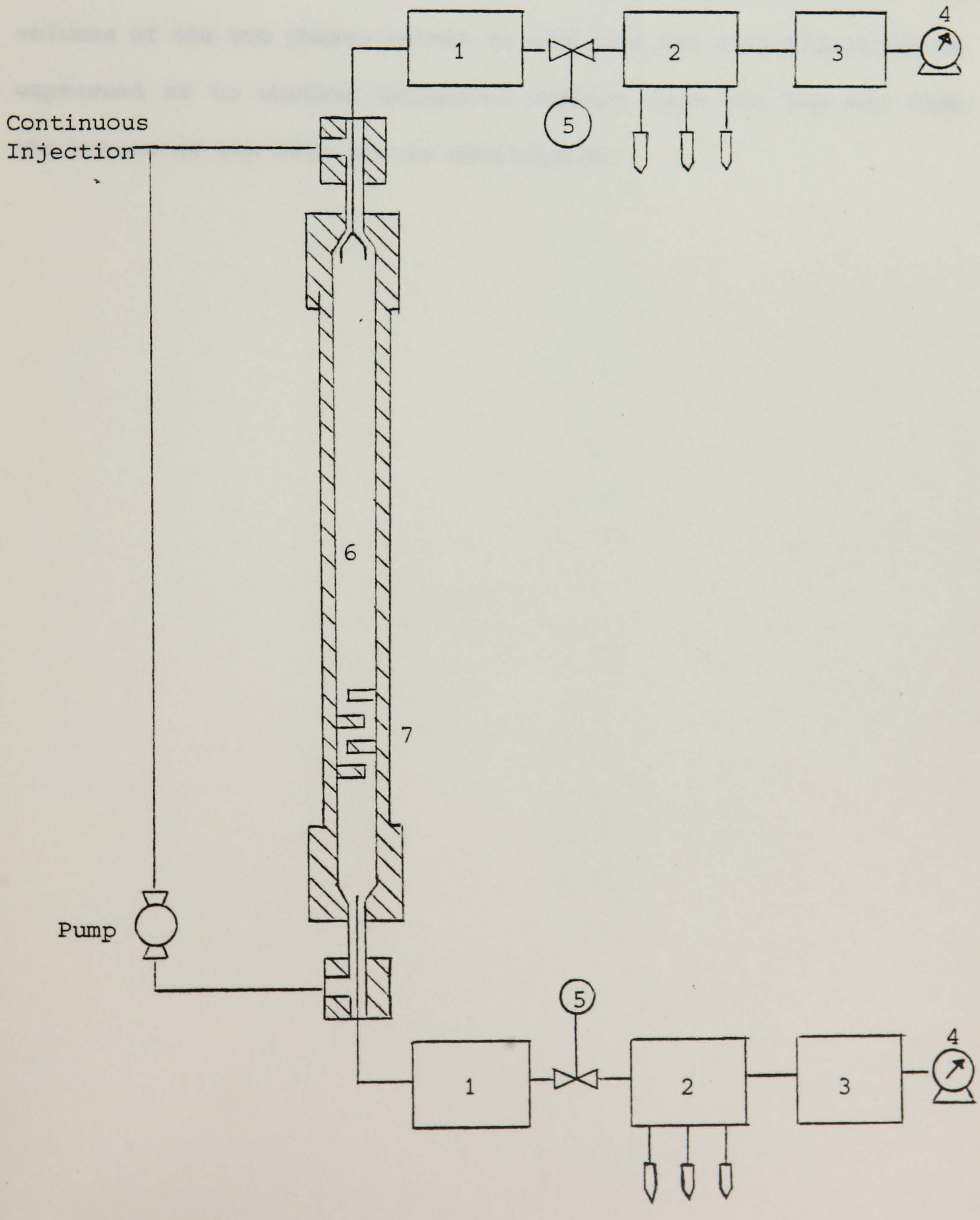

The advantage of the continuous multiple contact experiments over the static phase equilibrium ones, is that they are substantially faster because they operate continuously rather than in discrete steps, and that also an unlimited number of contacts can be simulated at the same run since there is no net loss of fluids between experiments.

As a disadvantage of the method it can be mentioned that the volumes of the two phases cannot be measured and some doubts can be expressed as to whether collected samples from the top and from the bottom of the cell are in equilibrium.

TABLE 10-1

CALIBRATION MIXTURE COMPOSITION

N-Alkane	Weight %
N-C 5	1.627
N-C 6	4.649
N-C 7	10.548
N-C 8	5.913
N-C 9	8.763
N-C 10	6.383
N-C 11	11.984
N-C 12	5.650
N-C 13	6.618
N-C 14	4.912
N-C 15	4.486
N-C 16	5.531
N-C 17	6.057
N-C 18	4.151
N-C 19	2.504
N-C 20	2.271
N-C 21	1.517
N-C 22	1.685
N-C 23	1.522
N-C 24	1.310
N-C 25	0.119
N-C 26	0.838
N-C 28	0.344
N-C 30	0.619

TABLE 10-2

RELATIVE RESPONSE FACTORS FOR HYDROCARBON C_5-C_{30}

C_5	113.34
C_6	110.65
C_7	109.89
C_8	107.90
C_9	106.59
C_{10}	104.89
C_{11}	103.53
C_{12}	101.97
C_{13}	99.85
C_{14}	100.00
C_{15}	99.52
C_{16}	98.50
C_{17}	96.60
C_{18}	95.76
C_{19}	94.86
C_{20}	92.10
C_{21}	92.17
C_{22}	88.88
C_{23}	91.53
C_{24}	88.55
C_{25}	87.00
C_{26}	85.16
C_{27}	82.00
C_{28}	78.07
C_{29}	70.00
C_{30}	63.49

TABLE 10-3

GAS CHROMATOGRAPH OPERATING CONDITIONS

Analysis	Temperature		Column	Sample Size
	Inj.port	Detector		
Liquid samples	375°C	300°C	20°C-350°C 20°C/min rate 8 min final hold	0.2µl
Gas samples	375°C	300°C	-70°C-250°C 20°C/min rate 2 min initial hold no final hold	100µl
High pressure samples	375°C	300°C	-70°-350°C 20°C/min rate 2 min initial hold 8 min final hold	4.0µl

TABLE 10-4

% MOLAR COMPOSITION OF GAS STANDARD MIXTURE

C_1	14.74
N_2	1.40
CO_2	76.76
C_2	3.20
C_3	3.05
C_4	0.52
C_5	0.33

TABLE 10-5

RELATIVE RESPONSE FACTORS FOR HYDROCARBONS C_1-C_5

Carbon Number	RRF_i
C_1	98
C_2	121
C_3	119
C_4	119
C_5	113.3

TABLE 10-6

THERMAL CONDUCTIVITY DETECTOR RESPONSE FACTORS[5]

Component	RRF_i
N_2	42
CO_2	48
C_1	35.7
C_2	51.2
C_3	64.6
C_4	85.0
C_5	105.0

TABLE 10-7

MEASURED WEIGHT % COMPOSITION OF A CALIBRATION MIXTURE USING THE DIRECT SAMPLING METHOD

Component	Actual Weight %	Calculated Composition
C_5	15.181	15.7142
C_6	12.486	12.0631
C_7	11.001	12.2016
C_8	11.034	11.3102
C_9	10.965	11.3782
C_{10}	8.201	8.3098
C_{12}	8.823	8.9413
C_{15}	8.063	7.4566
C_{16}	6.289	5.7517
C_{18}	5.183	4.3666
C_{20}	2.764	2.5067

LIST OF REFERENCES

1. Orr, R.M. Jr., Silva, M.K., Lien, C.L. and Pelletier, M.T.: "Laboratory Experiments to Evaluate Field Projects for CO_2 Flooding", SPE Paper No 9534.

2. Sigmund, P.M., Aziz, K. and Lee, J.: "Laboratory CO_2 Floods and their Computer Simulation", Proceedings of 10th World Petroleum Congress, 1979.

3. Orr, F.M. Jr., and Taber, J.J.: "Displacement of Oil by Carbon Dioxide", Final Report, March 1981.

4. Practical Gas Chromatography, Perkin-Elmer Handbook, 1973.

5. Dietz, W.A.: "Response Factors for Gas Chromatographic Analysis", J. Gas Chromatography 5, 68-71 (1967).

6. Graue, D.J. and Zana, E.: "Study of Possible CO_2 Flood in the Rangely Field, Colarado" SPE 5th Symposium on EOR, Tulsa, April 16-19, 1978.

7. Huang, e.T.S. and Tracht, J.H.: "The Displacement of Residual Oil by CO_2" SPE paper 4735,1974.

8. Peterson, A.V.: "Optimal Recovery Experiments with N_2 and CO_2", Pet. Eng. (November, 1978) 40-50.

9. Shelton, J.L. and Yarborough, L.: "Multiple Phase Behaviour in Porous Media During CO_2 or Rich Gas Flooding", J. Pet. Tech., 19 September 1977, 1171-1178.

10. Simon, R., Rosman, A. and Zana, E.: "Phase Behaviour Properties of CO_2-Reservoir Oil Systems", SPE paper No 6387, 1977.

11. Orr, F.M., Yu, A.D. and Lien, C.L.: "Phase Behaviour of CO_2 and Crude Oil in Low Temperature Reservoirs", SPE paper No 8813, 1980.

12. Henry, R.L. and Metcalfe, R.S.: "Multiple Phase Generation During CO_2 Flooding", SPE paper No 8812, 1980.

13. Menzie, D.E. and Nielsen, R.F.: "A Study of the Vapourisation of Crude Oil by CO_2 Repressuring", J. Petr. Techn., November 1963 p 1217.

14. Meldrum, A.H. and Nielsen, R.F.: "A Study of Three Phase Equilibria for CO_2-Hydrocarbon Mixtures", Produc. Monthly, August 1955.

15. Mahers, E.G. and Dawe, R.A.:
"The Role of Diffusion and Mass Transfer Phenomena in the Mobilisation of Oil During Displacement",
2nd European EOR Symposium, Paris, 1982.

16. Wang, G.C. and Knight, E.V.:
"Visual Study of Miscibility Development of CO_2-Crude Systems", 2nd European EOR Symposium, Paris, 1982.

17. Stewart, W.C. and Nielsen, R.F.:
"Phase Equilibria for Mixture of CO_2 and Several Normal Saturated Hydrocarbons",
Producers Monthly, 1954, Vol 18, 27-32.

18. Yarborough, L. and Vogel, J.:
"A New System for Obtaining Vapour and Liquid Sample Analyses to Facilitate the Study of Multicomponent Mixtures at Elevated Pressures",
Chem. Eng. Prog. Symp. Series, 1967, Vol 63 pp 1-9.

19. Stalkup, F.I.:
"Displacement of Oil by Solvent at High Water Saturation",
Soc. Pet. Eng. J. 10, December 1970, 337-348.

20. Metcalfe, R.S. and Yarborough, L.:
"Multiple Phase Behaviour in Porous Media During CO_2 or Rich-Gas Flooding",
J. Petr. Tech. 19 September 1977, 1171-1178.

21. Todd, M.R., Dietrich, J.K., Goldburg, A.J. and Larson, R.G.:
"Numerical Simulation of Competing Chemical Flood Designs",
SPE paper No 7077, 1978.

22. Gardner, J.W., Orr, F.M. and Patel, P.D.:
"The Effect of Phase Behaviour on CO_2 Flood Displacement Efficiency", SPE paper No 8367, 1979.

23. Orr, F.M. and Taber, J.J.:
"Displacement of Oil by CO_2",
Report to USDOE, November 1981.

24. "EOR and Improved Drilling Technology",
USA DOE 31 progress review, 1982.

CHAPTER 11

EXPERIMENTAL RESULTS AND SIMULATION OF THE PHASE BEHAVIOUR OF CO_2-HYDROCARBON MIXTURES

11.1 INTRODUCTION

11.2 PHASE BEHAVIOUR AND PHYSICAL PROPERTIES OF A CO_2-SYNTHETIC OIL MIXTURE

11.2.1 Saturation Pressure as a Function of CO_2 Content

11.2.2 Densities of Saturated Liquids as Function of CO_2 Content

11.2.3 Oil Phase Swelling as a Function of CO_2 Content

11.2.4 K-values Measurement

11.3 EXPERIMENTS ON A NORTH SEA STOCK TANK OIL-CO_2 MIXTURES

11.3.1 Bubble Point Pressure and Densities as a Function of CO_2 Content

11.3.2 Equilibrium Single Contacts of Oil A-CO_2 Mixtures

11.3.3 Multiple Contacts of Oil A-CO_2 Mixtures

11.3.4 Quantitative Estimation of the Hydrocarbons Distribution in the Vapour and Liquid Phase

11.1 INTRODUCTION

In order to study the change in the phase behaviour of hydrocarbon systems in contact with injection gas at reservoir conditions, a series of experiments were performed. The systems used were a synthetic oil consisting of two hydrocarbons and the stock tank oil of a North Sea reservoir.

Since the synthetic oil used contained only known pure components the heaviest of which was C_{12}, it was relatively easy to study experimentally and therefore it helped to provide valuable experience for the study of the more complicated real systems. A stock tank oil is a reservoir fluid from which all the volatile components have been stripped off and it constitutes a stabilised liquid phase at ambient temperature and atmospheric pressure. Since such an oil does not contain enough light components it cannot be miscible with carbon dioxide at reasonable pressures. Experiments on live oils were not tried due to the lack of samples. Carbon dioxide was used as the injection gas.

The change in saturation pressure, the change in the mixture's volume (swelling) as CO_2 dissolves in the liquid phase were studied, as well as the ability of CO_2 to extract hydrocarbons from the oil phase and to dissolve in the liquid phase. The experimental findings were compared against the VLE's predictions to test the accuracy of the theoretical approach, as well as to detect possible experimental errors.

11.2 PHASE BEHAVIOUR AND PHYSICAL PROPERTIES OF A CO_2-SYNTHETIC OIL MIXTURE

The synthetic oil is a two component mixture of normal alkanes with Perrocene added to the extent of 1% by mass of the final mixture. The composition of the sythetic oil is (mole fraction):

C_6 :0.1

C_{12}:0.9

The Perrocene can be used as a tracer in a future displacement study, due to the fact that it can be activated when exposed to radiation. The partition of Perrocene between the vapour and the liquid phase is of great importance for an associated displacement project. It has to remain solely in the liquid phase at the conditions of the run, to qualify as a tracer of the miscible displacement front.

The following studies were carried out for mixtures of CO_2 and synthetic oil at 60°C, to investigate experimentally the effect of carbon dioxide on the physical properties and on the phase behaviour of the two components "oil":

(i) Determination of the saturation pressure as a function of the CO_2 overall mole fraction

(ii) Measurement of the liquid phase density as a function of the CO_2 content

(iii) Measurement of the liquid phase swelling as a function of CO_2 content

(iv) Study of the partition of the components between the vapour and the liquid phase for different mixtures of CO_2 and synthetic oil and at different pressures.

These experiments were carried out in the multiple contact rig.

11.2.1 Saturation Pressure as a Function of CO_2 Content

The experiments to determine the saturation pressure of mixtures of synthetic oil and carbon dioxide were performed according to the experimental procedures outlined in Appendix III.

Measurements were taken for mixtures of different CO_2 content ranging from 0.2 up to 0.92 mole fraction. The results are given in Table 11.1. The saturation pressures were determined graphically by plotting pressure against volume data. The bubble point measurement at 0.88 mole fraction CO_2 was confirmed by visual observation of the first bubble formed on the top of the saturated liquid. A 0.92 mole fraction CO_2 mixture was studied as well, but this time by lowering the pressure, a liquid phase began to form on top of the mixture-mercury interface. A saturation pressure of 2250 psia was determined to be the dew point pressure for that composition. The 0.9 mole fraction CO_2 mixture can be regarded as approximately the critical point of the mixture.

The experimental saturation pressures as functions of the CO_2 content, are plotted in Figure 11-1 against VLE's predictions. The Peng-Robinson Equation of State was used with a default value for the interaction parameters for CO_2 and the normal alkanes, $k_{ij} = 0.1$. The predicted bubble point curve in this case underestimates the saturation pressure particularly at high CO_2 concentration. VLE's bubble point curve option, was run again using a slightly higher value for the interaction parameter ($k_{ij} = 0.11$). This time the fit on the experimental data is very good and the predicted critical point is 0.875 mole fraction CO_2. The fact that the two curves do not fit on each other all along, is thought

BUBBLE POINT CURVE FOR CO2-nC6-C12 SYNTHETIC MIXTURE
TEMPERATURE=60C P-R EOS

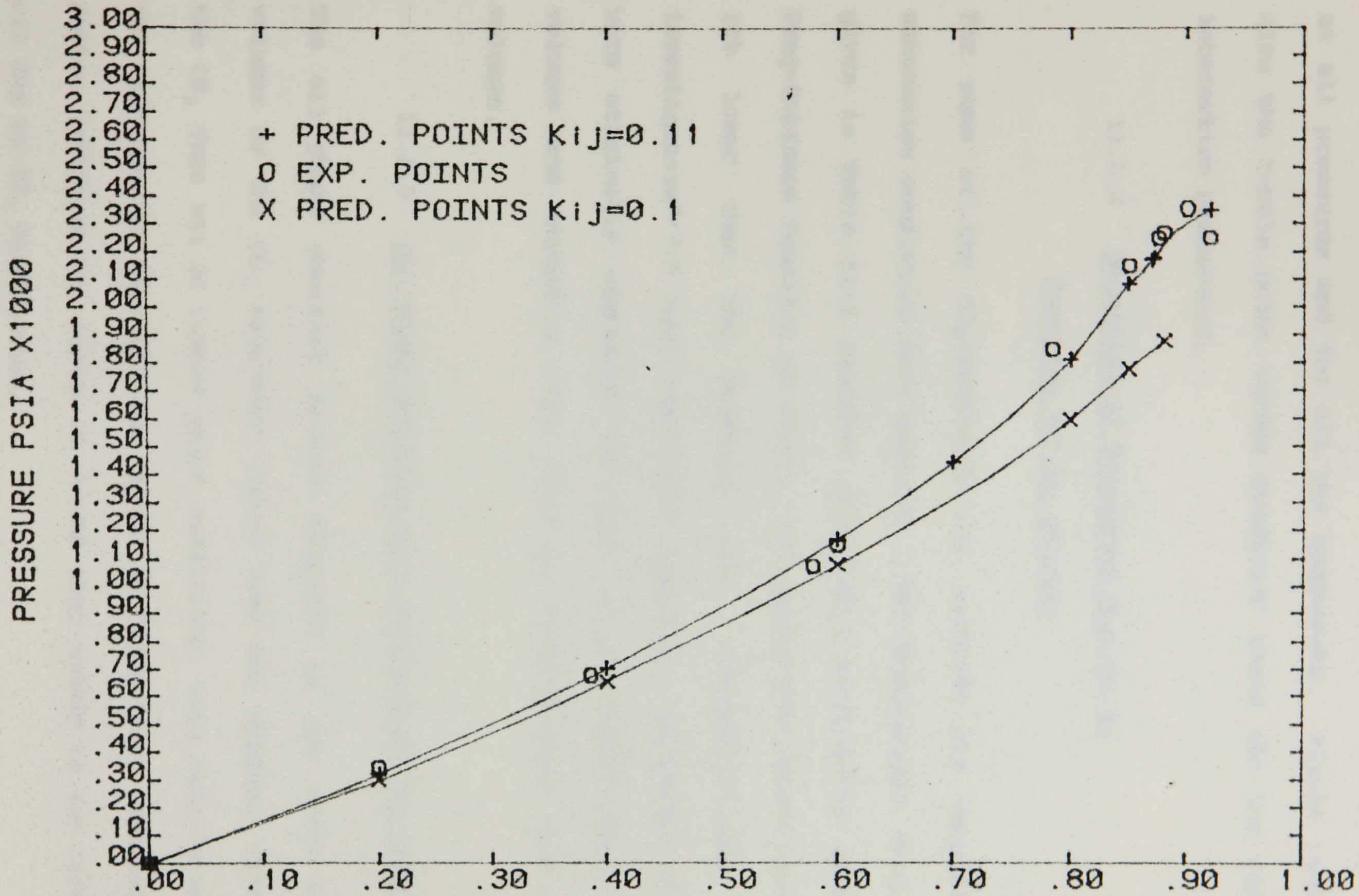

FIGURE 11-1

to be due to the constant value of the interaction parameter used at all pressures and for all the components. Figure 11-1 shows also the bubble point curves predicted using the two different interaction parameters.

11.2.2 Densities of Saturated Liquids as Function of CO_2 Content

For some of the CO_2-synthetic oil mixtures the densities at saturation conditions were measured. The experimental results are given in Table 11-2 together with VLE's predictions using the Peng-Robinson Equation of State. All calculated values are up to 10% lower than the measured ones, confirming what other investigators[2,3,4] have repeatedly reported. Equations of state were originally expressed and used to calculate vapour phase volumes and therefore they tend to underestimate the liquid volumes.

11.2.3 Oil Phase Swelling as a Function of CO_2 Content

The oil phase swelling factors regarded as the ratio of the volumes of the CO_2 saturated liquid over the original volume of the CO_2 free oil at bubble point conditions, were calculated from the experimental data and are listed in Table 11-3. The swelling factor indicates the change of volume that occurs to the reservoir oil due to CO_2 dissolution.

11.2.4 K-Value Measurements

To study the partition of the components between the vapour and the liquid phase, the K-values for specified temperature and pressure should be determined. Given volumes of the synthetic oil

and CO_2 were mixed and the resulting phases were allowed to equilibrate. Both phases were flashed to ambient after phase volumes and densities were measured. K-values information were obtained for two different CO_2-synthetic oil mixtures at 60°C.

(1) <u>80% CO_2-20% "oil" (mole), 1350 PSIA 60°C</u>

The experimentally measured liquid and vapour phase compositions together with the compositions predicted by the VLE are listed in Table 11-4. No liquid drop out was collected when the vapour phase was blown down to atmospheric conditions and for that reason, no C_{12} was measured. To be able to measure dodecane in the vapour phase a bigger sample should have been used. The Peng-Robinson Equation of State was used with the optimised value for the interaction parameter for carbon dioxide and hydrocarbons to simulate the contact. Ferrocene was given the properties of C_{14} since its boiling point is very close to the boiling point of C_{14}.

Table 11-5 gives the experimental and the predicted values for the phase densities. The vapour phase volume saturation measured was 40.5% compared with 44.18% predicted. To check the accuracy of the results the component material balance for the two phases at room conditions, was compared to the overall composition of the mixture. The results are tabulated in Table 11-6. The agreement between the predicted and measured data is regarded as very good given that in a mixture with such high CO_2 concentration, some components are present in a very small amount and therefore experimental error does not allow an exact measurement of their weight fraction. The predicted liquid phase density has been again underestimated and the material balance check agrees with the overall mixture composition.

(2) 87% CO_2-13% "oil" (Mole) 1650 PSIA 60°C

The experimentally measured liquid and vapour phase compositions are listed in Table 11-7 compared with the VLE's predictions. The experimental values for the phase densities are presented in Table 11-8 against the calculated values. The vapour phase volume saturation measured was 36.76% compared with 54% predicted. The component material balance for the two phases was compared to the overall composition of the mixture and the results are tabulated in Table 11-9.

The discrepancy between the experimental and calculated vapour phase volume is interpreted as due to the uncertainty on the volume saturations for mixtures as close to their critical point as the 87% overall CO_2 mixture under study. Figure 11-2 shows the almost vertical direction of the volume saturation lines at around the critical composition, for mixtures of a US reservoir oil and carbon dioxide[1]. A small experimental error in the volumes of the phases charged in the cell can cause a small difference in the overall composition and hence a significant error in the phase saturation. This interpretation is also reinforced by the fact that discrepancies occur as well between the calculated and measured K-values and phase densities. Around the critical region the equilibrium constants are very sensitive to composition.

11.3 EXPERIMENTS ON NORTH SEA STOCK TANK OIL-CO_2 MIXTURES

The effect of carbon dioxide on a real reservoir oil was studied on a North Sea stock tank oil which from now on will be referred to as oil A. The received sample was analysed using the Perkin Elmer F17 chromatograph. The conditions for the analysis were the ones

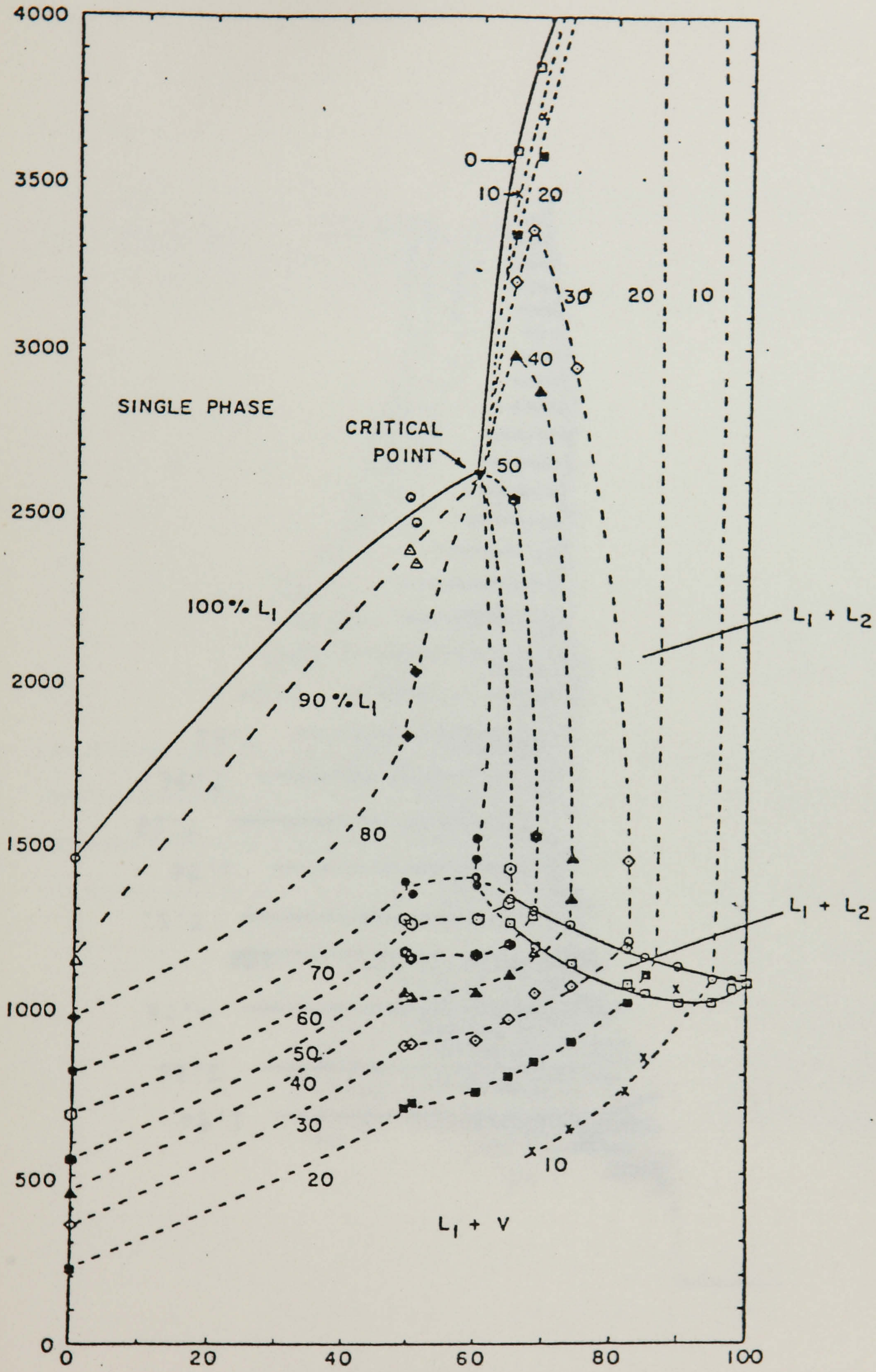

FIGURE 11-2

THREE PHASE EQUILIBRIA[23]

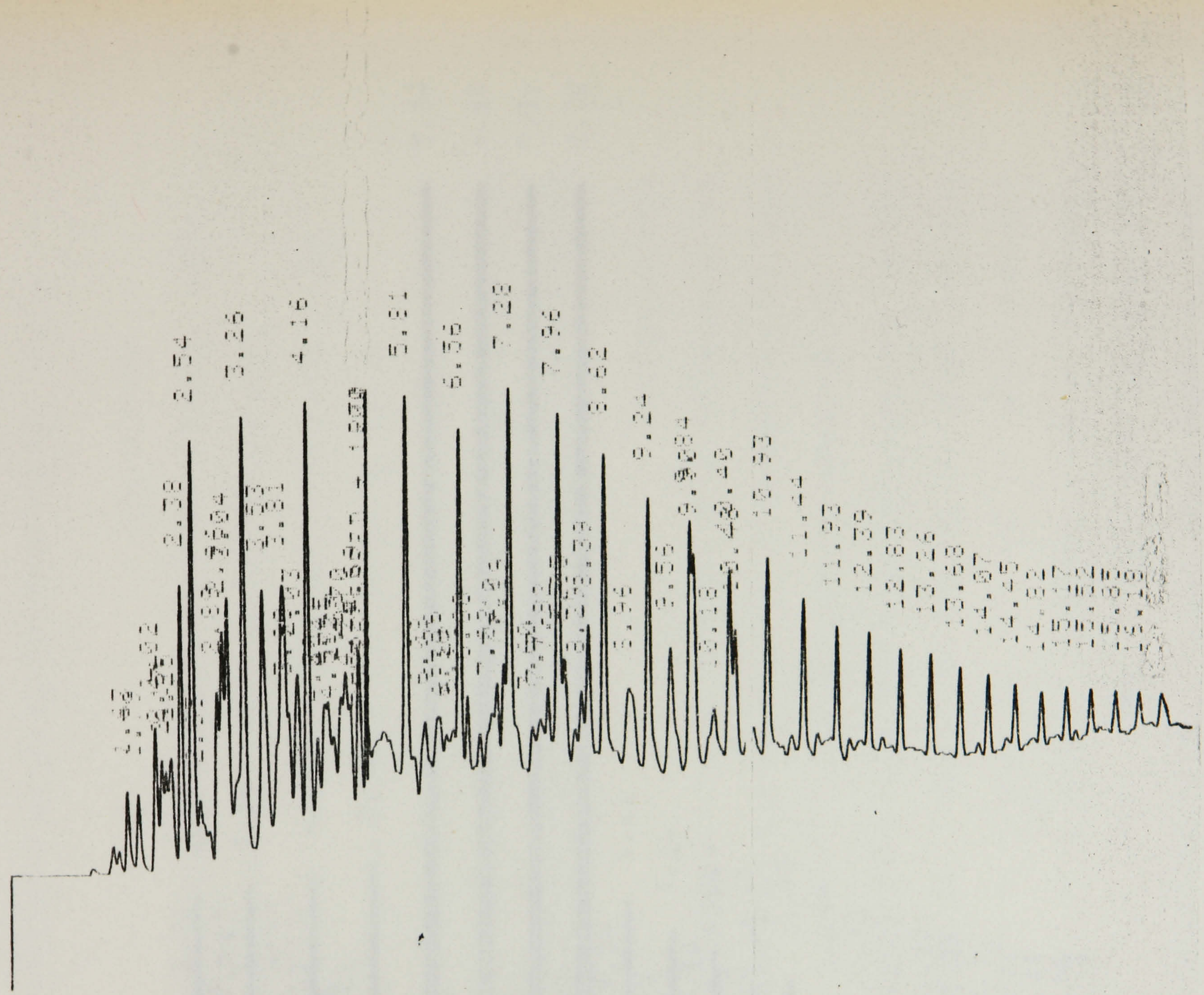

FIGURE 11-3 OIL A GAS CHROMATOGRAPHIC ANALYSIS

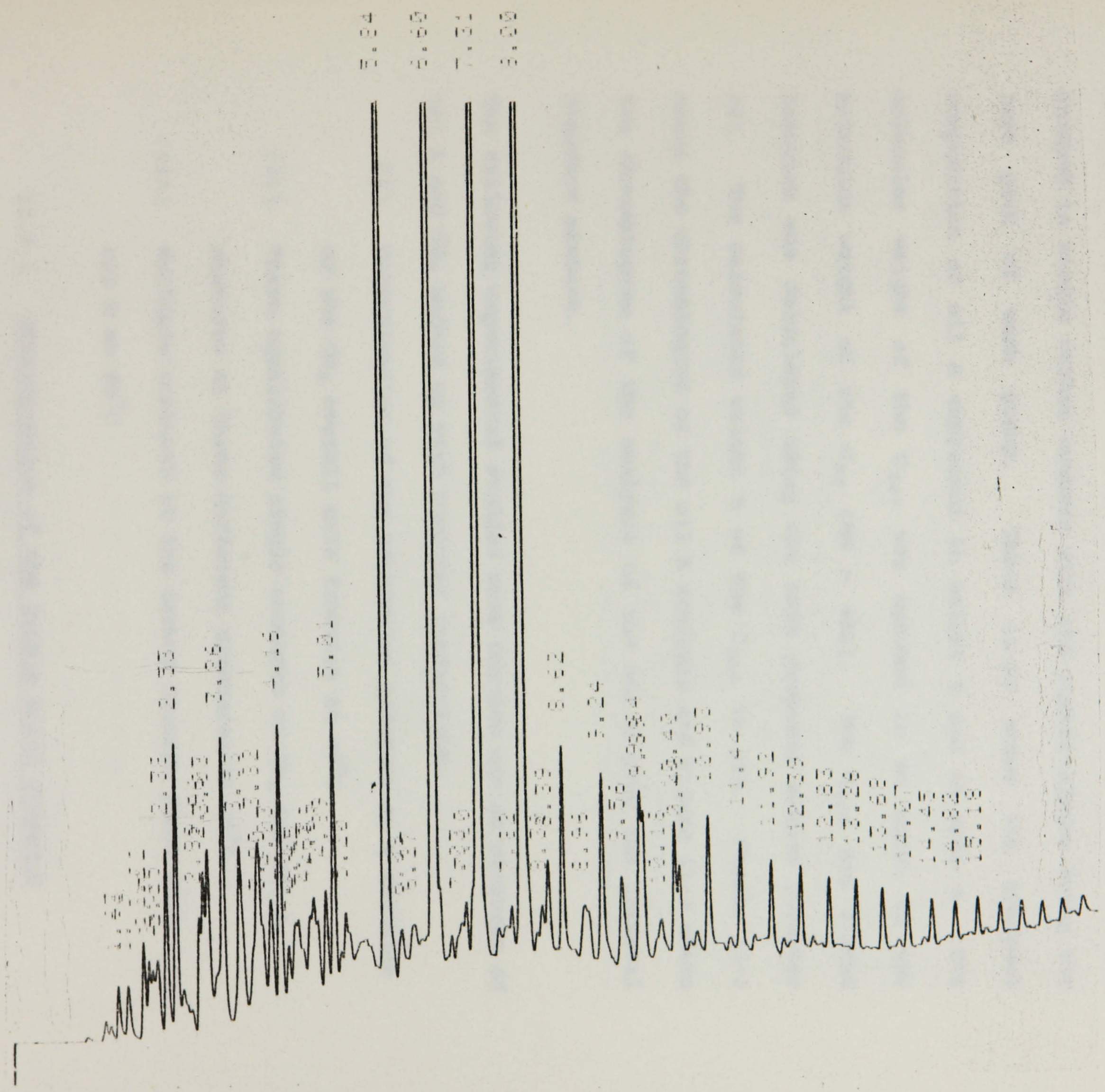

FIGURE 11-4 CHROMATOGRAM OF OIL A PLUS STANDARD MIXTURE

specified for the analysis of liquid hydrocarbon samples (Chapter 10). Horizontal baseline projection was used for the measurements of the peak areas in the chromatogram. The hydrocarbons were grouped in single carbon numbers with the normal alkane being the last peak of each group. Table 11-10 shows the analysed composition of oil A expressed in weight % and in mole %. The molecular weight of the C_{30+} was assumed to be equal to the molecular weight of the C_{35} (MW = 492). The C_{30+} non eluted fraction was calculated using the ASTM proposed method (Chapter 10). The calculated weight % of the C_{30+} is 33%. Figure 11-3 shows the chromatogram of the oil A analysis and Figure 11-4 shows the chromatogram of the analysis of the oil A plus the internal standard mixture.

The following experimental studies were carried out on mixtures of oil A and CO_2 backed up with computer predictions:

(i) Determination of the saturation pressure as a function of the CO_2 overall mole fraction at 80°C

(ii) Three equilibrium single contacts of CO_2 and oil A mixtures at three different pressures at 80°C

(iii) Multiple contacts of the carbon dioxide phase with oil A at 80°C

11.3.1 Determination of the Bubble Point Pressure and Saturation Density as a Function of CO_2 Content at 80° C

The experiments to determine the bubble point pressure of mixtures of oil A and carbon dioxide were performed according to the experimental procedures outlined in Appendix III.

The bubble point pressure was measured for nine different CO_2 overall mole fractions. The results are presented in Table 11-11. For a few CO_2-oil A saturated mixtures, the density at the conditions of the experiment was measured. The results are given in Table 11-12.

To use the phase behaviour simulator to predict the saturation data for the mixtures of CO_2 and oil A, the extended chromatographic analysis of the oil (11.2) had to be reduced to a total number of 14 components; 10 pure hydrocarbons C_5-C_{14}, and four pseudocomponents C_{15}-C_{20}, C_{21}-C_{24}, C_{25}-C_{30} and C_{30+}. Three different methods were tried to tune the Peng-Robinson EOS to match the experimental data of the saturation pressures and densities.

(i) T_{CMOD}, P_{CMOD} coefficients were used to alter the critical properties of all four pseudocomponents after their values have been predicted from Cavett's correlations.

(ii) T_{CMOD}, P_{CMOD} coefficients were used to alter the critical properties of only the heaviest pseudo component; the other pseudos' P_C and T_C were given the values calculated from the correlations.

(iii) T_{CMOD}, P_{CMOD} coefficients equal to 1.0 were used. The values of the boiling point (BP), molecular weight (MW) and specific gravity (SG) of the heaviest pseudocomponent were altered and Cavett's correlations were used to calculate the critical properties of the pseudocomponents.

(i) Katz-Firoozabadi's tables were used to obtain the values for the SG of the four pseudocomponents using the molecular weights and boiling points calculated from chromatography. These values are given in Table 11-13. Bergman's correlations gave the values for the critical properties and the acentric factors of the pseudos presented in Table 11-14. These values failed to match the experimentally predicted liquid density (0.685 gr/cc compared with 0.819 gr/cc experimental for 0.27 CO_2 overall mole fraction, 500 psia and 80°C). After various runs where the T_{CMOD} and P_{CMOD} were given different values the following conclusions were reached:

(1) An increase on either the critical temperature or the critical pressure of the pseudocomponents, causes an increase in the saturation pressure of the mixture.

(2) An increase in the critical temperature of the pseudocomponents causes a decrease in the liquid density, whereas an increase in the critical pressure increases the saturation density.

Due to the fact that the predicted density had to be corrected upwards, the critical temperature was decreased and the critical pressure was increased. This combined action had as an effect a substantial increase of the saturation density while the bubble point pressure was changed only slightly. The optimum values found for T_{CMOD} and P_{CMOD} were

$$T_{CMOD} = 0.86 \qquad P_{CMOD} = 1.18$$

The critical properties and the acentric factors of the pseudos that match the experimental saturation pressures and densities are given in Table 11-15. The predicted bubble point curve for oil A

and CO_2 mixtures after matching, is shown in Figure 11-5, where the predicted values are compared to the experimental data. An interaction coefficient value of 0.12 was used for CO_2 and the pseudocomponents. The value of this parameter affects the slope of the latest part of the curve. For carbon dioxide and pure hydrocarbons, the value of k_{ij} used was 0.1.

The predicted critical point of the mixture is 7782 psia at 0.872 overall CO_2 mole fraction. The slope of the curve in the vicinity of the critical point in Figure 12-5, indicates how sensitive to composition the saturation pressure is around the critical region.

The calculated saturation densities are listed together with the experimental values in Table 11-12 and in general, there is a close agreement between them. Because the EOS was tuned to match the saturated liquid density for 0.27 CO_2 overall mole fraction only, the density predictions further along the bubble point curve are slightly off the laboratory values. This implies that for the Peng-Robinson EOS a single density matching point is not enough to ensure accurate predictions over a wide range of pressure and composition.

(ii) All the efforts to match the experimental data by altering only the critical properties of the heaviest pseudocomponent were unsuccessful.

(iii) Default values of 1.0 were used for T_{CMOD} and P_{CMOD}. The boiling point, specific gravity and molecular weight of the heaviest pseudocomponent were altered and Cavett's correlations were used to predict the critical properties. The best combination of values for C_{30+} were found to be:

BUBBLE POINT CURVE FOR OIL A-CO_2 MIXTURE
TEMPERATURE=80C P-R EOS

FIGURE 11-5

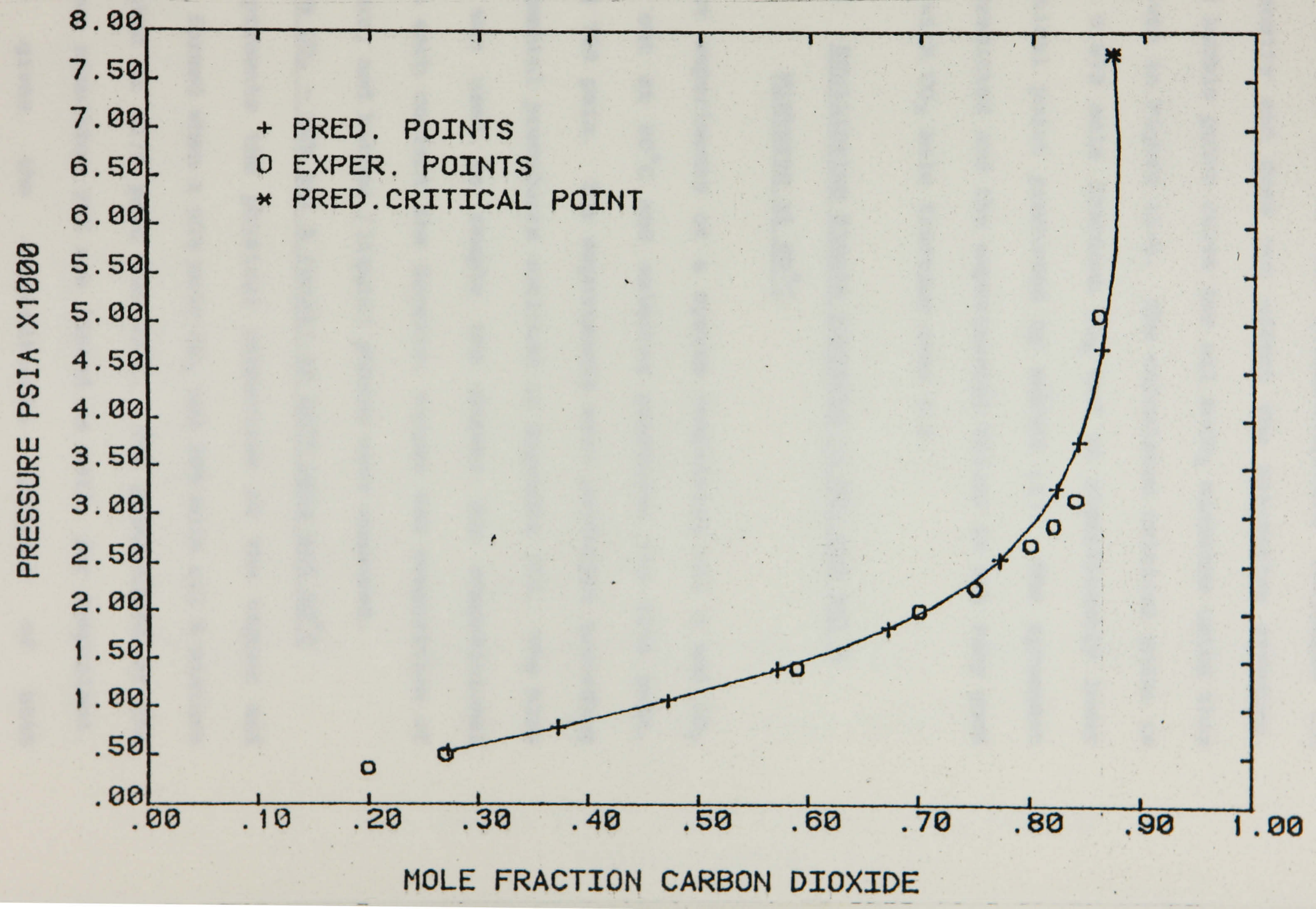

BP = 890°F, SG = 0.89, MW = 800.0

An increase in the MW of the pseudocomponent increases the saturation density and does not affect the saturation pressure. The predicted bubble point curve for oil A–CO_2 mixtures using this method, is given in Figure 11-6. The calculated critical point is 5385 psia at 0.873 mole fraction CO_2 and is significantly lower than the critical point predicted by method (i). The agreement between the predicted and the experimental values is not very good for mixtures with CO_2 mole fraction over 0.8.

11.3.2 Equilibrium Single Contacts of CO_2 and oil A Mixtures at 80°C

Single contact experiments of a system comprising oil A and CO_2 were carried out at 80°C and selected pressures viz 2175 psia, 1455 psia and 725 psia. The experiments were performed according to the experimental procedures outlined in Appendix III. The blow down method was used to sample the phases for compositional analysis. In each contact the density, volume and composition of the top (vapour) and bottom (liquid) phases were measured.

(1) 80% CO_2 - 20% oil A (mole) at 2175 psia and 80°C

Table 11-16 presents the physical properties of the vapour and liquid phases formed when a 80% mole CO_2 and 20% mole oil A mixture was equilibrated at 2175 psia and 80°C. The predictions of the phase behaviour simulator VLE are listed as well, for comparison. Table 11-17 gives the compositional analysis of both phases, experimental and calculated values. Table 11-18 presents the material balance check on the component's overall mole fractions.

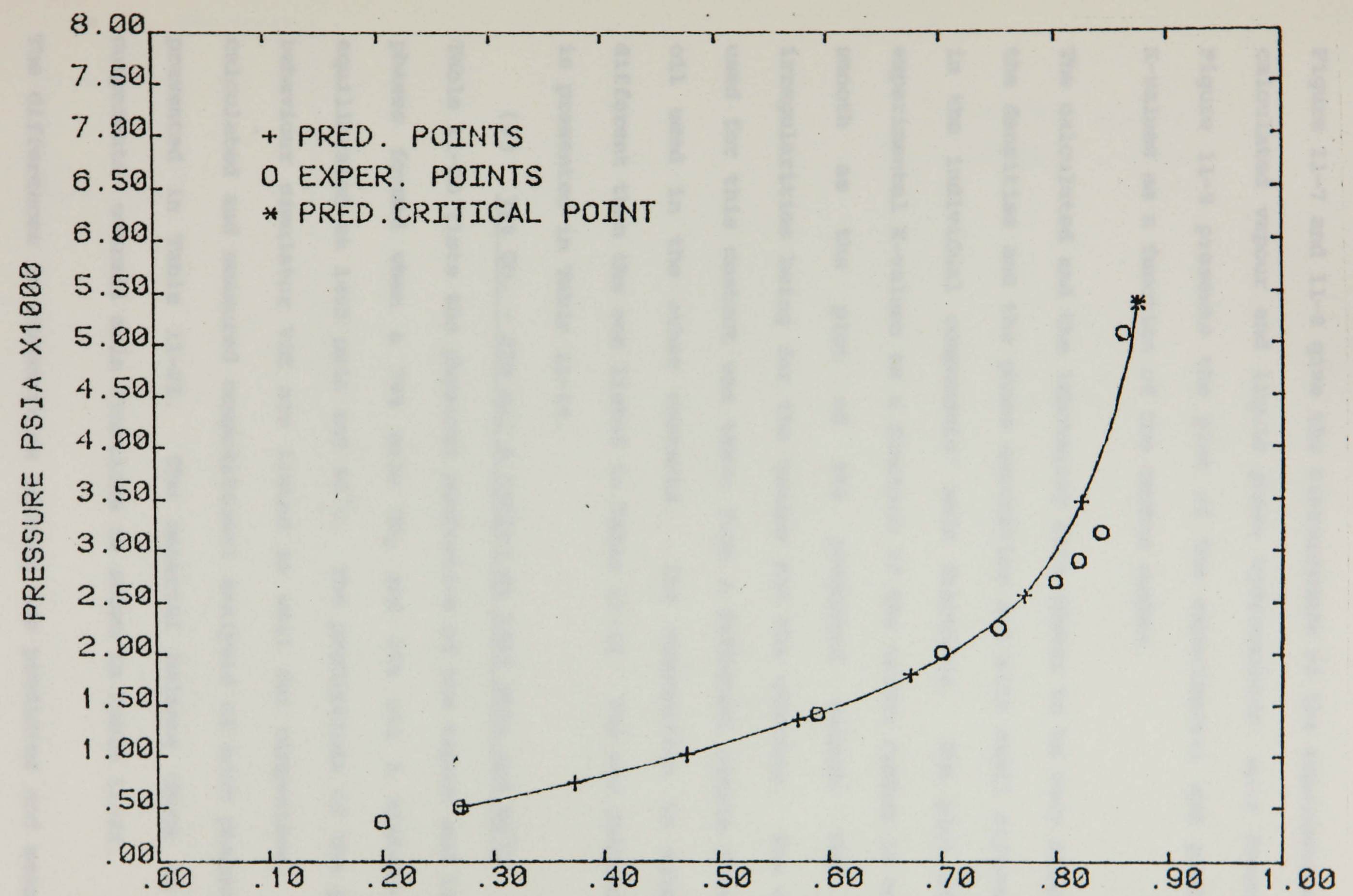

FIGURE 11-6

BUBBLE POINT CURVE FOR OIL A-CO_2 MIXTURE
TEMPERATURE=80C P-R EOS

Figure 11-7 and 11-8 give the histogrammes of the experimental and calculated vapour and liquid phase hydrocarbons' mole fractions. Figure 11-9 presents the plot of the experimental and predicted K-values as a function of the carbon number.

The calculated and the laboratory data appear to be very close for the densities and the phase saturation and with small differences in the individual components' mole fractions. The plot of the experimental K-values as a function of the carbon number is not as smooth as the plot of the predicted values; the main irregularities being for the hexane and the undecane. The oil A used for this contact was taken from a different sample than the oil used in the other contacts. Its composition is slightly different than the one listed in Table 11-10. The new composition is presented in Table 11-19.

(2) <u>78% CO_2 - 22% oil A (mole) at 1455 psia and 80°C</u>

Table 11-20 lists the physical properties of the vapour and liquid phases formed when a 78% mole CO_2 and 22% oil A mixture was equilibrated at 1455 psia and 80°C. The predictions of the phase behaviour simulator VLE are listed as well for comparison. The calculated and measured compositional analysis of both phases are presented in Table 11-21. The material balance check on the components' overall mole fractions is shown in Table 11-22.

The differences in composition between the predicted and measured liquid and vapour phases are attributed to an error in the measurement of the CO_2 volume eluted when each phase was flashed to the atmosphere. For that contact a gas wetmeter was used and given the CO_2 solubility in water and the reduced accuracy of the device at high gas rates, an underestimation of the eluted CO_2 can

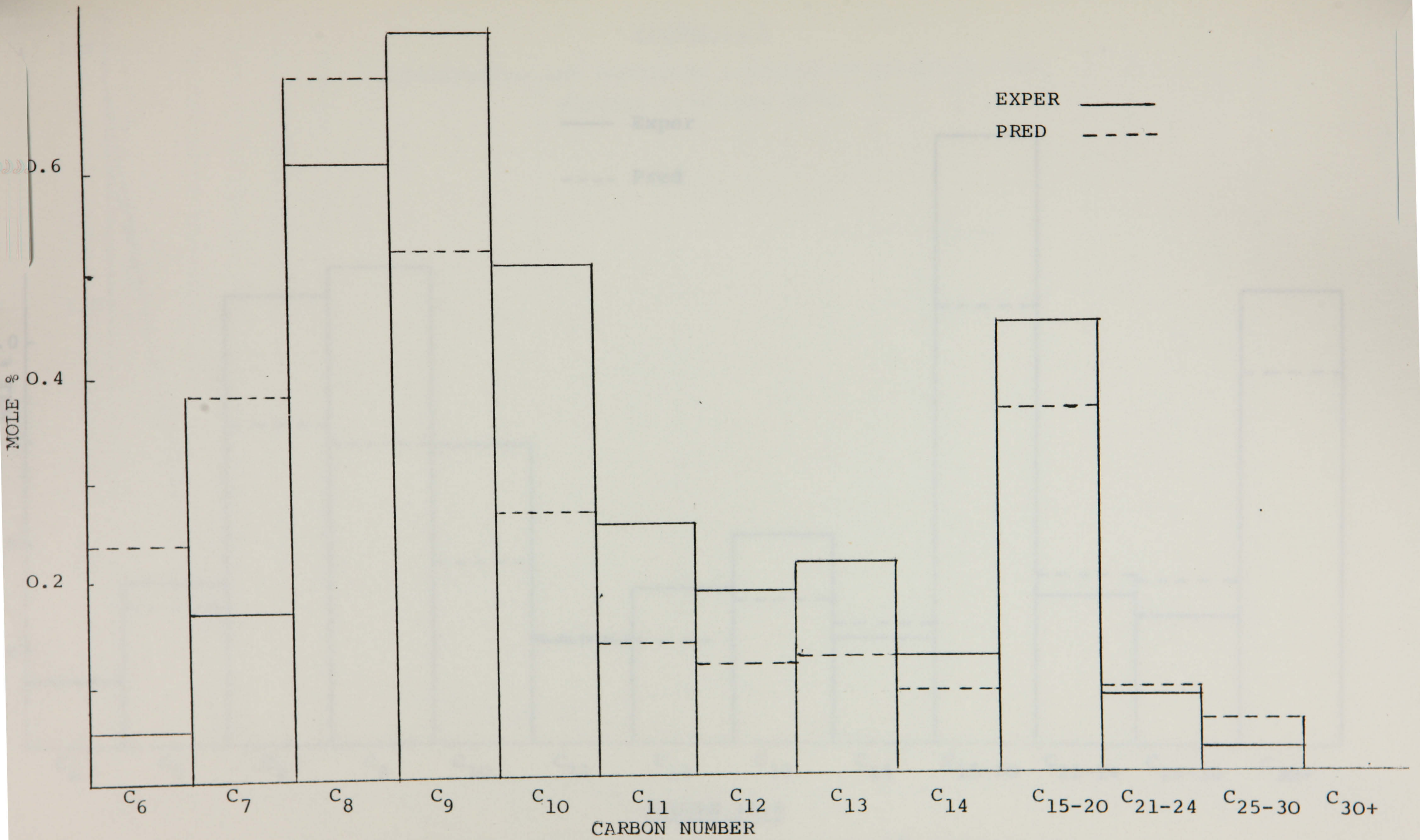

FIGURE 11-7 OIL A - CO_2 MIXTURE (80% MOLE) 2175PSI 80°C UPPER PHASE

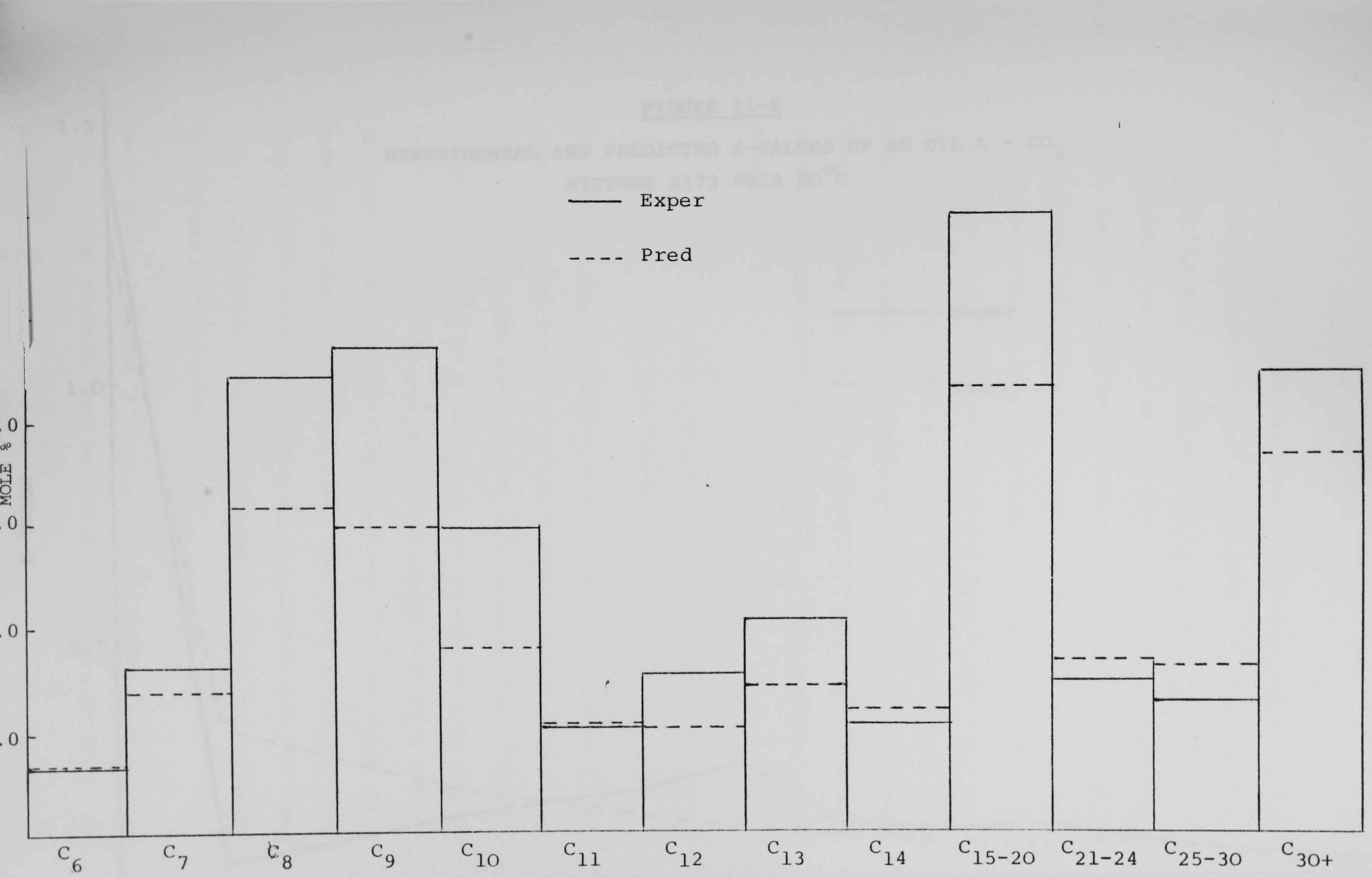

FIGURE 11-8

OIL A - CO_2 MIXTURE (80% MOLE) 2175 PSI 80°C LOWER PHASE

FIGURE 11-9

EXPERIMENTAL AND PREDICTED K-VALUES OF AN OIL A - CO_2 MIXTURE 2175 PSIA 80°C

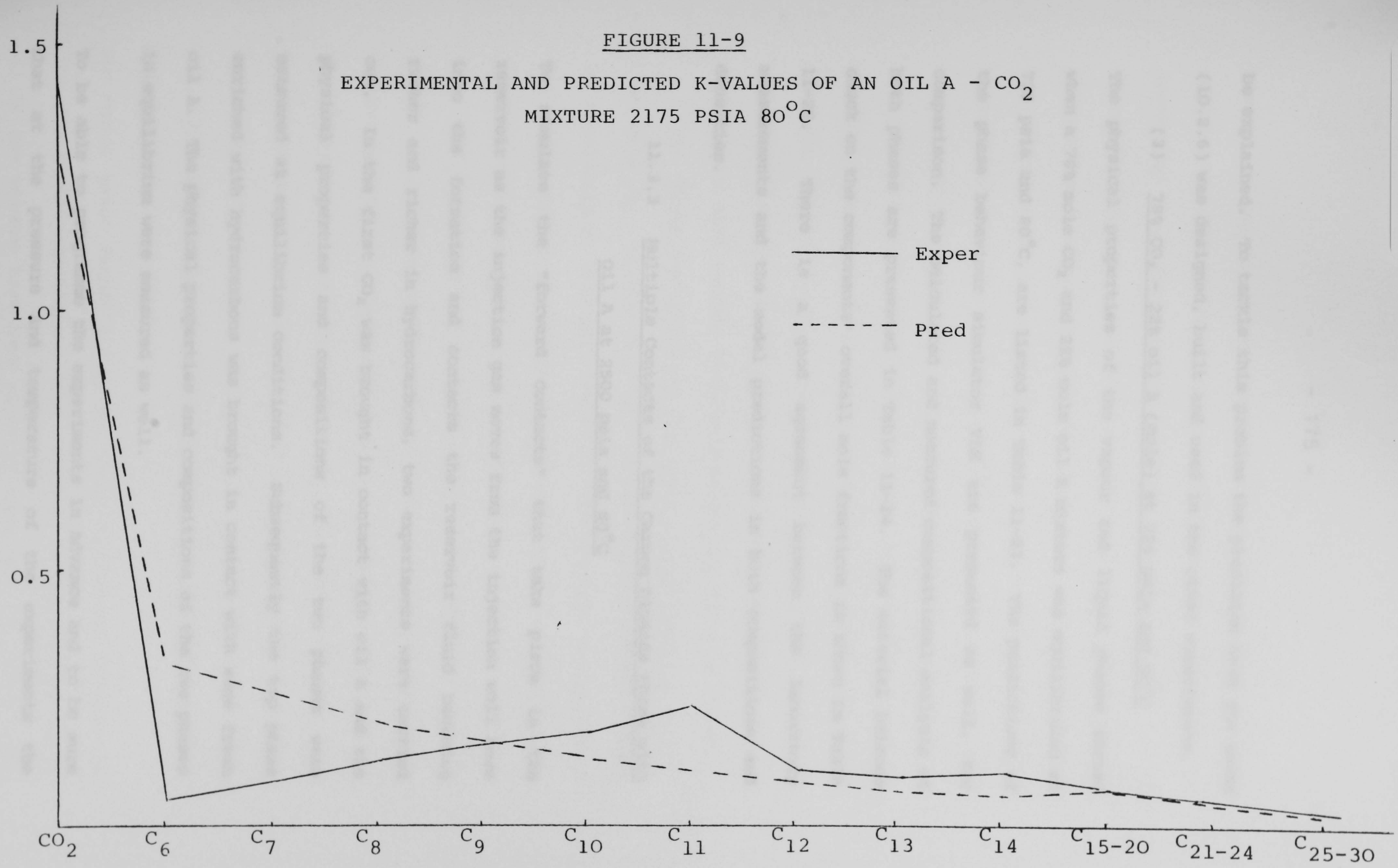

be explained. To tackle this problem the precision bore gas meter (10.2.6) was designed, built and used in the other experiments.

(3) 78% CO_2 - 22% oil A (mole) at 725 psia and 80°C

The physical properties of the vapour and liquid phases formed when a 78% mole CO_2 and 22% mole oil A mixture was equilibrated at 725 psia and 80°C, are listed in Table 11-23. The predictions of the phase behaviour simulator VLE are presented as well, for comparison. The calculated and measured compositional analysis of both phases are presented in Table 11-24. The material balance check on the components' overall mole fractions is shown in Table 11-25. There is a good agreement between the laboratory measurements and the model predictions in both compositions and densities.

11.3.3 Multiple Contacts of the Carbon Dioxide Phase with Oil A at 2500 psia and 80°C

To simulate the "forward contacts" that take place in the reservoir as the injection gas moves from the injection well bore into the formation and contacts the reservoir fluid becoming richer and richer in hydrocarbons, two experiments were carried out. In the first CO_2 was brought in contact with oil A and the physical properties and compositions of the two phases were measured at equilibrium conditions. Subsequently the top phase enriched with hydrocarbons was brought in contact with some fresh oil A. The physical properties and compositions of the two phases in equilibrium were measured as well.

To be able to programme the experiments in advance and to be sure that at the pressure and temperature of the experiments the

mixture charged in the equilibrium cell will be in the two phase region, the VLE phase behaviour simulator was run using the previously tuned Peng-Robinson equation of state, to predict the phase envelope of the system at 2500 psia and 80°C which is presented on a ternary diagram (Figure 11-10). In the same Figure the dashed area indicates the locus of the reservoir fluid compositions that can be miscible with the carbon dioxide at 2500 psia and 80°C (Chapter 4). Oil's A composition indicated by A, lies clearly outside the miscible area and therefore it can not be miscible with CO_2 at the conditions noted previously. When the oil A-CO_2 mixture becomes rich enough in C_5 - C_{14} hydrocarbons so that the extension of its tie-line will pass through the oil A composition, then further enrichment of the top phase is halted.

(1) <u>First contact of CO_2 and oil A at 2500 psia and 80°C</u>

A 92% mole CO_2 - 8% mole oil A mixture was prepared and was brought in equilibrium at 2500 psia and 80°C. The physical properties of the vapour and liquid phases formed are listed in Table 11-26 together with the predictions of the phase behaviour simulator VLE. The calculated and measured compositional analysis of both phases are presented in Table 11-27. The material balance check on the components' overall mole fractions is shown in Table 11-28. The agreement between the laboratory and the predicted data appears to be very good for the phase densities as well as for the compositions.

(2) <u>Second contact of the CO_2 rich phase and oil A at 2500 psia and 80°C</u>

The vapour phase formed during the first contact was transferred into the second equilibrium cell, where it contacted some fresh oil A; the volumes have been adjusted such that the overall CO_2

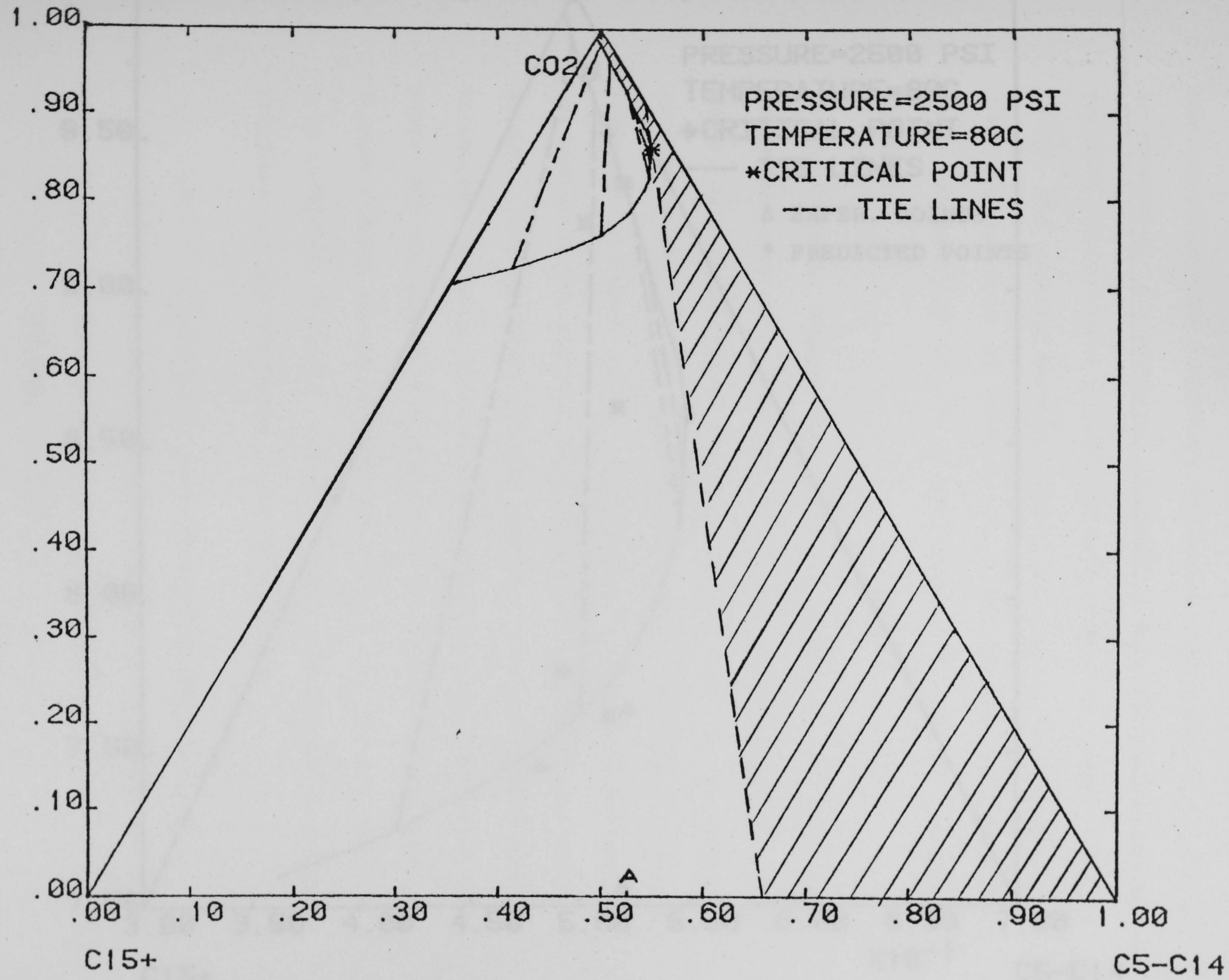

FIGURE 11-10 TERNARY DIAGRAM FOR OIL A - CO_2 MIXTURE

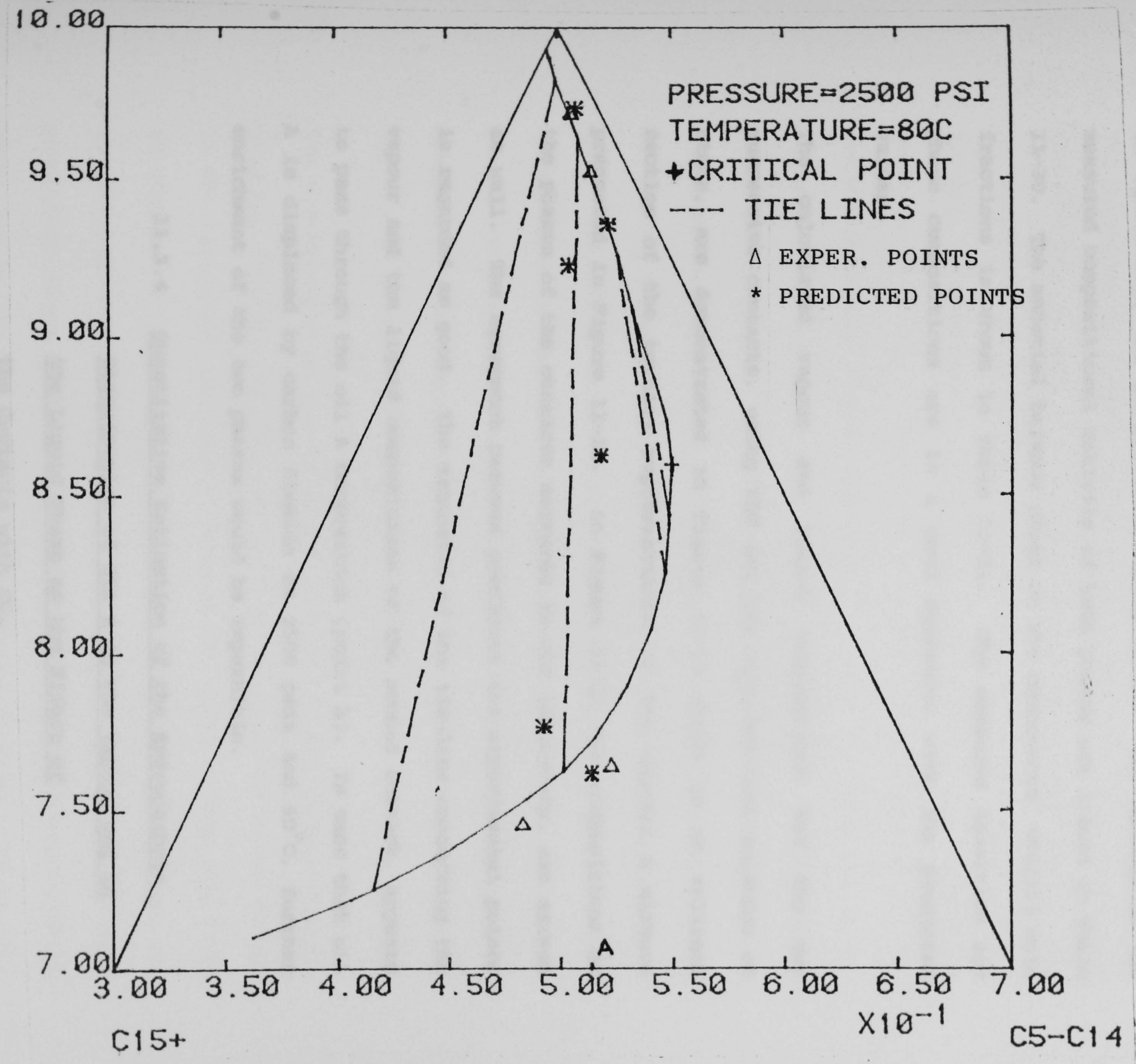

FIGURE 11-11 TERNARY DIAGRAM FOR OIL A - CO2 MIXTURE

mole fraction in the mixture would be 0.86. The measured and calculated physical properties of the new vapour and liquid phases in equilbrium, are presented in Table 11-29. The calculated and measured compositional analysis of both phases are listed in Table 11-30. The material balance check on the components' overall mole fractions is shown in Table 11-31. The measured densities and phase compositions are in a good agreement with the predicted values.

The calculated vapour and liquid compositions for the two successive contacts, using VLE and the Peng-Robinson equation of state, are demonstrated in Figure 11-11 which is an enlarged section of the ternary representation of the CO_2-oil A mixture presented in Figure 11-10. In Figure 11-11 the compositions of the phases of the contacts measured in the laboratory, are marked as well. The agreement between predicted and experimental points is regarded as good. The extension of the tie-line connecting the vapour and the liquid compositions of the second contact, appears to pass through the oil A composition (point A). In case that oil A is displaced by carbon dioxide at 2500 psia and 80°C, further enrichment of the two phases would be impossible.

11.3.4 Quantitative Estimation of the Hydrocarbons Distribution of Oil A in the Vapour and in the Liquid Phase as the Effect of the Contacts with CO_2

The mass transfer of light and intermediate hydrocarbons from the oil phase to the advancing injection gas phase, is what makes a gas injection flooding attractive for the recovery of the oil that

remains trapped in the reservoir and cannot be produced by waterflooding.

The experimental results presented in 11.3.3 were used to estimate the mobility of each single carbon number group among phases, and in particular to study how the composition of each group of the ternary representation (C_5–C_{14}, C_{15+}), changes with successive contacts with CO_2. Figure 11-12 gives the histogramme of the molar composition of each component in the C_6–C_{14} group for oil A. Figures 11-13 and 11-14 show the same histogramme for the vapour phase of the first and of the second contact. As expected, the contribution of the light hydrocarbons C_6–C_9 in the group C_6–C_{14} of the CO_2 phase is increasing as the injection gas contacts more oil. Figures 11-15 and 11-16 give the histogramme of the molar composition of each component in the C_6–C_{14} group for the liquid phases of the first and of the second contact respectively. Remarkably, the carbon dioxide strips hydrocarbons as high as C_{11}–C_{14} as it makes more contacts with oil A.

The histogrammes of the molar composition of each pseudocomponent (C_{15}–C_{20}, C_{21}–C_{24}, C_{25}–C_{30} and C_{30+}) in the C_{15+} cut in oil A, and in the liquid and the vapour phase of the first contact are given in Figures 11-17, 11-18, 11-19. The C_{15+} in the original oil consists of about 38% of the pseudocomponent C_{15}–C_{20} while this percentage rises to almost 50% in the vapour phase and drops to about 25% in the liquid phase of the first contact. The C_{21}–C_{24} mole fraction in the liquid phase remains almost the same as in oil A, while the C_{25}–C_{30} and C_{30+} mole percentages are raised (17% against 15% and 47% compared with 33%). Figure 11-20 presents the same histogramme for the C_{15+}, in the second contact's overall

composition. This appears to be almost identical with oil A's components distribution (Figure 11-17). The C_{15}-C_{20} percentage is slightly higher this time, due to the fact that the vapour phase has carried some intermediate hydrocarbons from the first contact. Figures 11-21 and 11-22 provide the histogrammes of the molar compositions of the four pseudocomponents in C_{15+}, for the liquid and the vapour phase of the second contact. The main characteristic of this contact is that the C_{25}-C_{30} contribution in C_{15+}, rises in the vapour phase in comparison with the same percentage in the vapour phase of the first contact.

Finally, Figure 11-23 demonstrates what values the molar ratio C_6-C_{14}/C_{15+} takes in the different phases of the different contacts. Starting from a value of around 1.0 (oil A) it reaches at 3.5 (Vapour phase - First contact) and 6.2 (Vapour phase - Second contact). The same ratio in the liquid phases, changes very little.

Figures 11-12, 11-13, 11-14, 11-15, 11-16, 11-17, 11-18, 11-19, 11-20, demonstrate how approximate the results will be, in case that a multicomponent mixture's phase behaviour is simulated using a reduced compositional representation. Such representation considers that at any time the ratios of the single carbon number hydrocarbons remain the same in the lumped pseudocomponent, where they have been grouped. The above Figures suggest that obviously this is not the case, when an injection gas is mixed with the reservoir fluid in a miscible displacement, and more pseudocomponents should be chosen to characterise the oil mixture.

FIGURE 11-12

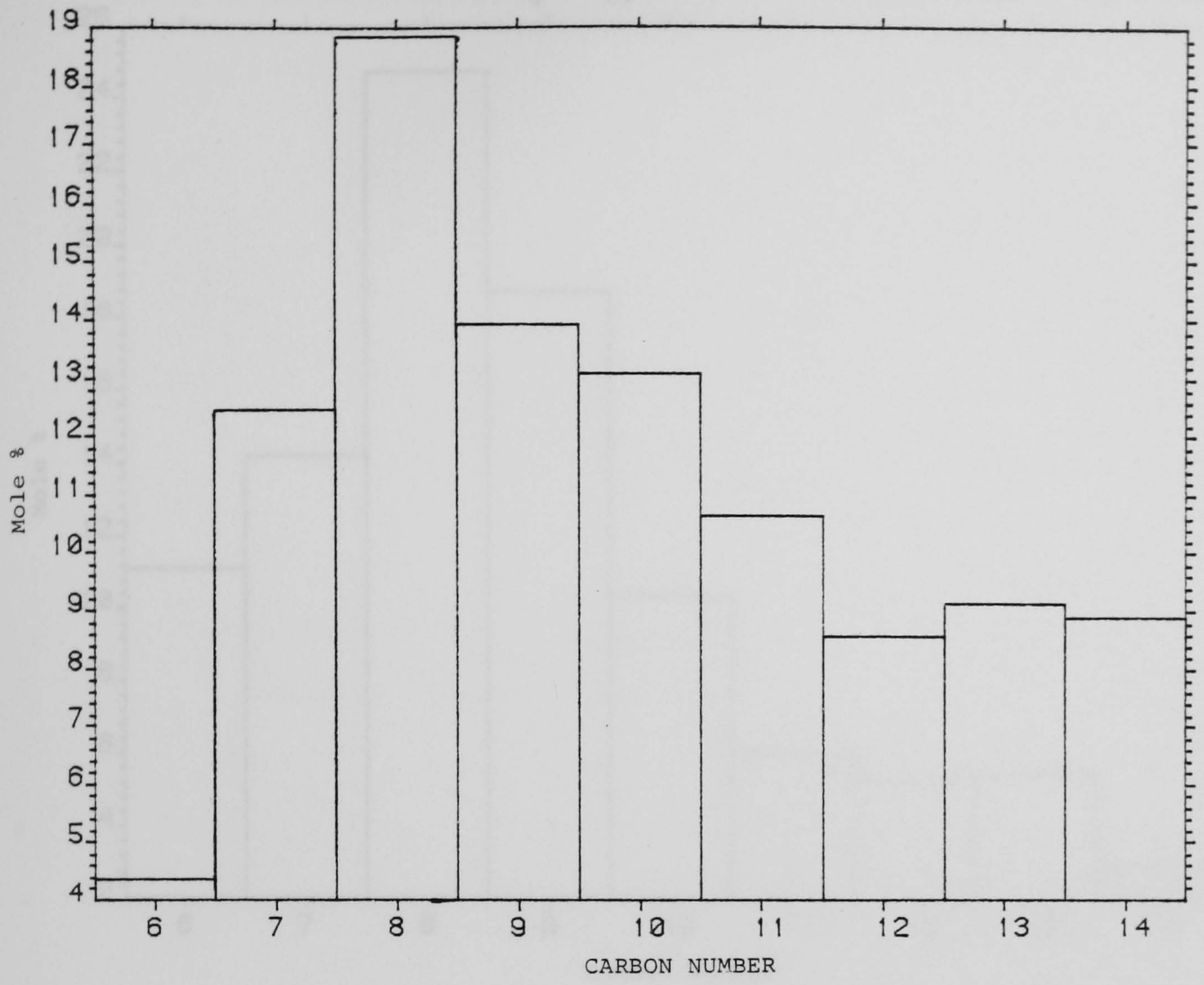

FIGURE 11-13

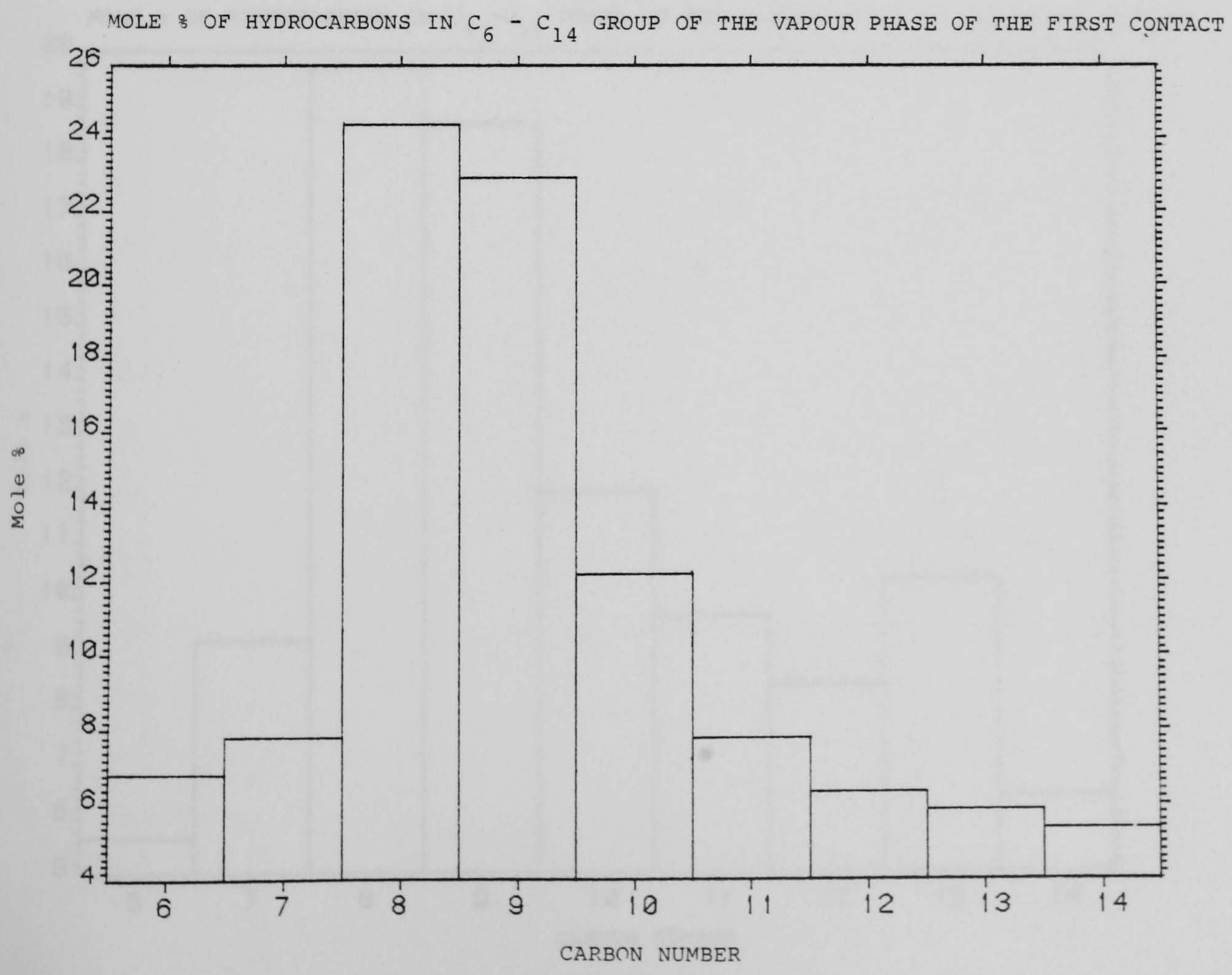

FIGURE 11-14

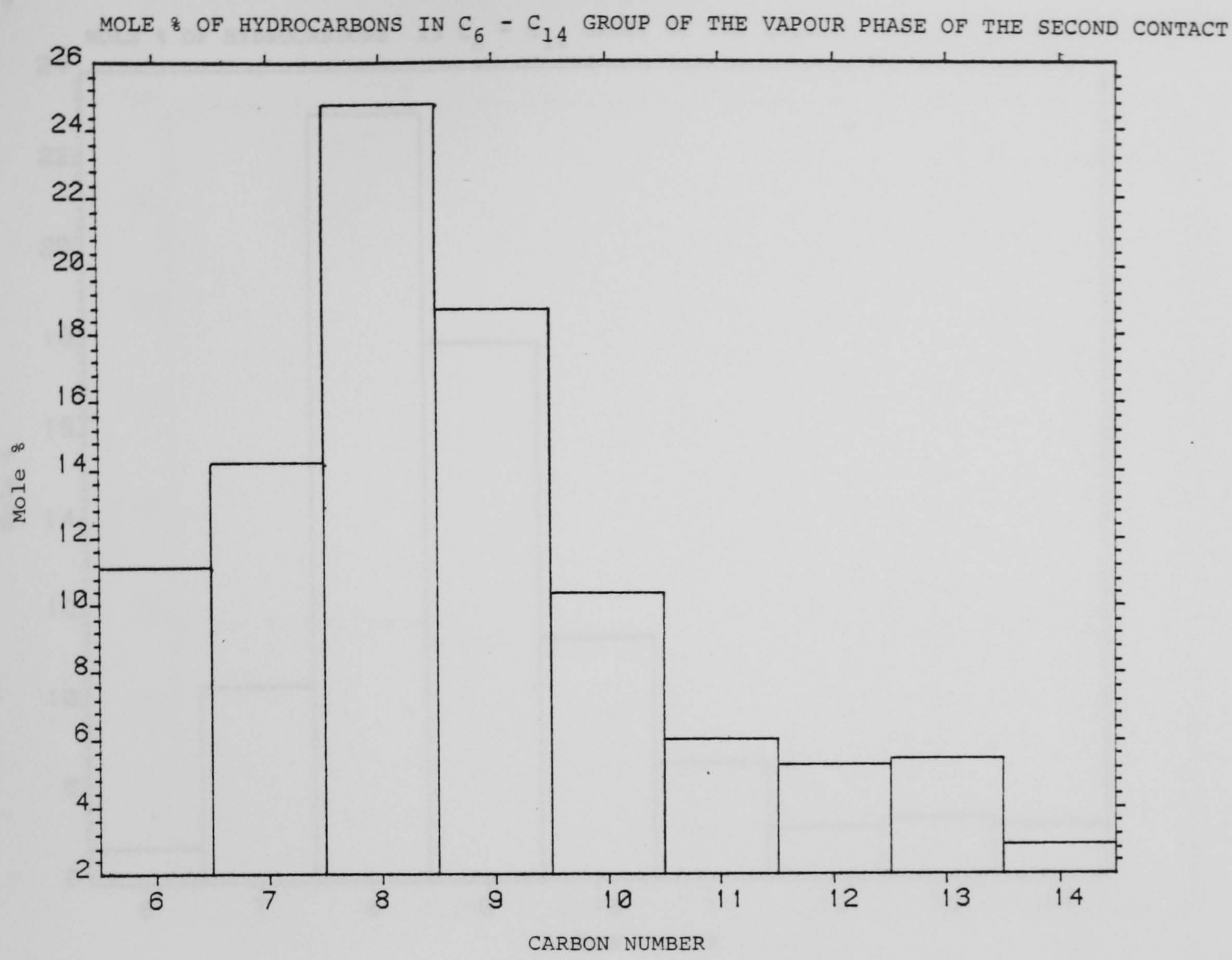

FIGURE 11-15

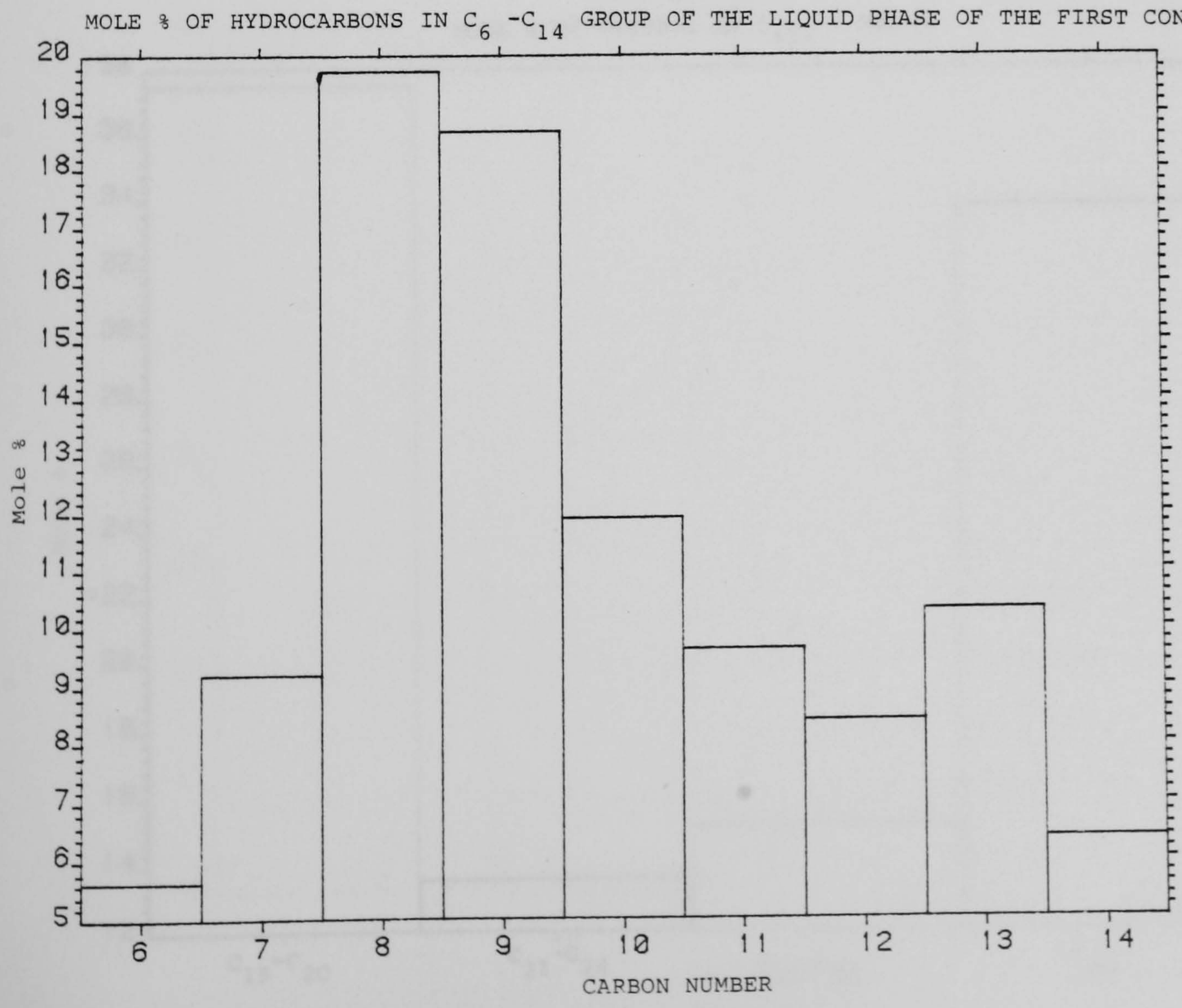

FIGURE 11-16

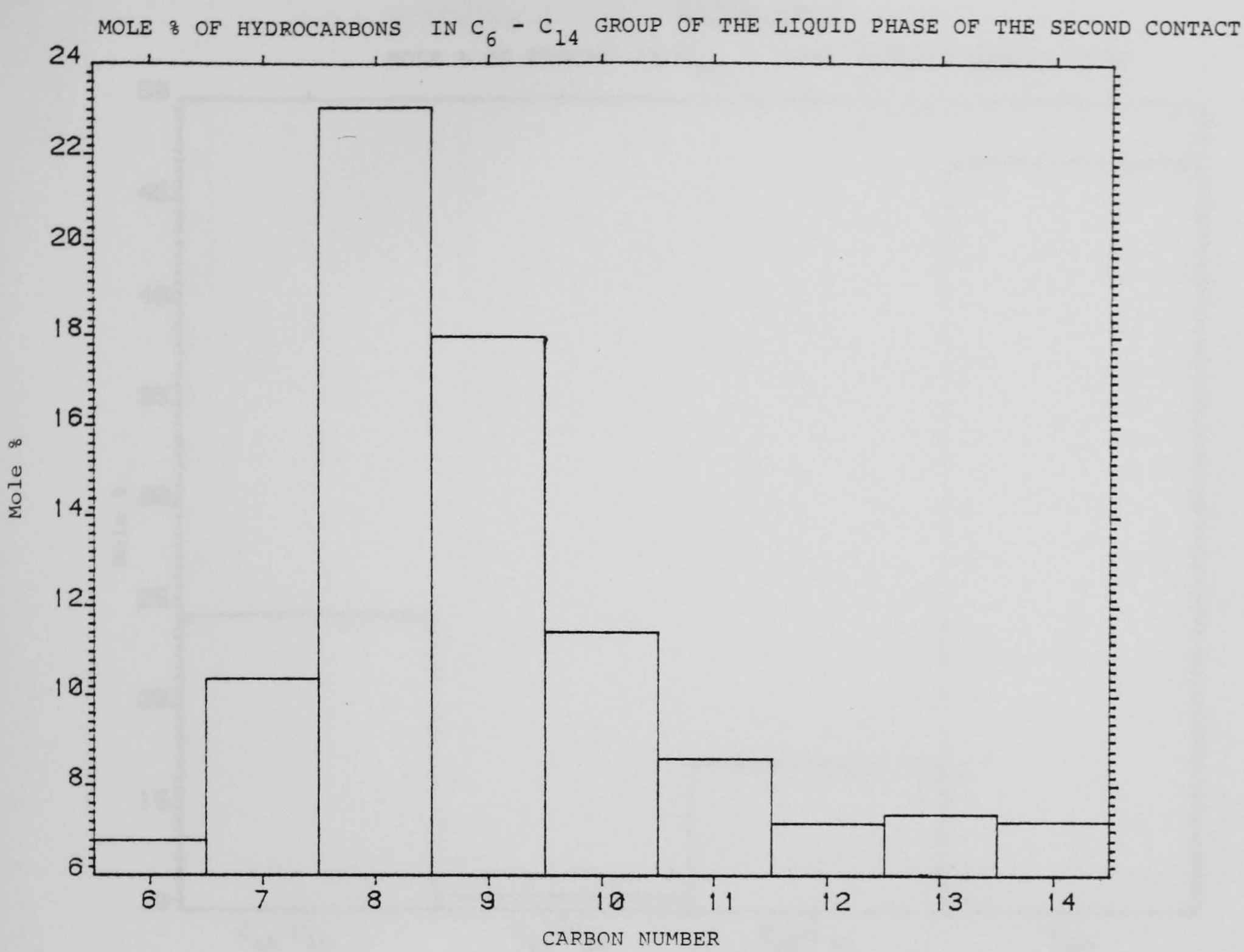

FIGURE 11-17

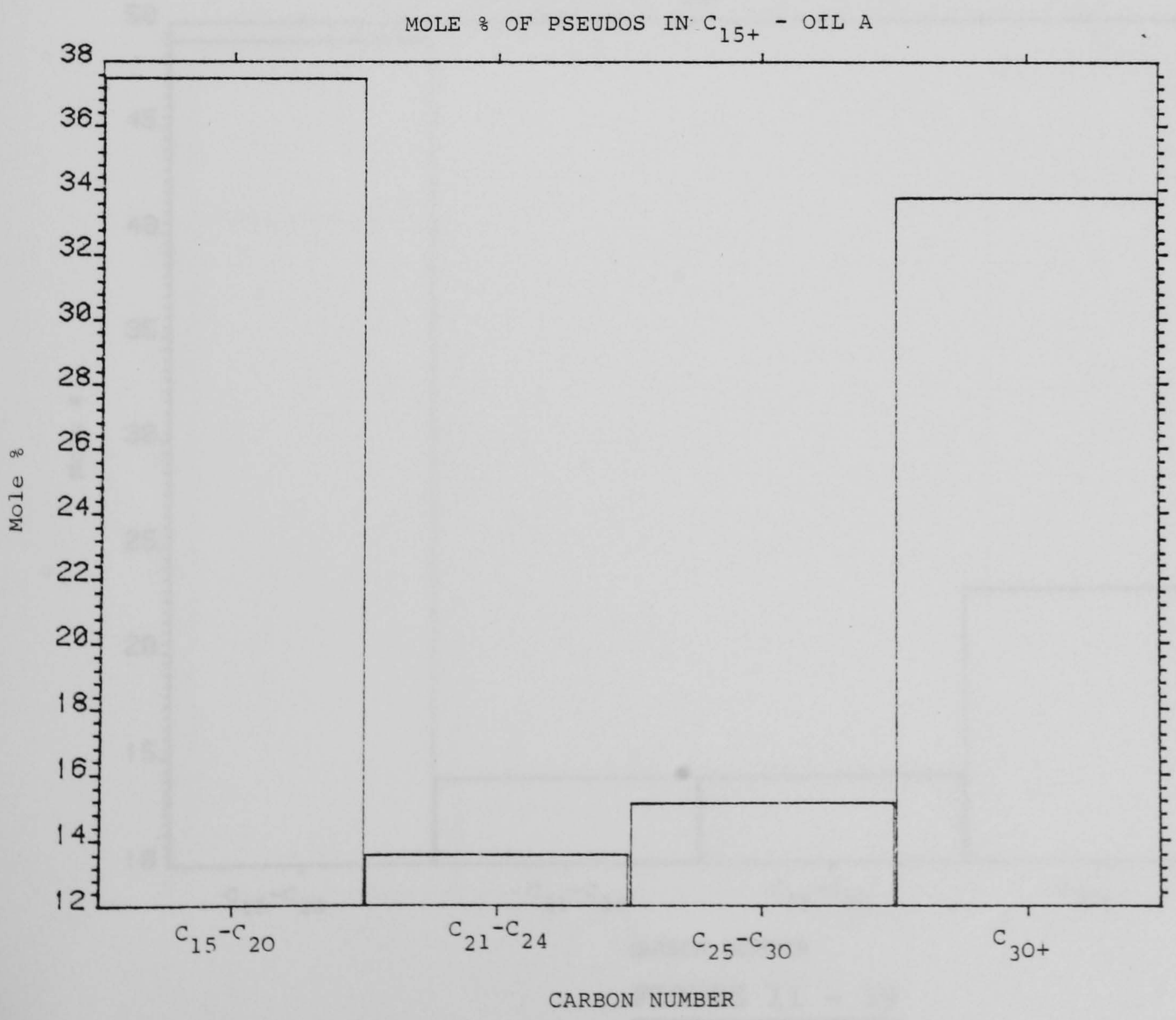

FIGURE 11-18

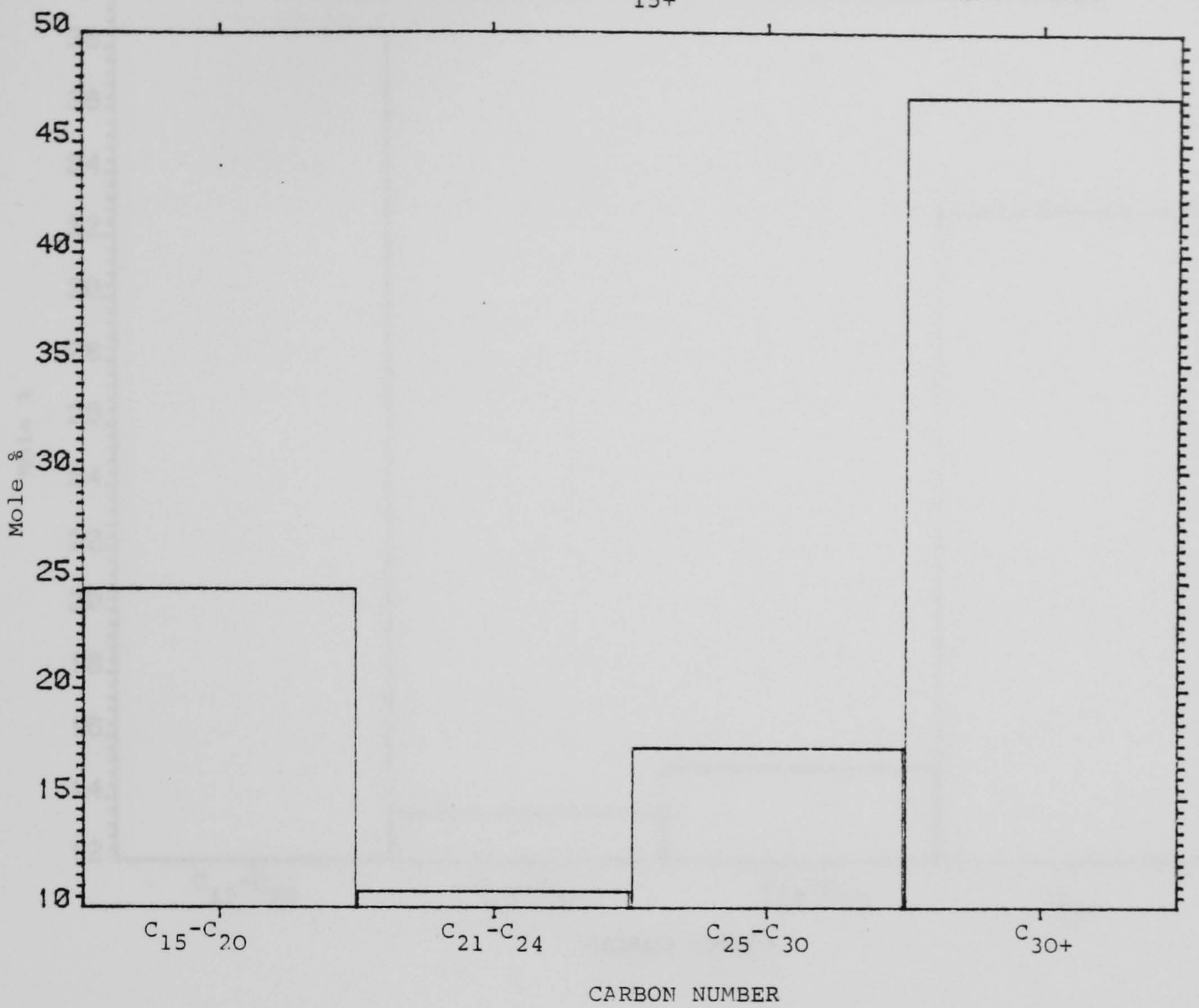

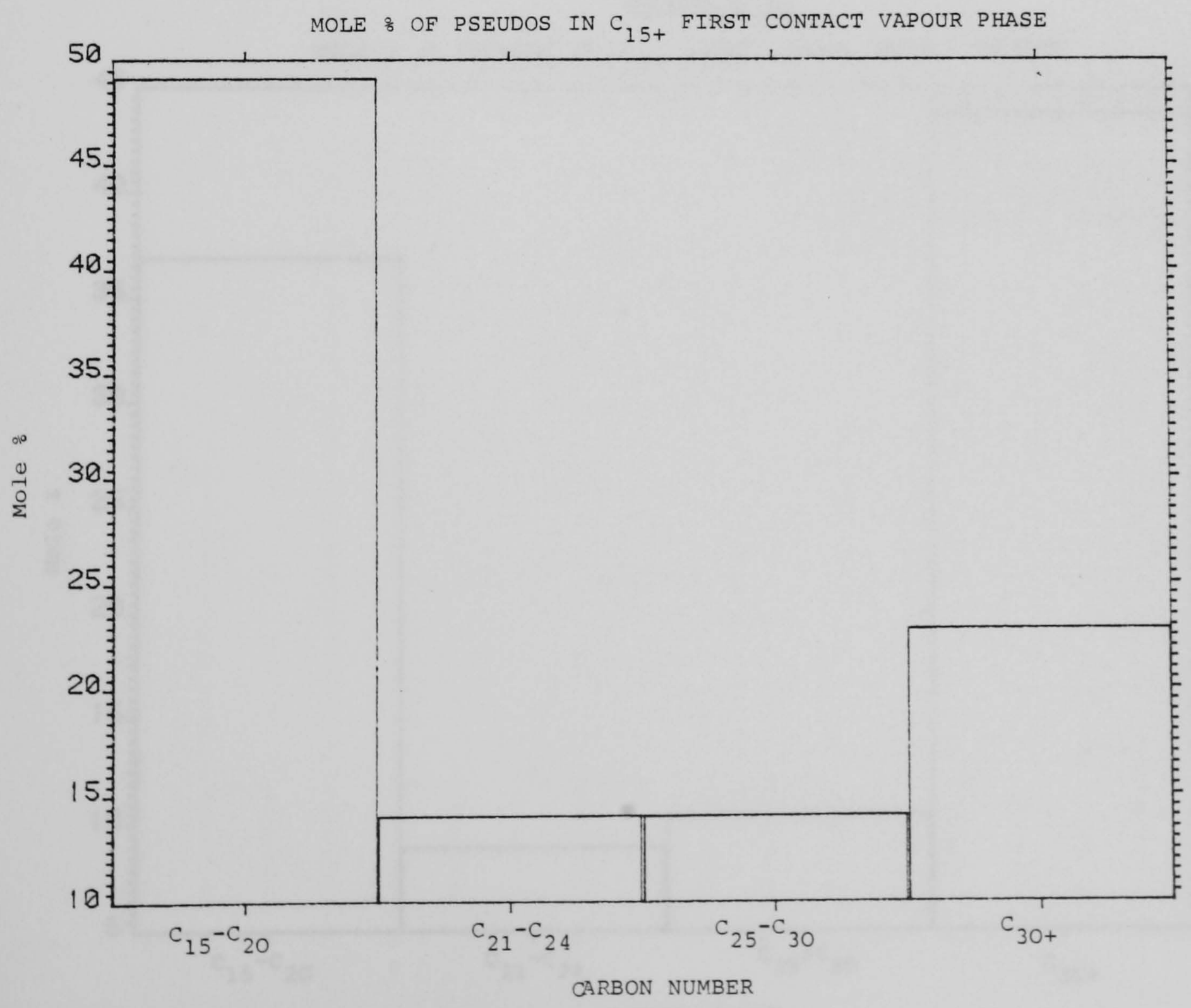

FIGURE 11 - 19

FIGURE 11-20

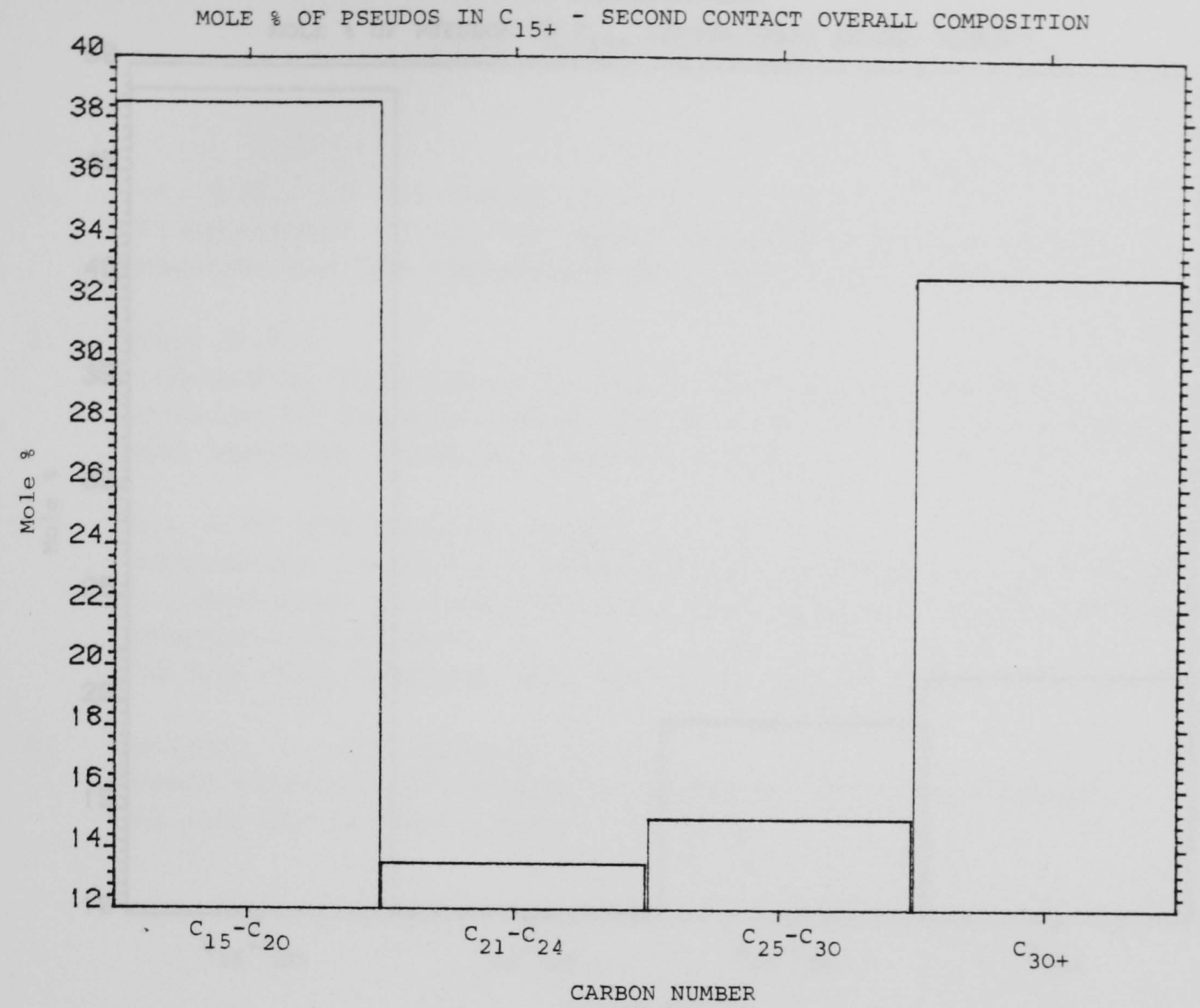

FIGURE 11-21

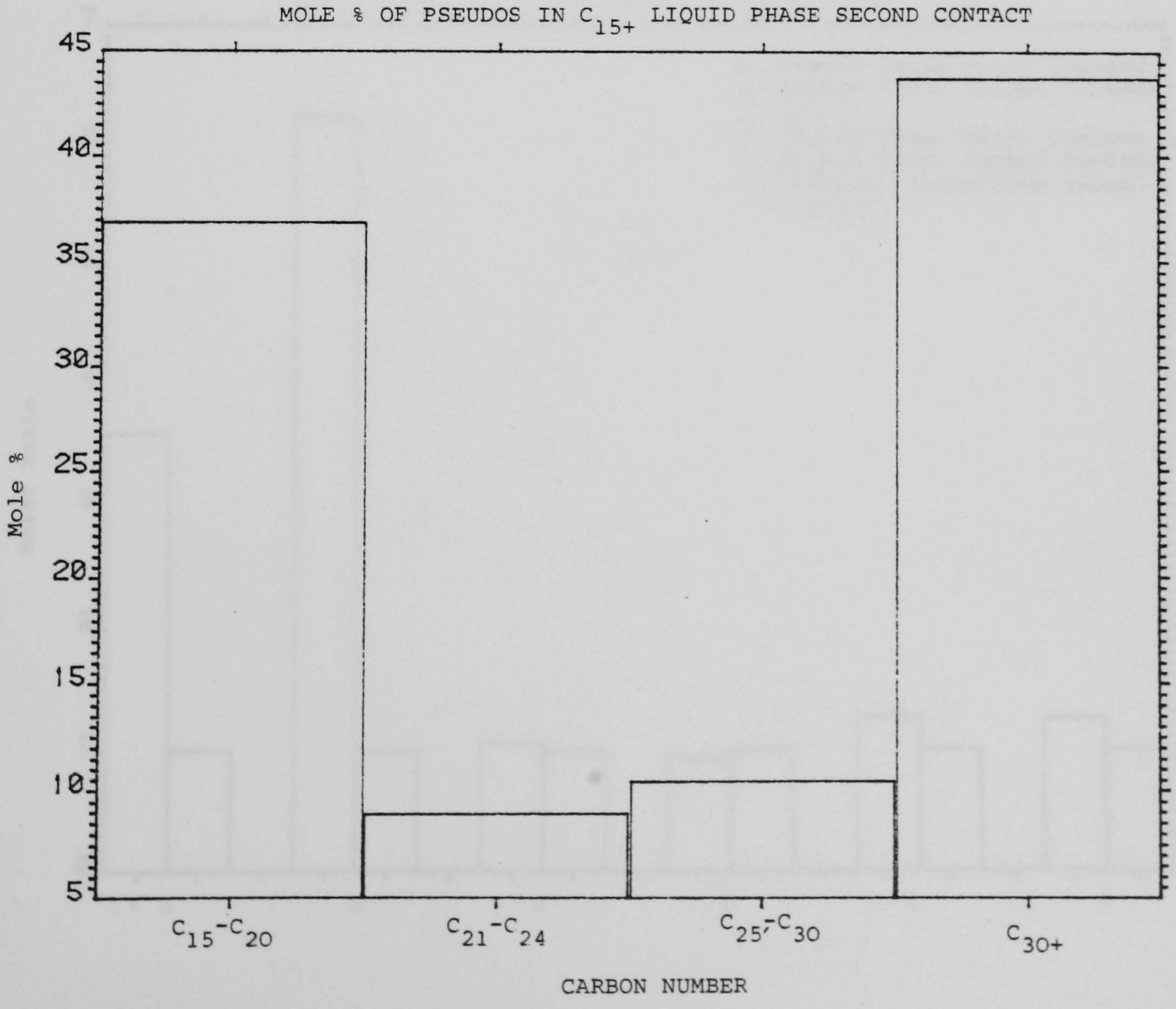

FIGURE 11-22

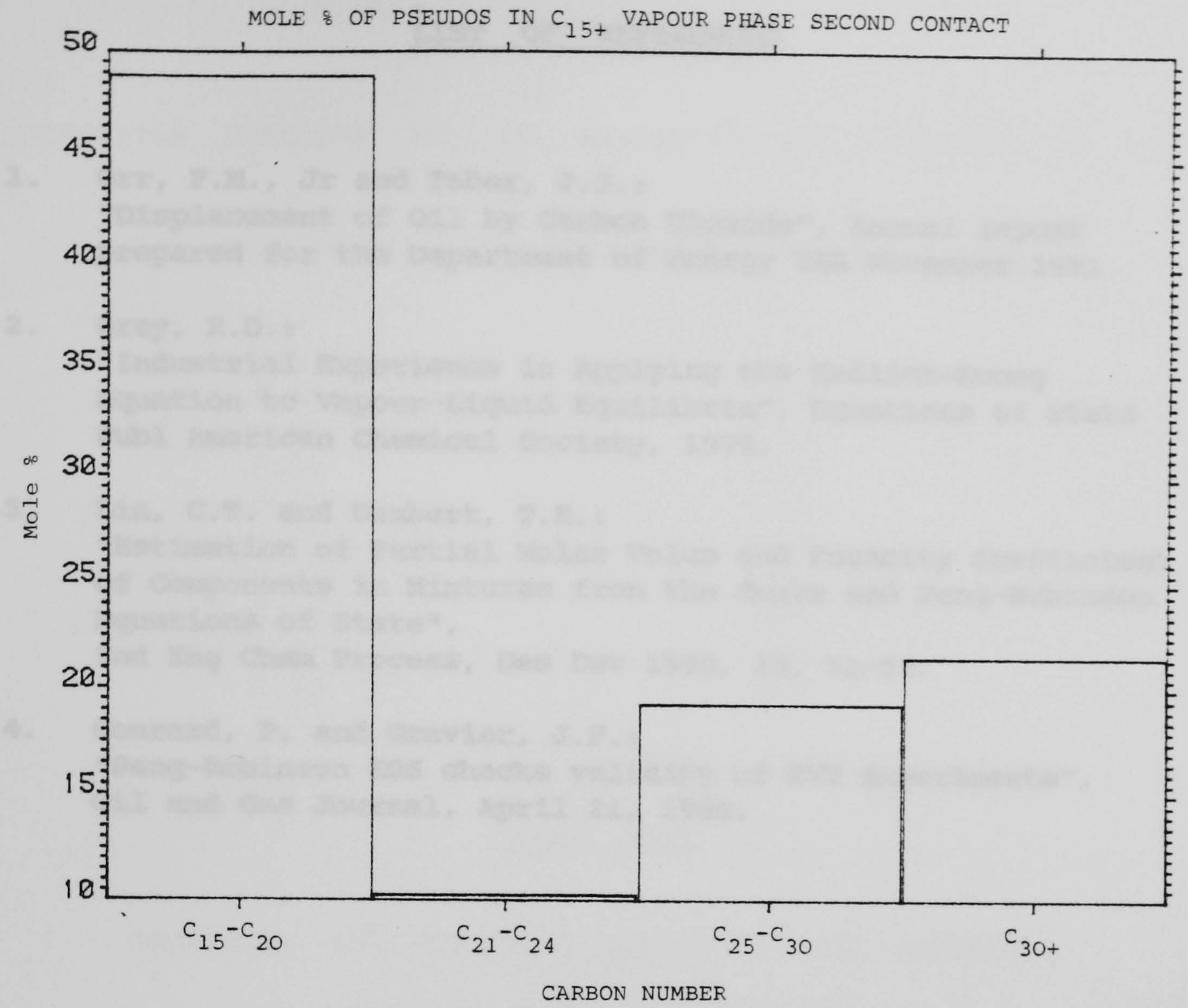

FIGURE 11-23

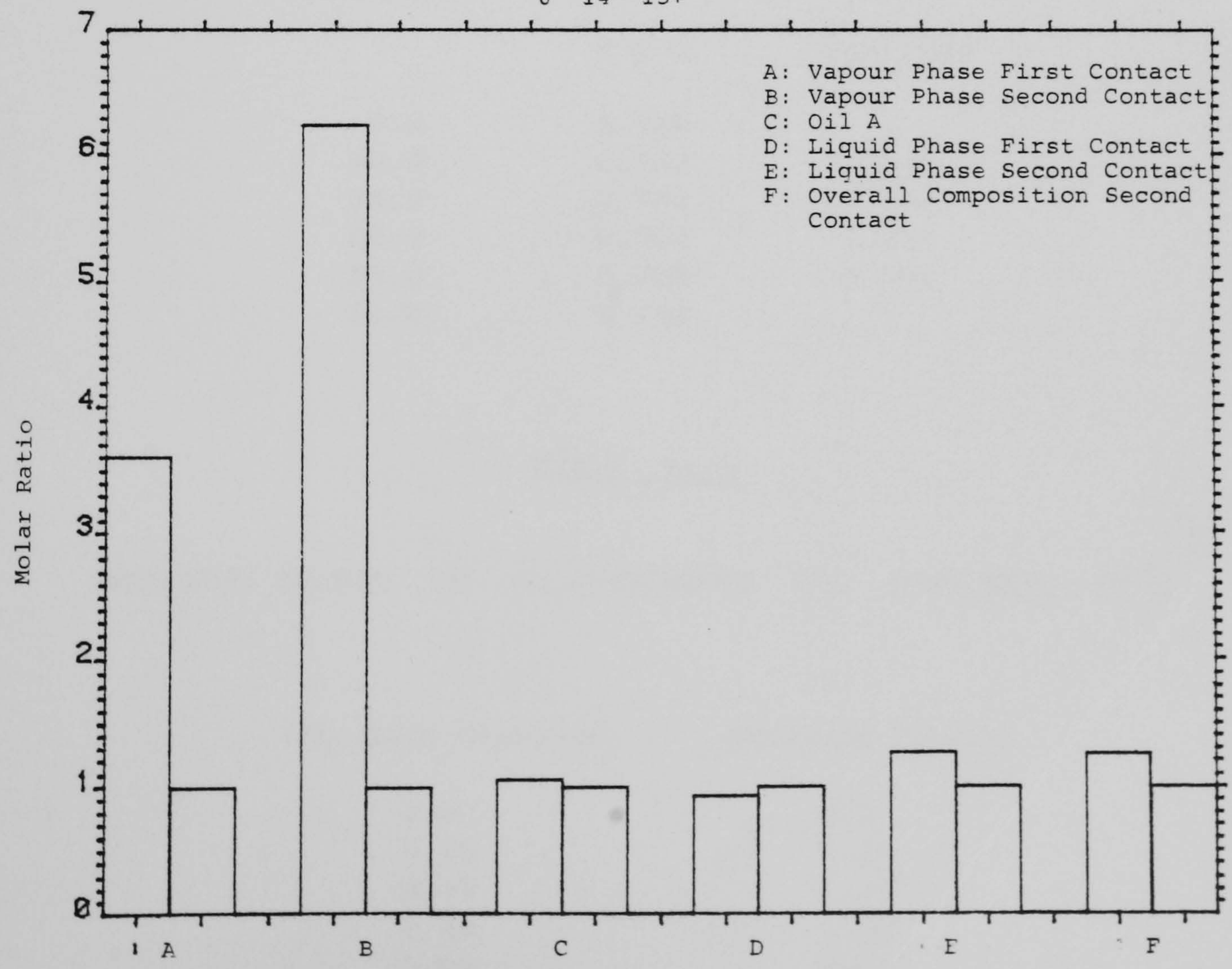

LIST OF REFERENCES

1. Orr, F.M., Jr and Taber, J.J.:
"Displacement of Oil by Carbon Dioxide", Annual report prepared for the Department of Energy USA November,1981.

2. Gray, R.D.:
"Industrial Experience in Applying the Redlich-Kwong Equation to Vapour-Liquid Equilibria", Equations of State Publ American Chemical Society, 1979.

3. Lin, C.T. and Daubert, T.E.:
"Estimation of Partial Molar Volum and Fugacity Coefficient of Components in Mixtures from the Soave and Peng-Robinson Equations of State",
Ind Eng Chem Process, Des Dev 1980, 19, 51-59.

4. Conrard, P. and Gravier, J.F.:
"Peng-Robinson EOS checks validity of PVT Experiments",
Oil and Gas Journal, April 21, 1980.

TABLE 11-1

SATURATION PRESSURE FOR CO_2-SYNTHETIC OIL MIXTURES AT 60°C

CO_2 Mole Fraction	Saturation Pressure (psia)
0.0	-
0.20	345
0.39	680
0.58	1075
0.60	1150
0.78	1850
0.85	2150
0.875	2250
0.88	2270
0.90	2355
0.92	2250

TABLE 11-2

PREDICTED AND MEASURED DENSITIES FOR SATURATED CO_2-SYNTHETIC OIL MIXTURES AT 60°C

CO_2 Mole %	Density gr/cc	
	Exper	Predicted
0.0	0.723	-
20.0	0.713	0.649
39.0	0.742	0.658
60.0	0.759	0.672
85.0	0.755	0.691
92.0	0.752	-

TABLE 11-3

SWELLING FACTOR OF CO_2-SYNTHETIC OIL MIXTURES, 60°C

CO_2 Mole Fraction	Swelling Factor
0.0	1.0
0.20	1.08
0.39	1.14
0.60	1.34
0.85	2.44
0.92	3.97

TABLE 11-4

COMPOSITIONS OF SYNTHETIC OIL–CO_2 MIXTURES 1350 PSIA–60°C

	Vapour Phase % Mole		Liquid Phase % Mole		K-Values	
	Predict	Exper	Pred	Exper	Pred	Exper
CO_2	99.4	99.69	66.44	65.83	1.5	1.51
nC_6	0.34	0.31	3.12	2.66	0.1	0.12
C_{12}	0.25	–	29.80	31.27	0.008	–
Ferr	–	–	0.27	0.24	–	–

TABLE 11-5

DENSITIES OF CO_2-SYNTHETIC OIL MIXTURES 1350 PSIA-60°C

	Vapour Density gr/cc	Liquid Density gr/cc
Predicted	0.27	0.68
Experimental	0.309	0.712

TABLE 11-6

MATERIAL BALANCE CHECK

	Blow Down Material Balance	Overall Composition
CO_2	0.780	0.800
nC_6	0.018	0.020
C_{12}	0.200	0.178
Ferr	0.002	0.002

TABLE 11-7

COMPOSITIONS OF SYNTHETIC OIL–CO_2 MIXTURE 1650 PSIA–60°C

	Vapour Phase Mole %		Liquid Phase Mole %		K-Values	
	Pred	Exper	Pred	Exper	Pred	Exper
CO_2	98.41	94.78	74.1	84.82	1.33	1.12
nC_6	0.51	0.5	2.18	1.27	0.23	0.39
C_{12}	1.07	4.69	23.50	13.8	0.05	0.34
Ferr	0.01	0.03	0.22	0.1	0.05	0.3

TABLE 11-8

DENSITIES OF SYNTHETIC OIL–CO_2 MIXTURES

	Vapour Phase Density gr/cc	Liquid Density gr/cc
Predicted	0.688	0.43
Experimental	0.717	0.531

TABLE 11-9

MATERIAL BALANCE CHECK

	Blow Down Material Balance	Overall Composition
CO_2	0.88	0.87
nC_6	0.01	0.01
C_{12}	0.11	0.12
Ferr	0.0	0.0

TABLE 11-10

CHROMATOGRAPHIC ANALYSIS OF OIL A (I)

Component	Weight %	Mole %
C_5	0.075	0.255
C_6	0.695	1.985
C_7	2.595	6.375
C_8	4.482	9.658
C_9	3.717	7.134
C_{10}	3.877	6.706
C_{11}	3.460	5.448
C_{12}	3.038	4.391
C_{13}	3.508	4.684
C_{14}	3.676	4.561
C_{15}	3,760	4.357
C_{16}	3.087	3.355
C_{17}	3.139	3.213
C_{18}	3.036	2.936
C_{19}	2.446	2.242
C_{20}	2.530	2.204
C_{21}	2.260	1.876
C_{22}	2.220	1.759
C_{23}	2.0180	1.530
C_{24}	2.006	1.458
C_{25}	2.479	1.730
C_{26}	1.918	1.287
C_{27}	3.989	2.579
C_{28}	1.020	0.636
C_{29}	0.934	0.562
C_{30}	1.034	0.602
C_{30+}	33.000	16.476

TABLE 11-11

SATURATION PRESSURES OF MIXTURES OF OIL A AND CO_2 AT 80°C AS A FUNCTION OF CO_2 OVERALL MOLE FRACTION

CO_2 Mole Fraction	Bubble Point Pressure (psia)
0.2	350
0.27	500
0.59	1400
0.70	2000
0.75	2250
0.80	2700
0.82	2900
0.84	3170
0.86	5080

TABLE 11-12

PREDICTED AND MEASURED DENSITIES FOR SATURATED CO_2-OIL A MIXTURES AT 80°C

CO_2 Mole Fraction		Density gr/cc	
		Exper	Predicted
0.27		0.8195	0.821
0.59	(1600 psia)	0.8402	0.806
0.70	(2500 psia)	0.8370	0.795
0.84		0.7704	0.803

TABLE 11-13

PSEUDOCOMPONENTS' PROPERTIES

	BP(°F)	SG	MW
C_{15}-C_{20}	576.46	0.846	245.02
C_{21}-C_{24}	706.04	0.874	317.26
C_{25}-C_{30}	816.53	0.893	397.2
C_{30+}	914.0	0.917	492.0

TABLE 11-14

PSEUDOCOMPONENTS CRITICAL PROPERTIES AND ACENTRIC FACTORS

	T_C (°K)	P_C (atm)	ω
C_{15}-C_{20}	757	16.08	0.637
C_{21}-C_{24}	821	12.36	0.744
C_{25}-C_{30}	873	10.02	0.85
C_{30+}	920	8.82	0.976

TABLE 11-15

CRITICAL PROPERTIES AND ACENTRIC FACTORS OF PSEUDOS

	T_C (°K)	P_C (atm)	ω
C_{15}–C_{20}	651	18.99	0.637
C_{21}–C_{24}	706	14.59	0.744
C_{25}–C_{30}	750	11.82	0.854
C_{30+}	791	10.4	0.975

TABLE 11-16

PREDICTED AND MEASURED PHYSICAL PROPERTIES, 2175 PSIA-80°C

	Experim	Predicted
Vapour volume saturation	23.9%	27%
Vapour density gr/cc	0.456	0.472
Liquid density gr/cc	0.774	0.798

TABLE 11-17

COMPOSITIONAL ANALYSIS OF VAPOUR AND LIQUID PHASES, 2175 PSIA-80°C

Component	Vapour Phase % Mole Exper	Vapour Phase % Mole Predicted	Liquid Phase % Mole Exper	Liquid Phase % Mole Predicted
CO_2	96.69	97.66	66.43	71.48
C_5	0.0	0.02	0.0	0.06
C_6	0.035	0.15	0.561	0.52
C_7	0.156	0.38	1.17	1.70
C_8	0.601	0.46	4.434	2.64
C_9	0.7053	0.27	4.717	1.99
C_{10}	0.497	0.21	2.961	1.89
C_{11}	0.245	0.13	1.045	1.55
C_{12}	0.175	0.09	1.521	1.26
C_{13}	0.204	0.07	2.075	1.36
C_{14}	0.110	0.06	1.049	1.32
C_{15}–C_{20}	0.441	0.33	6.555	5.27
C_{21}–C_{24}	0.069	0.06	1.150	1.93
C_{25}–C_{30}	0.020	0.04	1.284	2.17
C_{30+}	–	0.05	4.503	4.86

TABLE 11-18

MATERIAL BALANCE CHECK, 2175 PSIA-80°C

Component	Material Balance Mole Fraction	Overall Mole Fraction
CO_2	0.75	0.8
C_5	0.0	0.0
C_6	0.04	0.004
C_7	0.013	0.011
C_8	0.033	0.025
C_9	0.036	0.023
C_{10}	0.023	0.014
C_{11}	0.008	0.008
C_{12}	0.011	0.008
C_{13}	0.015	0.011
C_{14}	0.008	0.009
$C_{15}-C_{20}$	0.048	0.033
$C_{21}-C_{24}$	0.008	0.013
$C_{25}-C_{30}$	0.009	0.012
C_{30+}	0.032	0.027

TABLE 11-19

COMPOSITIONAL ANALYSIS OF OIL A (II)

Component	Mole Fraction
C_5	0.003
C_6	0.020
C_7	0.064
C_8	0.097
C_9	0.071
C_{10}	0.067
C_{11}	0.054
C_{12}	0.044
C_{13}	0.047
C_{14}	0.046
$C_{15}-C_{20}$	0.183
$C_{21}-C_{24}$	0.067
$C_{25}-C_{30}$	0.074
C_{30+}	0.165

TABLE 11-20

PREDICTED AND MEASURED PHYSICAL PROPERTIES, 1455 PSIA-80°C

	Experim	Predicted
Vapour Volume Saturation	54.66%	52.12%
Vapour Density gr/cc	0.2434	0.236
Liquid Density gr/cc	0.8303	0.808

TABLE 11-21

COMPOSITIONAL ANALYSIS OF VAPOUR AND LIQUID PHASES, 1455 PSIA AND 80°C

Component	Liquid Phase % Mole Exper	Liquid Phase % Mole Predicted	Vapour Phase % Mole Exper	Vapour Phase % Mole Predicted
CO_2	46.68	58.34	98.47	99.21
C_5	0.12	0.09	0.06	0.02
C_6	1.00	0.75	0.19	0.09
C_7	3.07	2.50	0.23	0.20
C_8	4.86	3.89	0.22	0.19
C_9	4.00	2.93	0.21	0.09
C_{10}	3.66	2.78	0.09	0.06
C_{11}	2.96	2.27	0.06	0.03
C_{12}	2.37	1.84	0.04	0.02
C_{13}	2.51	1.97	0.05	0.01
C_{14}	2.74	1.92	0.05	0.01
C_{15}–C_{20}	8.35	7.68	0.03	0.01
C_{21}–C_{24}	2.98	2.79	0.01	0.0
C_{25}–C_{30}	4.22	3.12	0.0	0.0
C_{30+}	10.48	7.13	0.0	0.0

TABLE 11-22

MATERIAL BALANCE CHECK, 1455 PSIA-80°C

Component	Material Balance Mole Fraction	Overall Fraction Fraction
CO_2	0.759	0.784
C_5	0.001	0.001
C_6	0.005	0.005
C_7	0.014	0.014
C_8	0.022	0.029
C_9	0.018	0.015
C_{10}	0.016	0.014
C_{11}	0.013	0.012
C_{12}	0.011	0.009
C_{13}	0.011	0.010
C_{14}	0.012	0.010
$C_{15}-C_{20}$	0.037	0.039
$C_{21}-C_{24}$	0.013	0.014
$C_{25}-C_{30}$	0.019	0.016
C_{30+}	0.047	0.036

TABLE 11-23

PREDICTED AND MEASURED PHYSICAL PROPERTIES

725 PSIA - 80°C

	Experim	Predicted
Vapour Volume Saturation	79.48%	81.8%
Vapour Density gr/cc	0.0875	0.0909
Liquid Density gr/cc	0.8268	0.8215

TABLE 11-24

COMPOSITIONAL ANALYSIS OF VAPOUR AND LIQUID PHASES, 725 PSIA-80°C

Component	Vapour Phase % Mole		Liquid Phase % Mole	
	Exper	Predicted	Exper	Predicted
CO_2	99.66	99.52	35.64	34.56
C_5	0.04	0.02	0.01	0.13
C_6	0.10	0.09	1.20	1.14
C_7	0.10	0.15	2.83	3.91
C_8	0.07	0.12	4.17	6.15
C_9	0.04	0.05	3.19	4.63
C_{10}	0.0	0.02	2.94	4.39
C_{11}	0.0	0.01	2.57	3.58
C_{12}	0.0	0.0	2.41	2.90
C_{13}	0.0	0.0	3.02	3.09
C_{14}	0.0	0.0	3.92	3.01
$C_{15}-C_{20}$	0.0	0.02	14.29	12.08
$C_{21}-C_{24}$	0.0	0.0	4.90	4.38
$C_{25}-C_{30}$	0.0	0.0	5.38	4.89
C_{30+}	0.0	0.0	13.53	11.17

TABLE 11-25

MATERIAL BALANCE CHECK, 725 PSIA-80°C

Component	Material Balance Mole Fraction	Overall Mole Fraction
CO_2	0.766	0.784
C_5	0.0	0.0
C_6	0.005	0.004
C_7	0.011	0.014
C_8	0.015	0.021
C_9	0.012	0.015
C_{10}	0.011	0.014
C_{11}	0.010	0.012
C_{12}	0.009	0.009
C_{13}	0.011	0.010
C_{14}	0.014	0.010
$C_{15}-C_{20}$	0.052	0.040
$C_{21}-C_{24}$	0.018	0.014
$C_{25}-C_{30}$	0.019	0.016
C_{30+}	0.049	0.036

TABLE 11-26

PREDICTED AND MEASURED PHYSICAL PROPERTIES,

2500 PSIA-80°C - FIRST CONTACT

	Experim	Predicted
Vapour Volume Saturation	65.10%	70.04%
Vapour Density gr/cc	0.545	0.555
Liquid Density gr/cc	0.837	0.812

TABLE 11-27

COMPOSITIONAL ANALYSIS OF VAPOUR AND LIQUID PHASES,

2500 PSIA-80°C - FIRST CONTACT

Component	Vapour Phase % Mole Exper	Vapour Phase % Mole Predicted	Liquid Phase % Mole Exper	Liquid Phase % Mole Predicted
CO_2	97.38	97.21	78.24	74.04
C_6	0.14	0.13	0.59	0.36
C_7	0.16	0.33	0.96	1.13
C_8	0.50	0.45	2.06	1.89
C_9	0.47	0.30	1.95	1.51
C_{10}	0.25	0.25	1.24	1.52
C_{11}	0.16	0.18	1.01	1.33
C_{12}	0.14	0.13	0.88	1.12
C_{13}	0.12	0.12	1.08	1.26
C_{14}	0.11	0.10	0.67	1.29
$C_{15}-C_{20}$	0.28	0.49	2.79	4.81
$C_{21}-C_{24}$	0.08	0.12	1.22	1.95
$C_{25}-C_{30}$	0.08	0.09	1.96	2.33
C_{30+}	0.13	0.12	5.33	5.45

TABLE 11-28

MATERIAL BALANCE CHECK, 2500 PSIA-80°C - FIRST CONTACT

Component	Material Balance Mole Fraction	Overall Mole Fraction
CO_2	0.917	0.92
C_6	0.003	0.002
C_7	0.004	0.005
C_8	0.010	0.008
C_9	0.009	0.006
C_{10}	0.005	0.005
C_{11}	0.004	0.004
C_{12}	0.004	0.004
C_{13}	0.004	0.004
C_{14}	0.003	0.004
$C_{15}-C_{20}$	0.010	0.015
$C_{21}-C_{24}$	0.004	0.005
$C_{25}-C_{30}$	0.006	0.006
C_{30+}	0.017	0.013

TABLE 11-29

PREDICTED AND MEASURED PHYSICAL PROPERTIES,
2500 PSIA-80°C - SECOND CONTACT

	Exper	Predicted
Vapour Volume Saturation	48.49%	43.08%
Vapour Density gr/cc	0.564	0.571
Liquid Density gr/cc	0.80	0.79

TABLE 11-30

COMPOSITIONAL ANALYSIS OF VAPOUR AND LIQUID PHASES, 2500 PSIA-80°C - SECOND CONTACT

Component	Vapour Phase % Mole		Liquid Phase % Mole	
	Experim	Predicted	Experim	Predicted
CO_2	93.63	96.25	76.17	75.58
C_6	0.62	0.22	0.90	0.54
C_7	0.79	0.44	1.38	1.33
C_8	1.36	0.69	3.06	2.46
C_9	1.04	0.48	2.38	2.03
C_{10}	0.57	0.34	1.52	1.67
C_{11}	0.33	0.22	1.14	1.34
C_{12}	0.29	0.16	0.95	1.10
C_{13}	0.30	0.14	0.98	1.18
C_{14}	0.16	0.12	0.96	1.15
$C_{15}-C_{20}$	0.43	0.56	3.89	4.23
$C_{21}-C_{24}$	0.12	0.13	0.95	1.56
$C_{25}-C_{30}$	0.17	0.10	1.10	1.78
C_{30+}	0.19	0.14	4.62	3.98

TABLE 11-31

MATERIAL BALANCE CHECK, 2500 PSIA-80°C - SECOND CONTACT

Component	Material Balance Mole Fraction	Overall Mole Fraction
CO_2	0.856	0.861
C_6	0.007	0.004
C_7	0.011	0.009
C_8	0.021	0.016
C_9	0.017	0.012
C_{10}	0.010	0.010
C_{11}	0.007	0.007
C_{12}	0.006	0.006
C_{13}	0.006	0.006
C_{14}	0.005	0.006
$C_{15}-C_{20}$	0.020	0.024
$C_{21}-C_{24}$	0.005	0.008
$C_{25}-C_{30}$	0.006	0.009
C_{30+}	0.022	0.024

densities and compositions are regarded as rather insensitive to it. There is strong evidence that the interaction parameters vary with components, pressure and temperature.

(4) The Peng-Robinson Equation of State was found to give better answers for liquid phase densities than the Modified Soave-Redlich-Kwong and the Modified Redlich-Kwong ones. But even the Peng-Robinson EOS, under-estimates liquid densities, sometimes to the extent of 5-10%. The experimental data can be matched by tuning the critical properties of the pseudocomponents but if matching is done at saturation conditions, the predictions at atmospheric pressure underestimate the stock tank oil density. The vapour phase density is predicted accurately.

(5) For the computer model to match experimental results, two sets of parameters have to be tuned; the interaction parameters and the correction factors for the critical properties of the pseudocomponents. Two reference data are necessary at least; saturation pressure and the saturated liquid density. The interaction parameter is tuned against the pressure, while the correction factors are tuned against the liquid density.

(6) The model, in a few cases of mixtures being very close to their critical point, had converged in an unstable trivial solution. A good initial estimate provided by the continuation technique sometimes can overcome the problem.

(7) The use of the continuation technique was proved very effective on reducing the number of iterations needed to achieve convergence and to ease calculations near and around the critical point. The saving in computer time was often more than 50%.

(8) For the very first phase behaviour calculation, a Newton type method, like the method used in this study, requires good initial values for the iteration variables. The available correlations to provide initial values for the saturation pressure are inadequate and therefore the operator should select it accordingly to his judgement and experience.

(9) A ternary representation of the phase behaviour although useful, proved conceptually inadequate to describe the mass transfer that takes place between phases in a gas miscible flooding process. To run a displacement simulator of a miscible process, more than three components are needed to describe the mixture.

(10) The use of the computer model had facilitated the vapour-liquid equilibrium experiments and had helped on the detection of experimental errors.

(11) The blow-down method used to analyse equilibrium phases proved to be a source of errors in some experiments. On the one hand, the large number of measurements it involves, and on the other the risk of light components in the gas phase condensing in the lines between the sampling loop and the gas meter, as well as the risk of the coating of the heavy waxes

on the pipe bore, make the method unattractive. On the contrary, the direct sampling method appears to be very promising.

12.2 RECOMMENDATIONS FOR FUTURE WORK

Further improvements and applications of both the phase behaviour model and the experimental system will be considered in turn.

The available empirical correlations provide very poor starting values for the unknown phase compositions, estimating K-values which have a very wide spread, particularly when a light gas (C_1, CO_2, N_2) and a heavy lumped pseudocomponent coexist in the mixture. A first priority must be to acquire more data from North Sea reservoir fluids' phase behaviour, including common oils, volatile oils and gas condensate systems. A study of the profile of the K-values at different pressures and temperatures, could possibly provide a generalised spread of the equilibrium values for the different components. It appears that the K-values of a gas condensate fluid exhibit a different profile than the ones of a crude oil.

The need for better liquid density predictions require the search for a more efficient EOS than the ones used in this study. Already within the Department, the Schmidt-Wenzel EOS has been tried with very encouraging results. The improved values it provides for the calculation of the liquid volume should be confirmed over a wider range of reservoir fluid systems and over different pressures and temperatures. The possibility of using the Peng-Robinson EOS for the phase composition calculations, and a different EOS (like the

Benedict-Webb-Rubin)[1] or a correlation (like the Alany-Kennedy)[2] for the liquid density determination, can also be considered.

To improve the characterisation of the heavy end of reservoir fluids and overcome the problem of poor laboratory data, probability functions should be considered for the molar distribution of the single carbon numbers. A study has already started in the Department using Whitson's three parameter gamma distribution and Lohrenz's exponential distribution. More effort should be put into developing methods of selecting the appropriate number of pseudocomponents out of an extended analysis, in order to be able to match accurately the laboratory data. This applies more for condensate systems where the accurate prediction of the liquid drop out in a constant volume depletion process is a fine art. For condensate fluids, the effect the aromatic and cyclo-components, and in particular those having boiling points between hexane and decane, have on the phase behaviour calculations, should be investigated. The components coming out of a chromatographic column, for example between heptane and octane, can hardly be given the properties of the normal octane. It is strong evidence that the presence of cyclos and aromatics, effects the vapour-liquid predictions and therefore it appears that these groups of components should be handled as pseudos rather than normal hydrocarbons.

It appears to be evident that the interaction parameters of CO_2, N_2, C_1 and hydrocarbons are functions of the pressure and the temperature of the system, and of the nature of hydrocarbons. An investigation has already started in the Department to study all the available binary data of hydrocarbons and CO_2, N_2, and C_1 and

endeavour to develop correlations for the interaction parameter as a function of reduced pressure, reduced temperature and acentric factor. These correlations should be incorporated as a subroutine in VLE and therefore variable values of the binary coefficients would be used with the Equations of State.

Experience has shown that the ternary representation is inadequate to describe the phase behaviour occurring in a gas miscible flooding and gives poor results for condensate studies. The development of quaternary phase envelopes with the additional dimension it provides, can give considerably improved results. Phase behaviour data derived for different pressures and stored as quaternary representations can be called by a displacement simulator, avoiding the solution of the system of nonlinear equations at each time step and for each block. This method, although it might seem approximate, eliminates the risk of the simulator crushing during the run because of a non convergence problem. A method of interpolation between pressures should be devised for the quaternary phase envelopes.

The study of the behaviour of Gibbs free energy function should be considered around the area of the solution of the phase behaviour problems, to ensure that the roots which equalise the phases' chemical potentials provide also the system with the lowest possible Gibbs energy at the temperature and pressure of the problem.

As far as the experimental part of this study is concerned, a rationalisation of the transfer loop between the two high pressure equilibrium cells is required. In particular the dead volume of

the manifold should be minimised to reduce the volume loss of phases after each contact. This modification will make possible the run of several multiple contacts of mixtures of reservoir fluid and injection gas.

Computer models used to simulate the gas miscible displacement in a reservoir, require viscosity data for the vapour and the liquid phases. The available correlations give satisfactory results for the vapour phase viscosity but they can be very erroneous for the liquid phase. A simple experimental facility can be incorporated in the transfer loop of the experimental system to measure the viscosity of the liquid phase. A few meters coil of 1/16" S.S pipe can cause a moderate drop to the flowing phase pressure and this pressure drop can be recorded by a differential pressure transducer. Poiseuille's law can be used to provide a value for the liquid phase viscosity.

Multiple contacts - including "forward" and "backward" contacts - of mixtures of live North Sea crude oils with a variety of injection gases like CO_2 and N_2 should be made to investigate the feasibility of such processes from the reservoir engineering point of view. The experimental facilities backed up with a robust phase behaviour simulator can provide a comprehensive investigation as to the application of gas miscible flooding as an enhanced oil recovery method in the North Sea reservoirs.

LIST OF REFERENCES

1. Benedict, M., Webb, G.B. and Rubin, L.C.:
   J Chem Phys, 1940, 8, 334.

2. Alani, G. and Kennedy, H.:
   "Volumes of Liquid Hydrocarbons at High Temperatures and Pressures", Pet Trans AIME, Vol 219, 1960, p 280.

APPENDIX I

DESCRIPTION OF THE INPUT PARAMETERS THE VARIABLES AND THE SUBROUTINES USED IN VLE

INPUT PARAMETERS

MAIN PROGRAM

Input Parameter	Description
IPRINT	Flag for explanatory comments on the usage of the program. 0 for minimum information. 1 for full explanatory comments. 3 for minimum information from the main program but full output from the quasi-Newton subroutines. (New users should type 1).
IRTD	Flag for input data to be presented with titles and comments. 0 option not used. 1 option used.
KVAL	Flag for the use of the appropriate equation of state. 1 for the modified Redlich-Kwong. 2 for the modified Soave-Redlich-Kwong. 3 for the Peng-Robinson.
kPROP	Flag for the method of calculating fraction properties. 0 for lumped analysis. 1 for PNA analysis.
NCOMP	Number of pure components and pseudo-components in the mixture (maximum = 20)

NPSEUD	Number of pseudo-components in the mixture (maximum = 10).
ICOMP	Vector of pure component data bank identifying numbers.
TITLE	Title for pseudo-component identification.
BPF	Vector of boiling points of pseudo-components ($^{\circ}$F), eg 150, 200, 300. A value must be assigned.
SGSRK	Vectors of specific gravity of pseudo-components. If no value is provided correlations will be used to calculate the specific gravity.
MWT	Vector of molecular weight of pseudo-components. If no value is provided correlations will be used to calculate the molecular weight.
TCMOD	Correction constant for pseudo-component critical temperature. (If no modification is needed TCMOD = 1.0).
PCMOD	Correction constant for pseudo-component critical pressure. (If no modification is needed PCMOD = 1.0).
ICASE	Flag for mode of calculation. 2 isothermal flash calculation. 3 dew point or bubble point pressure or temperature calculation. 4 ternary phase diagram. 5 optimisation of binary interaction parameter.

6 constant volume depletion or differential vapourisation.

z — Vector of mole fractions. A basis of 1 k-mol feed is employed.

The rest of the input parameters are dependent upon the choice of calculation and are self explanatory with IPRINT = 1.

The main program also contains some of the common blocks used in the program. The following is a list of all the common block names along with the variables they contain.

```
common/kVALUE/k, kB, kD
      /SYSTEM/ IN, IOUT
      /COMPNO/ ICOMP
      /CODE/ ICODE
      /NINE/ MHYP
      /TEN/ TCMOD, PCMOD
      /ELEVEN/ kVAL
      /IE/ IE
      /IPHASE/ IPE
      /THIRTEEN/ TITLE
      /SIX/ ZCR, WT
      /FOURTEEN/ RHOL, RHOV, AVLMW, AVVMW
      /FIFTEEN/ ICASE, kPROP
      /IDEW/ IDEW
```

The variables in the common blocks represent the following:

(a) <u>kVALUE</u>:

This contains the calculated equilibrium ratios.

k = vector of equilibrium ratios.

kB = vector of bubble point equilibrium ratios.

kD = vector of dew point equilibrium ratios.

(b) SYSTEM

This contains the machine dependent input and output device identifiers.

IN = device number for reading in data from the terminal (5 for the Honeywell 66/6000)

IOUT = device number for writing out data to the terminal (6 for the Honeywell 667/6000)

(c) COMPNO

ICOMP = vector of pure component data bank identifying numbers.

(d) kODE:

ICODE = indicator for use in specific subroutines

2 saturation temperature calculation

4 saturation pressure calculation

(e) NINE

MHYP = number of pseudo-components in the mixture.

(f) TEN:

This contains data associated with the pseudo-components.

TCMOD = correction constant for pseudo-component critical temperature

PCMOD = correction constant for pseudo-component critical pressure

(g) ELEVEN

kVAL = indicator for the appropriate equation of state.

(h) IE

IE = indicator used to store data

(i) IPHASE

IPE = indicator used in a series of bubble point, dew point or flash calculations so that the terminal compositions of previous solutions can be extrapolated to provide initial compositions for the new calculation.

ϕ option not used

1 option used

(j) THIRTEEN;

TITLE = title for pseudo-component identification.

(k) SIX:

ZCR = vector of pure component data bank critical compressibility factors.

WT = vector of pure component data bank molecular weights

(l) FOURTEEN:

RHOL = liquid phase density

RHOV = vapour phase density

AVLMW = liquid phase molecular weight

AVVMW = vapour phase molecular weight

(m) FIFTEEN:

ICASE = indicator for mode of calculation

kPROP = indicator for the method of calculating fraction properties

(n) IDEW

IDEW = 1 Dew point calculation

IDEW = 0 Bubble point calculation

The preceeding list of common blocks are commoned between the main program and various subroutines. As well as containing a list of all the common blocks the main program has dimension statements for variables which enter and return from the subroutines through the subroutine parameter lists.

LIST OF PRINCIPAL VARIABLES - MAIN PROGRAM DEFINITION

Program Symbol	Definition
Z	Vector containing mixture variables. (3) = pressure (4) = temperature (5) - (24) = mole fraction of each component in the mixture
ZL	Vector containing vapour feed stream variables. the elements are defined as for Z.
ZV	Vector containing vapour phase variables. The elements are defined as for Z.
Y	Vector containing liquid and vapour phase variables. (5) -(45) = liquid and vapour mole fractions
YB	Vector containing liquid and vapour phase variables at bubble point conditions The elements are defined as for Y.
YD	Vector containing liquid and vapour phase variables at dew point conditions. The

elements are defined as for Y.

HIP — Iteration matrix for isothermal flash calculation.

HB — Iteration matrix for bubble point calculation.

HD — Iteration matrix for dew point calculation

PAR — Parameter vector used to pass variables from the main program to various sub-routines.

VP — Vector of component vapour pressures.

ZZ — Vector of phase compressibility factors.
(1) = liquid phase compressibility factor
(2) = vapour phase compressibility factor

NOTE ON SUBROUTINE DESCRIPTIONS

Where an argument of a subroutine is the same as that defined in a preceding subroutine description, then the argument is taken to have that definition unless otherwise stated.

MAIN SUBROUTINES

SUBROUTINE OUTPUT

This routine controls the printed output for the various calculations performed.

LIST OF PRINCIPAL VARIABLES - OUTPUT

Program Symbol	Definition
NC	Total number of pure components and

	pseudo-components.
ICOMP	Vector of pure component data bank identifying numbers.
Y	Vector containing liquid and vapour phase variables. (5)-(45) = liquid and vapour mole fractions
K	Vector of component equilibrium ratios.
TITLE	Vector of titles for pseudo-component identification.

Subroutine TEMPST

This routine provides a starting temperature for bubble point and dew point calculations where the system pressure, P is specified.

Subroutine PRESST

This routine provides a starting pressure for bubble point and dew point calculations where the system temperature is specified.

Subroutine VAPRES

This routine calculates the initial estimates of the K-values at the specified temperature and pressure.

Subroutine ASDATA

This routine takes the appropriate data out of the arrays in the data block. The data corresponding to the specified pure component numbers held in vector ICOMP is taken out of the common blocks containing the data for the fifty six pure components.

This routine allows smaller arrays to be commoned between subroutines. The maximum number of pure components is twenty.

Subroutine HYPIN

This routine calculates the properties of the pseudocomponents in the mixture. There are two options depending upon the value of KPROP specified in the main program. If KPROP = 0 the lumped analysis method is used. If KPROP = 1 the paraffin-napthene-aromatic analysis is used. The routine is dimensioned for ten pseudo components.

Subroutine QUADRA

This routine calculates the coefficients of the quadratic equation that fits the three previous solutions (ALM, BELT, CIV). If linear extrapolation has to be used the coefficients of the line connecting the two previous solutions are determined (WAL, VOL). Finally if the calculation is very close to the critical point the subroutine extrapolates the values of the iteration variables up to the critical point (PHO).

Subroutine ZUZU

This routine gives predictions for the values of the iteration variables at the new value of the continuation parameter using the functions calculated in QUADRA.

Subroutine CBUBPT

This routine calls the quasi-Newton subroutines which solve the bubble point equations for a specified pressure or temperature.

If ICODE = 4 then temperature is specified and if ICODE = 2, pressure is specified.

LIST OF PRINCIPAL VARIABLES - CBUBPT

Program Symbol	Description
TBUB	Bubble point temperature.
PBUB	Bubble point pressure
ZCB	Liquid compressibility factor at bubble point.
NN	Dummy variable used to specify the dimensions of the iteration matrix in quasi-Newton routine SONEM2.
IPRINT	Integer which controls printing from SONEM2. ϕ no printing 1 full printing at each cycle of iteration
YBO	Vector containing the liquid and vapour mole fractions of the previous calculation in a series of bubble point calculations
LIFO	Counter used for the application of the continuation technique.

Subroutine CDEWPT

This routine is identical to subroutine CBUBPT except that it solves the dew point equations which are specified in subroutine DEWPT called by the quasi-Newton subroutine SONEM2.

Subroutine CILF

This routine calls the quasi-Newton subroutines which solve the isothermal flash equations for a specified pressure and temperature.

Subroutine PHASEN

This routine calls the driving subroutines for the calculation of the ternary phase envelope of a mixture at given temperature and pressure.

Subroutine COVODE

This routine calls the driving subroutines for the calculation of the constant volume depletion of a gas condensate mixture (IRUN = 1) or the differential vapourisation of a crude oil (IRUN = 2)

LIST OF PRINCIPAL VARIABLES - COVODE

ALPHA	Vapour molar fraction
VOLY	Volume occupied by 1 mole of gas at dew point conditions (cc)
VOVY	Volume of gas displaced per mole of feed (cc)
AOMOL	Moles of gas displaced per mole of feed
CUMU	Cumulative moles of gas displaced per mole of feed.
FEED	Moles remaining in the system per mole of feed.

Subroutine FAX

This routine calls the driving routines for the bubble point

calculation during the optimisation of the binary interaction parameter. It contains an objective function which the optimum value of the interaction parameter minimises.

Subroutine FBUP

This routine calls the subroutines used in the evaluation of the chosen equation of state and returns the calculated k-values, the compressibility factors and the residuals of the error equations for each iteration of the bubble point calculation.

Subroutine DEWPT

This routine operates in all respects in the same way as FBUP but for a dew point calculation.

Subroutine FUGA

This routine calls the subroutines that evaluate the appropriate equation of state. Each equation of state is called once for the liquid phase and once for the vapour phase returning the phase fugacity and compressibility to FUGA. The equilibrium ratios, average liquid and vapour molecular weights and densities are then calculated in FUGA.

LIST OF PRINCIPAL VARIABLES - FUGA

Program Symbol	Description
YL	Vector of liquid compositions
YV	Vector of vapour compositions
ZZ	Vector of compressibility factors

	(1) = liquid phase
	(2) = vapour phase
FUGL	Vector of liquid phase fugacity coefficients
FUGV	Vector of vapour phase fugacity coefficients
PAR	Vector of variables passed through from other subroutines
	(24) = pressure
	(2) = temperature
	(3) = kVAL, indicator for the selection of the appropriate equation of state.

Subroutine PENG

This routine calculates the mixture compressibility factor using the cubic Peng-Robinson equation of state written in terms of the compressibility factor. Firstly, subroutine INTER is called to calculate the binary interaction coefficients. Next the coefficients A(1), A(2), A(3), of the cubic equation are calculated. Subroutine CUBEQN is called to evaluate the roots of the cubic which are then sorted in subroutine SORT and the appropriate root selected for use in PENG.

LIST OF PRINCIPAL VARIABLES - PENG

Program Symbol	Description
Y	Vector of liquid or vapour compositions

	passed from subroutine FUGA
ZM	Compressibility factor returned to FUGA
IFASE	Indicator used for the selection of the appropriate real root of the cubic equation of state. 0 = smallest real root is selected 1 = largest real root is selected
FUG	Vector of fugacity coefficients

The following is a list of the named common blocks which are introduced in PENG:

```
common /CC/ A(3)
       /CS/ Z(3), MTYPE
       /ROO/ ZZ
```

(a) /CC/:

This block contains the coefficients of the cubic equation of state, written in terms of compressibility factor, A(1), A(2) and A(3), ie

$Z^3 + A(1)\ Z^2 + A(2)\ Z + A(3) = 0$

(b) /CS/:

Z = vector containing the three roots of the equation of state.

MTYPE = indicator for the types of roots.

0 = 3 real roots, 2 equal

1 = 1 real root, 2 complex

-1 = 3 real unequal roots

(c) /ROO/:

ZZ = the chosen root returned to PENG from subroutine SORT.

Subroutine SRKEQU

This routine calculates the mixture compressibility factor using the cubic modified Soave-Redlich-Kwong equation of state. The only difference in operation between PENG and SRKEQU is that SRKEQU calls subroutine SRINTER for the binary interaction coefficients for the Soave-Redlich-Kwong equation of state.

Subroutine RKEQU

This routine calculates the mixture compressibility factor using the cubic modified Redlich-Kwong equation of state. Subroutine BICO is called to calculate the binary interaction parameters.

Subroutine INTER

This routine evaluates the binary interation parameters used in the Peng-Robinson equation of state. The parameters are stored in data statement FFK for pure hydrocarbon components methane through to tetradecane, together with carbon dioxide and nitrogen. If the mixture contains pseudocomponents then interaction parameters are only assigned for binaries with methane, propane, ethane, carbon dioxide and nitrogen. The indicator IC is set equal to one on the first call in INTER so that the routine is bypassed on subsequent calls from subroutine PENG.

Subroutine SRINTER

This routine is identical to subroutine INTER except that it

provides the interaction parameters for the Modified Soave-Redlich-Kwong equation of state.

Subroutine SONEM2

This subroutine implements Broyden's n-dimensional quasi-Newton method with step size control which is used for the solution of n-nonlinear algebraic equations in n variables. The routine operates on a subroutine, FX, whose main purpose is to return the function values F_i corresponding to the value of the variables X_i. When SONEM2 is called the argument FX is replaced by the name of the specific subroutine required. If an error occurs in the evaluation of the functions or in the call of subroutine STEP error messages are printed out.

LIST OF PRINCIPAL VARIABLES - SONEM2

Program Symbol	Description
X	vector of implicit variables.
FX	external subroutine name.
F	array containing function values - F_i.
SFX	vector containing scale factors for X.
FDX	factor for changing X values.
H	iteration matrix.
PI	performance index.
IC	step counter for iteration loops.
ICS	choice of the use of step control. 0 - required 1 - not required

ILP	iteration cycle limitation integer.
NN	dummy variable used to specify the dimensions of the iteration matrix, H.
Z, PAR, Y	vectors of variables passed through from the main driving program.
IPRINT	integer which controls printing from SONEM2. 0 - no printing 1 - full printing at each cycle of iteration and call of subroutine PRINT
INDIC	control integer 2 - a starting vector, X, is available on entry to SONEM2, but the initial iteration matrix, H, is calculated 3 - both the staring vector, X, and initial iteration matrix, H, are available from a previous calculation
IED	error return from subroutine STEP
IER	error return from SONEM2 0 - iteration converged successfully 1 - iteration failed to converge in the allowed number of cycles.
TOL	accuracy required - tolerance.

Subroutine STEP

This routine takes the increments in the X variables held in vector P and evaluates the function values, F_i, at the Newton step X + P by a call of subroutine FX. The iteration matrix, H, is then updated using Broyden's Rank-one update formula. The routine is

called by subroutine SONEM2. The subroutine arguments are the same as in SONEM2 with the following additions:

LIST OF PRINCIPAL VARIABLES - STEP

Program Symbol	Description
P	vector containing incremental steps taken by the implicit variables.
ICOUNT	counter used to store the number of calls in STEP of the subroutine FX.
IUPD	integer which controls updating of iteration matrix. 0 - no updating 1 - updating required (IUPD is assigned in SONEM2)
IK	counter used to store the number of slashings of alpha (step-size control factor).
N	dimension of vector of implicit variables, X.
ISMAX	number of times alpha can be slashed.
IER	error return from STEP 1 - IK has exceeded allowable value, ISMAX 2 - elements of iteration matrix, H, are zero 3 - error return from subroutine FX

Subroutine SCALEV

This routine scales the variables solved by SONEM2. SCALEV operates under the direction of the integer variable ICODE. ICODE and SFX are specified in the call of SCALEV from SONEM2

ICODE = 1 variables divided by scale factors

ICODE = 2 variables multiplied by scale factors.

APPENDIX II

TABLES OF CONSTANTS USED IN THE PHASE BEHAVIOUR CALCULATIONS

TABLE II.1

MOLECULAR WEIGHTS, BOILING POINTS AND CRITICAL COMPRESSIBILITY FACTORS

The molecular weights of the hydrocarbons are used to change the units in the program, ie quantities evaluated on the basis of weight are changed to ones evaluated on a mole basis, eg J/kg °K is changed to J/kg.mole °K.

	T_B °C	M.Wt.	Z_C
hydrogen	-252.78	2.016	0.306
methane	-161.49	16.042	0.29
ethane	- 88.63	30.068	0.288
propane	- 42.07	44.094	0.278
iso butane	- 11.73	58.12	0.283
nor butane	- 0.5	58.12	0.274
iso pentane	27.852	72.146	0.269
nor pentane	36.074	72.146	0.268
hexane	68.74	86.172	0.264
heptane	98.427	100.198	0.26
octane	125.665	114.224	0.256
nonane	150.798	128.25	0.25
decane	174.123	142.276	0.246
undecane	195.89	156.292	0.242
dodecane	216.278	170.323	0.237
tridecane	235.44	184.354	0.23
tetradecane	253.57	198.38	0.23
pentadecane	270.63	212.406	0.23
hexadedcane	286.793	226.432	0.22
heptadecane	301.82	240.458	0.22
ethylene	-103.71	28.052	0.29
propylene	- 47.7	42.078	0.274
1 butene	- 6.26	56.104	0.277
cis 2 butene	3.72	56.104	0.276
trans 2 butene	0.88	56.104	0.276
1,3 butadiene	- 4.413	54.088	0.271
1 pentene	29.968	70.13	0.27

TABLE II.1 (CONTD)

	T_B °C	M.Wt.	Z_C
cis 2 pentene	36.942	70.13	0.268
trans 2 pentene	36.353	70.13	0.268
2 methyl 2 butene	31.163	70.13	0.268
3 methyl 1 butene	20.061	70.13	0.27
2 methyl 2 butene	38.568	70.13	0.268
1 hexene	63.485	84.156	0.265
cyclopentane	49.262	70.13	0.276
methylcyclopentane	71.812	84.156	0.273
cyclohexane	80.738	84.156	0.2767
methlcyclohexane	100.934	98.182	0.252
benzene	80.1	78.108	0.274
toluene	110.625	92.134	0.263
O-xylene	144.411	106.16	0.26
m-xylene	139.103	106.16	0.27
p-xylene	138.353	106.16	0.25
ethylbenzene	136.186	106.16	0.266
neopentane	9.503	72.146	0.269
ethylcyclohexane	131.783	122.203	0.244
ethylcyclopentane	103.466	98.182	0.269
1 heptane	93.643	98.182	0.26
1,2 butadiene	10.85	54.088	0.271
propadiene	- 34.5	40.062	0.27
nitrogen	-195.7	28.016	0.291
oxygen	-183.0	32.0	0.292
carbon monoxide	-191.3	28.01	0.294
carbon dioxide	- 78.3	44.01	0.274
hydrogen sulphide	- 61.6	34.08	0.268
sulphur dioxide	- 9.8	64.06	0.268

TABLE II.2

CRITICAL TEMPERATURE AND PRESSURE

The critical temperature and pressure are used in the calculation of the equation of state constants.

The critical constants of the fifty hydrocarbons are stored in degrees Kelvin and atmospheres respectively.

	TC	PC		TC	PC
hydrogen	33.3	12.8	1,3 butadiene	425.0	42.7
methane	191.0	45.8	1 pentene	474.0	40.0
ethane	306.0	48.2	cis 2 pentene	481.1	35.29
propane	370.0	42.0	trans 2 pentene	479.4	35.09
iso butane	408.0	36.0	2 methyl 1 butene	472.2	34.99
nor butane	425.0	37.5	3 methyl 1 butene	461.7	34.49
iso pentane	461.0	32.9	2 methyl 2 butene	483.3	35.89
nor pentane	470.0	33.3	1 hexene	511.1	32.09
hexane	508.0	29.9	cyclopentane	511.7	44.56
heptane	540.0	27.0	methylcyclopentane	532.7	37.35
octane	569.0	24.6	cyclohexane	553.0	40.0
nonane	596.1	22.6	methylcyclohexane	572.3	34.31
decane	618.9	20.7	benzene	562.0	48.6
undecane	641.1	19.2	toluene	594.0	41.6
dodecene	660.0	17.0	o-xylene	632.4	36.05
tridecane	677.8	17.0	p-xylene	619.4	34.69
tetradecane	695.0	16.0	m-xylene	618.4	34.01
pentadecane	710.0	14.96	ethylbenzene	619.9	36.73
hexadecane	723.9	14.01	neopentane	433.6	32.62
heptadecane	737.8	12.99	1 butene	419.0	31.02
ethylene	282.0	50.0	ethlcyclohexane	575.0	26.25
propylene	365.0	45.6	ethlcyclopentane	569.3	34.64
1 butene	420.0	39.7	1 heptane	535.0	28.29
cis 2 butene	427.8	40.82	1,2 butadiene	443.6	45.91
trans 2 butene	427.8	40.82	propadiene	393.0	43.6
nitrogen	126.2	33.5	carbon dioxide	304.2	72.9
oxygen	154.8	50.1	hydrogen suphide	373.6	88.9
carbon monoxide	133.0	34.5	sulphur dioxide	430.7	77.7

TABLE II.3

VAPOUR PRESSURE CONSTANTS FOR THE ANTOINE EQUATION

The vapour pressure of component i is given by the Antoine equation ie

$$\ln P_i = A_i - \frac{B_i}{t + C_i}$$

where:

P_i = vapour pressure of component i.

A_i, B_i, C_i = constants for component i

t = temperature in $^{\circ}C$

	A_i	B_i	C_i
hydrogen	5.92088	71.615	276.337
methane	6.61184	389.93	266.0
ethane	6.80266	656.4	256.0
propane	6.28973	813.2	248.0
iso butane	6.81	955.0	243.0
nor butane	6.83029	945.9	240.0
isopentane	6.8038	1027.25	234.0
nor pentane	6.85221	1064.64	232.0
hexane	6.8773	1171.53	224.366
heptane	6.90319	1268.586	216.954
octane	6.92394	1355.126	209.517
nonane	6.93764	1430.459	201.803
decane	6.95707	1503.566	194.738
undecane	6.97712	1572.752	188.054
dodecane	6.98291	1627.714	180.521
tridecane	7.00925	1693.684	174.815
tetradecane	7.2007	2018.879	170.591
pentadecane	7.03121	1795.065	161.891
hexadecane	7.03519	1835.21	151.868
heptadecane	6.97509	1851.699	149.263
ethylene	6.74756	585.0	255.0

TABLE II.3 (CONTD)

	A_i	B_i	C_i
propylene	6.8196	785.0	247.0
1 butene	6.8429	926.1	240.0
cis 2 butene	6.86102	956.398	236.572
trans 2 butene	6.87825	964.897	240.498
1,3 butadiene	6.85364	933.586	239.511
1 pentene	6.84268	1043.206	233.344
cis 2 pentene	6.87497	1069.243	230.759
trans 2 pentene	6.90546	1083.828	232.945
2 methyl 1 butene	6.86263	1048.876	232.194
3 methyl 1 butene	6.82643	1013.605	236.833
2 methyl 2 butene	6.92322	1099.075	233.317
1 hexene	6.8688	1154.646	226.064
cyclopentane	6.90325	1132.868	232.375
methylcyclopentane	6.8664	1188.05	226.276
cyclohexane	6.84498	1203.526	222.863
methylcyclohexane	6.82827	1273.673	221.723
benzene	6.89745	1206.35	220.237
toluene	6.95334	1343.943	219.377
o-xylene	7.00154	1476.393	213.872
p-xylene	7.00646	1460.183	214.827
m-xylene	6.9882	1451.792	215.111
ethylbenzene	6.9565	1423.543	213.091
neopentane	6.73812	950.84	237.0
ethylcyclohexane	0.80225	1823.831	218.053
ethylcyclopentane	6.88709	1298.599	220.675
1 heptane	6.88709	1257.505	219.18
1,2 butadiene	7.1619	1121.0	251.0
propadiene	5.6457	441.0	194.0
nitrogen	6.9898	308.365	273.2
oxygen	6.866	370.76	273.2
carbon monoxide	6.2402	230.274	260.0
carbon dioxide	8.154	799.02	230.0
hydrogen sulphide	7.7351	1051.8	277.0
sulphur dioxide	7.3278	1022.8	240.0

TABLE II.4

LIQUID MOLAR VOLUME AND ACENTRIC FACTOR

The acentric factor, ω_i, is dimensionless, and the liquid molar volume, v_i, has units

of ml/grm.mole.

	ω_i	v_i
hydrogen	0.0	31.0
methane	0.0115	52.0
ethane	0.0908	68.0
propane	0.1454	84.0
iso butane	0.1756	105.5
nor butane	0.1928	101.4
iso pentane	0.2273	117.4
nor pentane	0.2510	116.1
hexane	0.2957	131.6
heptane	0.3506	147.5
octane	0.3942	163.5
nonane	0.4437	179.6
decane	0.4902	196.0
undecane	0.5349	212.2
dodecane	0.5622	228.6
tridecane	0.6231	244.9
tetradecane	0.6797	261.3
pentadecane	0.7060	277.8
hexadecane	0.7418	294.1
heptadecane	0.7699	310.4
ethylene	0.0856	61.0
propylene	0.1477	79.0
1 butene	0.1874	95.3
cis 2 butene	0.2044	91.2
trans 2 butene	0.2138	93.8
1,3 butadiene	0.1814	88.0
1 pentene	0.2450	110.4
cis 2 pentene	0.2403	107.8
trans 2 pentene	0.2372	109.0
2 methyl 1 butene	0.2321	108.7

TABLE II.4 (CONTD)

	ω_i	v_i
3 methyl 1 butene	0.2285	106.7
2 methyle 2 butene	0.2837	106.7
1 hexane	0.2848	125.8
cyclopentane	0.1923	94.7
methylcyclopentane	0.2395	113.1
cyclohexane	0.2144	108.7
methylcyclohexane	0.2333	128.3
benzene	0.2100	89.4
toluene	0.2566	106.8
o-xylene	0.3136	121.2
p-xylene	0.3311	123.5
m-xylene	0.3243	124.0
ethylbenzene	0.3011	123.1
neopentane	0.1970	123.3
1 butene	0.1874	95.4
ethylcyclohexane	0.2426	119.2
ethylcyclopentane	0.2826	177.2
1 heptane	0.3580	192.3
1,2 butadiene	0.3394	109.4
propadiene	0.3135	96.5
nitrogen	0.045	25.34
oxygen	0.019	28.71
carbon monoxide	0.093	25.84
carbon dioxide	0.231	63.65
hydrogen sulphide	0.100	50.81
sulphide dioxide	0.246	50.81

APPENDIX III

E X P E R I M E N T A L P R O C E D U R E S

III.1 INTRODUCTION

III.2 CHARGING THE FLUIDS INTO THE CELLS

III.3 MIXING OF THE FLUIDS IN THE CELL, MEASUREMENT OF PHASE VOLUMES OR SATURATION PRESSURE

III.4 TRANSFER OF PHASES, DENSITY MEASUREMENT AND COMPOSITIONAL CHARACTERISATION

III.5 CLEANING OF EQUILIBRIUM CELLS AND TRANSFER LINES

III.1 INTRODUCTION

The apparatus shown in Figure 10-1 was used to perform both the volumetric and the vapour-liquid equilibrium experiments according to the classification of Section 10.1. The experiments can be divided into the following stages

(i) Charge of the reservoir fluid and injection gases to the equilibrium cells.

(ii) Mixing of the fluids in the cells, and measurement of phase volumes or saturation pressure.

(iii) Transfer of phases between cells, density measurement sampling and compositional characterisation and/or preparation for the next contact.

(iv) Cleaning of equilibrium cells and transfer lines.

III.2 CHARGING THE FLUIDS INTO THE CELLS

The reservoir fluids, stock tank oils or synthetic hydrocarbon mixtures used in this study were stored in the recombination cell (Fig 10-2). Before any transfer was made the recombination cell was rocked for at least ten minutes in case it contained fluid with very heavy components. The heating jacket was switched on to warm up the mixture at moderate temperatures of about 30-35°C to ensure the dissolution of the waxes and the existence of a homogeneous phase in the cell. In the meantime, the barrels of the pumps were filled with mercury, the cell in which the experiment was going to take place was filled to the top with mercury and pressurised to the chosen pressure of the transfer. This pressure had to be either a very small positive pressure for mixtures not containing any components more volatile than C_5, or slightly higher than the

mixtures' saturation pressure for live systems, to ensure a single phase. Using the second pump the mixture in the recombination cell was brought to the same pressure. Next, the top valve of the rocking cell was opened very slowly with the pressure continuously re-established to the initial value, to avoid any phase separation. In this way all the valves in the loop between the recombination cell and the equilibrium cell were opened one by one.

When the fluid had reached the top valve of the high pressure cell, the pressure in both pumps was checked to be equal to the transfer pressure and the pumps were engaged to the motor in such a way that the pump connected to the equilibrium cell would displace mercury out of it and the pump connected to the rocking cell would inject mercury into it. The displacing pump scale reading was recorded and the motor was started at the same time as the top valve of the cell was opened. This step has to be synchronised to keep the pressure of the system constant and avoid having any mercury on the top lines which could cause problems to the density cell. The displaced fluid is driven into the equilibrium cell at the same rate as the mercury is withdrawn from it. The pressure during the transfer practically remains constant if the storing vessel and the high pressure cell are kept at the same temperature. After the required volume of fluid had been charged in the cell, the pump, the top valve of the equilibrium cell and the top valve of the recombination cell were turned off. The displaced fluid that had remained in the transfer loop was removed through the drain and the lines were washed out with solvents, dried and evacuated to be ready for the displacement of the injection gas.

One of the mercury pumps was connected to the CO_2 storing high pressure cylinder to record its pressure and the gas intensifier was switched on to pressurise the gaseous CO_2 to the pressure of transfer. At the temperature of the transfer this pressure was slightly higher than the critical pressure of the CO_2 to keep it in the liquid phase. The pump connected to the cell was pressurised to the pressure of transfer as well, and both pumps were engaged to the motor. The valves in the transfer loop between the storing vessel and the equilibrium cell were opened one by one and when the chosen pressure was achieved and stabilised, the gas booster was switched off, the top valve of the cell was opened and simultaneously the displacement pumps were turned on. After the required volume of gas was displaced into the cell, the pumps and both the top valves of the cell and the storing cylinder were turned off. The lines were cleaned, dried and evacuated to be ready for the transfer of the phases from the one equilibrium cell to the other.

III.3 MIXING OF THE FLUIDS IN THE CELL AND MEASUREMENT OF PHASE VOLUMES OR SATURATION PRESSURE

The mixture of injection gas and reservoir fluid was allowed to equilibrate in the cell at the temperature of the experiment. To speed up the mass transfer between phases, the rocking mechanism was switched on for a long time. The establishment of equilibrium inside the cell could be certified by the stability of the pressure reading over a long period of time.

In the case of a contact, the volumes of the two phases in equilibrium should be measured. The television monitor system and

the camera were switched on and the centre of the dark cross at the end of the boroscope was focused on the top of the cell window. The scale reading on the airbath door was taken and the platform which holds the camera was allowed to slide down by the use of an adjusting screw until the centre of the cross on the television screen coincided with the interface of the vapour and liquid phase. The scale reading was taken to determine the height of the top phase in the cell. The height of the phase was multiplied by calibration coefficients to give the volume of the phase, and the already pre-measured dead volume of the top of the equilibrium cell was added to that volume.

The volume of the bottom phase was measured in the same way between the vapour-liquid interface and the liquid-mercury one. In case that the height of both the vapour and liquid phases or the height of one of them, exceeded the length of the cell window, then the cell had to be inverted (always with top and bottom valves off) and the volume of the mercury and of the bottom phase were measured. The volume of the top phase was determined from these two volumes and the predetermined total volume of the cell.

To measure the bubble point pressure of a mixture, the pressure in the cell was raised high enough to ensure that it had exceeded the saturation pressure, all the gas had gone into solution and the mixture was a single phase fluid. At the next step some mercury was pulled back into the pump barrel to increase the volume of the mixture and therefore decrease the pressure. The cell was rocked for about half an hour and if the pressure remained constant, the pump reading and the pressure were recorded. The pressure was decreased in small steps and at each step both the volume and the

pressure were taken. The volume-pressure pair of values were plotted on a x-y chart, the pressures being the y-axis. When the mixture was in the single phase it was highly incompressible and small changes in volume caused dramatic changes in pressure and the P-V relationship was linear. As the saturation pressure was approached, and the time that the mixture was allowed to equilibrate was not enough, the P-V function became slightly curved. In the two phase region, and when the gas cushion that was formed was relatively large, the mixture became highly compressible and the P-V relationship became linear again having a very small slope this time. The discontinuity in the compressibility of the mixture determines the saturation pressure. To measure graphically the bubble point pressure of the mixture the two straight lines of the P-V diagram were extrapolated. The conjunction of these lines determine the bubble point pressure of the mixture. Sometimes it became difficult to choose the two phase compressibility line because it was not very clear which were the first set of points on the two phase region. Experience has shown that the two phase line has to be drawn between the first few points which lie on a straight line just after the curved part of the P-V relationship. In case that a line passing through points lying further down was chosen, then the bubble point pressure was underestimated.

III.4 TRANSFER OF PHASES-DENSITY MEASUREMENT-COMPOSITIONAL CHARACTERISATION

After the volumes of the phases in the cell were measured, the densities and the compositions of the phases had to be determined.

While maintaining the pressure in the equilibrium cell containing the mixture, the other pump filled the second cell with mercury and pressurised it at the pressure of the experiment. Both cells were kept at the same pressure. The top valve of the first cell was opened very slowly and the mercury pump was used to re-establish the original pressure to avoid any phase separation. All valves in the transfer loop between the two cells were opened in the same way until the top phase had reached the top valve of the second cell. Both mercury pumps were engaged and the motor was turned on. The top phase moved out of the first cell, passed through the density cell and displaced the mercury from the second cell. A continuous flow of the phases through the density cell was required to ensure that the measurement was representative of the fluid under test. As the fluids were flowing through the densitometer, the period of oscillation of the tube was automatically recorded and a continuous density read out was available. Before each run the parameters A and B had to be calculated for the conditions of the run and stored in one of the densitometer memories.

To measure the composition, two methods were available. Either a small volume (≈ 4cc) of the phase was trapped in a sampling loop, isolated from the rest of the mixture and then blown down to atmospheric pressure or the high temperature direct sampling system was used. Both systems have been described earlier.

To use the blow down system (Fig 10-2, 10-3) the sample was trapped and isolated in the sampling loop, and the centrifuge tube which had previously been accurately weighed, was connected to the drain. The elastic cap of the centrifuge tube was secured using a

plastic strip. The gas chromatograph was set at the conditions for the gas analysis (Table 10-3), the gas sampling valve was turned at the fill position and the position of the bottom of the Teflon plug in the gas meter was recorded. The valve at the bottom of the sampling loop was then cracked very carefully so that the eluted gas would not burst the centrifuge or carry with it liquid droplets which would be deposited in the lines and would avoid measurement. The liquid drop out accumulated at the bottom of the tube, while the gas flowed through the sampling valve and was collected in the gas meter. After sufficient gas had displaced all the air that was initially in the lines, the VALCO valve was switched to the inject position and a volume of approximately 100$\mu\ell$ was injected into the column. After all the sample had been separated, the bottom valve of the gas meter was closed and the new position of the Teflon plug was recorded to calculate the volume of the eluted gas. The centrifuge tube with the liquid drop out in it, was removed from the sampling system, sealed and weighed again to determine the mass of the separated liquid. The chromatograph was set at the conditions for the liquid samples analysis (Table 10-3) and using a Hamilton 1.0 μ syringe, 0.2 μ of sample were injected in the column. In case that the mixture contained hydrocarbons heavier than C_{30}, a small volume of the liquid drop out was spiked with a certain volume of a mixture of pure hydrocarbons (C_{14}-C_{17}). Next an injection of the spiked mixture was made to determine the fraction of the sample that remained in the column.

If the direct sampling system was used, then during the transfer of the phase from one cell to the other, the valve shown on the top

line of the airbath (Figure 10-1) was closed to force circulation of the fluid through the sampling system. The side box which contained the VALCO valve was kept at the temperature of the oven in order that the phase equilibrium would not be disturbed. The sampling valve was then turned to the inject position and 4 μ of fluid were directed to the flow of the hot carrier gas which carried the sample into the column. At the same time the sampling system was isolated from the rest of the mixture in the oven and the heater of the side box was switched on to raise the temperature of the VALCO valve at 300°C. The temperature program of the VALCO valve and the temperature program of the chromatographic column were following each other in pace.

When a second contact was required, a predetermined volume of the top phase was displaced into the second cell, where a known volume of reservoir fluid had been charged before. The top valve of the second cell was closed and the remaining of the top phase was displaced from the system into one of the auxiliary vessels with the pressure remaining constant during the transfer and equal to the pressure of the experiment. All top valves of the cells were closed and the lines were cleaned and evacuated to be ready for the transfer of the bottom phase. The measurement of the bottom phase density and its compositional characterisation were performed in precisely the same way as with the top phase. The remaining liquid was driven to a second auxiliary vessel and the lines were evacuated. For the remaining contacts the same procedure was followed.

III.5 CLEANING OF EQUILIBRIUM CELLS AND TRANSFER LINES

To clean the cells and the lines from any residual left after the completion of every stage during the phase equilibrium experiments, two solvents were used; naptha and acetone. Nitrogen at pressure of about 100 psi was injected from the top of the naptha cylinder, displacing naptha out of the container and through the top lines into the part of the system which required cleaning. After the lines and/or the cells were flashed several times and naptha was coming out clean and colourless, the nitrogen flow was diverted to the top of the acetone cylinder and several flashes of acetone were made. Finally the valves of the solvent containers were turned off and nitrogen was allowed to flow through the lines and/or the cells and dry the acetone that was left inside.